Pedro Emanuel Alves Flores de Oliveira Gala

THE FICTITIOUS FORCE METHOD AND ITS APPLICATION TO THE NONLINEAR MATERIAL ANALYSIS OF SKELETAL STRUCTURES

Doctor of Philosophy Thesis in Civil Engineering, specialisation in Structures, supervised by Professor Paulo Manuel Mendes Pinheiro da Providência e Costa and by Professor Vitor Dias da Silva and submitted to the Faculty of Sciences and Technology of the University of Coimbra

July 2013

Universidade de Coimbra

Pedro Emanuel Alves Flores de Oliveira Gala

THE FICTITIOUS FORCE METHOD AND ITS APPLICATION TO THE NONLINEAR MATERIAL ANALYSIS OF SKELETAL STRUCTURES

Doctor of Philosophy Thesis in Civil Engineering, specialisation in Structures, supervised by Professor Paulo Manuel Mendes Pinheiro da Providência e Costa and by Professor Vitor Dias da Silva and submitted to the Faculty of Sciences and Technology of the University of Coimbra

July 2013

UNIVERSIDADE DE COIMBRA

Abstract

Structural analysis and design have evolved, in the last decades, with the objective of a more accurate consideration of the material and geometrical nonlinearities, increasing the security of the structures, improving their behaviour and reducing their cost. The simplicity of the linear models and analysis methods, particularly the one dimensional models for skeletal structures, has determined their dissemination by the technical community, which often regards nonlinear models and methods as a last resort because of their complexity.

Moreover, because of the remarkable performance reached nowadays by current personal computers, the choice of the more appropriate numerical analysis tool is not exclusively determined by its numerical efficiency – other characteristics, such as being user-friendly, must also be considered. Hence, the survival of the linear 1D model, even for nonlinear structural problems, appears to be determined not by its less demanding computational requirements but by its intrinsic simplicity.

The P-delta method, which is based on a linear 1D model, is the most popular geometrically nonlinear analysis method of skeletal structures. This iterative method uses an additional system of equivalent forces to indirectly simulate the reduction of the linear stiffness of the structure. The large success of this method was the starting idea for creating a similar structural method for nonlinear material analysis.

The Fictitious Force Method, presented in this thesis, is an iterative method for the quasi-static nonlinear elastic analysis of plane skeletal structures. In order to model the nonlinear material behaviour this method replaces the original constitutive relations by auxiliary linear relations and considers an additional fictitious force system. This fictitious force system models the "nonlinear" component of the deformations according to one of two alternative approaches: initial stresses or the initial deformations.

These two possibilities correspond to the Fictitious Force Method by deformations, which is an application of the Initial Stress Method of Zienkiewicz and co-authors and to the Fictitious Force Method by stresses which is an application of the Initial Strain Method of Argyris and co-authors. From a numerical point of view, these methods are applications of the Fixed Point Iteration Method.

The thesis includes the study of three common elemental bar models, the determination of the corresponding fictitious force systems, the fully description of the iterative procedures of the Fictitious Force Method (FFM), the explanation of these procedures from both physical and mathematical points of view, the development of their convergence conditions, and it thoroughly investigates the influence of the auxiliary stiffness field on the numerical efficiency of FFM.

Several examples are presented to illustrate the application of FFM and to discuss its convergence and other general issues. These examples are complemented with the flowcharts required for the implementation of FFM in current linear elastic structural analysis programs. In fact, FFM was implemented in one program of that type, EvalS, and this implementation was successfully used by other authors.

Resumo

A análise estrutural evoluiu, nas últimas décadas, no sentido de modelar de forma mais rigorosa as não linearidades material e geométrica, o que permite aumentar a segurança das estruturas, melhorar o seu desempenho e reduzir o seu custo. A simplicidade dos modelos e métodos de análise lineares, particularmente dos modelos unidimensionais para estruturas reticuladas, determinou a sua disseminação na comunidade técnica, que muitas vezes encara os modelos e métodos não lineares como um último recurso, em virtude da sua complexidade.

Por outro lado, o desempenho dos computadores pessoais atingiu tal patamar, que a selecção dos programas numéricos de análise estrutural deixou de ser determinada exclusivamente pela sua eficiência numérica, devendo ser também consideradas outras características tais como a simplicidade de utilização. Deste modo, a sobrevivência do modelo linear 1D, inclusivamente em problemas não lineares, aparenta ser determinada não só pelos seus menores requisitos computacionais mas sobretudo pela sua simplicidade intrínseca, que o torna mais facilmente compreensível.

O método P-delta, baseado no modelo linear 1D, é o método de análise geometricamente não linear de estruturas reticuladas mais popular. Este método iterativo usa um sistema adicional de forças equivalentes que simula indirectamente a redução da rigidez linear da estrutura. A grande popularidade deste método levou a que se pensasse em criar um método semelhante para a análise materialmente não linear de estruturas reticuladas.

O Método das Forças Fictícias, apresentado nesta tese, é um método iterativo para a análise elástica não linear quase-estática de estruturas reticuladas planas. Para modelar o comportamento material não linear este método substitui as relações constitutivas originais por relações lineares auxiliares e considera um sistema adicional de forças fictícias. Este sistema de forças fictícias modela a componente “não linear” das deformações por meio de uma de duas abordagens alternativas: tensões iniciais ou deformações iniciais.

Estas duas possibilidades correspondem, respectivamente, ao Método das Forças Fictícias por Deformações e ao Método das Forças Fictícias por Tensões, as quais podem ser interpretadas como aplicações do Método das Tensões Iniciais de Zienkiewicz e colaboradores e do Método

das Deformações Iniciais de Argyris e colaboradores. De um ponto de vista numérico, estes métodos são aplicações do Método do Ponto Fixo.

A tese inclui o estudo de três modelos elementares correntes de barra, a determinação dos correspondentes sistemas de forças fictícias, a descrição detalhada dos procedimentos iterativos do Método das Forças Fictícias (MFF), a explicação destes procedimentos dos pontos de vista físico e matemático, a determinação de condições de convergência e investiga a influência do campo auxiliar de rigidez na eficiência numérica do método.

Os vários exemplos apresentados na tese permitem ilustrar a aplicação do MFF e discutir a sua convergência e outros aspectos mais gerais. Estes métodos são complementados com fluxogramas que possibilitam a implementação do MFF em programas correntes de análise elástica linear de estruturas reticuladas. Efectivamente, o MFF já foi implementado na última versão do programa EvalS, a qual já foi utilizada com sucesso por outros autores.

Keywords

Fictitious Force Method

Initial Strain Method

Initial Stress Method

Iterative Method

Nonlinear Material Analysis

Skeletal Structures

Palavras-chave

Análise Materialmente Não Linear

Estruturas Reticuladas

Método das Deformações Iniciais

Método das Forças Fictícias

Método das Tensões Iniciais

Método Iterativo

Acknowledgments

My first acknowledgment goes to Professor Paulo Providência e Costa and Professor Vitor Dias da Silva, by the permanent support in the supervision of this work. I wish to thank Professor Paulo Providência for the countless hours of teaching and discussion not only about this work but also other subjects on structural analysis. For that, I am immensely grateful.

I wish to express my gratitude to Engineer Miguel Ferreira for the countless hours of debate about this work and for his brilliant ideas on how to improve it. At last, but not least, I what to express my gratitude for his friendship which means so much to me.

I wish also to express my gratitude to Professor Ricardo Costa, for the immense support, for the meticulous corrections of this work, and finally for his friendship.

I want to thank Professors Alfredo Dias and Anísio Andrade for the incentive and support, so important in the most difficult days.

I wish to thank Professor Luís Cruz Simões, head of the Structural Analysis Group at University of Coimbra, for the conditions offered for the development of this work.

I am very grateful to the Polytechnic Institute of Leiria for all its incentives and for giving me the conditions to develop this work.

I wish also to thanks André Varge for all the good advises and for the privilege of his friendship which means so much to me.

My deepest gratitude goes to my family, particularly, to my parents and to Isabel.

Table of Contents

List of Figures

List of Tables

List of Symbols

Latin lower case letters

b	self-equilibrated bending moment field
e	axial extension of a fibre
f	dimensionless function
g	influence function; elemental field; dimensionless function
h	cross section depth
i_{r}	cross-sectional radius of gyration with respect to r -axis
m	distributed moment; number of linear elements
n	shape function; number of nodal generalized displacements
o	origin of Cartesian system of coordinates
p	axial distributed load
q	transverse distributed load
u	axial component of displacement
w	transverse component of displacement
x, y, z	axes of Cartesian system of coordinates

Latin upper case letters and expressions

D	region of space corresponding to a cross section
E	modulus of elasticity
E_{EI}	average modulus of elasticity weighted by the cross-sectional second moment of area distribution
E_{A}	average modulus of elasticity weighted by the cross-sectional area distribution
E_{ES}	average modulus of elasticity weighted by the cross-sectional static moment distribution
EI	bending stiffness
EA	axial stiffness
ES	generalized static moment
F	effective force system; flexibility
F_0	normalised flexibility
G	functional operator
I	second moment of area

K stiffness; Banach space

K_0 normalised stiffness

L length of a linear element

$\mathbb{M}$ point moment

M bending moment

N axial force

P axial point load

Q transverse point load

R generalized stresses

S static moment

T functional operator

V shear force

Greek lower case letters

α contractivity constant; real number

β relative differences of bending stiffness

χ curvature

δ variation; corrective term

ε axial strain

ϕ rotation at the element end section w.r.t. its chord; relative rotation

φ axial elongation

γ dimensionless static moment

η generalized strains

λ eigenvalue

μ reduced bending moment

ρ spectral radius of a matrix

σ stress

Greek upper case letters

Δ variation; jump discontinuity; concerning a discretized function or entity

Lower indices

a concerning a linear matrix operator in the context of Initial Load Technique

ap	approximated
A	auxiliary
b	concerning a linear matrix operator in the context of Initial Load Technique; bottom fibre
C	compatible
Def	concerning FFM *by deformations*
ex	exact
E	elastic
EA	concerning axial stiffness
EI	concerning bending stiffness
ES	concerning stiffness generalized static moment
F	fictitious
F2	related to FFM_2
F3	related to FFM_3
incr	increment
lim	concerning the limit of proportionality
L	linear
max	maximum value
min	minimum value
M	concerning FFM$(M)_S$
N	concerning FFM$(N)_S$
NL	nonlinear
NL2	nonlinear related to FFM_2
NL3	nonlinear related to FFM_3
P	plastic; pseudo
r	reduced
ref	reference
R	restoring
RI	concerning generalized initial stresses
S	concerning FFM *by stresses*
t	top fibre; tangent
y	concerning the *y*-axis
χ, ε, η	concerning FFM_{Def}
δ	concerning a corrective field or entity
δ,eq	equivalent to the corrective term δ
ηp	concerning a plastic deformation
Δ	concerning an interpolation field or entity
I	initial; concerning specific measures of a relative error
II	concerning specific measures of a relative error

1 concerning left end section

2 concerning right end section

3 concerning midspan section

Upper indices

el elemental directions

gl global directions

(i) ith iteration

M concerning model M

MN concerning model MN

N concerning model N

T transpose

I linear structural operator

II nonlinear cross-sectional operator

Additional Symbols

$\overrightarrow{ab}$ oriented segment (from point a to b)

$\tilde{g}$ generic elemental field (function of x)

$\hat{g}$ generic constitutive function of a cross section

$\widehat{g}$ generic constitutive function of a fibre

$\bar{\mathbf{g}}$ generic elemental vector or matrix; concerning a modified structure

$\bar{\bar{\mathbf{g}}}$ generic elemental vector or matrix

$\underline{\mathbf{g}}$ global vector

$\hat{\mathbf{g}}$ generic eigenvalue

$\|\mathbf{g}\|$ Euclidean norm of vector $\mathbf{g}$

Bold latin letters (matrices)

$\mathbf{A}$ transformation matrix

$\mathbf{C}$ compatibility matrix

$\mathbf{D}$ Boolean connectivity matrix

$\mathbf{F}$ Force vector

$\mathbf{I}_i$ $i \times i$ identity matrix

$\mathbf{J}$ Jacobian matrix

$\mathbf{K}$	stiffness matrix
$\mathbf{P}$	permutation matrix
$\mathbf{T}$	matrix operator
$\mathbf{U}$	boolean pointer matrix
$\mathbf{W}$	symmetric square “compressed” stiffness matrix
$\mathbf{Z}$	influence matrix
$\mathbf{\Phi}$	elemental vector collecting strain resultants
$\mathbf{1}_{\mathrm{i}}$	dimension i vector with unit entries
$\mathbf{0}_{\mathrm{i}}$	$i \times i$ null matrix
$\mathbf{0}_{i\times 1}$	dimension i vector with null entries
$\mathbf{I}_{\mathrm{i}}$	$i \times i$ unit matrix

Abbreviations

const	constant function
FEM	Finite Element Method
FFM	Fictitious Force Method
$\mathrm{FFM}_{\mathrm{Def}}$	Fictitious Force Method *by deformations*
$\mathrm{FFM}_{\mathrm{S}}$	Fictitious Force Method *by stresses*
FFM(*M*)	Fictitious Force Method for *model M*
$\mathrm{FFM}(M)_2$	basic discrete description of FFM(*M*)
$\mathrm{FFM}(M)_3$	improved discrete description of FFM(*M*)
FFM(*MN*)	Fictitious Force Method for *model MN*
$\mathrm{FFM}(MN)_2$	discrete description of FFM(*MN*)
FFM(*N*)	Fictitious Force Method for *model N*
$\mathrm{FFM}(N)_2$	discrete description of FFM(*N*)
FFM_2	short form for $\mathrm{FFM}(M)_2$, $\mathrm{FFM}(N)_2$ or $\mathrm{FFM}(MN)_2$
FFM_3	short form for $\mathrm{FFM}(M)_3$
g.c.	geometrical centre
sup	supreme
tol	tolerance
w.r.t.	with respect to

Chapter 1
Introduction

1.1. Motivation

Structural analysis and design have evolved, in the last decades, with the objective of a more accurate consideration of the material and geometrical nonlinearities, increasing the security of the structures, improving their behaviour and reducing their cost. The simplicity of the linear models and analysis methods, particularly the one dimensional models suitable for the analysis of skeletal structures, determined their dissemination by the technical community, which often regards nonlinear models as a last resort because of their complexity.

On the other hand, the major advances in computer science and technology achieved over the same period motivated the developing of more advanced software tools for structural analysis, many of them far beyond the understanding of the common analyst and designer, more used to the linear 1D model. Moreover, today's computational capabilities of common personal computers are such that, very often, the choice of the numerical analysis tools is not determined by the numerical efficiency of the software itself.

In this context, the survival of the linear 1D model, even for nonlinear problems, appears to be determined not by its less demanding computational requirements but by its intrinsic simplicity, making it easily intelligible by the analyst.

The P-delta method, or Equivalent Force Method (Reis and Camotim, 2001), is perhaps the more popular method for the nonlinear geometrical analysis of skeletal structures, which is based on a linear 1D model. Its popularity may explain why so many variants and designations for this method can be found in the literature.

Two of the best descriptions of the Equivalent Force Method are those of Adams (1974), who uses the designation Fictitious Lateral Load Method, and Lui (1988), who calls it the Pseudo Load Approach, see also Chen and Lui (1991). The description of these methods presented by Gala (2007) proves that they are variants of the same general method. Actually, they only differ in the format of the system of equivalent forces: the fictitious force system of Adams is a discretization of the pseudo-forces of Lui.

The Equivalent Force Method consists in establishing an additional force system that, when applied to the structure together with the effective force system, simulates the equilibrium in the deformed configuration. In other words, the linear equilibrium equation written for the initial configuration with the effective plus equivalent forces is equal to the equilibrium equation written for the deformed configuration with the effective forces only. This is the same to say that the additional system of equivalent forces simulates the stiffness reduction of the structure, corresponding to the replacement of its linear stiffness by the geometric stiffness.

These equivalent forces are also problem unknowns because the deformed configuration is not known in advance. They can be determined in a simple iteration procedure, using the linear solution as the initial guess. For the analyst, the method presents a simple interpretation: it is as if the structure is being progressively pushed towards the exact configuration, or as if small configuration corrections are successively added. Mathematically, in the case of the differential 1D model, the procedure reflects an application of Picard's method (Bailey *et al.* (1968), Simmons (1991) and Shampine (1968)), while in the case of the discrete 1D model it is an application of the fixed point iteration method (Atkinson and Han (2001), Pina (2010) and Ortega and Rheinboldt (1970)).

The high efficiency of the Equivalent Force Method, which gives accurate results after just a few iterations, appears as an additional advantage, allowing it to be applicable even by hand. However, the method is also easily implemented in automated routines, because it only requires common linear analysis operations. Moreover, such an automated implementation in

the context of the finite element method (FEM), benefits from the fact that the stiffness matrix needs to be computed and inverted only once.

The large success of the Equivalent Force Method justifies the following question: is it possible to generalize or adapt this method in order to model nonlinear material behaviour? If the answer is affirmative, a second question immediately emerges: what requirements should such nonlinear material analysis method satisfy? In our view, these requirements are the following:

(i) The method should consist of simple operations, similar to those of a linear analysis method, repeating several times the same procedure;

(ii) This repeated procedure should use a constant stiffness on every iteration, because the calculation and inversion of stiffness matrices require large amounts of time;

(iii) The application of the method should be versatile enough;

(iv) The primary version of the method should be based on a small number of simplifying assumptions.

Actually, some methods aiming to extend the Equivalent Force Method to the nonlinear material analysis can be found in the literature. For example, the inelastic analysis method proposed by Lui and Zhang (1990) is an extension of the pseudo load approach (Lui 1988) to the nonlinear material analysis. However, this method does not fulfil the second requirement given above since the stiffness must be re-evaluated in every iteration. Blaauwendraad (1972) presents a method which considers the nonlinear material behaviour of the linear elements of skeletal structures directly in the stiffness matrix used in the routines for nonlinear geometric analysis. However, this method also violates the second requirement given above.

In order to operate with a constant stiffness, for instance, the initial tangent stiffness, an additional force system can be used to emulate the nonlinear material behaviour. These additional forces shift the structure from the “linear” configuration to the effective configuration corresponding to the nonlinear constitutive relation. The analogy with the Equivalent Force Method is obvious. The additional forces can also be seen as modelling the nonlinear material behaviour by means of initial deformations or initial stresses. The problem of determining the effect of a given field of initial deformations, like that due to a thermal action, in a structure with linear behaviour, is easily solved by Duhamel’s Method (Arantes e

Oliveira 1999). Note that it is also possible to use initial deformations to model the geometrical nonlinearity, see for instance Mari *et al.* (1982).

Because of the nonlinear character of the problem these additional forces are not known in advance. This is the same to say that the corresponding initial deformations or initial stresses are not known in advance, just like the effective deformed configuration is an unknown of the geometrically nonlinear problem tackled by the Equivalent Force Method. Hence, the calculation of these additional forces, named fictitious forces in opposition to the effective loads, requires appropriate numerical procedures. The adoption of a fictitious force system, modelling the nonlinear material behaviour, together with a simple iteration procedure and appropriate simplifying assumptions, are all that is required for a nonlinear material analysis method, fulfilling the four requirements given before. This is the basic idea of the Fictitious Force Method (FFM), established in Gala (2007), further developed since then and presented in this thesis, which is an iterative method for the quasi-static nonlinear analysis of plane skeletal structures.

Gala (2007) established two simple iteration procedures, which are now designated the Fictitious Force Method *by deformations* (FFM_{Def}) and the Fictitious Force Method *by stresses* (FFM_S). These two iterative versions of the Fictitious Force Method can be seen as applications of the Initial Stress Method of Ziewnkiewicz *et al.* (1969) and of the Initial Strain Method of Argyris and Scharpf (1972), originally proposed in the context of the Finite Element Method (FEM). On the other hand, the format of the fictitious forces employed in FFM has also a close relation to the Equivalent System of Fertis (2006).

The constant stiffness used in FFM can be the initial tangent stiffness; actually, this is a rather intuitive option. However, the constant stiffness which can be used is to some extent arbitrary. Moreover, the choice of an adequate constant stiffness is crucial not only to assure the convergence of the numerical procedure but also to decrease the required number of iterations.

FFM was originally formulated for flexure behaviour only, corresponding to beam *model M*. In this thesis, it is extended to the truss *model N* and to the general beam-column model *MN*, which combines the previous two. The formulation accomplished with *model MN* fulfils the requirements of the methodology proposed by Blaauwendraad (1972).

1.2. Objectives of the thesis

The central objective of this thesis is to present the 1D Fictitious Force Method. This main objective can be divided in the following sub-objectives:

(i) Establish the fictitious force system for three 1D bar models: *M*, *N* and *MN*;

(ii) Establish the FFM iterative procedures and clarify their meaning from both the physical and mathematical points of view;

(iii) Determine the convergence conditions of the FFM and, based on these conditions, define the admissible choices for the auxiliary stiffness;

(iv) Determine the influence of the auxiliary stiffness on the numerical efficiency of the FFM;

(v) Illustrate and discuss the application of FFM.

1.3. Structure of the thesis

This thesis contains seven chapters, including this introductory one. In the second chapter one reviews several methods, presented in the literature, that use either fictitious force systems or initial deformations to model nonlinear material behaviour or other structural phenomena. Duhamel's method for the solution of the initial deformations linear problem is presented in this context. The Fixed Point Iteration Method is also presented, from the functional analysis viewpoint, and FFM is shown to belong to this category of methods.

In the third chapter, the simplifying hypotheses which support the 1D flexural Euler-Bernoulli model are first clarified and subsequently FFM is formulated for this model, the so-called beam *model M*. The convergence conditions for FFM are then derived in the context of *model M* with all the required generality. A simple example is then presented as a first illustration of the method. The chapter closes with more advanced aspects of the application of FFM in the context of *model M*, including the development of the exact expressions of the fictitious force format.

The fourth chapter presents the application of FFM in the context of the truss *model N*, including once again the development of the fictitious force format exact expressions. The discretization procedure commonly adopted for linear material behaviour is not valid in the

nonlinear case. An example is given which illustrates the application of FFM in the context of *model N*.

The fifth chapter presents the application of FFM in the context of the beam-column *model MN*, with a special focus on the specific convergence conditions. An example is presented which illustrates the method in the context of *model MN*. The examples presented in chapters 3 to 5 were analysed with the help of the algebra package *Mathematica* (Wolfram, 2008).

The sixth chapter presents some applications of FFM, *via EvalS*, to the nonlinear analysis of reinforced concrete skeletal structures. *EvalS* (Ferreira, 2011) is a software for the analysis of plane skeletal structures that uses the Equivalent Force Method to model geometrically nonlinear behaviour and the Fictitious Force Method to perform nonlinear material analyses.

The last chapter summarizes the main conclusions of this work and indicates topics requiring further investigation.

Chapter 2
Fictitious Forces in Structural Analysis

2.1. Introduction

This chapter presents a review of the literature on the use of fictitious forces and initial deformations in structural analysis problems and, particularly, in nonlinear material problems. It begins with an historical perspective on the use of initial deformations in structural analysis. Then, the Initial Stress Method of Zienkiewicz *et al.* (1969) and the Initial Strain Method of Argyris and Scharpf (1972) are described. In the sequel to these methods, a brief but general description of the Fixed Point Iteration Method is presented.

In the remaining sections other methods are reviewed, beginning with the method proposed by Lin (1968) for the nonlinear elastic-plastic analysis of beams, which is a direct application of Duhamel's method. Next comes the Imposed Deformations Method of Aguado (1980) which, in spite of not using fictitious forces, employs initial deformations to model nonlinear material behaviour in an iterative procedure that approximates the strain fields like the Initial Strain Method.

The chapter is concluded with the description of three additional methods which also employ fictitious forces and/or initial deformations: the Method of Equivalent Systems of Fertis (2006), which employs a system of auxiliary forces similar to the FFM fictitious force system, and two reanalysis methods.

2.2. The use of initial deformations in structural analysis

The state of deformation and stress caused by a given field of initial deformations was first analysed by Duhamel in 1838 (Arantes e Oliveira, 1999). Duhamel did not consider an arbitrary field of initial deformations; instead, he supposed that the structure was subjected to a given thermal action, which is a particular case of an initial deformations field. Duhamel's method can be described in various ways, all sharing the same basic idea (Arantes e Oliveira, 1999). The problem considers a structure subjected to an action formed by (i) a thermal action, or any other initial deformation, and (ii) a system of exterior forces. To this action corresponds a general solution in terms of displacement, strain and stress fields. If the problem is linear, the effect of the initial deformations can be calculated subtracting the effects of the exterior forces to the general solution (superposition principle). In chapter 3, Duhamel's method is presented in detail in the context of Euler-Bernoulli beam element and FFM.

Initial deformations can be used to disguise the nonlinear character of nonlinear material problems, *i.e.* to replace their nonlinear governing equations by an iteratively solved series of linear equations. This corresponds to the substitution of the nonlinear material problem by a simpler linear elastic problem. However, the intrinsic nonlinear character of the former problem does obviously not vanish: even though it is not present in each iteration of the latter problem, it modifies its linear equations from one iteration to the next one.

The use of initial deformations in the analysis of nonlinear material problems results from the conjunction of:

(i) a linear solver capable of determining the structural response to an arbitrary initial deformations field;

(ii) an iterative procedure which updates the initial deformations field in every iteration.

This methodology is used by FFM for the quasi-static analysis of structures made of materials presenting nonlinear elastic constitutive laws.

This procedure is not restricted to nonlinear material problems; it can also be applied to other types of structural problems. In fact, the Method of Cut-Outs of Argyris (1960) (see also Argyris and Kelsey (1957)) and its variations, were probably the first to use initial deformations to model generic actions rather than thermal actions and, particularly, to model structural modifications in the reanalysis procedures of optimization, reliability and redesign problems.

This method appears in the context of matrix structural analysis, developed about the same time, see Argyris and Kelsey (1957)[1] – this method became the basis for several reanalysis methods, some of which are reviewed in § 2.8.

Some years later, Argyris (1965) created the Initial Strain Method, employing initial strains again, this time to model plasticity in structures and, later on, Zienkiewicz *et al.* (1969) presented the closely related Initial Stress Method. Together with Maier (1970 and 1972), these were the first authors to use initial strains with this purpose. Teixeira de Freitas (1990) presents the work of Argyris and Scharpf (1972) and Zienkiewicz *et al.* (1969) as the backbone for elastic-plastic methods of analysis which can be divided in two main categories: those employing iterative procedures and those based on the application of mathematical programming theory.

The relation between the Initial Strain Method and the Initial Stress Method was proven by Argyris and Scharpf (1972), who treated them as particular instances of the Initial Load Technique, which is the appropriate framework to model initial deformations and initial stresses in the context of the Finite Element Method (FEM). Argyris and Scharpf (1972) systematization of the initial stress and initial strain methods also clarifies their iterative nature: they result from the combination of the Initial Load Technique with numerical iterative procedures of the simplest kind – *e.g.* fixed point iteration methods, see Atkinson and Han (2001) and Pina (2010). Argyris and Scharpf (1972) presented also an exhaustive convergence study of both initial strain and stress methods, in the context of a specific 3D FEM problem. The next section presents these methods with some detail.

2.3. The Initial Stress and Initial Strain Methods

2.3.1. Initial Stress Method

As mentioned before, the Initial Stress Method was firstly proposed by Zienkiewicz *et al.* (1969), in the context of the Finite Element Analysis, as an iterative method to determine the elastic-plastic solution of general structural problems. Zienkiewicz *et al.* (1969) describe the application of the method to the calculation of the structural response to a given load

[1] See also Felippa (2001).

increment $\Delta\mathbf{F}$, supposing there are pre-existing states of stress or deformation. The method starts with the calculation, with a linear elastic analysis based on a constant stiffness matrix, of the increments of stress $\Delta\mathbf{R}_{\mathrm{L}}$ and strain $\Delta\boldsymbol{\eta}_{\mathrm{L}}$ occurring when the load increment $\Delta\mathbf{F}$ is applied to the structure. Thence, the linear solution ($\Delta\boldsymbol{\eta}_{\mathrm{L}}$,$\Delta\mathbf{R}_{\mathrm{L}}$) is the first estimative of the iterative procedure, *i.e.* $\Delta\boldsymbol{\eta}^{(1)} = \Delta\boldsymbol{\eta}_{\mathrm{L}}$ and $\Delta\mathbf{R}_{\mathrm{A}}^{(1)} = \Delta\mathbf{R}_{\mathrm{L}}$, where the subscript "A" in $\Delta\mathbf{R}_{\mathrm{A}}^{(i)}$ means that these stresses correspond to a constant stiffness, the so-called auxiliary stiffness. The true increment of stress $\Delta\mathbf{R}^{(1)}$ corresponding to $\Delta\boldsymbol{\eta}^{(1)}$ is also calculated using the effective nonlinear constitutive law.

A set of forces equilibrating the initial or fictitious stress $\Delta\mathbf{R}_{\mathrm{F}}^{(1)} = \Delta\mathbf{R}_{\mathrm{A}}^{(1)} - \Delta\mathbf{R}^{(1)}$ is then introduced. This defines the fictitious force system of the second iteration. Subsequently, with these fictitious forces, a new linear elastic analysis is performed with the same constant stiffness matrix, causing the additional strain increment $\Delta\boldsymbol{\eta}^{(2)}$ and the linear stress increment $\Delta\mathbf{R}_{\mathrm{A}}^{(2)}$. In each iteration, the value $\left\|\Delta\mathbf{R}_{\mathrm{F}}^{(i)}\right\|$ is calculated. The procedure is iteratively repeated until the difference between two successive values of $\left\|\Delta\mathbf{R}_{\mathrm{F}}^{(i)}\right\|$ gets smaller than the predefined numerical tolerance, $\left|\left\|\Delta\mathbf{R}_{\mathrm{F}}^{(i+1)}\right\| - \left\|\Delta\mathbf{R}_{\mathrm{F}}^{(i)}\right\|\right| < tol$. This concludes the analysis of the first load increment $\Delta\mathbf{F}$; the analysis is then repeated for each of the remaining load increments.

2.3.2. Initial Load Technique

Argyris and Scharpf (1972) established the Initial Load Technique, in the context of FEM, for the analysis of the structural response to the action of a generic field of initial strains or the corresponding initial stresses. If the vectors $\boldsymbol{\eta}_{\mathrm{I}}$ and $\mathbf{R}_{\mathrm{I}}$ correspond to the discrete representation of these fields of initial strains and stresses, respectively, they satisfy the following linear relationship

$$\mathbf{R}_{\mathrm{I}} = -\mathbf{K}_{\mathrm{A}}^{*}\,\boldsymbol{\eta}_{\mathrm{I}} \tag{2.1}$$

The global vectors $\boldsymbol{\eta}_{\mathrm{I}}$ and $\mathbf{R}_{\mathrm{I}}$ collect the elemental vectors containing the initial strains and stresses at given interpolation points; the initial strains and stresses at any other point of the structure can be calculated by interpolation. The matrix $\mathbf{K}_{\mathrm{A}}^{*}$ is block diagonal and collects the linear elastic stiffness matrices at the interpolation points. The displacement response to these actions is given by the solution of the finite element equation

$$\mathbf{F} = \mathbf{K}_{\mathrm{A}}\,\mathbf{d} + \mathbf{F}_{\mathrm{I}} \tag{2.2}$$

where $\mathbf{K}_A$ is the assembled stiffness matrix, $\mathbf{d}$ the displacement vector, $\mathbf{F}$ the effective force vector and $\mathbf{F}_I$ the initial force vector corresponding to the initial strains

$$\mathbf{F}_I = \mathbf{F}_{\eta_I}\left[\eta_I\right] \tag{2.3}$$

The effective strains η are compatible with the displacement vector $\mathbf{d}$, *i.e.*

$$\eta = \eta\left[\mathbf{d}\right] \tag{2.4}$$

and the elastic strains are given by

$$\eta_E \equiv \eta - \eta_I \tag{2.5}$$

and satisfy the linear constitutive relationship

$$\mathbf{R} = \mathbf{K}_A^* \, \eta_E \tag{2.6}$$

where $\mathbf{R}$ is the effective stress vector. Hence, substituting (2.5) and (2.1) into (2.6), gives,

$$\mathbf{R} = \mathbf{K}_A^* \, \eta + \mathbf{R}_I \tag{2.7}$$

It is possible, with these relations, to establish a linear matrix operator $\mathbf{T}_a$ which transforms the effective force vector $\mathbf{F}$ and the initial deformation vector η_I into the effective stress vector,

$$\mathbf{R} = \mathbf{T}_a\left[\mathbf{F}\,,\,\eta_I\right] \tag{2.8}$$

Similarly, it is possible to establish a linear matrix operator $\mathbf{T}_b$ which transforms the effective force vector $\mathbf{F}$ and the initial stresses $\mathbf{R}_I$ into the effective strains,

$$\eta = \mathbf{T}_b\left[\mathbf{F}\,,\,\mathbf{R}_I\right] \tag{2.9}$$

These two relations are used in the Initial Strain Method and Initial Stress Method, respectively.

2.3.2.1. Initial Strain Method

Within the general framework of the Initial Load Technique, Argyris and Scharpf (1972) presented the Initial Strain Method for the calculation of the response to a load increment $\Delta\mathbf{F}$ of a structure with an elastic-plastic constitutive relation satisfying Von-Mises yield criterion.

The solution to this problem is characterized by the global vectors of strain $\Delta\boldsymbol{\eta}$ and stress $\Delta\mathbf{R}$ increments.

Based on an auxiliary elastic stiffness $\mathbf{K}_{\mathrm{A}}^{*}$ corresponding to the initial tangent stiffness, Argyris and Scharpf (1972) additively decompose the effective increment of strain of the elastic-plastic problem $\Delta\boldsymbol{\eta}$ into an elastic component $\Delta\boldsymbol{\eta}_{\mathrm{E}}$ and a plastic component $\Delta\boldsymbol{\eta}_{\mathrm{P}}$, *i.e.*

$$\Delta\boldsymbol{\eta} \equiv \Delta\boldsymbol{\eta}_{\mathrm{E}} + \Delta\boldsymbol{\eta}_{\mathrm{P}} \tag{2.10}$$

Next, the authors assume that the effective stress increment $\Delta\mathbf{R}$ is known in advance, and write the plastic deformations $\Delta\boldsymbol{\eta}_{\mathrm{P}}$ in terms of the stresses in a constitutive relation of the type

$$\Delta\boldsymbol{\eta}_{\mathrm{P}} = \Delta\boldsymbol{\eta}_{\mathrm{P}}\left[\Delta\mathbf{R}\right] \tag{2.11}$$

where $\Delta\boldsymbol{\eta}_{\mathrm{P}}\left[\Delta\mathbf{R}\right]$ aggregates a collection of nonlinear constitutive relations defined for each interpolation point of the discretized continuum. Each of these relations depends on both the auxiliary elastic stiffness $\mathbf{K}_{\mathrm{A}}^{*}$, and the effective nonlinear constitutive relation.

The authors treat the plastic strain component $\Delta\boldsymbol{\eta}_{\mathrm{P}}$ as an initial deformation, in the framework of Initial Load Technique. Thence, substituting $\Delta\boldsymbol{\eta}_{\mathrm{P}}$ on the right-hand side of the incremental form of (2.8) and substituting the resulting expression on the right-hand side of (2.11) gives

$$\Delta\boldsymbol{\eta}_{\mathrm{P}} = \Delta\boldsymbol{\eta}_{\mathrm{P}}\left[\mathbf{T}_{\mathrm{a}}\left[\Delta\mathbf{F}\,,\,\Delta\boldsymbol{\eta}_{\mathrm{P}}\right]\right] \tag{2.12}$$

or

$$\Delta\boldsymbol{\eta}_{\mathrm{P}} = \mathbf{T}_{\eta\mathrm{p}}\left[\Delta\mathbf{F},\Delta\boldsymbol{\eta}_{\mathrm{P}}\right] \tag{2.13}$$

in which $\mathbf{T}_{\eta\mathrm{p}}$ is the nonlinear operator resulting from the composition of the linear operator $\mathbf{T}_{\mathrm{a}}$ defined in (2.8) with the nonlinear constitutive relations at the points of the discretised continuum gathered in (2.11). For a fixed vector $\Delta\mathbf{F}$, this operator $\mathbf{T}_{\eta\mathrm{p}}$ transforms the plastic deformation $\Delta\boldsymbol{\eta}_{\mathrm{P}}$ into itself. Thence, $\Delta\boldsymbol{\eta}_{\mathrm{P}}$ is a fixed point of $\mathbf{T}_{\eta\mathrm{p}}$ (Atkinson and Han, 2001). However, the presence of $\Delta\boldsymbol{\eta}_{\mathrm{P}}$ in both members of (2.12) and (2.13) is a direct consequence of the hypothesis, formulated by the authors, that the effective stress $\Delta\mathbf{R}$ is known in advance. Since, in general, this is not true, the expression (2.13) determines the following simple iteration procedure

$$\Delta\boldsymbol{\eta}_{\mathrm{P}}^{(i+1)} = \mathbf{T}_{\eta\mathrm{p}}\left[\Delta\mathbf{F},\Delta\boldsymbol{\eta}_{\mathrm{P}}^{(i)}\right] \tag{2.14}$$

This means that in a generic iteration the plastic deformations $\Delta\boldsymbol{\eta}_{\mathrm{P}}^{(i)}$, corresponding to the effective stresses $\Delta\mathbf{R}^{(i)}$, are considered to be initial strains applied to the structure. The matrix operator $\mathbf{T}_{\eta\mathrm{p}}$ in (2.14), based on the Initial Load Technique, then transforms $\Delta\boldsymbol{\eta}_{\mathrm{P}}^{(i)}$ into the next estimative $\Delta\boldsymbol{\eta}_{\mathrm{P}}^{(i+1)}$. This iterative procedure stops when the difference between the plastic deformations determined in successive iterations satisfies the convergence criterion.

2.3.2.2. Initial Stress Method revisited by Argyris and Scharpf

The Initial Stress Method is also revisited by Argyris and Scharpf (1972), as a particular case of the Initial Load Technique, when they investigate the elastic-plastic problem previously described. They start by establishing the incremental elastic-plastic constitutive relations

$$\Delta\mathbf{R} = \mathbf{K}^{*}\,\Delta\boldsymbol{\eta} \tag{2.15}$$

where $\mathbf{K}^{*}$ is a block diagonal matrix gathering the material elastic-plastic tangent stiffness matrices at the points of the discretized continuum. They next replace this constitutive equation by the affine relation (2.7), written now in the incremental form,

$$\Delta\mathbf{R} = \mathbf{K}_{\mathrm{A}}^{*}\,\Delta\boldsymbol{\eta} + \Delta\mathbf{R}_{\mathrm{I}} \tag{2.16}$$

This substitution is possible for the following initial stresses

$$\Delta\mathbf{R}_{\mathrm{I}} = -\left(\mathbf{K}_{\mathrm{A}}^{*} - \mathbf{K}^{*}\right)\Delta\boldsymbol{\eta} \tag{2.17}$$

This global relation gathers a collection of analogous relations defined at the points of the discretized continuum. This matrix relation is symbolically represented by

$$\Delta\mathbf{R}_{\mathrm{I}} = \Delta\mathbf{R}_{\mathrm{I}}\left[\Delta\boldsymbol{\eta}\right] \tag{2.18}$$

which is dual of (2.11). It is useful to admit, as Zienkiewicz *et al.* (1969) did, that the correct effective strain increment $\Delta\boldsymbol{\eta}$, and therefore $\Delta\mathbf{R}_{\mathrm{I}}$, are known in advance. Thence, substituting the incremental form of (2.9) on the right-hand side of (2.18), gives

$$\Delta\mathbf{R}_{\mathrm{I}} = \Delta\mathbf{R}_{\mathrm{I}}\left[\mathbf{T}_{\mathrm{b}}\left[\Delta\mathbf{F}\,,\,\Delta\mathbf{R}_{\mathrm{I}}\right]\right] \tag{2.19}$$

or

$$\Delta\mathbf{R}_{\mathrm{I}} = \mathbf{T}_{\mathrm{RI}}\left[\Delta\mathbf{F}, \Delta\mathbf{R}_{\mathrm{I}}\right] \tag{2.20}$$

where $\mathbf{T}_{\mathrm{RI}}$ is the nonlinear operator resulting from the composition of the linear operator $\mathbf{T}_{\mathrm{b}}$ defined in (2.9) with the nonlinear constitutive relations at the points of the discretised continuum gathered in (2.18). For a fixed force vector increment $\Delta\mathbf{F}$, the operator $\mathbf{T}_{\mathrm{RI}}$ transforms the initial stress $\Delta\mathbf{R}_{\mathrm{I}}$ into itself. Thence, $\Delta\mathbf{R}_{\mathrm{I}}$ is a fixed point of $\mathbf{T}_{\mathrm{RI}}$. Recall that the presence of $\Delta\mathbf{R}_{\mathrm{I}}$ in both members of (2.20) is a direct consequence of the hypothesis, formulated by Argyris and Scharpf (1972) and Zienkiewicz *et al.* (1969), that the effective strains $\Delta\boldsymbol{\eta}$ are known in advance. Since, in general, this is not true, the expression (2.20) determines the following simple iteration procedure

$$\Delta\mathbf{R}_{\mathrm{I}}^{(i+1)} = \mathbf{T}_{\mathrm{RI}}\left[\Delta\mathbf{F}, \Delta\mathbf{R}_{\mathrm{I}}^{(i)}\right] \tag{2.21}$$

This means that a generic iteration of the method consists in considering the initial stresses $\Delta\mathbf{R}_{\mathrm{I}}^{(i)}$, corresponding to the effective strains $\Delta\boldsymbol{\eta}^{(i)}$, that are transformed into the next estimative $\Delta\mathbf{R}_{\mathrm{I}}^{(i+1)}$ by the matrix operator $\mathbf{T}_{\mathrm{RI}}$ in (2.21). This iterative procedure stops when the difference between the initial stresses of successive iterations verifies the convergence criterion.

Finally, it is worth noting that the iterative procedure expressed by (2.21) can be used even if the effective problem to be solved is linear; in that case, the auxiliary stiffness matrix $\mathbf{K}_{\mathrm{A}}^{*}$ is different from the now also linear $\mathbf{K}^{*}$. A similar conclusion can be drawn for the Initial Strain Method. In that case, $\Delta\boldsymbol{\eta}_{\mathrm{P}}$ are no longer plastic deformations; instead, they are components of the decomposition $\Delta\boldsymbol{\eta} \equiv \Delta\boldsymbol{\eta}_{\mathrm{E}} + \Delta\boldsymbol{\eta}_{\mathrm{P}}$ determined by the auxiliary stiffness $\mathbf{K}_{\mathrm{A}}^{*}$ and, therefore, the relation $\Delta\boldsymbol{\eta}_{\mathrm{P}} = \Delta\boldsymbol{\eta}_{\mathrm{P}}\left[\Delta\mathbf{R}\right]$ becomes linear. It is this possibility that makes these methods suitable for reanalysis procedures.

Sometimes, the Initial Strain Method and Initial Stress Method are referred to as applications of the modified Newton-Rhapson method, because of the relation between these two general iterative methods.

2.3.2.3. Alternative iteration formulas for Initial Strain and Initial Stress Methods

The close relation between the Initial Strain Method and $\mathrm{FFM}_{\mathrm{Def}}$ and between the Initial Stress Method and $\mathrm{FFM}_{\mathrm{S}}$ is proven in chapter 3. Such relation is best understood if other iteration formulas, equivalent to (2.14) and (2.21), are considered.

In the context of the Initial Strain Method, let us consider again (2.8) and (2.11). Note that, apart from its iterative character, the iteration formula (2.14) results from substituting (2.8) into (2.11). If, alternatively, (2.11) is substituted into the incremental form of (2.8), one gets

$$\Delta\mathbf{R} = \mathbf{T}_{\mathrm{a}}\left[\Delta\mathbf{F}\,,\,\Delta\boldsymbol{\eta}_{\mathrm{P}}\left[\Delta\mathbf{R}\right]\right] \tag{2.22}$$

or

$$\Delta\mathbf{R} = \mathbf{T}_{\mathrm{R}}\left[\Delta\mathbf{F}\,,\,\Delta\mathbf{R}\right] \tag{2.23}$$

This equation can then be converted into the iterative form, giving

$$\Delta\mathbf{R}^{(i+1)} = \mathbf{T}_{\mathrm{R}}\left[\Delta\mathbf{F}\,,\,\Delta\mathbf{R}^{(i)}\right] \tag{2.24}$$

which is equivalent to (2.14) and related to FFM *by Stresses* presented in the next chapter.

In the context of the Initial Stress Method, let us consider again (2.9) and (2.18). Apart from its iterative character, the iteration formula (2.21) results from substituting (2.9) into (2.18). Once again, consider instead the substitution of (2.18) into the incremental form of (2.9)

$$\Delta\boldsymbol{\eta} = \mathbf{T}_{\mathrm{b}}\left[\Delta\mathbf{F}\,,\,\Delta\mathbf{R}_{\mathrm{I}}\left[\Delta\boldsymbol{\eta}\right]\right] \tag{2.25}$$

or

$$\Delta\boldsymbol{\eta} = \mathbf{T}_{\eta}\left[\Delta\mathbf{F}\,,\,\Delta\boldsymbol{\eta}\right] \tag{2.26}$$

This equation can then be converted into the iterative form, giving

$$\Delta\boldsymbol{\eta}^{(i+1)} = \mathbf{T}_{\eta}\left[\Delta\mathbf{F}\,,\,\Delta\boldsymbol{\eta}^{(i)}\right] \tag{2.27}$$

which is equivalent to (2.21) and is related to FFM *by Deformations* presented in the next chapter.

The operators $\mathbf{T}_{\mathrm{a}}$ and $\mathbf{T}_{\mathrm{b}}$ are related to the operators $G_{\mathrm{M}}^{\mathrm{I}}$ and G_{χ}^{I} introduced in § 3.2.5 in the context of the FFM.

Iteration formulas (2.14) and (2.21) (and therefore also (2.24) and (2.27)) correspond to the application of the Fixed Point Iteration Method which is described next.

2.4. The Fixed-Point Iteration Method

The Fixed Point Iteration Method[2] is now presented from the viewpoint of functional analysis (Atkinson and Han, 2001). Generically, the Fixed Point Iteration Method is used to solve nonlinear functional equations of the type

$$v = T\left[u\right] \tag{2.28}$$

where $T:\ K \to K$ stands for a nonlinear operator in a complete space K with a norm represented by $\left\|.\right\|$, see (Atkinson and Han, 2001). A fixed-point of T is an element of K which satisfies the expression

$$u = T\left[u\right] \tag{2.29}$$

The operator T is classified as Lipschitzian if

$$\left\|T\left[u\right]-T\left[v\right]\right\| \le L\left\|u-v\right\| \quad \forall u,v \in K,\ L \ge 0 \tag{2.30}$$

as non-expansive if $L = 1$ in the above expression, *i.e.*

$$\left\|T\left[u\right]-T\left[v\right]\right\| \le \left\|u-v\right\| \quad \forall u,v \in K \tag{2.31}$$

and as contractive if $0 \le L < 1$ in the above expression, *i.e.*

$$\left\|T\left[u\right]-T\left[v\right]\right\| \le \alpha\left\|u-v\right\| \quad \forall u,v \in K \quad \text{and} \quad \alpha \in \left[0,1\right[\tag{2.32}$$

where α is the contractivity constant. It can be concluded that a non-expansive operator is also Lipschitzian and a contractive operator is also non-expansive and, therefore, Lipschitzian.

Suppose that $T:\ K \to K$ is a nonlinear contractive operator. According to the Fixed Point Theorem (Atkinson and Han, 2001):

i) There is a unique fixed point $u = T\left[u\right]$ in K;

ii) Whatever the initial element $u^{(1)}$ of K, the sequence $\left\{u^{(i)}\right\}$ defined by

$$u^{(i+1)} = T\left[u^{(i)}\right] \tag{2.33}$$

converges to the fixed point u, *i.e.* $\left\|u^{(i+1)} - u\right\| \to 0$ when $i \to \infty$;

[2] Other designations are also used, such as the Principle of Contraction Mappings (Bailey *et al.*, 1968).

iii) The error of the *i*th iteration is limited by the following bound,

$$\left\|u^{(i)}-u\right\| \leq \alpha \left\|u^{(i-1)}-u\right\| \tag{2.34}$$

From this bound a second bound for that error can be immediately deduced using Schwarz inequality

$$\left\|u^{(i)}-u\right\| \leq \frac{\alpha}{1-\alpha}\left\|u^{(i-1)}-u^{(i)}\right\| \tag{2.35}$$

and from this one and the contractive operator condition (2.32) a third error bound is also easily established

$$\left\|u^{(i)}-u\right\| \leq \frac{\alpha^{i-1}}{1-\alpha}\left\|u^{(1)}-u^{(2)}\right\| \tag{2.36}$$

This theorem suggests a numerical method for solving nonlinear functional equations of the type (2.28), which is known by Fixed Point Iteration Method. The simplest application of the Fixed Point Iteration Method is to determine the solution of a nonlinear equation with domain $D_1 \subset \mathbb{R}$, which can be written as (Pina, 2010, Chapra and Canale, 2010)

$$f\left[x\right]=a, \quad a \in D_1 \tag{2.37}$$

This equation can be converted to the fixed-point equation format

$$x=t\left[x\right] \tag{2.38}$$

with

$$t\left[x\right]= f\left[x\right]+x-a \tag{2.39}$$

The application of the Fixed Point Iteration Method to solve (2.38) gives

$$x^{(i+1)}=t\left[x^{(i)}\right] \tag{2.40}$$

Let M be the maximum absolute value of the first derivative of $t\left[x\right]$ in the domain D_1, *i.e.*,

$$M=\max_{x \in D_1}\left|t'\left[x\right]\right| \tag{2.41}$$

Then, the iteration formula (2.40) converges if $M<1$. In this case, M is the contractivity constant α, *i.e.*,

$$\alpha = M=\max_{x \in D_1}\left|t'\left[x\right]\right|<1 \tag{2.42}$$

In this one-dimensional case, the convergence of the iterative procedure has a clear graphical representation, as illustrated by the example presented in § 3.3.

Another application of the Fixed Point Iteration Method is the calculation of the solution of a system of nonlinear equations of the type (Pina, 2010)

$$\mathbf{F}[\mathbf{x}] = \mathbf{a} \tag{2.43}$$

where $\mathbf{F}$: $D_n \to D_n$ with $D_n \subset \mathbb{R}^n$ is a map between elements of D_n, that can be written as

$$\begin{cases} f_1[x_1, x_2, ..., x_n] = a_1 \\ f_2[x_1, x_2, ..., x_n] = a_2 \\ \quad\vdots \\ f_n[x_1, x_2, ..., x_n] = a_n \end{cases} \tag{2.44}$$

where x_j and a_j are the components of $\mathbf{x}$ and $\mathbf{a}$. The system of equations (2.43) can be converted into the fixed-point system

$$\mathbf{x} = \mathbf{T}[\mathbf{x}] \tag{2.45}$$

with

$$\mathbf{T}[\mathbf{x}] = \mathbf{F}[\mathbf{x}] + \mathbf{x} - \mathbf{a} \tag{2.46}$$

The application of the Fixed Point Iteration Method to solve (2.45) gives

$$\mathbf{x}^{(i+1)} = \mathbf{T}\left[\mathbf{x}^{(i)}\right] \tag{2.47}$$

Let $\mathbf{J}[\mathbf{x}]$ be the Jacobian matrix of $\mathbf{T}[\mathbf{x}]$ and let S be the supreme norm of $\mathbf{J}[\mathbf{x}]$ in D_n, *i.e.*,

$$S = \sup_{\mathbf{x} \in D_n} \left\| \mathbf{J}[\mathbf{x}] \right\| \tag{2.48}$$

Then, the iteration formula (2.47) is convergent if $S < 1$. In this case, S is the contractivity constant α, *i.e.*,

$$\alpha = S = \sup_{\mathbf{x} \in D_n} \left\| \mathbf{J}[\mathbf{x}] \right\| < 1 \tag{2.49}$$

As demonstrated in chapter 3, the discrete descriptions of FFM are applications of the Fixed Point Iteration Method that satisfy conditions of this type.

2.5. Lin's nonlinear material method

This section presents a method proposed by Lin (1968) employing fictitious forces to perform a nonlinear material analysis of one dimensional beams, assuming Euler-Bernoulli kinematic hypothesis. The following exposition presents the fictitious force form adopted by this author and the related system of governing equations.

Lin analyses a built-in beam made of a material with a nonlinear constitutive stress-strain relation $\sigma[e]$, see Figure 2.1, which is subjected to a system of exterior forces. The constitutive relation has an initial linear branch, characterized by stiffness E_0, which is followed by a generic nonlinear branch, so that plastic strains e_{P} develop when the strain reaches this second branch[3]. The transition point between these two branches is defined by the proportionality limit stress σ_{lim} see Figure 2.1. To this non-holonomic elastic-plastic problem corresponds a similar holonomic nonlinear elastic problem if no load reversal is considered.

The solution to the beam problem is given by the effective nonlinear bending moment field $M[x]$, the effective curvature field $\chi[x]$ and the corresponding deflections field, where x is a coordinate along the beam longitudinal axis. Suppose that $M_{\mathrm{L}}[x]$ represents the bending moment field calculated with a linear elastic analysis using the initial elastic bending stiffness EI_0, determined by E_0 and by the cross-sectional geometry. The increment of the bending moment field $M_{\mathrm{incr}}[x]$ can now be defined as

$$M_{\mathrm{incr}}[x] = M[x] - M_{\mathrm{L}}[x] \tag{2.50}$$

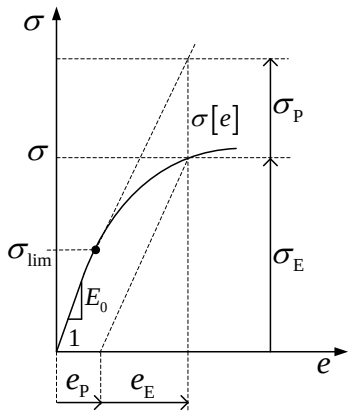

Figure 2.1. Lin's problem: nonlinear constitutive relation.

[3] The constitutive relation is symmetric with respect to the origin, which means that there are three branches, one linear and two nonlinear. But the generality of the exposition is not lost if one keeps imagining positive stresses and strains.

If the stress at all points of every cross section is below the proportionality limit stress σ_{lim}, the solution is linear elastic and $M_{\text{incr}}[x]=0$. For the general case, Lin determines the bending moment field $M_{\text{incr}}[x]$ by means of a physical model employing fictitious forces, described next, which corresponds to the application of Duhamel's method.

2.5.1. Lin's fictitious force system

Let us consider a generic segment of the beam with length Δx, see Figure 2.2a, and suppose that the fields of curvatures χ and bending moments M, caused by a system of forces, are approximated by seccionally constant fields with a constant value in this segment. Imagine that this segment is cut out of the original beam so that its bending moments are relieved. The segment then gets the deformed configuration corresponding to the plastic curvatures χ_{P}, see Figure 2.2b. The initial configuration of the beam will be restored if the restoring moments $\mathcal{M}_{\text{R}}$ corresponding to the bending moments $-M_{\text{P}}=-EI_0\,\chi_{\text{P}}$, represented in Figure 2.2c, are applied to the segment ends. The sign conventions are represented in Figure 2.3, for positive internal forces and positive applied point forces and moments at a generic cross section, and in Figure 2.4, for a positive curvature.

Suppose that the beam has been partitioned into several elements of length Δx all cut out as described before. In general, due to the residual plastic strains the deformed configurations of the cut out contiguous segments are not compatible with the hyperstatic beam boundary conditions. Compatibility is restored if each segment is straightened by means of the application of the restoring moments $\mathcal{M}_{\text{R}}$. The pairs of plastic moments M_{P}, and, therefore, the restoring moments $\mathcal{M}_{\text{R}}$, will generally have different values in adjacent segments. Hence, at the generic *j*th section, connecting two adjacent segments, the sum of their plastic moments defines the resultant restoring moment $\Delta\mathcal{M}_{\text{R},j}=\mathcal{M}_{\text{R},j}-\mathcal{M}_{\text{R},j\text{-}1}=-M_{\text{P},j}+M_{\text{P},j\text{-}1}$, see Figure 2.5 and Figure 2.6. At this stage, the conditions of Duhamel's method are established: the combined effect of the residual curvature χ_{P} and of a system of exterior forces, defined by the restoring moments $\Delta\mathcal{M}_{\text{R},j}$, corresponds to a known solution, which is determined by the initial configuration and the plastic bending moments -M_{P}.

Hence, Lin considers χ_{P} and -M_{P} as initial curvatures and initial bending moments, respectively, acting on the beam that is now considered to have the linear auxiliary constitutive relation determined by the auxiliary bending stiffness EI_0. A beam equal to the original beam except that the effective constitutive relation is replaced by the auxiliary constitutive relation will be

called auxiliary beam. The difference between this nonlinear material problem and the linear problem of Duhamel is that the initial curvatures and initial bending moments are unknowns

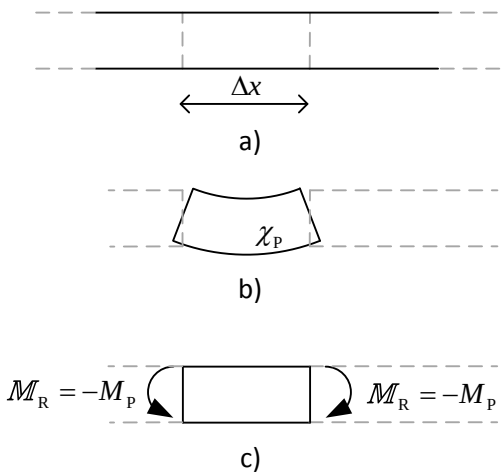

Figure 2.2. Lin's problem: residual plastic deformation and straightening of a beam segment.

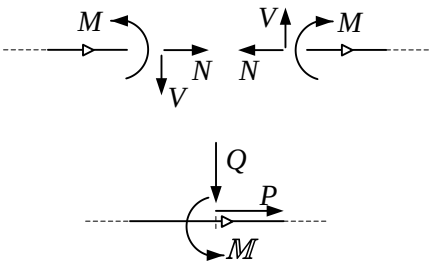

Figure 2.3. Sign conventions: positive internal forces and positive point forces and moments.

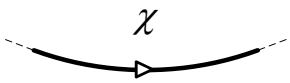

Figure 2.4. Sign convention: initially straight beam under positive curvature.

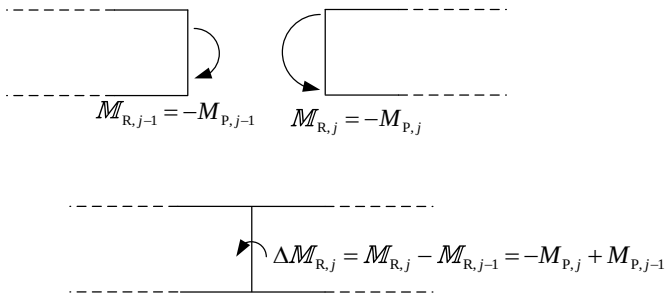

Figure 2.5. Lin's problem: restoring moments in two adjacent elements.

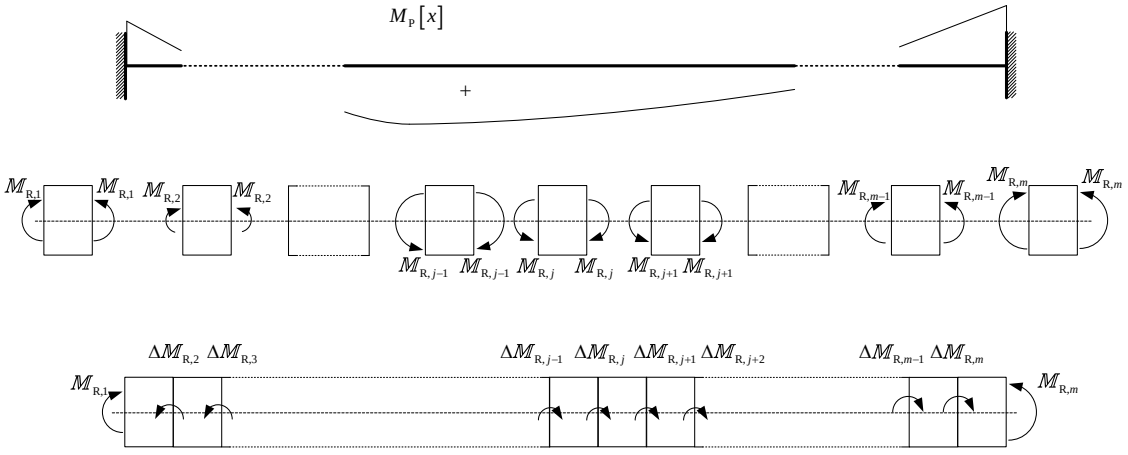

Figure 2.6. Lin's problem: elemental restoring moments and their resultant moments.

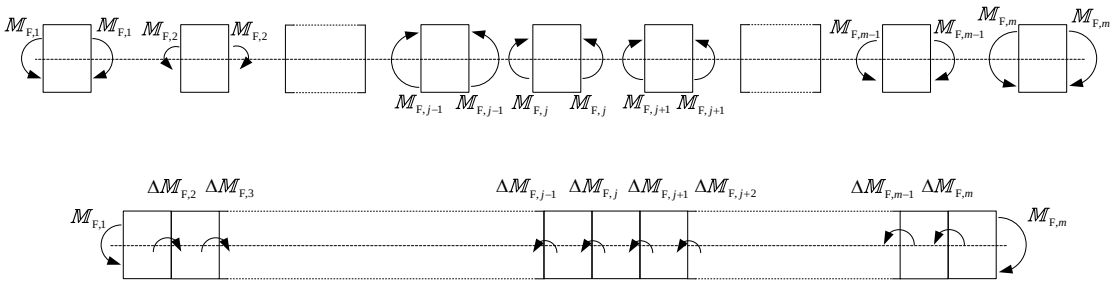

Figure 2.7. Lin's problem: system of fictitious moments.

of the problem in the former case, since they depend on the solution itself. This is the source of nonlinearity of the problem.

The effect of the residual curvatures χ_{P} can be calculated subtracting the linear elastic effect of the exterior forces to this solution. In the physical model of Lin, a system of fictitious forces formed by the fictitious moments $M_{\mathrm{F}} = -M_{\mathrm{R}}$, *i.e.* formed by moments symmetric to M_{R}, must be applied to the beam, as represented in Figure 2.7.Thence, the intuitive physical model proposed by Lin defines a fictitious "force" system which simulates the residual curvatures χ_{P} on the auxiliary beam.

The combination of this fictitious system of (generalized) forces with the effective force system, when applied to the auxiliary beam, corresponds to the auxiliary bending moment field $M_{\mathrm{A}}[x]$. The increment of the bending moments field corresponding solely to the fictitious system of moments is therefore

$$M_{\mathrm{A,incr}}[x] = M_{\mathrm{A}}[x] - M_{\mathrm{L}}[x] \tag{2.51}$$

which, when added to the plastic bending moment field $-M_{\mathrm{P}}[x]$, gives the effective increment of the bending moment field

$$M_{\mathrm{incr}}[x] = M_{\mathrm{A,incr}}[x] - M_{\mathrm{P}}[x] \tag{2.52}$$

In order to determine the bending moments $M_{\mathrm{A,incr}}[x]$ introduced by the fictitious force system, Lin uses the influence function $g[x,x']$ which gives the bending moment at section x caused by a unit moment applied at section x', *i.e.* $g[x,x']$ is the influence line of the bending moment at a fixed section x for a unit moment moving along the beam. Note that for the adopted sign conventions, represented in Figure 2.3,

$$g[x,x^{+}] = g[x,x^{-}] + 1 \tag{2.53}$$

where x^{-} and x^{+} are the sections just before and just after section x.

In the case of hyperstatic beams this function $g[x,x']$ depends on the bending stiffness distribution. Recall that the use of influence lines assumes that structural behaviour is linear, which is the case of the auxiliary beam.

The variation of the bending moment at section x caused by the fictitious moment $\Delta\mathcal{M}_{\mathrm{F}} = -\Delta M_{\mathrm{P}}$, see Figure 2.8, applied at section x', is given by

$$M_{\mathrm{A,incr}}[x] = g[x,x']\,\Delta\mathcal{M}_{\mathrm{F}} = -g[x,x']\,\Delta M_{\mathrm{P}}[x'] \tag{2.54}$$

If this moment has an elementary magnitude then

$$dM_{\mathrm{A,incr}}[x] = -g[x,x']\,dM_{\mathrm{P}}[x'] \tag{2.55}$$

or

$$dM_{\mathrm{A,incr}}[x] = -g[x,x']\frac{dM_{\mathrm{P}}[x']}{dx'}dx' \tag{2.56}$$

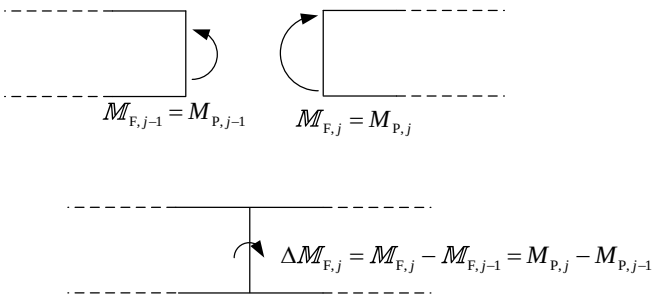

Figure 2.8. Lin's problem: fictitious moments in two adjacent elements.

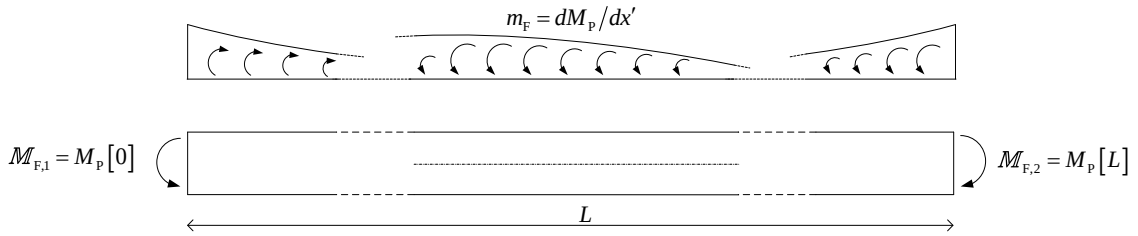

Figure 2.9. Lin's problem: differential description of the system of fictitious forces.

Hence, the field $M_{\mathrm{A,incr}}[x]$ is given by the integration of the differential increments $dM_{\mathrm{A,incr}}[x]$

$$M_{\mathrm{A,incr}}[x] = -\int_0^L g[x,x']\frac{dM_{\mathrm{P}}[x']}{dx'}dx' \tag{2.57}$$

The influence function $g[x,x']$ is in fact a Green's function of the governing differential equation of the beam problem (Veiskarami and Pourzeynali, 2012).

The derivative dM_{P}/dx' in the expression above is a distributed fictitious moment $m_{\mathrm{F}} = dM_{\mathrm{P}}/dx'$ which is obtained when the partition norm $\Delta x' \to 0$. Thence, a self-equilibrated fictitious force system is established by Lin, which is formed by this fictitious distributed moment and the two fictitious moments $\mathscr{M}_{\mathrm{F},1} = M_{\mathrm{P}}[0]$ and $\mathscr{M}_{\mathrm{F},2} = -M_{\mathrm{P}}[L]$ at the element end sections, see Figure 2.9.

2.5.2. Governing nonlinear integral equation

The fictitious force system of Lin leads to expression (2.57) that is now converted into the governing integral equation of the method. Assuming that M_{P} is continuous and integrating by parts the integral in this expression

$$\begin{aligned}
-\int_0^L g[x,x']\frac{dM_{\mathrm{P}}[x']}{dx'}dx' &= -\int_0^x g[x,x']\frac{dM_{\mathrm{P}}[x']}{dx'}dx' - \int_x^L g[x,x']\frac{dM_{\mathrm{P}}[x']}{dx'}dx' \\
&= -\Big[M_{\mathrm{P}}[x']\,g[x,x']\Big]_0^{x^-} + \int_0^x M_{\mathrm{P}}[x']\frac{\partial g[x,x']}{\partial x'}dx' \\
&\quad -\Big[M_{\mathrm{P}}[x']\,g[x,x']\Big]_{x^+}^{L} + \int_x^L M_{\mathrm{P}}[x']\frac{\partial g[x,x']}{\partial x'}dx' \\
&= -g[x,L]\,M_{\mathrm{P}}[L] + g[x,0]\,M_{\mathrm{P}}[0] + \Big(g[x,x^+] - g[x,x^-]\Big)M_{\mathrm{P}}[x] \\
&\quad + \int_0^x M_{\mathrm{P}}[x']\frac{\partial g[x,x']}{\partial x'}dx' + \int_x^L M_{\mathrm{P}}[x']\frac{\partial g[x,x']}{\partial x'}dx'
\end{aligned} \tag{2.58}$$

Substituting (2.53) into this expression and introducing the result in expression (2.57) gives

$$M_{\mathrm{A,incr}}[x] = M_{\mathrm{P}}[x] + \int_0^x M_{\mathrm{P}}[x'] \frac{\partial g[x,x']}{\partial x'} dx' + \int_x^L M_{\mathrm{P}}[x'] \frac{\partial g[x,x']}{\partial x'} dx' - g[x,L] M_{\mathrm{P}}[L] + g[x,0] M_{\mathrm{P}}[0] \tag{2.59}$$

Since the beam end sections are built-in[4], $g[x,0] = g[x,L] = 0$,

$$M_{\mathrm{A,incr}}[x] = M_{\mathrm{P}}[x] + \int_0^x M_{\mathrm{P}}[x'] \frac{\partial g[x,x']}{\partial x'} dx' + \int_x^L M_{\mathrm{P}}[x'] \frac{\partial g[x,x']}{\partial x'} dx' \tag{2.60}$$

Thence, the effective increments of bending moments (2.52) are given by

$$M_{\mathrm{incr}}[x] = \int_0^x M_{\mathrm{P}}[x'] \frac{\partial g[x,x']}{\partial x'} dx' + \int_x^L M_{\mathrm{P}}[x'] \frac{\partial g[x,x']}{\partial x'} dx' \tag{2.61}$$

and the nonlinear bending moments are given by, see (2.50),

$$M[x] = M_{\mathrm{L}}[x] + \int_0^x M_{\mathrm{P}}[x'] \frac{\partial g[x,x']}{\partial x'} dx' + \int_x^L M_{\mathrm{P}}[x'] \frac{\partial g[x,x']}{\partial x'} dx' \tag{2.62}$$

where the integral expression on the second member is nonlinear because the plastic bending moments $M_{\mathrm{P}}[x']$ depend on the effective bending moments $M[x]$.

2.6. The Imposed Deformations Method

Another method for the nonlinear material analysis of skeletal structures is the Imposed Deformations Method proposed by Aguado (1980) and Aguado *et al.* (1981). This method is an iterative nonlinear material analysis method that considers the nonlinear behaviour by means of initial deformations. The application of this method requires the previous computation of the nonlinear constitutive bending moment-curvature relations $\chi[M]$. Aguado and his co-authors used the method for the analysis of reinforced concrete beams, but the method can also be applied to general skeletal structures. The method was extended to model also geometrically nonlinear behaviour by means of initial deformations (Mari *et al.*, 1982). The method fulfils the requirements established in the framework of the General Method of CEB Buckling Manual (CEB,1974). Other authors, like Ferry Borges and Arantes e Oliveira (1964) and Macchi (1973), also developed related methodologies fulfilling these requirements.

[4] If any of them was free, the corresponding bending moment would be zero, therefore $M_{\mathrm{P}} = 0$, and the expression (2.60) would be obtained once more.

Actually, the Imposed Deformations Method can be seen as a direct extension of the Imposed Rotations Method of Macchi (1973), cited by Aguado (1980). The Imposed Deformations Method is also similar to the method proposed by Morisset (1976) for the nonlinear geometrical and material analysis of reinforced concrete beam-columns.

The Imposed Deformations Method considers an auxiliary linear constitutive relation between bending moment and curvature, see Figure 2.10, characterized by EI_0, the initial bending stiffness of the effective constitutive relation. With this auxiliary linear relation a first solution is determined, defined by the fields of bending moments $M^{(1)}$ and curvatures $\chi^{(1)}$; this is the initial guess of the iterative procedure.

With (i) this initial guess and (ii) the effective nonlinear constitutive relation $\chi\left[M\right]$, the initial curvature $\chi_{\mathrm{I}}^{(1)}$ is defined by, see Figure 2.10,

$$\chi_{\mathrm{I}}^{(1)} = \chi\left[M^{(1)}\right] - \chi^{(1)} \tag{2.63}$$

These initial curvatures, considered at specific cross sections, are then treated as initial deformations acting on the skeletal structure that is now considered to have the linear auxiliary constitutive relation determined by the bending stiffness EI_0, being therefore designated auxiliary skeletal structure. In isostatic structures the method ends here, since the initial curvature $\chi_{\mathrm{I}}^{(1)}$ produces a variation of the displacement field of the structure, and therefore of the curvature field, but does not change the bending moments $M^{(1)}$. In that case, these bending moments do not obviously depend on the bending stiffness EI_0. In the general case, to the initial curvatures $\chi_{\mathrm{I}}^{(1)}$ corresponds the variation of the bending moments $\Delta M^{(2)} = M^{(2)} - M^{(1)}$, *i.e.* to the initial deformations $\chi_{\mathrm{I}}^{(1)}$ corresponds a new solution characterized by the fields of curvatures $\chi^{(2)}$ and bending moments $M^{(2)}$. This new solution

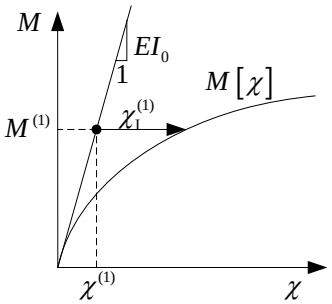

Figure 2.10. Imposed Deformations Method: Effective nonlinear and auxiliary linear constitutive relations and initial curvature.

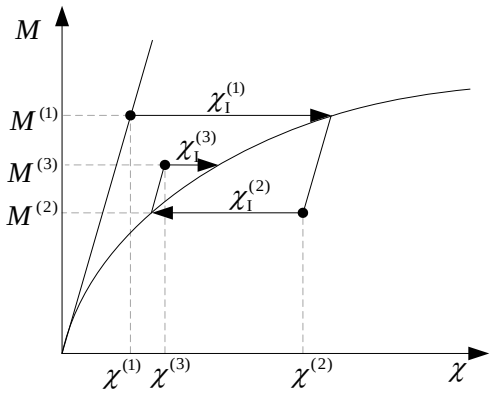

Figure 2.11. Imposed Deformations Method: schematic representation of iterative procedure.

satisfies equilibrium and compatibility but not the nonlinear constitutive relation. Based on this new solution a new initial curvature $\chi_{\mathrm{I}}^{(2)}$ is defined by

$$\chi_{\mathrm{I}}^{(2)} = \chi\left[M^{(2)}\right] - \chi^{(2)} \tag{2.64}$$

This initial curvature is treated again as an initial deformation acting on the auxiliary skeletal structure, to which corresponds the new solution $\left(M^{(3)}, \chi^{(3)}\right)$. The iterative procedure proceeds as described above and, in the generic *i*th iteration, the initial curvature is given by

$$\chi_{\mathrm{I}}^{(i)} = \chi\left[M^{(i)}\right] - \chi^{(i)} \tag{2.65}$$

to which corresponds the next solution $\left(M^{(i+1)}, \chi^{(i+1)}\right)$, see Figure 2.11.

The iterative procedure ends when the solution converges, *i.e.* the norm of the initial curvatures becomes less than the specified tolerance. An equivalent criterion may be established for the variation of bending moments

$$\Delta M^{(i)} = M^{(i)} - M^{(i-1)} \tag{2.66}$$

which is the one apparently chosen by Aguado. Whatever the used convergence criterion, it must indicate that, at a generic section, the convergent solution $\left(M^{(j)}, \chi^{(j)}\right)$ is close enough to the effective nonlinear constitutive relation. In other words, this solution satisfies the constitutive relation within a specified tolerance.

To sum up, starting from a given initial guess, the Imposed Deformations Method proceeds by iterations. Supposing that the *i*th approximation $\left(M^{(i)}, \chi^{(i)}\right)$ was already calculated, the next iteration consists of two basic steps:

(i) Evaluate, at all cross sections, the initial deformations determined by the auxiliary linear and effective nonlinear constitutive relations;

(ii) Determine the linear structural response to these initial deformations.

Aguado (1980) proposes a methodology to determine the structural response referred to in item (ii) above. Generically speaking, influence lines can be used as an operator to determine the structural response. This operator is mathematically represented by the function $g_{\mathrm{I}}[x,x']$ which gives the bending moment at section x caused by a unit relative rotational deformation at section x', see Figure 2.12. Thence, when a relative rotational deformation ϕ_{I} is applied at section x', the bending moment at section x is given by

$$M[x]=\phi_{\mathrm{I}}\, g_{\mathrm{I}}[x,x'] \tag{2.67}$$

In the case of a beam of length L, the bending moment variation (2.66) at a specific section x in the ith iteration, is given by

$$\Delta M^{(i)}[x]=M^{(i)}[x]-M^{(i-1)}[x]=\int_0^L g_{\mathrm{I}}[x,x']\,\chi_{\mathrm{I}}^{(i-1)}[x']dx' \tag{2.68}$$

because $\chi_{\mathrm{I}}=d\phi_{\mathrm{I}}/dx$. If the constitutive relation $M[\chi]$ has an initial branch with bending stiffness EI_0, as represented in Figure 2.13, expression (2.68) is replaced by

$$\Delta M^{(i)}[x]=\sum_{j=1}^{n}\int_{x_{j,1}}^{x_{j,2}} g_{\mathrm{I}}[x,x']\,\chi_{\mathrm{I}}^{(i-1)}[x']dx' \tag{2.69}$$

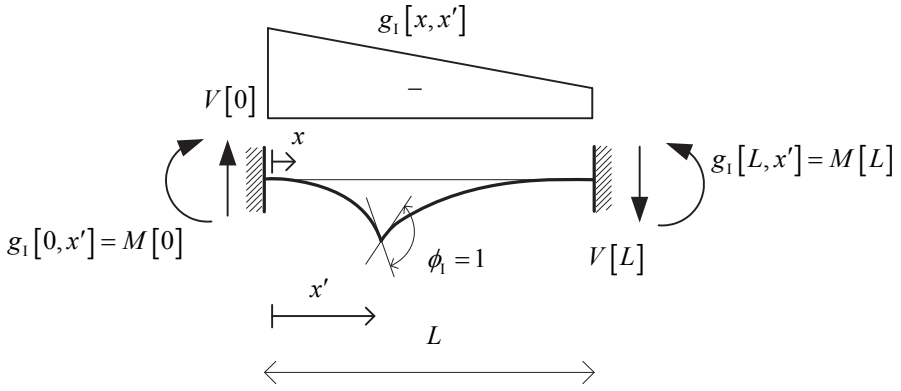

Figure 2.12. Imposed Deformations Method: relative rotational deformation applied to beam element.

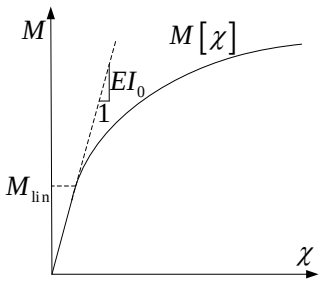

Figure 2.13. Imposed Deformations Method: effective nonlinear and auxiliary linear constitutive relations.

where *n* is the number of beam segments where the bending moment exceeds $M_{\lim}$ and $x_{j,1}$ and $x_{j,2}$ are the abscissas of the left and right end sections of each segment. Thence, according to the initial curvature definition (2.65),

$$\Delta M^{(i)}[x] = \sum_{j=1}^{n} \int_{x_{j,1}}^{x_{j,2}} g_{\mathrm{I}}[x,x'] \left(\chi\left[M^{(i-1)}[x'] \right] - \chi^{(i-1)}[x'] \right) dx' \tag{2.70}$$

The integrand on the right-hand side is nonlinear because the constitutive relation $\chi[M]$ is nonlinear. Even though Aguado (1980) does not present expressions (2.68) to (2.70) in this particular format, they are implicit in his description.

Aguado (1980) presents strategies for the automatic analysis of general skeletal structures by the Imposed Deformations Method. For the generic element represented in Figure 2.12, the internal forces due to a relative rotational deformation ϕ_{I} at cross section x' are given by

$$M[x\,,x'] = \left(1 - \frac{x}{L}\right) M_1[x'] + \frac{x}{L} M_2[x'] \tag{2.71}$$

$$V[x'] = \frac{-M_1[x'] + M_2[x']}{L} \tag{2.72}$$

where

$$M_1[x'] = M[0] = -\frac{2EI_0}{L^2} \phi_{\mathrm{I}} (2L - 3x') \tag{2.73}$$

$$M_2[x'] = M[L] = -\frac{2EI_0}{L^2} \phi_{\mathrm{I}} (3x' - L) \tag{2.74}$$

The initial deformations along the beam have to be integrated by an expression similar to (2.68). In order to get acceptable results, Aguado integrates these deformations in a simplified

way, subdividing each beam or column into three equal length beam elements (of the type represented in Figure 2.12).

Aguado (1980) also proposed an improvement of the method described above where the iterative procedure is accelerated by means of suitable guesses of the final solution.

2.7. The Equivalent Systems Method

The Equivalent Systems Method of Fertis *et al.* (1990, 1991, 2006) is a method particularly appropriate for the analysis of beams and beam-columns. The method deals with very distinct structural problems, but it seems to be particularly useful for the analysis of geometrically nonlinear problems and non-prismatic elements such as tapered elements. This method can also be used for the analysis of nonlinear material problems under certain particular circumstances. The basic idea of the method is to rewrite the structural equations for a given effective problem into a simpler form, corresponding to an auxiliary problem defined by (i) a regular geometry, in case the original problem had some irregularity, and/or (ii) a linear constitutive relation, in case the original problem is nonlinear elastic. This transformation is made possible by an auxiliary force system reflecting the difference between the original problem and the auxiliary problem. Probably, the best way to present the fundamental concepts of the method, and particularly its equivalent force system, is by considering its application to the analysis of a tapered beam (Fertis, 2006).

2.7.1. Equivalent force system

The analysis of a slender tapered cantilever beam by the Equivalent Systems Method considers an auxiliary problem defined by (i) an auxiliary prismatic cantilever beam with constant auxiliary bending stiffness EI_{A} and (ii) an equivalent force system, such that the curvature and the deflection fields of the effective (tapered) and auxiliary (prismatic) problems coincide.

Consider the tapered cantilever beam and loading represented in Figure 2.14. According to Euler-Bernoulli beam theory,

$$M[x] = E[x]\, I_y[x]\, \chi[x] \tag{2.75}$$

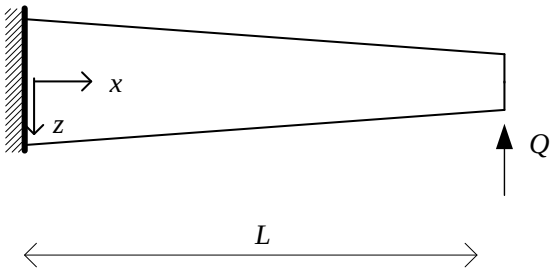

Figure 2.14. Equivalent Systems Method: Slender tapered cantilever beam.

where $E[x]$ is a function giving the modulus of elasticity at each cross section, $I_y[x]$ is the second moment of area and $\chi[x]$ is the curvature field of this element.

Suppose that the distributions $E[x]$ and $I_y[x]$ are defined by

$$E[x] = E_{\mathrm{A}}\ f[x] \tag{2.76}$$

$$I_y[x] = I_{y,\mathrm{A}}\ g[x] \tag{2.77}$$

where E_{A} and $I_{y,\mathrm{A}}$ are arbitrary constant values of the modulus of elasticity and second moment of area and $f[x]$ and $g[x]$ are dimensionless functions of the axial *x*-coordinate along the beam. The substitution of these expressions into (2.75) gives a constitutive relation similar to that of a prismatic element

$$M_{\mathrm{A}}[x] = EI_{\mathrm{A}}\ \chi[x] \tag{2.78}$$

where $M_{\mathrm{A}}[x]$ is an equivalent or auxiliary bending moment field given by

$$M_{\mathrm{A}}[x] \equiv \frac{M[x]}{f[x]\,g[x]} \tag{2.79}$$

and $EI_{\mathrm{A}} \equiv E_{\mathrm{A}}\ I_{y,\mathrm{A}}$. This equivalent bending moment field is in equilibrium with the equivalent shear forces field

$$V_{\mathrm{A}}[x] = \frac{dM_{\mathrm{A}}[x]}{dx} \tag{2.80}$$

and the equivalent distributed transverse force

$$q_{\mathrm{A}}[x] = -\frac{dV_{\mathrm{A}}[x]}{dx} \tag{2.81}$$

as illustrated in Figure 2.15a.

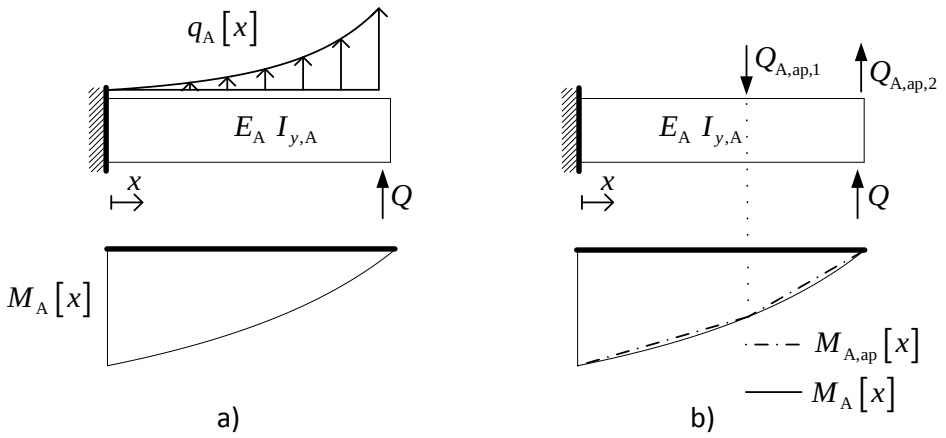

Figure 2.15. Equivalent Systems Method: Equivalent force system: a) exact; b) approximated.

Even though this it is not mentioned by Fertis, sometimes the equivalent force system must also include point loads in order to guarantee equilibrium with the equivalent internal forces.

In order to simplify this equivalent force system, Fertis (2006) proposes the substitution of the exact equivalent bending moment field $M_A[x]$ by an approximated piecewise linear field $M_{A,ap}[x]$, like the one represented in Figure 2.15b. In this case, the equivalent force system is formed by transverse point loads located at the discontinuity sections of the derivative of $M_{A,ap}[x]$, see Figure 2.15b.

2.7.2. Nonlinear material analysis

The Equivalent Systems Method can be applied to the analysis of nonlinear material problems under certain circumstances. Fertis (2006) applies his method to statically determined beams by means of the auxiliary system of forces briefly illustrated in the previous section and a reduced modulus of elasticity E_r (Timoshenko 1976), as described in what follows.

Let us consider again the symmetric tapered cantilever beam represented in Figure 2.14 with a rectangular cross section with constant breadth b and variable depth $h[x]$ and suppose that its longitudinal fibres satisfy a symmetric nonlinear stress-strain constitutive relation, $\sigma[e]$, such as the one represented in Figure 2.16. At each cross section, the bending moment is given by

$$M = b \int_{-h/2}^{h/2} \sigma\, z\, dz \tag{2.82}$$

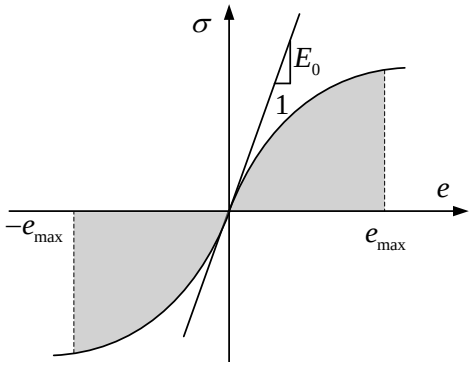

Figure 2.16. Equivalent Systems Method: symmetric nonlinear constitutive relation.

But, according to Euler-Bernoulli hypothesis,

$$z = \frac{e}{\chi} \tag{2.83}$$

and therefore

$$\chi = 2\frac{e_{\max}}{h} \tag{2.84}$$

where $e_{\max}$ is the maximum axial strain, at the top and bottom fibres of the cross section, see Figure 2.16. Hence, changing the integration variable in expression (2.82) according to (2.83), gives

$$M = \frac{b}{\chi^2}\int_{-e_{\max}}^{e_{\max}} \sigma\, e\, de \tag{2.85}$$

Defining the reduced modulus of elasticity (Timoshenko 1976)

$$E_{\mathrm{r}} \equiv \frac{12}{\chi^3 h^3}\int_{-e_{\max}}^{e_{\max}} \sigma\, e\, de \tag{2.86}$$

and substituting this definition in (2.85), gives

$$M = E_{\mathrm{r}}\, I_y\, \chi \tag{2.87}$$

which is a particularization of (2.75) for a specific cross section.

Introducing (2.84) into (2.86) gives

$$E_{\mathrm{r}} = \frac{3}{2e_{\max}^3}\int_{-e_{\max}}^{e_{\max}} \sigma\, e\, de \tag{2.88}$$

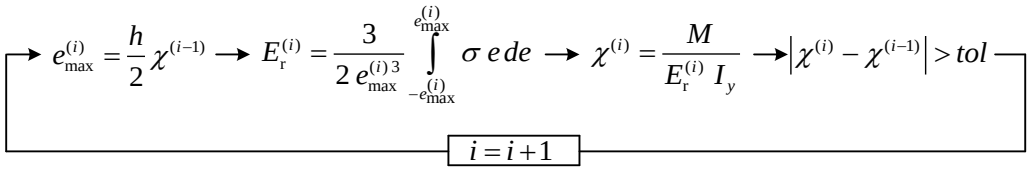

Figure 2.17. Equivalent Systems Method: trial-and-error iterative procedure for the determination of $E_{\mathrm{r}}[x]$.

Therefore, for a given constitutive relation, the value of E_{r} at each cross section depends solely on the maximum strain $e_{\max}$ at the top and bottom fibres, which are unknown. This strain changes from one cross section to another and so does E_{r}, corresponding to the fields $e_{\max}[x]$ and $E_{\mathrm{r}}[x]$. For this particular problem $e_{\max}[x]$ depends solely on the curvature field $\chi[x]$. These fields can be determined in a discrete manner, *i.e.* the functions $e_{\max}[x]$, $\chi[x]$ and $E_{\mathrm{r}}[x]$ can be determined at a fixed set of cross sections, by means of the trial-and-error iterative procedure schematized in Figure 2.17. This procedure determines the deformation corresponding to the bending moment produced by the external loads and determined solely by the equilibrium relations.

This iterative procedure is therefore equivalent to determining the nonlinear bending moment-curvature constitutive relation of the beam cross sections. If there was also an axial force, the iterative procedure would have to include the search for both the curvature and the axial strain at the beam axis (or the axial strain at top and bottom fibres).

Once $E_{\mathrm{r}}[x]$ has been determined, a reference value can be chosen for E_{A}, for instance the maximum value of $E_{\mathrm{r}}[x]$, to determine the function $f[x]$ in (2.76). The equivalent force system established in the previous section can now be calculated and the deformed configuration of the beam determined.

2.8. Reanalysis methods employing fictitious forces

Several reanalysis methods, used for instance in optimization, reliability and redesign analysis, are also suitable for the analysis of nonlinear material problems. The relation between these two families of methods is patent in the relation between the method of cut-outs of Argyris (1956) and the Initial Stress and Initial Strain Methods of Zienkiewicz *et al.* (1969) and Argyris and Scharpf (1972). Like other methods, these reanalysis methods are based on the repeated solution of a simple linear problem, which makes them very versatile.

Kolakowski *et al.* (2008) present an exhaustive review of these reanalysis methods, in a paper dedicated to the Virtual Distortion Method of Holnicki-Szulc (1989,1991). The versatility of the Virtual Distortion Method reflects itself in its application to different structural problems, see Kolakowski *et al.* (2008), from static analysis to dynamic analysis, and even to some non-structural problems, due to the analogy between structural mechanical analysis and network analysis first observed by Cross (1936).

Makode *et al.* (1996, 1999a) presented the so-called Pseudo Distortion Method, which is an application of the Virtual Distortion Method to the analysis of skeletal structures. The Virtual Distortion Method and the Pseudo Distortion Method are also used for nonlinear material analysis. Moreover, Makode *et al.* (1999b) also use the Pseudo Distortion Method for the geometrically nonlinear analysis of skeletal structures.

Akgun *et al.* (2001) proved the equivalence between the Virtual Distortion Method and the general Sherman-Morrison-Woodbury formulas (Sherman and Morrison 1949 and Woodbury 1950) used by Deng and Ghosn (2001) in the Pseudo Force Method, which is another reanalysis method employing fictitious forces that can be used for nonlinear material analysis. In the next two sub-sections we describe the general framework of these two methods and, in particular, the linear solver used for both reanalysis and nonlinear material problems.

2.8.1. The Virtual Distortion Method and the Pseudo Distortion Method

The starting point of the Virtual Distortion Method and the related Pseudo Distortion Method is the modification of the original structure to be analysed establishing the so-called modified structure. Subsequently, these methods proceed with the determination of the structural response of the modified structure. Eventually, this solution to the modified structure is used to establish the solution to the original problem. Note that the problem of analysing a tapered beam with the Method of Equivalent Systems follows this kind of methodology. Actually, the Virtual Distortion Method operates directly with the original structure: it considers virtual distortions, whose magnitude is not known in advance, acting on the original structure and producing deformations equal to those occurring in the modified structure. The deformed configuration of the original structure caused by the virtual distortions is referred to as the distorted structure.

The Pseudo Distortion Method is an application of the Virtual Distortion Method to skeletal structures, where the pseudo-distortions are applied at the ends of each member. These pseudo-distortions can be relative rotations or relative transverse displacements. The term "distortion" is due to Nowacki (1970) and was adopted by Holnicki-Szulc (1989,1991): in our opinion, it is not a very logical designation, since it is by no means related to distortional deformations. Note also that the virtual and pseudo distortions are in fact initial strains as recognized by Kolakowski *et al.* (2008). The determination of the effects of these virtual and pseudo distortions clearly corresponds to an application of Duhamel´s method. Be aware that none of the two above methods employs fictitious forces in modelling those initial strains.

Makode *et al.* (1999a) summarize the procedure for determining the effects of unit pseudo-distortions in the following four steps:

(i) Impose a unit pseudo-rotation $\phi_{1,i} = 1$ at the end i of member m and compute the corresponding fixed-end moments and shear forces in the member;

(ii) Apply these fixed-end forces but with opposite direction to member m;

(iii) Apply to the structure nodal forces with the magnitude and direction of those fixed end forces. Calculate the nodal displacements.

(iv) Superimpose the results of steps (ii) and (iii) to obtain the actual displacements and member forces experienced by the skeletal structure.

These four steps clearly reflect an application of Duhamel's method for unit initial deformations of this type.

The application of the Pseudo Distortion or Virtual Distortion Methods in the context of nonlinear material problems is only possible if the plastic deformations are assumed to occur at specified sections, corresponding to the end sections of the elements, *i.e.* these methods adopt the plastic hinge approach (Chen and Powell (1982, 1986)). The plastic deformations at each hinge are considered as nonlinear pseudo-distortions. Moreover, the external loads are applied incrementally, which means that hinges show up and yield progressively.

The advantage of the Pseudo Distortion and Virtual Distortion Methods is that they avoid the recalculation the stiffness matrix every time a new plastic hinge shows up. Instead, the effect of the plastic deformations is modelled by means of pseudo-distortions.

2.8.2. The Pseudo Force Method

Like the Pseudo Distortion Method, the Pseudo Force Method (Deng and Ghosn, 2001) considers an auxiliary structure which results from the modification of the original structure. The finite element stiffness equations of the original and modified structures are, respectively,

$$\mathbf{K}\,\mathbf{d} = \mathbf{F} \tag{2.89}$$

$$\bar{\mathbf{K}}\,\bar{\mathbf{d}} = \mathbf{F} \tag{2.90}$$

where $\mathbf{F}$ is the effective force vector, $\mathbf{K}$ and $\mathbf{d}$ are the stiffness matrix and the displacement vector of the original structure, and $\bar{\mathbf{K}}$ and $\bar{\mathbf{d}}$ are the stiffness matrix and the displacement vector of the modified structure (a symbol with a bar on top refers to the modified structure).

Like the Pseudo Distortion Method, the Pseudo Force Method avoids the direct analysis of the modified structure. Instead, the structure modifications are considered by means of a fictitious force system, the so-called pseudo-load system (Deng and Ghosn 2001). Instead of solving (2.90), the displacement $\bar{\mathbf{d}}$ is determined from

$$\mathbf{K}\,\bar{\mathbf{d}} = \left(\mathbf{F} - \mathbf{F}_{\mathrm{F}}\right) \tag{2.91}$$

where $\mathbf{F}_{\mathrm{F}}$ is a fictitious or pseudo-force vector which allows to operate with $\mathbf{K}$ instead of $\bar{\mathbf{K}}$. In fact, this force vector is directly derived from the additive decomposition of the modified stiffness matrix,

$$\bar{\mathbf{K}} = \mathbf{K} + \Delta\mathbf{K} \tag{2.92}$$

Substituting this decomposition into (2.90) gives

$$\left(\mathbf{K} + \Delta\mathbf{K}\right)\bar{\mathbf{d}} = \mathbf{F} \tag{2.93}$$

Supposing that the stiffness matrix $\mathbf{K}$ has dimension n and that $\Delta\mathbf{K}$ has d^2 nonzero entries, then this $\Delta\mathbf{K}$ matrix can be decomposed as

$$\Delta\mathbf{K} = \mathbf{U}\,\mathbf{V} = \mathbf{U}\,\mathbf{W}\,\mathbf{U}^{\mathrm{T}} \tag{2.94}$$

where $\mathbf{V} = \mathbf{W}\,\mathbf{U}^{\mathrm{T}}$, $\mathbf{W}$ is a symmetric square "compressed" stiffness matrix, with dimension d, containing the nonzero entries of $\Delta\mathbf{K}$ and $\mathbf{U}$ is a $n \times d$ boolean matrix. For example, if

$$\mathbf{\Delta K} = \begin{bmatrix} \Delta k_{11} & 0 & 0 & 0 & \Delta k_{15} & 0 & 0 & 0 \\ 0 & 0 & 0 & 0 & 0 & 0 & 0 & 0 \\ 0 & 0 & 0 & 0 & 0 & 0 & 0 & 0 \\ 0 & 0 & 0 & 0 & 0 & 0 & 0 & 0 \\ \Delta k_{51} & 0 & 0 & 0 & \Delta k_{55} & 0 & 0 & 0 \\ 0 & 0 & 0 & 0 & 0 & 0 & 0 & 0 \\ 0 & 0 & 0 & 0 & 0 & 0 & 0 & 0 \\ 0 & 0 & 0 & 0 & 0 & 0 & 0 & 0 \end{bmatrix} \tag{2.95}$$

then $\mathbf{\Delta K}$ can be decomposed according to (2.94) with

$$\mathbf{U}^{\mathrm{T}} = \begin{bmatrix} 1 & 0 & 0 & 0 & 0 & 0 & 0 & 0 \\ 0 & 0 & 0 & 0 & 1 & 0 & 0 & 0 \end{bmatrix} \tag{2.96}$$

$$\mathbf{W} = \begin{bmatrix} \Delta k_{11} & \Delta k_{15} \\ \Delta k_{51} & \Delta k_{55} \end{bmatrix} \tag{2.97}$$

Substituting the decomposition (2.94) into equation (2.93) gives

$$\left(\mathbf{K} + \mathbf{U}\,\mathbf{W}\,\mathbf{U}^{\mathrm{T}}\right)\bar{\mathbf{d}} = \mathbf{F} \tag{2.98}$$

Next, Sherman-Morrison-Woodbury formula (Sherman and Morrison 1949, Woodbury 1950, Golub and Van Loan 1996), can be used to invert the stiffness matrix in the left-hand member, giving

$$\left(\mathbf{K} + \mathbf{U}\,\mathbf{W}\,\mathbf{U}^{\mathrm{T}}\right)^{-1} = \mathbf{K}^{-1}\left(\mathbf{I} - \mathbf{U}\left(\mathbf{I} + \mathbf{U}\,\mathbf{W}^{\mathrm{T}}\,\mathbf{K}^{-1}\,\mathbf{U}\right)^{-1}\mathbf{U}\,\mathbf{W}^{\mathrm{T}}\,\mathbf{K}^{-1}\right) \tag{2.99}$$

Substituting this inverse matrix into equation (2.93) gives

$$\bar{\mathbf{d}} = \mathbf{K}^{-1}\left(\mathbf{F} - \mathbf{U}\left(\mathbf{I} + \mathbf{U}\,\mathbf{W}^{\mathrm{T}}\,\mathbf{K}^{-1}\,\mathbf{U}\right)^{-1}\mathbf{U}\,\mathbf{W}^{\mathrm{T}}\,\mathbf{K}^{-1}\,\mathbf{F}\right) \tag{2.100}$$

Comparing this equation with (2.91) it can be concluded that the pseudo-force vector is given by

$$\mathbf{F}_{\mathrm{P}} = \mathbf{U}\left(\mathbf{I} + \mathbf{U}\,\mathbf{W}^{\mathrm{T}}\,\mathbf{K}^{-1}\,\mathbf{U}\right)^{-1}\mathbf{U}\,\mathbf{W}^{\mathrm{T}}\,\mathbf{K}^{-1}\,\mathbf{F} \tag{2.101}$$

or, introducing the finite element equation (2.89),

$$\mathbf{F}_{\mathrm{P}} = \mathbf{U}\left(\mathbf{I} + \mathbf{U}\,\mathbf{W}^{\mathrm{T}}\,\mathbf{K}^{-1}\,\mathbf{U}\right)^{-1}\mathbf{U}\,\mathbf{W}^{\mathrm{T}}\,\mathbf{d} \tag{2.102}$$

Comparing this expression with the decomposition (2.94), we see that the boolean matrix $\mathbf{U}$ can also be used to decompose the pseudo-force vector according to

$$\mathbf{F}_{\mathrm{P}} = \mathbf{U}\mathbf{R}_{\mathrm{P}} \tag{2.103}$$

where

$$\mathbf{R}_{\mathrm{P}} = \left(\mathbf{I} + \mathbf{U}\mathbf{W}^{\mathrm{T}}\mathbf{K}^{-1}\mathbf{U}\right)^{-1}\mathbf{U}\mathbf{W}^{\mathrm{T}}\mathbf{d} \tag{2.104}$$

is the rank d vector containing the local pseudo-forces acting on the modified members, corresponding to the degrees of freedom identified by $\mathbf{U}$. Using this vector and equation (2.89) the nodal displacements (2.100) can be written as

$$\bar{\mathbf{d}} = \mathbf{d} - \mathbf{K}^{-1}\mathbf{U}\mathbf{R}_{\mathrm{P}} = \mathbf{d} - \mathbf{Z}\mathbf{R}_{\mathrm{P}} \tag{2.105}$$

where

$$\mathbf{Z} = \mathbf{K}^{-1}\mathbf{U} \tag{2.106}$$

is the influence matrix which gives the response of the original structure to virtual unit loads placed at the degrees of freedom identified by $\mathbf{U}$.

Hence, the reanalysis procedure expressed by equation (2.105) is analogous to the Virtual Distortion Method, because the variation of the structural response caused by the modification of the structure is evaluated by means of an influence matrix corresponding to unit actions, which are in fact virtual distortions or pseudo-forces. Deng and Ghosn (2001) apply this framework to the incremental iterative nonlinear material analysis of structures, but the details of such application are omitted in this brief description.

Note that the original stiffness $\mathbf{K}$ of Deng and Ghosn (2001) is similar to the auxiliary stiffness of Fertis (2006). Moreover, the stiffness decomposition $\bar{\mathbf{K}} = \mathbf{K} + \Delta\mathbf{K}$ (2.92), leading to the pseudo forces $\mathbf{F}_{\mathrm{P}}$ (and to the internal forces $\mathbf{R}_{\mathrm{P}}$), is similar to the difference between the auxiliary and effective cross-sectional stiffness associated with the FFM fictitious force system presented in § 5.2.2.

2.9. Concluding remarks

The most important results presented in this chapter are now summarised and highlighted.

Firstly, it was clarified that the fictitious forces or initial deformations support the substitution of a nonlinear material analysis by an iterative application of linear analyses. This linear framework does not remove the intrinsic nonlinear character of the problem, but it creates the

conditions for application of the Fixed Point Iteration Method. The Initial Stress and Strain Methods, and therefore the Fictitious Force Method *by Deformations* and *by Stresses*, can be seen as applications of the Fixed Point Iteration Method. It is worth noting that the Imposed Deformations Method of Aguado adopts an iterative procedure similar to that of the Initial Stress Method and FFM_{Def}.

Methods employing fictitious forces or initial deformations to solve nonlinear material problems, or other problems, with the aid of different numerical strategies were also described. In this context, the fictitious forces of Lin, the equivalent force system of Fertis and the linear solvers of the Virtual Distortion Method, which uses initial deformations, and of the Pseudo-Force Method are presented. All these methods are based, like FFM, in the iterative application of linear analyses.

Chapter 3
The Fictitious Force Method

3.1. Problem description, simplifying assumptions and 1D models

This thesis considers the quasi-static nonlinear elastic analysis of skeletal structures, *i.e.* structures defined by a system of one-dimensional bars made of nonlinear elastic materials. The governing equations for such problems are established by a combination of linear kinematic relations, linear equilibrium relations and nonlinear elastic relations. The nonlinear character of these problems is therefore due to the third group of relations. As a preliminary presentation of these problems, the corresponding one-dimensional beam model is first described.

The bars composing the structure are three-dimensional prismatic straight beams, whose straight longitudinal axes are defined by the geometric centres of their cross sections. Only plane problems are considered: this means that the structure has a plane of symmetry which coincides with the loading plane and that all sections are symmetric with respect to this plane.

A local Cartesian system of coordinates $oxyz$ is associated with each three dimensional beam in such a way that, see Figure 3.1:

- the x-axis coincides with the beam axis and the origin is contained in the beam left end section;

- the *z*-axis is contained in the loading plane and is parallel to a cross-sectional axis of symmetry and
- the *y*-axis is orthogonal to the *xz*-coordinate plane.

Due to symmetry w.r.t. the *xz*-coordinte plane, the states of strain and stress at each point of a given three-dimensional beam are approximated by simple functions of x and z. In the corresponding one-dimensional beam model, the cross-sectional strains are functions of the *generalized strains* referred to the beam axis; the cross-sectional stress resultants relative to this axis are designated internal forces. The term "beam" will be used for designating both the one-dimensional beam model and the three-dimensional solid.

To reduce the physical space of the problem two basic hypotheses concerning the beam kinematics (Borkowsky,1988) are assumed: the plane problem hypothesis referred above and Euler-Bernoulli hypothesis – plane cross sections perpendicular to the undeformed beam axis, remain plane and perpendicular to the beam axis during deformation. According to these hypotheses, only two generalized strains are required to characterize the cross-sectional deformation state: the curvature χ and the axial strain ε, linearly related to the beam transverse (w) and axial (u) displacements, along z and x, respectively,

$$\chi = -\frac{d^2 w}{dx^2} \tag{3.1}$$

$$\varepsilon = \frac{du}{dx} \tag{3.2}$$

These generalized strains form a canonical basis of the cross-sectional deformation: χ determines the rotation increment and ε determines the longitudinal displacement increment of an element of length dx, see Figure 3.1.

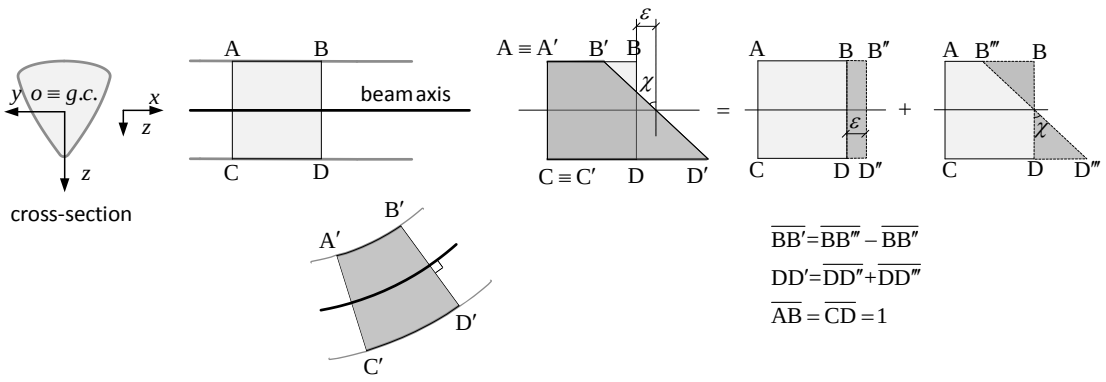

Figure 3.1. Beam segment with unit length and Euler-Bernoulli hypothesis.

The active internal forces, dual of χ and ε, are the bending moment M and the axial force N. These internal forces are linearly related by equilibrium to the generalized loads q and p, which are distributed forces acting along z and x, respectively,

$$q = -\frac{d^2 M}{dx^2} \tag{3.3}$$

$$p = -\frac{dN}{dx} \tag{3.4}$$

The loads p and q are the resultant forces in the 1D model, statically equivalent to the body and surface forces acting on the original three-dimensional beam[5].

This one-dimensional model, whose constitutive relation is expressed by generalized constitutive relations between the generalized strains (χ, ε) and internal forces (M , N), is designated as *model MN* (Borkowsky,1988).

In the 1D model all variables are referred to the cross-sectional geometric centre. Thence, the *linear* constitutive relations between generalized strains and internal forces are uncoupled, *i.e.*, they are given by two independent equations relating the corresponding internal forces and generalized strains. In that particular case, *model MN* can be separated into two simpler ones: *model M* and *model N*. These models consider cross-sectional deformations determined solely by the curvature χ in the case of *model M* and solely by the axial strain ε in the case of *model N*.

The linear beam *model M* is therefore characterized by the compatibility relation (3.1), the equilibrium relation (3.3) and the linear constitutive relation

$$M \equiv \hat{M}[\chi] = EI\,\chi \quad \text{or} \quad \chi \equiv \hat{\chi}[M] = \frac{M}{EI} \tag{3.5}$$

where the circumflex accent stands for a cross-sectional function and EI is the constant bending stiffness. Hence, at the element level, this model is independent of the axial displacement u, axial force N and axial distributed load p.

On the other hand, the linear rod *model N* is characterized by the compatibility relation (3.2), the equilibrium relation (3.4) and the linear constitutive relation

[5] If a distributed moment m about y had also been considered, the first of the above expressions would read $q + \frac{dm}{dx} = -\frac{d^2 M}{dx^2}$.

$$N \equiv \hat{N}\left[\varepsilon\right] = EA\,\varepsilon \quad \text{or} \quad \varepsilon \equiv \hat{\varepsilon}\left[N\right] = \frac{N}{EA} \tag{3.6}$$

where EA is the constant axial stiffness. Hence, this rod model is not affected by the transverse displacements w, bending moment M and transverse distributed load q.

If a Cartesian system whose x-axis no longer contains the cross-sectional geometric centre is used or if the constitutive relation is nonlinear, *model M* and *model N* obtained by decomposition of the general *model MN* are no longer independent or uncoupled. In fact, as shown in chapter 5, the nonlinear cross-sectional constitutive relation between generalized strains (curvature and axial strain) and internal forces is coupled by the equivalent cross-sectional static moment which is non null and variable. Physically, this coupling means that a variation of the curvature, at a specific cross section, corresponds to the variation of both internal forces (M and N), the same happening with a variation of the axial strain.

However, these simpler models may still be used for material nonlinear analysis in some particular contexts. For instance, *model N* can obviously be used for the nonlinear analysis of trusses and *model M* can be used for the nonlinear analysis of axially unrestrained beams. *Model M* can also be used for the analysis of plane skeletal structures if some simplifying assumptions consistent with the representation of the nonlinear constitutive relation in the uncoupled format are added - commonly, the consideration of (i) a linear relation $N = EA\,\varepsilon$ simultaneously with (ii) a nonlinear constitutive relation between bending moment and curvature, for a specific value, or range of values, of the axial force N, which may be known in advance. These simplifying assumptions are often adopted for the nonlinear analysis of frame structures.

This thesis considers an adequately supported generic skeletal structure which is made of nonlinear elastic materials, the so-called *effective structure*. The *effective problem* is determined by the application of a quasi-static *effective* loading system F, which excludes any imposed deformations, to this effective structure. It is admitted that the effective problem has got one and only one solution, which will be referred to as the *effective solution*.

In this chapter, the effective structure is a beam whose constitutive law is described, at each cross section, by

(i) a continuous nonlinear elastic relation between bending moment and curvature, denoted $\hat{M}[\chi]$ or $\hat{\chi}[M]$[6],

(ii) a linear relation between axial force N and axial strain ε.

As explained before, this corresponds to a simplification of a more general relation between generalized strains (χ, ε) and internal forces (M, N).

The cross-sectional tangent bending stiffness is defined by

$$EI \equiv \frac{d\hat{M}}{d\chi} \tag{3.7}$$

This function of χ (or M) is discontinuous at every point where the right and left derivatives are different. Its inverse, a cross-sectional bending flexibility, is denoted EI^{-1}. In this thesis, this tangent stiffness is admitted to be positive everywhere

$$EI > 0 \tag{3.8}$$

i.e., effective constitutive relations with either horizontal or softening branches are not considered.

3.2. Introduction to FFM

The particularization of FFM to *model MN*, *model M* and *model N* is denoted FFM(*MN*), FFM(*M*) and FFM(*N*), respectively, unless it is obvious which specific model is in use. Due to its simplicity, FFM(*M*) will be used in this section to present the fundamental concepts of the FFM, which will not be repeated for FFM(*N*) in chapter 4 and FFM(*MN*) in chapter 5. The more specific aspects of FFM(*M*) will then be addressed in the remaining sections of this chapter.

3.2.1. The auxiliary problem of FFM for the beam *model M*

FFM considers an *auxiliary structure* similar to the effective structure but whose cross sections follow a linear auxiliary constitutive relation

[6] Recall that a circumflex accent mark placed above a symbol denotes a cross-sectional function.

$$M_{\mathrm{A}} \equiv \hat{M}_{\mathrm{A}}\left[\chi\right] = EI_{\mathrm{A}}\,\chi \quad \text{or} \quad \chi_{\mathrm{A}} \equiv \hat{\chi}_{\mathrm{A}}\left[M\right] = \frac{M}{EI_{\mathrm{A}}} \tag{3.9}$$

instead of the effective nonlinear elastic relation. This auxiliary constitutive relation is a particular case of (3.5) and is determined by the cross-sectional bending stiffness field EI_{A}, whose values can be almost arbitrary; however, for reasons that will become clear later (§ 3.6.4), only positive values are considered, *i.e.* $EI_{\mathrm{A}} > 0$. This field may vary along the structure.

In order to circumvent, or correct, the use of this "fake" constitutive relation, the auxiliary problem requires an additional contribution, the fictitious force system F_{F}, which is added to the effective applied force system: their combination forms the auxiliary force system F_{A}. To this auxiliary force system corresponds, in the auxiliary structure, the deformation field observed in the effective problem. This auxiliary force system is conceptually similar to the auxiliary system established by Fertis (2006).

Figure 3.2 illustrates this procedure for a simple built-in beam where the chosen constant auxiliary constitutive relation is everywhere stiffer than the effective one, as shown for a specific, but arbitrary, section of the beam. As the figure illustrates, to the effective force system *F* correspond, in the auxiliary structure, the linear curvature field χ_{L} and the linear bending moment field M_{L}, with

$$M_{\mathrm{L}} = EI_{\mathrm{A}}\,\chi_{\mathrm{L}} \tag{3.10}$$

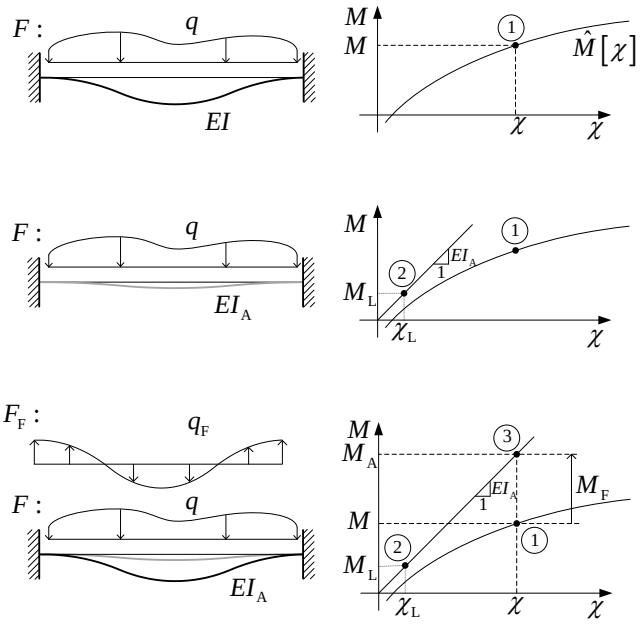

Figure 3.2. Illustrative example of the auxiliary problem of FFM, including fictitious forces.

at every section. This approximated solution (χ_{L},M_{L}), associated to the chosen field EI_{A}, is called a *linear solution* to the effective problem.

If the fictitious force system F_{F} is now added, the auxiliary structure moves into the deformed configuration corresponding to the effective nonlinear constitutive relation and the effective loading system, *i.e.*, the fictitious forces F_{F} produce the curvature increment

$$\chi_{\mathrm{incr}} = \chi - \chi_{\mathrm{L}} \tag{3.11}$$

To F_{F} corresponds also the additional fictitious bending moment field M_{F}, that, together with the effective bending moment field, define the auxiliary bending moments M_{A}, see Figure 3.2, which are thus in equilibrium with $F_{\mathrm{A}} = F + F_{\mathrm{F}}$. The fictitious bending moment field M_{F} is therefore given by the difference between the auxiliary and effective bending moment fields,

$$M_{\mathrm{F}} = M_{\mathrm{A}} - M \tag{3.12}$$

This relation expresses the auxiliary decomposition of the bending moment. In short, the auxiliary problem is defined by

(i) the auxiliary structure,

(ii) the auxiliary linear constitutive relation, characterized by a nowhere negative bending stiffness field, with EI_{A} constant at every section although it may vary from section to section, and

(iii) an auxiliary applied force system F_{A}, given by the effective force system F of the original problem *plus* a fictitious force system F_{F}.

This problem is called auxiliary owing to its assisting role in establishing the structural equations in FFM format. The solution to this auxiliary problem – the *auxiliary solution* – is defined by the effective curvature field χ and the auxiliary bending moment field M_{A} – the former coincides, by definition, with the solution to the effective problem but the latter does not. Table 3.1 represents the effective problem and the auxiliary problem side by side, showing that the fictitious force system allows FFM to operate with the auxiliary linear constitutive relation instead of the effective one.

Table 3.1 – Effective problem versus auxiliary problem of FFM.

problem	constitutive relation	load system	bending moment	curvature
effective	nonlinear	F	M	χ
auxiliary	linear	$F_{\mathrm{A}} = F + F_{\mathrm{F}}$	$M_{\mathrm{A}} = M + M_{\mathrm{F}}$	χ

3.2.2. FFM *by deformations* and FFM *by stresses*

Replacing the effective constitutive law by the auxiliary linear constitutive law does not, obviously, eliminate the intrinsic nonlinear character of the problem. The auxiliary problem is still nonlinear, because the fictitious forces depend on the solution itself, which is not known *a priori*. The reason why the auxiliary problem is so valuable is that it is particularly prone for iterative solution procedures. In fact, substituting into the fictitious bending moment definition (3.12) the linear auxiliary constitutive relation (3.9) gives either

$$M_{\mathrm{F}}\left[\chi\right] = EI_{\mathrm{A}}\,\chi - \hat{M}\left[\chi\right] \tag{3.13}$$

or

$$M_{\mathrm{F}}\left[M\right] = EI_{\mathrm{A}}\,\hat{\chi}\left[M\right] - M \tag{3.14}$$

Since χ and M are usually not known *a priori*, neither of these expressions can be directly used. Instead, two alternative iterative procedures can be established: the fictitious bending moment is determined, in the first procedure, as a function of the approximation $\chi^{(i)}$ to χ,

$$M_{\mathrm{F}}^{(i)} \equiv M_{\mathrm{F}}\left[\chi^{(i)}\right] = EI_{\mathrm{A}}\,\chi^{(i)} - \hat{M}\left[\chi^{(i)}\right] \tag{3.15}$$

and, in the second, as a function of the approximation $M^{(i)}$ to M,

$$M_{\mathrm{F}}^{(i)} \equiv M_{\mathrm{F}}\left[M^{(i)}\right] = EI_{\mathrm{A}}\,\hat{\chi}\left[M^{(i)}\right] - M^{(i)} \tag{3.16}$$

These two alternative ways of computing $M_{\mathrm{F}}^{(i)}$, schematised in Figure 3.3, lead to FFM *by deformations* ($\mathrm{FFM_{Def}}$) and FFM *by stresses* ($\mathrm{FFM_S}$). In $\mathrm{FFM_S}$, the *i*th approximation to the effective bending moment is given by an iterative version of the auxiliary decomposition (3.12)

$$M^{(i)} = M_{\mathrm{A}}^{(i)} - M_{\mathrm{F}}^{(i-1)} \tag{3.17}$$

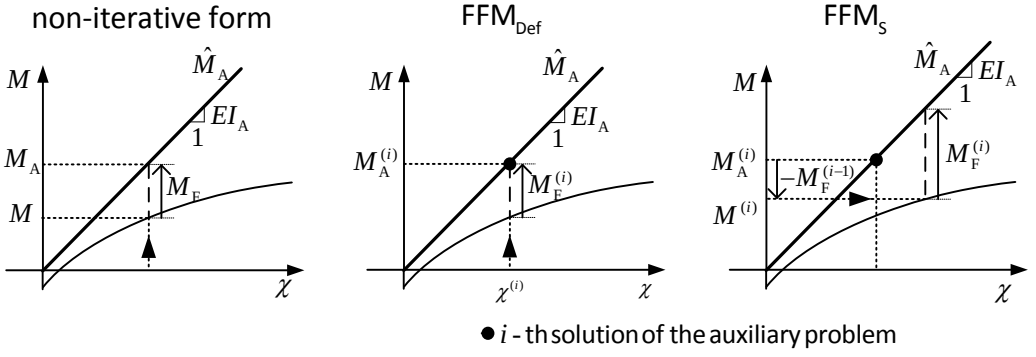

Figure 3.3. Fictitious bending moment.

see Figure 3.3c.

A null fictitious force system is used to compute the initial guess required to start either of the two iterative procedures. This means that

$$\begin{cases} \chi^{(1)} \equiv \chi_{\mathrm{L}} \\ M^{(1)} \equiv M_{\mathrm{L}} \end{cases} \tag{3.18}$$

i.e., the first iteration of FFM gives a linear solution to the effective problem, as defined by expression (3.9).

The flowcharts in Figure 3.4 summarise these iterative procedures. $\mathrm{FFM_{Def}}$, broadly described in this section, is an application of the Initial Stress Method proposed by Zienkiewicz *et al.* (1969) and developed by Argyris and Scharpf (1972) in the context of the Initial Force Method for the Finite Element Method (FEM). $\mathrm{FFM_S}$, also generically described in this section, is an application of the Initial Strain Method presented also in Argyris and Scharpf (1972).

3.2.3. Fictitious forces and initial deformations

In § 3.2.1, it was explained that the application of the fictitious force system F_{F} to the auxiliary structure causes the curvature increment $\chi_{\mathrm{incr}} \equiv \chi - \chi_{\mathrm{L}}$, *i.e.*, F_{F} shifts the structure from the "linear" configuration to the effective configuration corresponding to the effective nonlinear constitutive relation. It can also be said that the additional forces F_{F} model the nonlinear material behaviour by means of initial deformations (imposed deformations) or the corresponding initial stresses. Recall that, as explained in § 2.2, the use of initial strains (or initial stresses) to emulate the material nonlinear behaviour is the basis of the initial force concept of Argyris and Scharpf (1972). This explains the designations *Initial Strain Method* and *Initial Stress Method*. The relation between the fictitious forces of FFM and initial deformations is discussed in this section and in the next one.

The effective curvature at a given section can be formally decomposed into its auxiliary χ_{A} component, given by (3.9.2), and its "nonlinear" component χ_{NL},

$$\chi_{\mathrm{NL}} = \chi - \chi_{\mathrm{A}} \tag{3.19}$$

see Figure 3.5. This relation expresses the auxiliary decomposition of the curvature. Similarly,

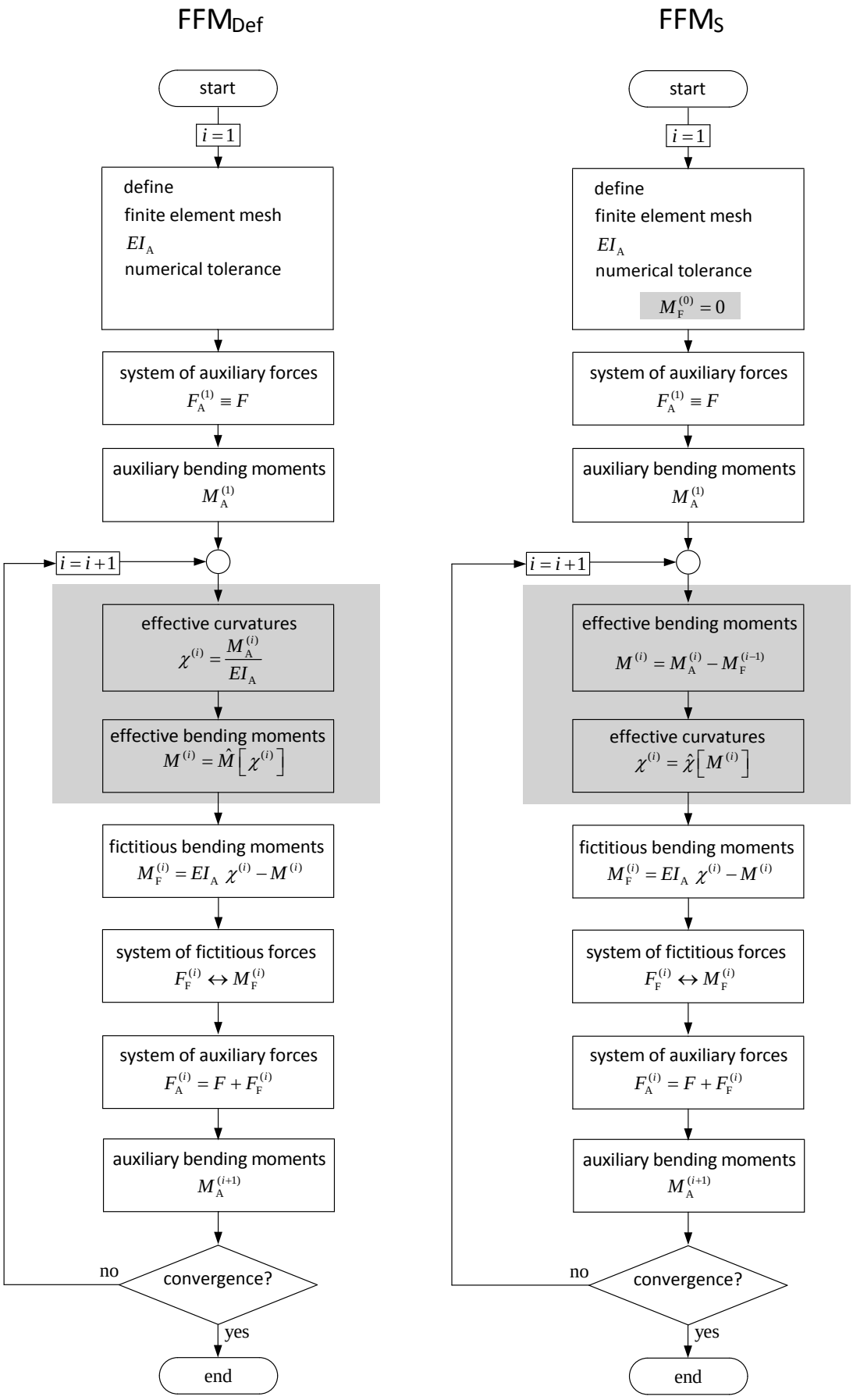

Figure 3.4. FFM(*M*) iterative procedures (differences identified with shaded boxes).

the effective bending moment can be decomposed into M_{A}, given by (3.9.1), and $-M_{\mathrm{F}}$. The dual character of these two decompositions is clearer if (3.12) is rewritten as

$$-M_{\mathrm{F}} = M - M_{\mathrm{A}} \tag{3.20}$$

and this relation is compared to (3.19). Note that the decompositions of the effective bending moment $M = M_{\mathrm{A}} - M_{\mathrm{F}}$ and effective curvature $\chi = \chi_{\mathrm{A}} + \chi_{\mathrm{NL}}$ are merely formal, not physical, since they are determined exclusively by the arbitrary value of EI_{A} – actually, even bending moments and curvatures associated by linear constitutive relations can be arbitrarily decomposed into such "linear" and "nonlinear" components. If one chooses for EI_{A} the initial tangent bending stiffness of the effective nonlinear constitutive relation it is quite natural to call the associated deformation component linear and the remaining deformation nonlinear. This particular case explains the adoption of the designations linear and nonlinear even when an arbitrary value is chosen for EI_{A}.

Substituting the two relations (3.9) in (3.20) and recalling (3.19), gives

$$M_{\mathrm{F}} = EI_{\mathrm{A}}\, \chi_{\mathrm{NL}} \tag{3.21}$$

see Figure 3.5. This expression shows that, for each value of EI_{A}, the curvature χ_{NL}, the fictitious bending moments M_{F} and the fictitious force system F_{F}, which is in equilibrium with M_{F}, are three equivalent and *alternative* forms of describing a given state. The curvature χ_{NL} (resp. bending moment M_{F}) can be regarded as an initial curvature (resp. initial bending moment) which, when applied to the auxiliary structure, produces the increments of curvature $\chi_{\mathrm{incr}} \equiv \chi - \chi_{\mathrm{L}}$ and bending moment $M_{\mathrm{incr}} \equiv M - M_{\mathrm{L}}$, see Figure 3.6.

The identification of the curvature χ_{NL} as an initial curvature transforms the auxiliary problem into the one treated by Duhamel's method, see Arantes e Oliveira (1999). This identification

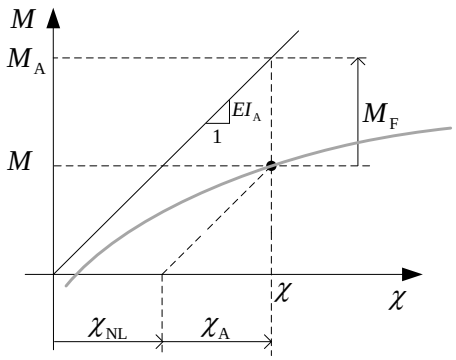

Figure 3.5. Fictitious bending moment and nonlinear component of curvature.

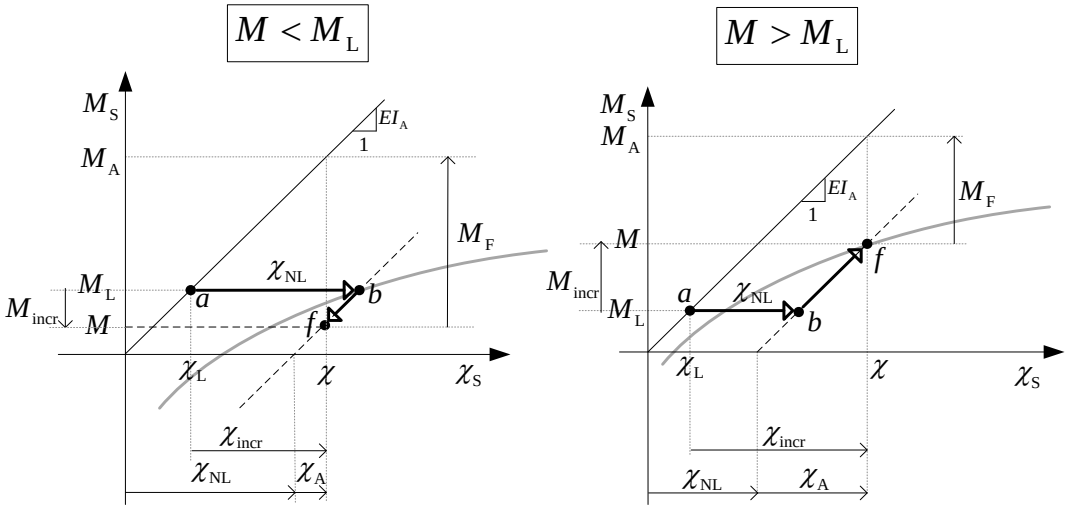

Figure 3.6. Representation of the fictitious bending moment, nonlinear component of curvature and increments of curvature χ_{incr} and bending moment M_{incr}.

was also employed by Lin (1968) in the analysis of the bending of a linear elastic beam, which was described in § 2.5. Thence, the plastic curvature χ_{p} of Lin is the nonlinear component of the curvature χ_{NL} defined for the initial tangent bending stiffness, treated as initial deformations in the context of Duhamel's method.

3.2.4. Links between FFM and Duhamel's method

Let us now describe in detail the application of Duhamel's method to determine the effective state of strain and stress caused by a thermal action (initial deformation), in order to better grasp its affinities with the nonlinear material problem tackled by FFM.

Consider a straight built-in beam, with the linear constitutive relation with stiffness EI_{A} (3.9), *i.e.*, with the constitutive relation of the auxiliary problem of FFM, subjected to a differential variation of temperature corresponding to the initial curvature field χ_{I}, see Figure 3.7a.

How can the corresponding curvature χ and bending moment M fields be determined? Well, the main purpose of Duhamel's method is to define the system of forces $-F_{\mathrm{R}}$ to be applied to the effective structure to simulate the kinematic effect of the thermal action.

Imagine that the beam is cut out from its supports (at least from one), becoming to deform under the thermal action, and acquires the curvature χ_{I}, represented in Figure 3.7b for the generic cross section S with a positive curvature. The unconstrained beam displacement field

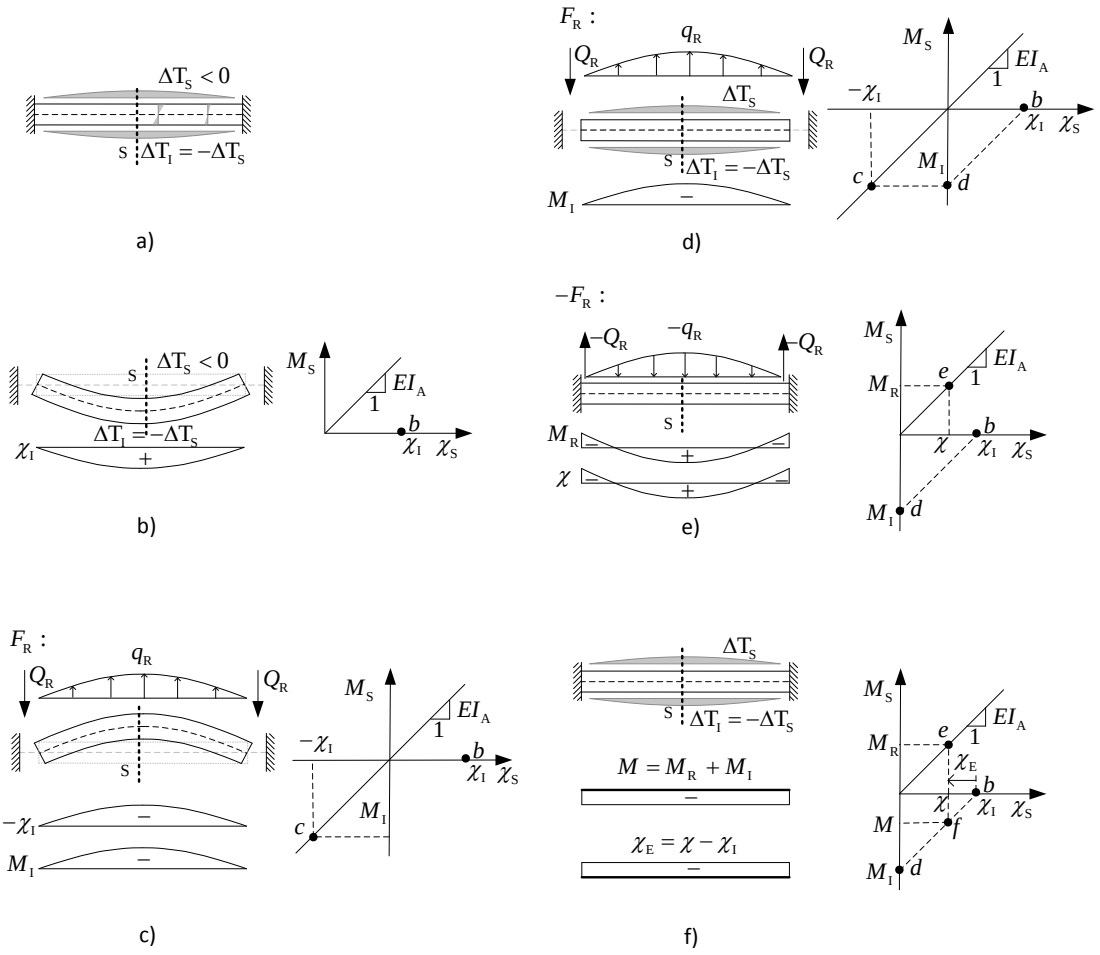

Figure 3.7. Duhamel's method applied to the analysis of a beam subjected to a thermal action.

is not compatible with the boundary conditions initially imposed by the supports, since the end sections are rotated w.r.t. the initial configuration. In order to restore compatibility, a self-equilibrated system of restoring forces F_{R} is introduced which reshapes the beam into its straight initial configuration, *i.e.* which adds the curvature field $-\chi_{\mathrm{I}}$ and the corresponding initial bending moments $M_{\mathrm{I}} = EI_{\mathrm{A}}\left(-\chi_{\mathrm{I}}\right)$, see Figure 3.7c. In the released beam, the combined action of the temperature variation, *i.e.* of the initial curvature χ_{I}, with F_{R} produces everywhere null total deformation and displacement fields, see Figure 3.7d.

The kinematic boundary constraints can now be reintroduced. In order to remove the fictitious force system F_{R} its symmetric $-F_{\mathrm{R}}$ is added to the previous state. To the system of forces $-F_{\mathrm{R}}$ corresponds the effective curvature χ and the resulting bending moments $M_{\mathrm{R}} = EI_{\mathrm{A}}\,\chi$, see Figure 3.7e. The effective bending moments are given by the sum of M_{R} with M_{I}, *i.e.* $M \equiv M_{\mathrm{R}} + M_{\mathrm{I}}$, see Figure 3.7f. These bending moment fields are proportional to the elastic curvatures $\chi_{\mathrm{E}} \equiv \chi - \chi_{\mathrm{I}}$, *i.e.* $M = EI_{\mathrm{A}}\,\chi_{\mathrm{E}}$, and they are obviously linear since there are no direct actions (*i.e.* forces) applied.

If the beam was isostatic, the above procedure would give $M = 0$, $\chi_E = 0$ and $\chi = \chi_I$, *i.e.*, the beam would deform freely under the action of the initial curvatures χ_I, since in this case they were compatible with the boundary conditions. Thence, the development of elastic deformations would not be required and no bending moments would occur.

Suppose now that, simultaneously with the thermal action, *i.e.* with the initial curvatures χ_I, the beam above is also subjected to an effective force system F corresponding to curvatures χ_L and bending moments M_L. Since the problem is linear, the superposition principle can be invoked and Duhamel's method can still be used to determine the increments of curvatures and bending moments

$$\chi_{incr} \equiv \chi - \chi_L \tag{3.22}$$

$$M_{incr} \equiv M - M_L \tag{3.23}$$

caused by the thermal action, *i.e.* the initial curvatures χ_I. In order to illustrate the application of Duhamel's method to this case, Figure 3.8 represents the successive states on the constitutive relation, corresponding to the stages of application of the two actions.

Figure 3.8a represents the linear solution (χ_L, M_L) corresponding to the applied forces. Next, this state is "frozen", the beam released and the variation of the deformation field of the beam, corresponding to the curvature χ_I, is considered, Figure 3.8b. Only then is the self-equilibrated system of restoring forces F_R defined; it introduces in the released beam the curvature $-\chi_I$ and the initial bending moments $M_I = EI_A(-\chi_I)$, see Figure 3.8c. The combined action of the applied forces, the thermal action and F_R is represented by point *d* in Figure 3.8d and corresponds to the deformation field χ_L.

The kinematic boundary constraints can now be replaced. In order to remove the fictitious forces F_R the corresponding symmetrical system $-F_R$ is added to the current state. The combined action of F and $-F_R$ corresponds to the effective curvatures χ and the bending moments $M_R = EI_A \chi$, *i.e.*, $-F_R$ corresponds to the increments of curvature χ_{incr} and bending moments $M_R - M_L$, see Figure 3.8e. Finally, the effective bending moments are obtained by adding together M_R and M_I, *i.e.* $M \equiv M_R + M_I$, see Figure 3.8f. The increment of bending moment due to the thermal action $M_{incr} \equiv M - M_L$ is proportional to the elastic curvature

$$\chi_E \equiv \chi_{incr} - \chi_I \tag{3.24}$$

i.e.

$$M_{incr} = EI_A \chi_E \tag{3.25}$$

Yet again, if the beam was isostatic, then $M_{\text{incr}} = 0$, $\chi_{\text{E}} = 0$ and $\chi_{\text{incr}} = \chi_{\text{I}}$.

Figure 3.9 is a clearer replica of Figure 3.8f. The path defined by the oriented line segments $\overrightarrow{ab}$ and $\overrightarrow{bf}$ representing the state of cross section S, reflects Duhamel's method: segment $\overrightarrow{ab}$ corresponds to the response of the freed structure (isostatic) to the application of the initial deformation χ_{I} and segment $\overrightarrow{bf}$ is the correction due to the kinematic constraints of the effectively hyperstatic structure. Thence, $\overrightarrow{bf}$ is null in the isostatic case.

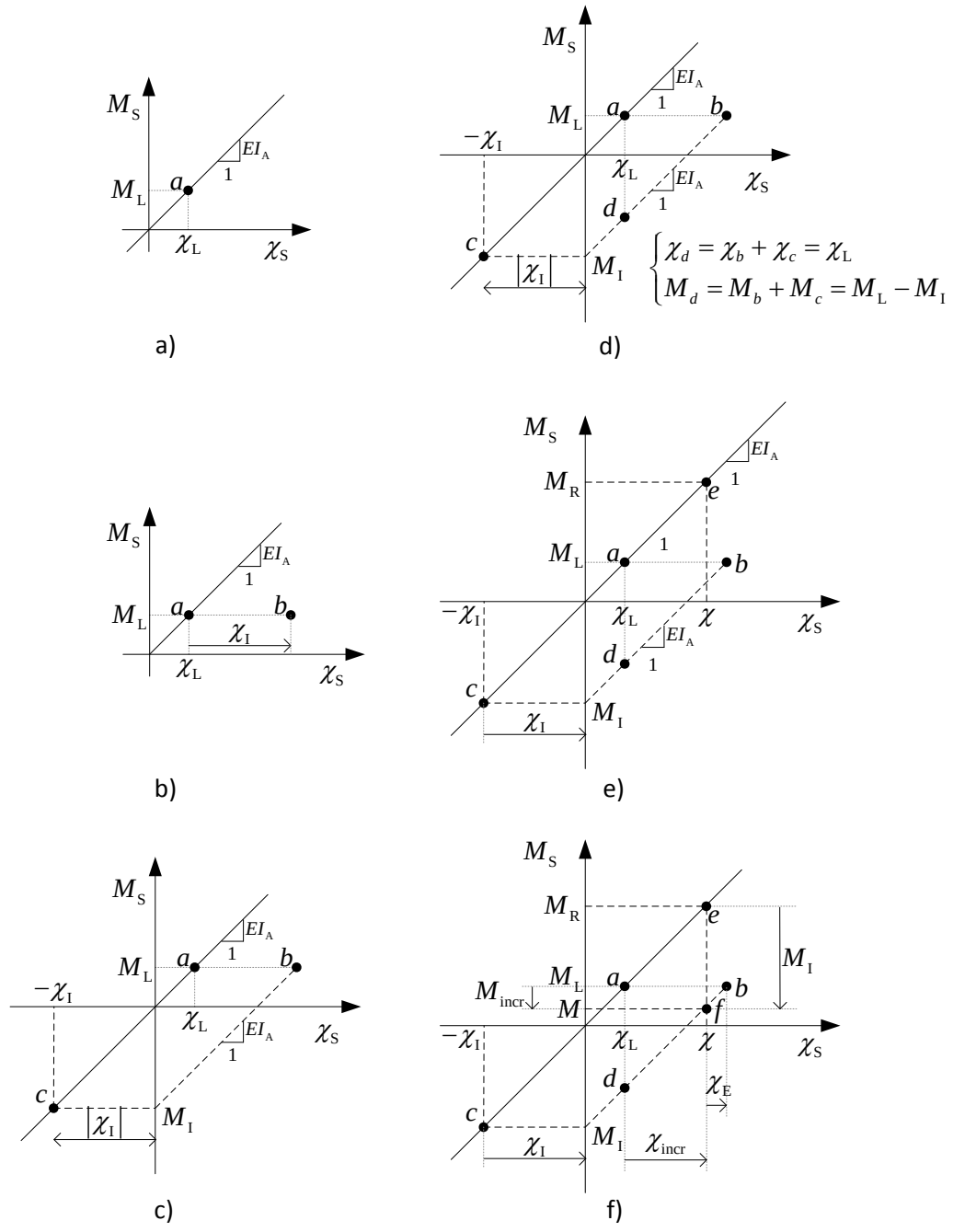

Figure 3.8. Duhamel's method applied to a problem which combines direct and indirect actions.

Let us consider again the nonlinear elastic problem analysed by FFM. The identification of the curvature χ_{NL} as an initial curvature makes this problem equivalent to the linear thermal problem analysed by Duhamel's method. Figure 3.10, whose top row replicates Figure 3.9, for both cases of $M_{\mathrm{L}} > M$ and $M_{\mathrm{L}} < M$, and whose bottom row replicates Figure 3.6, adding the points *a*, *b* and *f*, illustrates the equivalence between these two problems, depicting the successive states of the generic cross section S.

Considering this analogy between χ_{I} and χ_{NL} and comparing the top and bottom rows of Figure 3.10, it can be concluded that:

(i) the initial bending moment M_{I} and the fictitious bending moment M_{F} are symmetric;

(ii) the restoring force system F_{R} and the fictitious force system F_{F} are symmetric;

(iii) the resulting bending moment M_{R} is equivalent to the auxiliary bending moment M_{A};

(iv) the elastic curvature χ_{E} is equivalent to the difference between auxiliary curvature χ_{A} and linear curvature χ_{L}.

These results are gathered in Table 3.2.

3.2.5. FFM iteration formulas

In the last two sections it was shown that the analysis of nonlinear material problems by FFM is somewhat analogous to the analysis of the linear elastic problem of a structure subjected to initial deformations (or initial stresses) by Duhamel's method. However, in the first problem, the field χ_{NL}, and thus the field M_{F}, are not known *a priori*. This is what determines the need for $\mathrm{FFM_{Def}}$ and $\mathrm{FFM_S}$ iterative procedures. The former uses expression (3.15) and the latter (3.16) to estimate the fictitious bending moment M_{F} and the nonlinear curvature is afterwards estimated according to (3.19) by $\chi_{\mathrm{NL}}^{(i)} = M_{\mathrm{F}}^{(i)} / EI_{\mathrm{A}}$.

Let us define the operator T, relative to the auxiliary structure, which represents the transformation of a generic action, formed by an arbitrary initial curvature field, *e.g.* χ_{NL}, and an arbitrary force system F, into the effective curvature field χ

$$\chi = T\left[\chi_{\mathrm{NL}}, F\right] \tag{3.26}$$

Note that the use of a fictitious force system, *i.e.* the fictitious forces F_{F}, to emulate the initial deformations, corresponds to the identity $\chi = T\left[\chi_{\mathrm{NL}}, F\right] = T\left[0, F + F_{\mathrm{F}}\right]$.

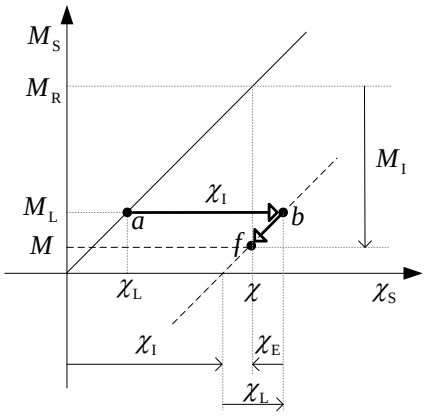

Figure 3.9. Summary of the application of Duhamel's method to a problem combining direct and indirect actions.

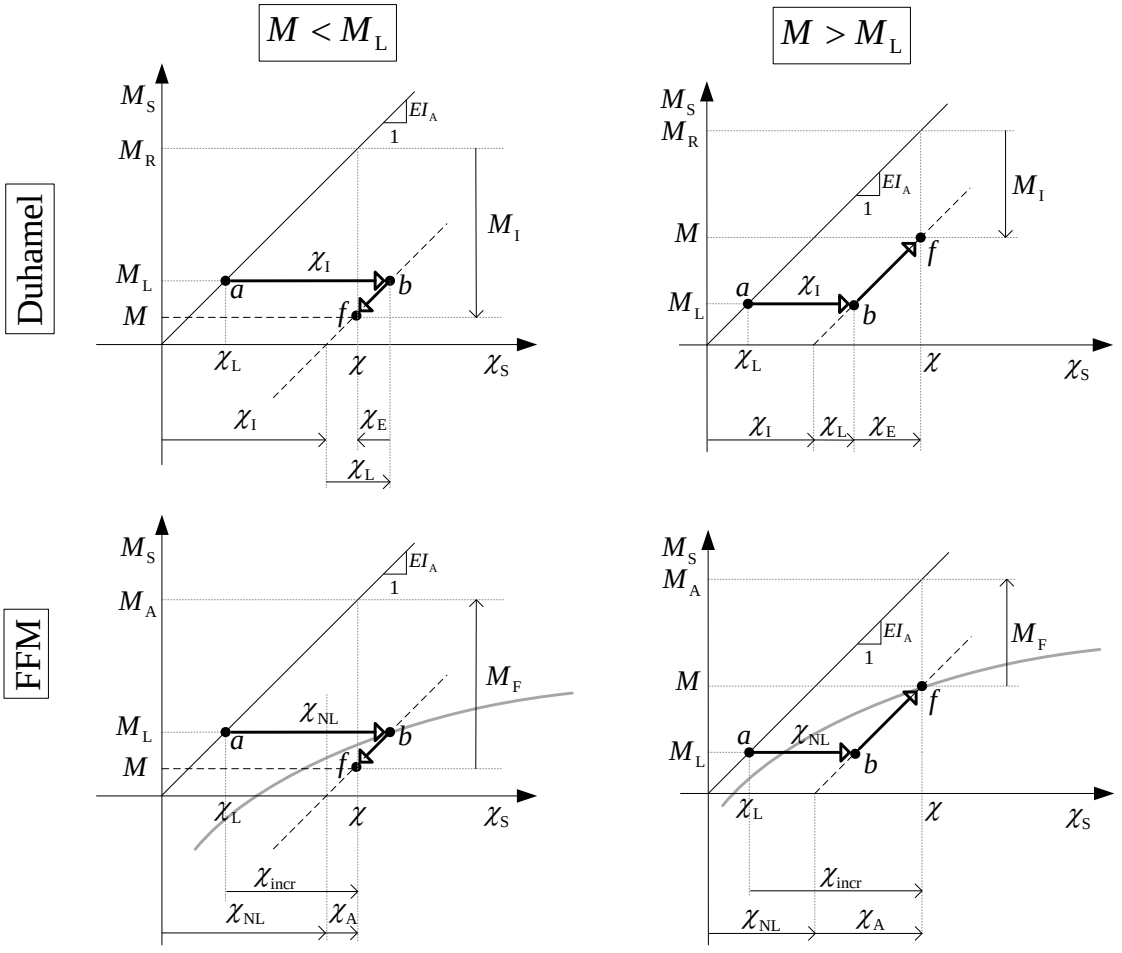

Figure 3.10. Equivalence of FFM and Duhamel's approaches.

Table 3.2 – Duhamel's *vs.* FFM approaches.

Duhamel	χ_I	M_I	F_R	M_R	χ_E
FFM	χ_{NL}	$-M_F$	$-F_F$	M_A	$\chi_A - \chi_L$

Even though the operator T is not bilinear it is linear in the pair (χ_{NL}, F), *i.e.* the total action, because

$$\begin{cases} T[\alpha\,\chi_{NL}, \alpha\,F] = \alpha\,T[\chi_{NL}, F] \\ T[\chi_{NL,1} + \chi_{NL,2}, F_1 + F_2] = T[\chi_{NL,1}, F_1] + T[\chi_{NL,2}, F_2] \end{cases} \tag{3.27}$$

Considering the second of these proprieties, expression (3.26) can be written as

$$\chi = T[\chi_{NL}, F] = T[\chi_{NL}, 0] + T[0, F] = T_\chi[\chi_{NL}] + \chi_L \tag{3.28}$$

where

$$\chi_L = T[0, F] \tag{3.29}$$

which is linear in F and represents the effect of the applied loads, and

$$T_\chi[\chi_{NL}] \equiv T[\chi_{NL}, 0] \tag{3.30}$$

which is linear in χ_{NL}. Hence, the operator G_χ^I which transforms (initial) curvatures χ_{NL} into effective curvatures is given by

$$\chi = G_\chi^I[\chi_{NL}] \equiv \chi_L + T_\chi[\chi_{NL}] \tag{3.31}$$

Subtracting χ_{NL} to both members of (3.31) and recalling that $\chi_A = \chi - \chi_{NL}$, (3.19), gives

$$\chi_A = \chi_L + T_\chi[\chi_{NL}] - \chi_{NL} \tag{3.32}$$

Multiplying both members by EI_A and recalling (3.9) and (3.10), gives

$$M = M_L + EI_A\,T_M[\chi_{NL}] \tag{3.33}$$

where

$$T_M[\chi_{NL}] \equiv T_\chi[\chi_{NL}] - \chi_{NL} \tag{3.34}$$

is a linear operator of χ_{NL}. Introducing (3.21) into (3.33) gives the operator G_M^I which transforms fictitious bending moments M_F into effective bending moments

$$M = G_M^I[M_F] = M_L + T_M[M_F] \tag{3.35}$$

Expressions (3.31) and (3.35), which convert (initial) curvatures χ_{NL} into effective curvatures χ, and (initial) fictitious bending moments M_F into effective bending moments M, are the backbone of FFM_{Def} and FFM_S iteration formulas.

Since χ_{NL} and M_{F} are usually not known in advance, it is necessary to estimate them. Substitution of (3.15) into (3.21) gives an approximation of the curvature filed χ_{NL}

$$\chi_{\mathrm{NL}}^{(i)} = G_{\chi}^{\mathrm{II}}\left[\chi^{(i)}\right] \equiv \frac{M_{\mathrm{F}}\left[\chi^{(i)}\right]}{EI_{\mathrm{A}}} \tag{3.36}$$

and of (3.16) into (3.21) gives an approximation to the bending moment field M_{F}

$$M_{\mathrm{F}}^{(i)} = G_{\mathrm{M}}^{\mathrm{II}}\left[M^{(i)}\right] \equiv M_{\mathrm{F}}\left[M^{(i)}\right] \tag{3.37}$$

Next, recalling that a null fictitious force system is used to compute the initial guess of the iterative procedures of FFM, *i.e.* $\chi^{(1)} \equiv \chi_{\mathrm{L}}$ and $M^{(1)} \equiv M_{\mathrm{L}}$, (3.18), and substituting the approximation (3.36) into (3.31) gives $\mathrm{FFM}_{\mathrm{Def}}$ fixed point iteration formula, see Atkinson and Han (2001) or Pina (2010),

$$\chi^{(i+1)} = G_{\chi}\left[\chi^{(i)}\right] \equiv G_{\chi}^{\mathrm{I}}\left[G_{\chi}^{\mathrm{II}}\left[\chi^{(i)}\right]\right] = \chi^{(1)} + T_{\chi}\left[\chi_{\mathrm{NL}}\left[\chi^{(i)}\right]\right] \tag{3.38}$$

On the other hand, substitution of approximation (3.37) into (3.35) gives $\mathrm{FFM}_{\mathrm{S}}$ fixed point iteration formula

$$M^{(i+1)} = G_{\mathrm{M}}\left[M^{(i)}\right] \equiv G_{\mathrm{M}}^{\mathrm{I}}\left[G_{\mathrm{M}}^{\mathrm{II}}\left[M^{(i)}\right]\right] = M^{(1)} + T_{\mathrm{M}}\left[M_{\mathrm{F}}\left[M^{(i)}\right]\right] \tag{3.39}$$

The compositions $G_{\chi} \equiv G_{\chi}^{\mathrm{I}}\left[G_{\chi}^{\mathrm{II}}\right]$ and $G_{\mathrm{M}} \equiv G_{\mathrm{M}}^{\mathrm{I}}\left[G_{\mathrm{M}}^{\mathrm{II}}\right]$ in (3.38) and (3.39) show that the nonlinear character of these iteration formulas is only caused by the operators G_{χ}^{II} and $G_{\mathrm{M}}^{\mathrm{II}}$, which depend on the nonlinear effective constitutive relation (through (3.15) and (3.16)). This result simplifies the determination of sectional sufficient convergence conditions of $\mathrm{FFM}_{\mathrm{Def}}$ and $\mathrm{FFM}_{\mathrm{S}}$ iterative procedures.

Finally, it can be noted that in isostatic structures the iterative procedure of $\mathrm{FFM}_{\mathrm{S}}$ gets reduced to a unique "iteration" after the initialization, since in those cases, unless geometric nonlinearities are relevant, the internal forces are independent of the material nonlinearities and do not change after the initial iteration of FFM, *i.e.* $M^{(1)} \equiv M$.

3.2.6. FFM convergence conditions

The convergence of the iteration formulas (3.38) and (3.39), corresponding to $\mathrm{FFM}_{\mathrm{Def}}$ and $\mathrm{FFM}_{\mathrm{S}}$ is now discussed. As explained in § 2.4, these iteration formulas will converge if the operators G_{χ} and G_{M} are contractive. According to the definition of contraction presented in that section

and recalling expression (3.38) (resp. (3.39)), if G_{χ}^{I} and G_{χ}^{II} (resp. $G_{\mathrm{M}}^{\mathrm{I}}$ and $G_{\mathrm{M}}^{\mathrm{II}}$) are non-expansive operators and at least one of them is contractive then G_{χ} (resp. G_{M}) is also contractive. Introducing the expressions (3.13) and (3.14) into (3.21), and deriving w.r.t. χ and M, gives

$$\frac{d\chi_{\mathrm{NL}}[\chi]}{d\chi}=1-\frac{1}{EI_{\mathrm{A}}}\frac{d\hat{M}}{d\chi}=\frac{EI_{\mathrm{A}}-EI[\chi]}{EI_{\mathrm{A}}} \tag{3.40}$$

$$\frac{dM_{\mathrm{F}}[M]}{dM}=EI_{\mathrm{A}}\,EI^{-1}[M]-1 \tag{3.41}$$

Defining the relative differences of bending stiffness

$$\beta_{\chi}\equiv\frac{EI_{\mathrm{A}}-EI}{EI_{\mathrm{A}}} \tag{3.42}$$

and

$$\beta_{\mathrm{M}}\equiv\frac{EI_{\mathrm{A}}-EI}{EI}=\frac{\beta_{\chi}}{1-\beta_{\chi}} \tag{3.43}$$

the above derivatives can be rewritten for a specific point of the constitutive law as

$$\frac{d\chi_{\mathrm{NL}}[\chi]}{d\chi}=\beta_{\chi} \tag{3.44}$$

and

$$\frac{dM_{\mathrm{F}}[M]}{dM}=\beta_{\mathrm{M}} \tag{3.45}$$

Hence, the derivatives of G_{χ}^{II} and $G_{\mathrm{M}}^{\mathrm{II}}$, see (3.36) and (3.37), are

$$\frac{dG_{\chi}^{\mathrm{II}}\left[\chi^{(i)}\right]}{d\chi^{(i)}}=\beta_{\chi} \tag{3.46}$$

$$\frac{dG_{\mathrm{M}}^{\mathrm{II}}\left[M^{(i)}\right]}{dM^{(i)}}=\beta_{\mathrm{M}} \tag{3.47}$$

Thence, for a continuous nonlinear constitutive law (§ 3.1), $G_{\chi}^{\mathrm{II}}\left[\chi^{(i)}\right]$ is contractive if the absolute value of the derivative (3.46) is bounded by a constant that is less than one, *i.e.*, if the linear auxiliary constitutive relation is everywhere such that

$$\left|\beta_{\chi}\right|<1 \tag{3.48}$$

and similarly $G_{\mathrm{M}}^{\mathrm{II}}\left[M^{(i)}\right]$ is contractive if the linear auxiliary constitutive relation is such that

$$\left|\beta_{\mathrm{M}}\right|<1 \tag{3.49}$$

These are sufficient conditions for convergence of FFM iteration formulas only if G_{χ}^{I} and $G_{\mathrm{M}}^{\mathrm{I}}$ are non-expansive operators. As a matter of fact, in § 3.6.2 and § 3.6.3 it is proved that, in the context of the discrete FFM methods, the operators G_{χ}^{I} and $G_{\mathrm{M}}^{\mathrm{I}}$ correspond to non-expansive transformations. In that case, expressions (3.48) and (3.49) represent sufficient conditions for convergence of FFM iterative procedures, which are proposed, tested and used in this work. These conditions are established at the cross-sectional level, *i.e.*, they must be satisfied at all sections of the structure.

3.3. First illustrative example

The application of FFM is now illustrated with the problem represented in Figure 3.11, with a beam of length $2L$.

The constitutive relation is constant in each half of the beam. In the left half, denoted by subscript 1, this relation is linear

$$\hat{M}_1[\chi]=EI_1\,\chi \quad \text{or} \quad \hat{\chi}_1[M]=\frac{M}{EI_1} \tag{3.50}$$

The right half, denoted by subscript 2, has the following nonlinear constitutive law, adapted from Richard and Abbott (1975)

$$\hat{M}_2[\chi]=\frac{EI_{2,0}\,\chi}{\sqrt{1+\left(\dfrac{EI_{2,0}\,\chi}{M_{\mathrm{ref}}}\right)^2}} \quad \text{or} \quad \hat{\chi}_2[M]=\frac{\dfrac{M}{EI_{2,0}}}{\sqrt{1-\left(\dfrac{M}{M_{\mathrm{ref}}}\right)^2}} \tag{3.51}$$

which is fully defined by two parameters: the bending stiffness at the origin $EI_{2,0}\equiv EI_2[0]$ and a reference value of the bending moment M_{ref} which bounds the constitutive law, *i.e.* $M=\pm M_{\mathrm{ref}}$ are horizontal asymptotes. This relationship has continuous first and second derivatives and is symmetric w.r.t. the origin.

The problem was solved for $M_{\mathrm{ref}}=1$ and $EI_{2,0}=4EI_1=1$, see Figure 3.12, reducing the above expressions to

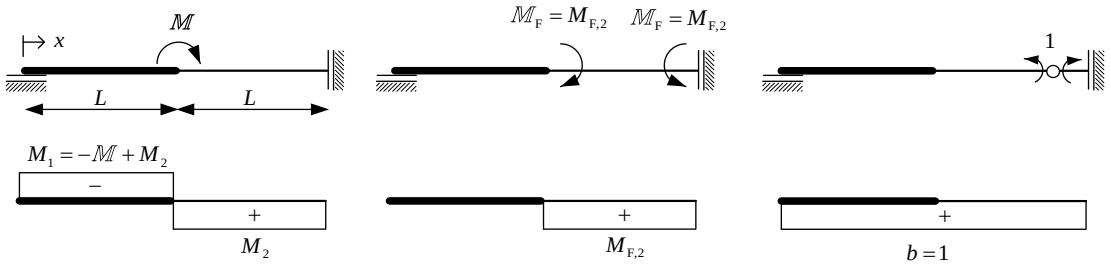

Figure 3.11. Example 3.1: (Left) Beam geometry and loading; (center) fictitious force system; (right) primary structure. The bending moment fields are represented below.

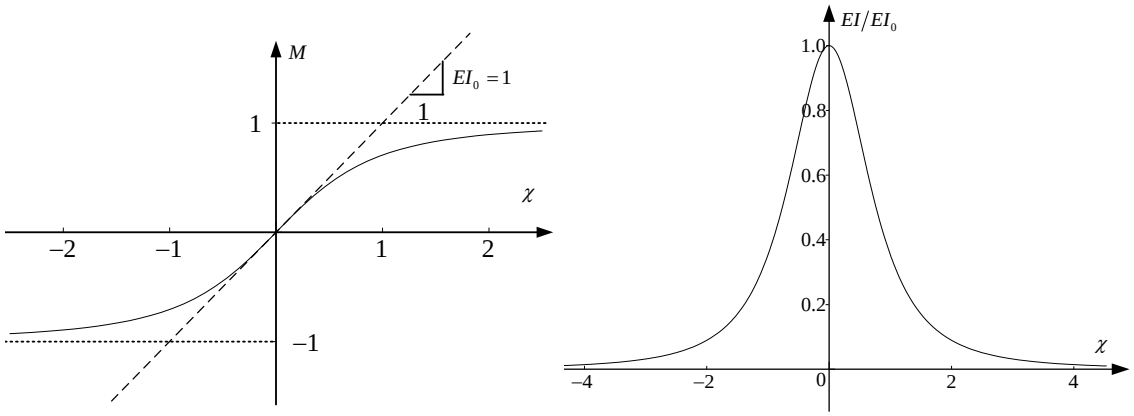

Figure 3.12. Example 3.1: Nonlinear constitutive relation and corresponding tangent stiffness.

$$\hat{M}_2[\chi] = \frac{\chi}{\sqrt{1+\chi^2}} \quad \text{or} \quad \hat{\chi}_2[M] = \frac{M}{\sqrt{1-M^2}} \tag{3.52}$$

The effective force system F comprises a unique moment with magnitude $\mathcal{M}=1$ applied at midspan. The bending moment and curvature fields are constant in each half of the beam. Hence, this structure is equivalent to two springs (point elements) in series with the constitutive laws (3.50) and (3.51).

Since this structure has a single degree of static indeterminacy, a primary structure can be defined by releasing the bending moment, for instance, at the beam right end section. Figure 3.11 represents this primary structure and the self-equilibrated constant bending moment distribution $b = 1$. The principle of virtual forces establishes the compatibility condition

$$\int_0^{2L} \tilde{b}\,\tilde{\chi}\,dx = \int_0^{2L} \tilde{\chi}\,dx = \chi_1\,L + \chi_2\,L = 0 \tag{3.53}$$

i.e.

$$\chi_1 + \chi_2 = 0 \tag{3.54}$$

where χ_1 and χ_2 are the values of the constant curvature fields in the left and right halves of the beam. The bending moment is also constant in each beam half and satisfies the equilibrium condition

$$M_2 = M_1 + 1 \tag{3.55}$$

Introducing first the constitutive functions (3.50) and (3.51) into the compatibility condition (3.54) and then the equilibrium condition (3.55), gives the nonlinear governing equation

$$\left(1 - \frac{1}{M_2}\right)\sqrt{1-\left(M_2\right)^2} + \frac{1}{4} = 0 \tag{3.56}$$

The solution to this equation is $M_2 = 0.732$, corresponding to $\chi_2 = 1.073$. In the right half of the beam, the tangent bending stiffness is given by

$$\widehat{EI}_2\left[\chi\right] \equiv \frac{\hat{M}_2\left[\chi\right]}{d\chi} = \left(1+\chi^2\right)^{\frac{-3}{2}} \quad ; \quad \widehat{EI}_2^{-1}\left[M\right] \equiv \frac{d\hat{\chi}_2\left[M\right]}{M} = \left(1-M^2\right)^{\frac{-3}{2}} \tag{3.57}$$

and therefore the above solution corresponds to $EI_2 = 0.317$. These three values define the exact solution of this problem.

The application of FFM begins with the definition of the auxiliary constitutive relation, which is chosen to be constant in each half of the beam,

$$\hat{M}_{\mathrm{A},1}\left[\chi\right] = EI_{\mathrm{A},1}\,\chi \tag{3.58}$$

$$\hat{M}_{\mathrm{A},2}\left[\chi\right] = EI_{\mathrm{A},2}\,\chi \tag{3.59}$$

Replacing these expressions into the compatibility condition (3.54), gives

$$\frac{M_{\mathrm{A},1}}{EI_{\mathrm{A},1}} + \frac{M_{\mathrm{A},2}}{EI_{\mathrm{A},2}} = 0 \tag{3.60}$$

In the left half of the beam the constant auxiliary stiffness value $EI_{\mathrm{A},1} = EI_1 = 1/4$ was chosen, which means that the auxiliary constitutive relation in this part of the beam is equal to the effective constitutive relation; thence, the fictitious bending moment is null in the left half of the beam. In the right half of the beam the constant auxiliary stiffness value $EI_{\mathrm{A},2}$ was varied, but always positive, in order to investigate its influence in the convergence of the method.

The fictitious force system F_{F} is formed by the two fictitious moments $\mathbb{M}_{\mathrm{F}} = M_{\mathrm{F},2}$ represented in Figure 3.11b. Hence, the auxiliary force system F_{A} is given by the auxiliary moment

$$\mathbb{M}_{\mathrm{A}} = 1 + \mathbb{M}_{\mathrm{F}} = 1 + M_{\mathrm{F},2} \tag{3.61}$$

applied at the beam midsection and by the fictitious moment at the beam right end, which affects the support reaction and has no other effect on the beam. This system of forces and the auxiliary bending moments satisfy an equilibrium equation similar to (3.55)

$$M_{\mathrm{A},2} = M_{\mathrm{A},1} + \mathbb{M}_{\mathrm{A}} \tag{3.62}$$

Solving the linear system of equations (3.60) and (3.62) gives the auxiliary bending moments

$$M_{\mathrm{A},1} = -\frac{EI_{\mathrm{A},1}}{EI_{\mathrm{A},1} + EI_{\mathrm{A},2}} \mathbb{M}_{\mathrm{A}} \tag{3.63}$$

$$M_{\mathrm{A},2} = \frac{EI_{\mathrm{A},2}}{EI_{\mathrm{A},1} + EI_{\mathrm{A},2}} \mathbb{M}_{\mathrm{A}} \tag{3.64}$$

Introducing (3.63) into (3.58) and recalling (3.54), gives the curvatures

$$\chi_2 = \frac{\mathbb{M}_{\mathrm{A}}}{EI_{\mathrm{A},1} + EI_{\mathrm{A},2}} = -\chi_1 \tag{3.65}$$

Making $M_{\mathrm{F},2} = 0$ in (3.61) and substituting the result into the three last expressions gives the linear solution of the auxiliary problem

$$M_{\mathrm{L},1} = -\frac{EI_{\mathrm{A},1}}{EI_{\mathrm{A},1} + EI_{\mathrm{A},2}} \tag{3.66}$$

$$M_{\mathrm{L},2} = \frac{EI_{\mathrm{A},2}}{EI_{\mathrm{A},1} + EI_{\mathrm{A},2}} \tag{3.67}$$

$$\chi_{\mathrm{L},2} = \frac{1}{EI_{\mathrm{A},1} + EI_{\mathrm{A},2}} = -\chi_{\mathrm{L},1} \tag{3.68}$$

Substituting (3.61) and (3.68) into (3.65) gives the curvature in the right half of the beam

$$\chi_2 = \chi_{\mathrm{L},2} + \frac{M_{\mathrm{F},2}}{EI_{\mathrm{A},1} + EI_{\mathrm{A},2}} \tag{3.69}$$

or, substituting (3.21),

$$\chi_2 = \chi_{\mathrm{L},2} + \frac{EI_{\mathrm{A},2}}{EI_{\mathrm{A},1} + EI_{\mathrm{A},2}} \chi_{\mathrm{NL},2} \tag{3.70}$$

Comparing this expression with (3.31), gives the general operator $G^{\mathrm{I}}_{\chi,2}$

$$\chi_2 = G^{\mathrm{I}}_{\chi,2}\left[\chi_{\mathrm{NL},2}\right] = \chi_{\mathrm{L},2} + T_{\chi,2}\,\chi_{\mathrm{NL},2} \quad \text{with} \quad T_{\chi,2} = \frac{EI_{\mathrm{A},2}}{EI_{\mathrm{A},1}+EI_{\mathrm{A},2}} \tag{3.71}$$

This expression corresponds to the iterative formula of $\mathrm{FFM}_{\mathrm{Def}}$

$$\chi_2^{(i+1)} = G_{\chi,2}\left[\chi_2^{(i)}\right] = \chi_2^{(1)} + T_{\chi,2}\,\chi_{\mathrm{NL},2}\left[\chi_2^{(i)}\right] \tag{3.72}$$

which is a particular case of (3.38).

Let us now use (3.19) to rewrite (3.71),

$$\chi_{\mathrm{A},2} = \chi_{\mathrm{L},2} + \left(T_{\chi,2} - 1\right)\chi_{\mathrm{NL},2} \tag{3.73}$$

Multiplying both members of this expression by $EI_{\mathrm{A},2}$, gives

$$M_2 = G^{\mathrm{I}}_{\mathrm{M},2}\left[M_{\mathrm{F},2}\right] = M_{\mathrm{L},2} + T_{\mathrm{M},2}\,M_{\mathrm{F},2} \quad \text{with} \quad T_{\mathrm{M},2} = T_{\chi,2} - 1 = -\frac{EI_{\mathrm{A},1}}{EI_{\mathrm{A},1}+EI_{\mathrm{A},2}} \tag{3.74}$$

This expression corresponds to the iterative formula of $\mathrm{FFM}_{\mathrm{S}}$

$$M_2^{(i+1)} = G_{\mathrm{M},2}\left[M_2^{(i)}\right] = M_{\mathrm{L},2}^{(1)} + T_{\mathrm{M},2}\,M_{\mathrm{F},2}\left[M_2^{(i)}\right] \tag{3.75}$$

Hence, the general operator T_{M} in (3.39) is given in this example by the scalar $-EI_{\mathrm{A},1}/\left(EI_{\mathrm{A},1}+EI_{\mathrm{A},2}\right)$.

Consider now the iteration formulas (3.72) and (3.75) and, specifically, the role played by the auxiliary constant bending stiffness $EI_{\mathrm{A},2}$ in the performance of these iterative procedures. These formulas can be seen as the composition of the operators G^{I}_{χ} (3.71) with G^{II}_{χ} (3.36) and $G^{\mathrm{I}}_{\mathrm{M}}$ (3.74) with $G^{\mathrm{II}}_{\mathrm{M}}$ (3.37).

Let us analyse the convergence of the iteration formula of $\mathrm{FFM}_{\mathrm{Def}}$ (3.72). This fixed point iteration formula is convergent if it is contractive, *i.e.* if

$$\left|\frac{dG_{\chi,2}\left[\chi_2^{(i)}\right]}{d\chi_2^{(i)}}\right| < 1 \tag{3.76}$$

The derivative in this expression is given by

$$\frac{dG_{\chi,2}\left[\chi_2^{(i)}\right]}{d\chi_2^{(i)}} = \frac{dG^{\mathrm{I}}_{\chi,2}\left[\chi^{(i)}_{\mathrm{NL},2}\right]}{d\chi^{(i)}_{\mathrm{NL},2}}\frac{G^{\mathrm{II}}_{\chi,2}\left[\chi_2^{(i)}\right]}{d\chi_2^{(i)}} = T_{\chi,2}\frac{d\chi_{\mathrm{NL},2}\left[\chi_2^{(i)}\right]}{d\chi_2^{(i)}} \tag{3.77}$$

Thence, recalling (3.44) and (3.42),

$$\frac{dG_{\chi,2}\left[\chi_2^{(i)}\right]}{d\chi_2^{(i)}} = T_{\chi,2}\,\beta_{\chi,2} \quad \text{with} \quad \beta_{\chi,2} = \frac{EI_{\mathrm{A},2} - EI_2}{EI_{\mathrm{A},2}} \tag{3.78}$$

and finally, introducing the expressions for $T_{\chi,2}$ (3.71.2) and for EI_2 (3.57.1),

$$\frac{d\chi_2^{(i+1)}}{d\chi_2^{(i)}} = \frac{dG_{\chi,2}\left[\chi_2^{(i)}\right]}{d\chi_2^{(i)}} = \frac{EI_{\mathrm{A},2} - \left(1+\left(\chi_2^{(i)}\right)^2\right)^{-\frac{3}{2}}}{EI_{\mathrm{A},2} + \frac{1}{4}} \tag{3.79}$$

Figure 3.13 represents this derivative for positive values of the curvature and for several values of $EI_{\mathrm{A},2}$ in the interval $[0,+\infty[$. This figure shows that if $EI_{\mathrm{A},2} > 0.375$, condition (3.76) is satisfied whatever the value of the curvature $\chi_2^{(i)}$; thence, $EI_{\mathrm{A},2} > 0.375$ is a sufficient condition for convergence of the iteration formula (3.72). However, this is not a necessary condition for convergence. Actually, formula (3.72) happened to converge numerically for $EI_{\mathrm{A},2} \geq 0.0334$. Figure 3.14 illustrates the beginning of the iterative procedure for $EI_{\mathrm{A},2} = 0.0334$. The sufficient convergence condition of $\mathrm{FFM_{Def}}$ (3.48) applied to this structure gives $\left|\beta_{\chi,2}\right| < 1$, *i.e.* $EI_{\mathrm{A},2} > \max EI_2/2 = 0.5$. However, condition (3.76) is also satisfied in the interval $0.375 < EI_{\mathrm{A},2} < 0.5$, because in this interval $\left|T_{\chi,2}\right| < 1$.

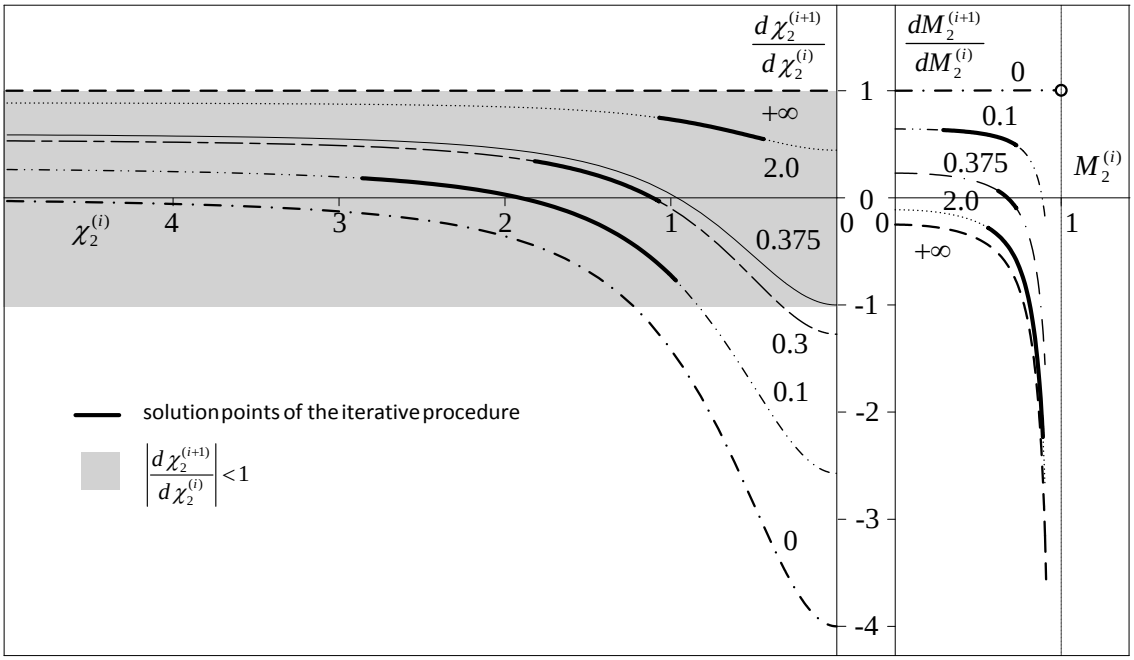

Figure 3.13. Example 3.1: Derivatives $d\chi_2^{(i+1)}/d\chi_2^{(i)}$ and $dM_2^{(i+1)}/dM_2^{(i)}$ for $EI_{\mathrm{A},2} \in \{0, 0.1, \cdots, \infty\}$.

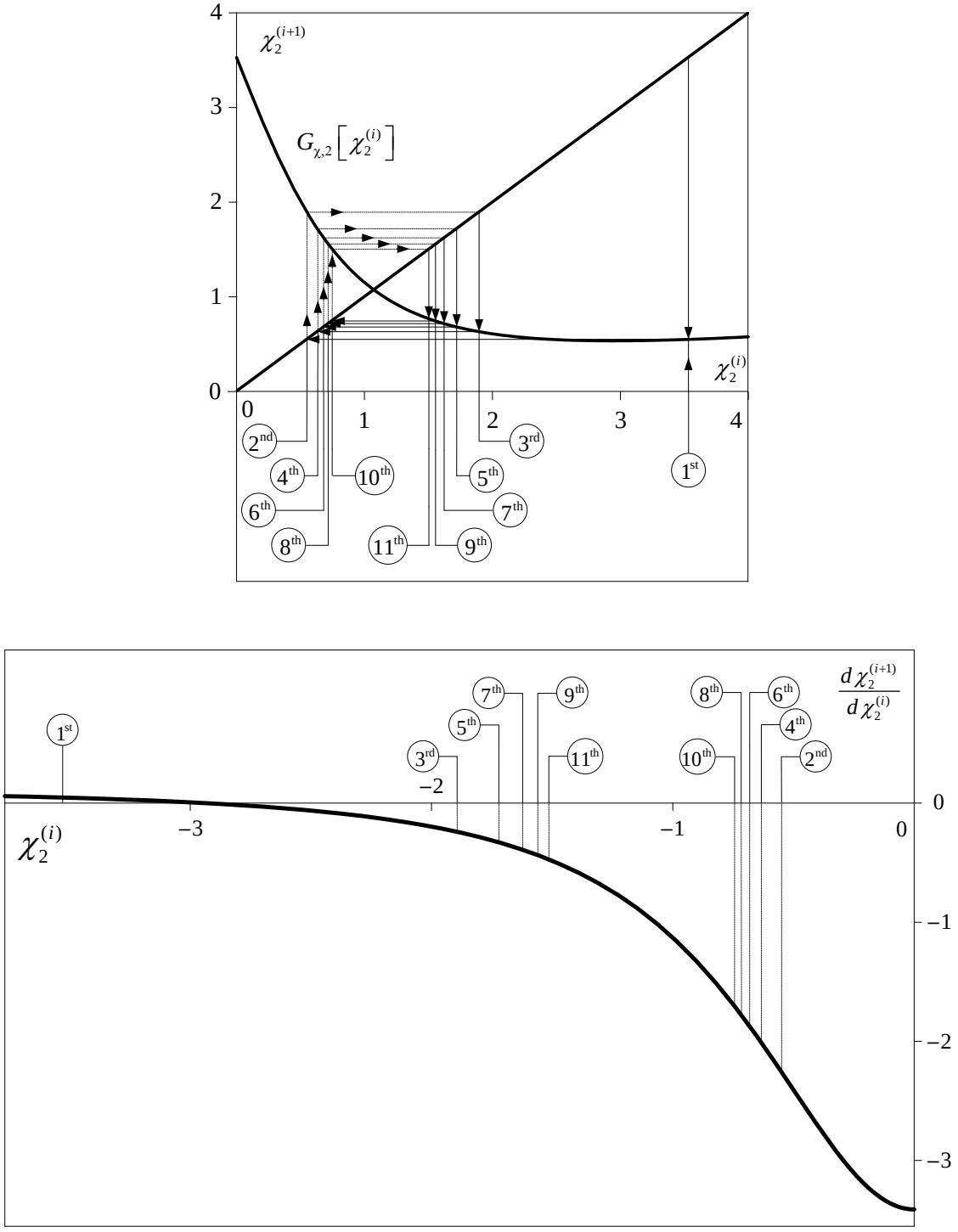

Figure 3.14. Example 3.1: Initial iterations of FFM_{Def} for $EI_{\text{A},2} = 0.0334$.

As a numerical criterion for FFM_{Def} to converge, the maximum relative error of the curvature value, when compared to the exact solution $\chi_{2,\text{ex}}$, must be less than a given tolerance, *i.e.* $\left|\left(\chi_2^{(j)} - \chi_{2,\text{ex}}\right)/\chi_{2,\text{ex}}\right| < tol$. Let us define a tolerance of $tol = 0.001$. Figure 3.15 shows the number of iterations required for FFM_{Def} to converge for values of $EI_{\text{A},2}$ in the interval $[0.1, 2.0]$. Note that the fastest convergence corresponds approximately to $EI_{\text{A},2} = 0.3$. Figure 3.13

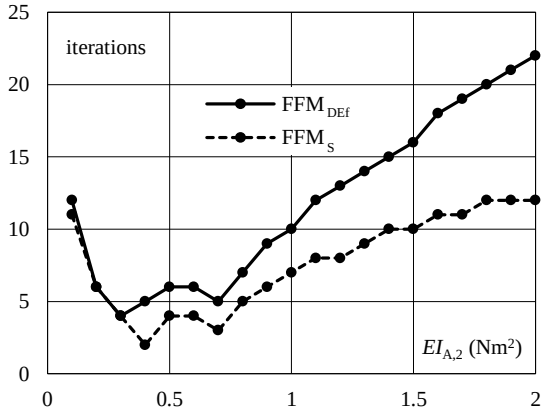

Figure 3.15. Example 3.1: Number of iterations required by FFM to converge.

representing the derivative (3.79) also represents the solution points of the iterative procedure for this value of $EI_{\mathrm{A},2}$ and also for 0.1 and 2.0. Figure 3.13 and Figure 3.15 show that, as expected, the number of iterations needed for $\mathrm{FFM}_{\mathrm{Def}}$ to converge is minimum when $\left| d\chi_2^{(i+1)} / d\chi_2^{(i)} \right|$ is minimum.

Let us now analyse $\mathrm{FFM}_{\mathrm{S}}$ iteration formula (3.75). This fixed point iteration formula is convergent if it is contractive, *i.e.*

$$\left| \frac{dG_{\mathrm{M},2}\left[M_2^{(i)} \right]}{dM_2^{(i)}} \right| < 1 \tag{3.80}$$

The derivative in the above condition is given by

$$\frac{dG_{\mathrm{M},2}\left[M_2^{(i)} \right]}{dM_2^{(i)}} = \frac{dG_{\mathrm{M},2}^{\mathrm{I}}\left[M_{\mathrm{F},2}^{(i)} \right]}{dM_{\mathrm{F},2}^{(i)}} \frac{dG_{\mathrm{M},2}^{\mathrm{II}}\left[M_2^{(i)} \right]}{dM_2^{(i)}} = T_{\mathrm{M},2} \frac{dM_{\mathrm{F},2}\left[M_2^{(i)} \right]}{dM_2^{(i)}} \tag{3.81}$$

or, according to expressions (3.45) and (3.43)

$$\frac{dG_{\mathrm{M},2}\left[M_2^{(i)} \right]}{dM_2^{(i)}} = T_{\mathrm{M},2}\ \beta_{\mathrm{M},2} \quad \text{with} \quad \beta_{\mathrm{M},2} \equiv \frac{EI_{\mathrm{A},2} - EI_2}{EI_2} \tag{3.82}$$

and finally, recalling (3.74.2) and (3.57.2),

$$\frac{dM_2^{(i+1)}}{dM_2^{(i)}} = \frac{dG_{\mathrm{M},2}\left[M_2^{(i)} \right]}{dM_2^{(i)}} = \frac{1 - EI_{\mathrm{A},2}\left(1 - \left(M_2^{(i)} \right)^2 \right)^{-\frac{3}{2}}}{1 + 4EI_{\mathrm{A},2}} \tag{3.83}$$

Figure 3.13 represents this derivative for positive values of the bending moment and for several positive values of $EI_{\mathrm{A},2}$. In this case, there is not an interval of values of $EI_{\mathrm{A},2}$ for which

condition (3.80) is satisfied for arbitrary values of $dM_2^{(i+1)}/dM_2^{(i)}$, see Figure 3.13, *i.e.* there is no sufficient condition for convergence of iteration formula (3.75). This result is coherent with the sufficient convergence condition of FFM_S (3.49), which, when applied to this structure, gives $\left|\beta_{\text{M},2}\right|<1$. This condition cannot be satisfied since $\min EI_2 \to 0$ and therefore

$$\beta_{\text{M},2}^{\max}=\frac{EI_{\text{A},2}-\min EI_2}{\min EI_2}\to+\infty \tag{3.84}$$

In spite of this result, iteration formula (3.75) happened to converge numerically for $EI_{\text{A},2}\le 8.582$. For $EI_{\text{A},2}>8.582$ the iterative procedure is interrupted as soon as $\left|M_2^{(j)}\right|>1$, because the constitutive relation (3.51.1) is defined only for $\left|M\right|<1$. For instance, for $EI_{\text{A},2}=9$ the iterative procedure is interrupted at the fifth iteration because $M_2^{(5)}=1.0069>1$, see Figure 3.16.

The numerical criterion for FFM_S to converge is similar to that adopted for FFM_{Def}. Thence, the maximum relative error of the bending moment value, when compared to the exact solution $M_{2,\text{ex}}$, must be less than the fixed tolerance of $tol = 0.001$, *i.e.* $\left|\left(M_2^{(j)}-M_{2,\text{ex}}\right)/M_{2,\text{ex}}\right|<tol$. Figure 3.15 also shows the number of iterations required for FFM_S to converge for several $EI_{\text{A},2}$ values in the range $[0.1,2]$. Figure 3.13 and Figure 3.15 show that number of iterations required for FFM_S to converge is also a minimum when the derivative $\left|dM_2^{(i+1)}/dM_2^{(i)}\right|$ is a minimum. Figure 3.15 also shows that, in this example FFM_S converges faster than FFM_{Def}.

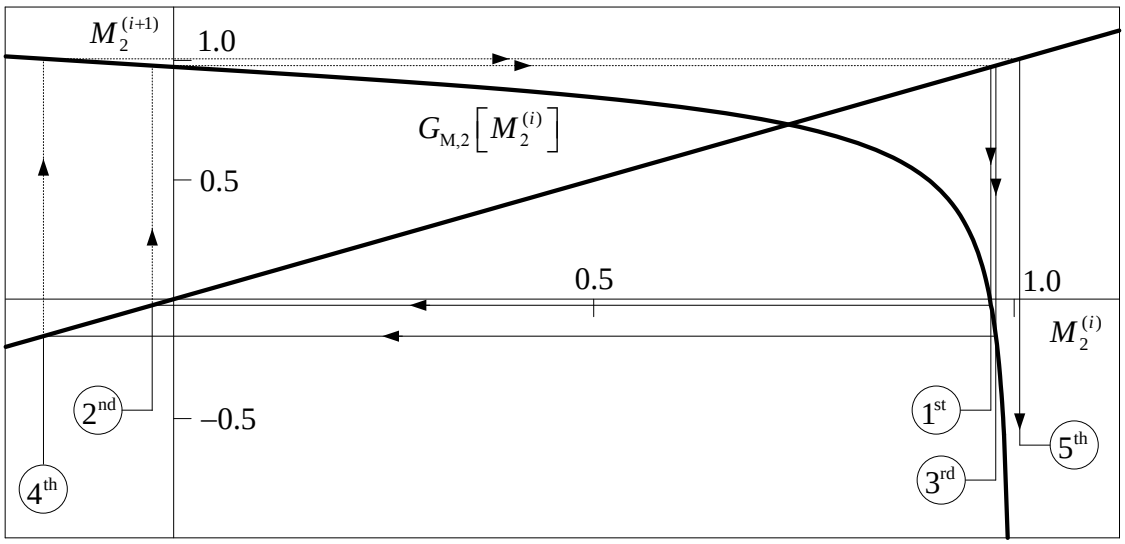

Figure 3.16. Example 3.1: Divergence of FFM_S for $EI_{\text{A},2}=9$.

3.4. Elemental fictitious force system

This section presents the fictitious force system of FFM(*M*) for a beam element. The definition of a mesh of beam elements (domain partition) and the description of the beam element are presented in § 3.4.1. The differential description of the fictitious force system is then presented in § 3.4.2. A decomposition of the elemental fields is presented in § 3.4.3. Finally, two discrete descriptions of the fictitious force system are presented in § 3.4.4.

3.4.1. Domain partition

Figure 3.17a illustrates part of a beam under a generic loading, composed of transverse distributed loads q, transverse point loads Q and moments $\mathcal{M}$. The bending moment and curvature fields in the beam are linked by the equivalent function compositions

$$\tilde{M} = \hat{M}\left[\tilde{\chi}\right] \quad \text{or} \quad \tilde{\chi} = \hat{\chi}\left[\tilde{M}\right] \tag{3.85}$$

The tilde over a symbol denotes a field, *i.e.* a function of x. For example, the function $\tilde{q}$ represents a transverse distributed load and $\tilde{M}$ and $\tilde{V}$ are the bending moment and shear force fields in the element. The jump discontinuity of the generic function of x, $\tilde{g}\left[x\right]$, at a given point, $x = x_0$, is defined by

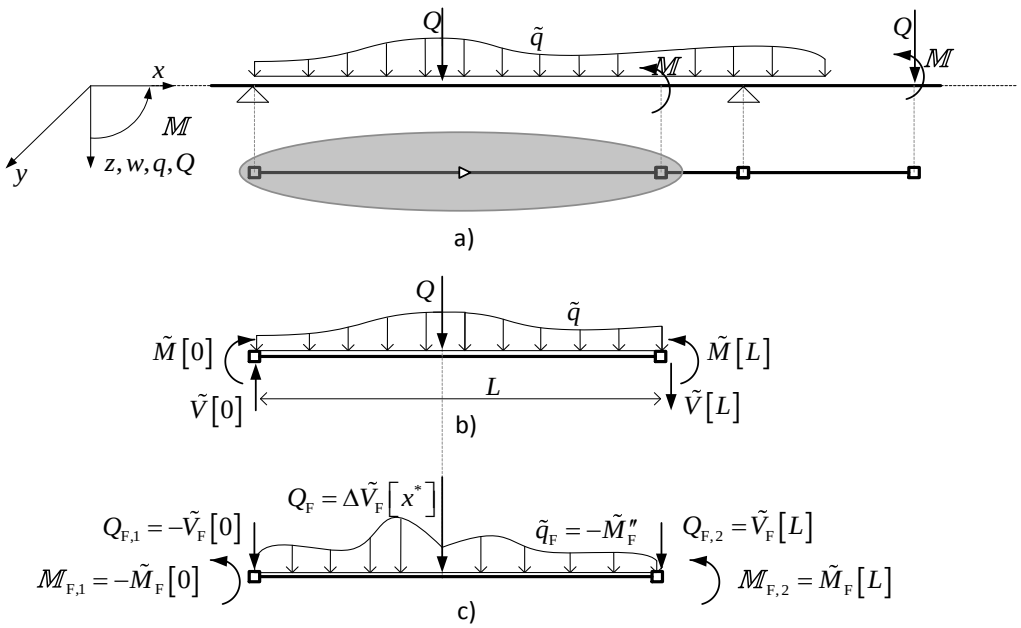

Figure 3.17. a) Beam partition b) effective and c) fictitious elemental force systems and corresponding internal forces at beam ends.

$$\Delta\tilde{g}\left[x_0\right] \equiv \tilde{g}\left[x_0^+\right] - \tilde{g}\left[x_0^-\right] \tag{3.86}$$

For example, if a transverse load Q is applied at section x_0, this is a point of discontinuity of $\tilde{V}$ and $\Delta\tilde{V}\left[x_0\right] = Q$.

Figure 3.17a shows a partition of the beam into elements, according to its geometry (each element is prismatic), supports and loading. The partition or mesh has a mandatory (or natural) node next to every support and, for the differential description presented in the following section, also at each section with an applied moment $\mathcal{M}$. Thence, the field $\tilde{M}$ is continuous in each element. Since $\hat{\chi}\left[M\right]$ is also continuous (§ 3.1) then, according to (3.85.2), $\tilde{\chi}$ is continuous in each element as well. The bending stiffness field is given by

$$\widetilde{EI} = \widehat{EI}\left[\tilde{\chi}\right] \quad \text{or} \quad \widetilde{EI} = \widehat{EI}\left[\tilde{M}\right] \tag{3.87}$$

A new system of coordinates is established for each element, obtained by a simple coordinate translation so that the element end sections correspond now to $x = 0$ and $x = L$, where L is the element length. For simplicity reasons the new system will also be denoted *oxyz*.

3.4.2. Differential description of the elemental fictitious force system

Until this point the auxiliary bending stiffness was allowed to vary from section to section. An important hypothesis, which will be adopted from now on, is the choice of a constant value for the auxiliary bending stiffness field in each element, *i.e.*

$$\widetilde{EI}_{\mathrm{A}}\left[x\right] = EI_{\mathrm{A}} = \mathrm{const} \tag{3.88}$$

Recalling the definition (3.9), the auxiliary bending moment field is given by

$$\tilde{M}_{\mathrm{A}} = \hat{M}_{\mathrm{A}}\left[\tilde{\chi}\right] \tag{3.89}$$

Thence, according to expressions (3.12), (3.89) and (3.85.1), the fictitious bending moment field can be written in terms of the curvature field, as required by $\mathrm{FFM_{Def}}$,

$$\tilde{M}_{\mathrm{F}} = \tilde{M}_{\mathrm{A}} - \tilde{M} = \hat{M}_{\mathrm{A}}\left[\tilde{\chi}\right] - \hat{M}\left[\tilde{\chi}\right] \tag{3.90}$$

Alternatively, according to expression (3.14), the fictitious bending moment field can be written in terms of the effective bending moment field, as required by $\mathrm{FFM_S}$,

$$\tilde{M}_{\mathrm{F}} = EI_{\mathrm{A}}\,\hat{\chi}\left[\tilde{M}\right] - \tilde{M} \tag{3.91}$$

Similarly, recalling again (3.9), the auxiliary component of the curvature field is given by

$$\tilde{\chi}_{\mathrm{A}} = \hat{\chi}_{\mathrm{A}}\left[\tilde{M}\right] \tag{3.92}$$

and, recalling (3.19), the nonlinear components of the curvature field is given by

$$\tilde{\chi}_{\mathrm{NL}} = \tilde{\chi} - \tilde{\chi}_{\mathrm{A}} \tag{3.93}$$

The elemental fictitious force system F_{F} is in equilibrium with the fictitious internal forces $\tilde{M}_{\mathrm{F}}$ and $\tilde{V}_{\mathrm{F}}$. It is therefore composed of:

(i) a transverse distributed force,

$$\tilde{q}_{\mathrm{F}} = -\tilde{M}_{\mathrm{F}}'' \tag{3.94}$$

(ii) transverse point forces at sections x_i,

$$Q_{\mathrm{F},i} = -\Delta\tilde{V}_{\mathrm{F}}\left[x_i\right] \tag{3.95}$$

(iii) in-plane moments at sections x_i,

$$\mathcal{M}_{\mathrm{F},i} = -\Delta\tilde{M}_{\mathrm{F}}\left[x_i\right] \tag{3.96}$$

The point forces and moments are located at the sections where the shear force $\tilde{V}_{\mathrm{F}}$ and bending moment $\tilde{M}_{\mathrm{F}}$ fields ($i > 2$), respectively, are discontinuous or at the ends of the element ($i = 1, 2$). Essentially, since $\tilde{M}_{\mathrm{F}}$ and $\tilde{V}_{\mathrm{F}}$ can have a non null value at the element boundaries, the corresponding elemental fictitious moments and point forces are given by

$$\begin{cases} Q_{\mathrm{F},1} = -\tilde{V}_{\mathrm{F}}\left[0\right] \\ \mathcal{M}_{\mathrm{F},1} = -\tilde{M}_{\mathrm{F}}\left[0\right] \end{cases} \tag{3.97}$$

at the beam left end and

$$\begin{cases} Q_{\mathrm{F},2} = \tilde{V}_{\mathrm{F}}\left[L\right] \\ \mathcal{M}_{\mathrm{F},2} = \tilde{M}_{\mathrm{F}}\left[L\right] \end{cases} \tag{3.98}$$

at the beam right end. These boundary forces assure self-equilibrated nature of the elemental fictitious force system.

It was shown in § 3.4.1 that, because of the hypotheses assumed so far, $\tilde{M}$ and $\tilde{\chi}$ are continuous in each element. Then, according to the expressions (3.90) and (3.91), the field $\tilde{M}_{\mathrm{F}}$ is also continuous in each element. Hence, according to (3.96), there are no fictitious moments $\mathcal{M}_{\mathrm{F}}$ inside any element. On the other hand, there may exist fictitious point forces Q_{F} inside an element, since $\tilde{V}_{\mathrm{F}}$ can be discontinuous at two types of sections: (i) sections where point loads

Q are applied and (ii) sections associated with discontinuity points of the cross-sectional bending stiffness $\widehat{EI}[\chi]$, see § 3.1. Figure 3.17c shows the fictitious force system for a beam element.

3.4.3. Decomposition of the elemental fields

A generic elemental field $\tilde{g}[x]$ can always be decomposed according to

$$\tilde{g} = \tilde{g}_{\Delta} + \tilde{g}_{\delta} \tag{3.99}$$

where the field

$$\tilde{g}_{\Delta} = \overline{\mathbf{n}}^{\mathrm{T}} \overline{\mathbf{g}} \tag{3.100}$$

is the linear interpolation of $\tilde{g}$ between its values at the element ends collected in the vector

$$\overline{\mathbf{g}} = \left[\tilde{g}[0] \quad \tilde{g}[L] \right]^{\mathrm{T}} \tag{3.101}$$

and

$$\overline{\mathbf{n}}^{\mathrm{T}} = \left[\tilde{n}_1 \quad \tilde{n}_2 \right] \tag{3.102}$$

is the vector of linear interpolation shape functions

$$\begin{cases} \tilde{n}_1 = 1 - \dfrac{x}{L} \\ \tilde{n}_2 = \dfrac{x}{L} \end{cases} \tag{3.103}$$

In this thesis, bold symbols denote matrices (upper case) or vectors (lower case, with a few exceptions) and a bar over a bold symbol denotes an elemental matrix or vector.

The corrective field $\tilde{g}_{\delta}$ is given by the deviation of $\tilde{g}$ w.r.t. the linear interpolation field $\tilde{g}_{\Delta}$ and thus $\tilde{g}_{\delta}[0] = \tilde{g}_{\delta}[L] = 0$. For example, the elemental decomposition of the curvature field and of its nonlinear component is given by

$$\tilde{\chi} = \tilde{\chi}_{\Delta} + \tilde{\chi}_{\delta} \tag{3.104}$$

$$\tilde{\chi}_{\mathrm{NL}} = \tilde{\chi}_{\mathrm{NL},\Delta} + \tilde{\chi}_{\mathrm{NL},\delta} \tag{3.105}$$

Since the curvature field $\tilde{\chi}_{\Delta}$ is linear, it is well characterized by two parameters, which are the rotations at the end sections w.r.t. the element chord (§ 3.5.1).

Similarly, the decomposition of the fields of effective bending moments is given by

$$\tilde{M} = \tilde{M}_{\Delta} + \tilde{M}_{\delta} \tag{3.106}$$

Moreover, according to the constitutive relation (3.9),

$$\tilde{M}_{\delta} = EI_{\mathrm{A}}\, \tilde{\chi}_{\mathrm{A},\delta} \tag{3.107}$$

The corrective field $\tilde{M}_{\delta}$ equilibrates the part of the force system applied between the element end sections and, because of its null value at the end sections, it can be viewed as the bending moment field in a simply supported element. Thence, in the case of a structure subjected to direct actions only, like those studied in this thesis (§ 3.1), the effective and the linear (3.10) corrective fields are one and the same,

$$\tilde{M}_{\mathrm{L},\delta} = \tilde{M}_{\delta} \tag{3.108}$$

Dividing both members of this expression by EI_{A} and introducing (3.107) and (3.10) it can also be concluded that

$$\tilde{\chi}_{\mathrm{L},\delta} = \tilde{\chi}_{\mathrm{A},\delta} \tag{3.109}$$

3.4.4. Discrete descriptions of the elemental fictitious force system

A discrete description of the 1D beam element represents the fields of displacements, generalized strains and internal forces by an interpolation of these fields at a finite number of sections of the element, the so-called interpolation sections. This process reduces the governing equilibrium, compatibility and constitutive field equations to a matrix form involving quantities defined at these sections.

In order to write in the discrete form the corrective terms $\tilde{M}_{\delta}$ (resp. $\tilde{\chi}_{\mathrm{A},\delta}$) and $\tilde{M}_{\mathrm{F},\delta}$ (resp. $\tilde{\chi}_{\mathrm{NL},\delta}$), the part of the elemental force system applied between nodes should be known in advance. This means that even though the discrete description of $\tilde{M}_{\delta}$ and $\tilde{\chi}_{\mathrm{A},\delta}$ is a trivial task, as shown above, the same cannot be said of $\tilde{M}_{\mathrm{F},\delta}$ and $\tilde{\chi}_{\mathrm{NL},\delta}$, because the fictitious force system is not known in advance. This difficulty can be overcome by imposing the form of the part of the force system between end nodes, *i.e.*, the shape of the elemental nonlinear component of the curvature $\tilde{\chi}_{\mathrm{NL},\delta}$, or the effective bending stiffness $\widetilde{EI}$, which is emulated by $\tilde{\chi}_{\mathrm{NL},\delta}$ in the auxiliary problem, see § 3.2.1. Of course, these constraints are in fact additional simplifying discretization assumptions at the element level. In what follows, two discrete

descriptions of the elemental fictitious force system of FFM are introduced, which emerge from two distinct simplifying assumptions for $\tilde{\chi}_{\mathrm{NL},\delta}$ and, therefore, $\tilde{M}_{\mathrm{F},\delta}$.

3.4.4.1. Basic discrete description of the elemental fictitious force system

In the basic discrete description of the elemental fictitious force system, the corrective field $\tilde{\chi}_{\mathrm{NL},\delta}$ and, therefore, $\tilde{M}_{\mathrm{F},\delta}$, are ignored,

$$\tilde{\chi}_{\mathrm{NL},\delta} = \tilde{\chi}_{\mathrm{NL2},\delta} = 0 \quad \text{and} \quad \tilde{M}_{\mathrm{F},\delta} = \tilde{M}_{\mathrm{F2},\delta} = 0 \tag{3.110}$$

Hence, the nonlinear component of the curvature and the fictitious bending moment fields become linear (affine) functions of x, *i.e.* it is assumed that $\tilde{\chi}_{\mathrm{NL}} = \tilde{\chi}_{\mathrm{NL},\Delta}$ and $\tilde{M}_{\mathrm{F}} = \tilde{M}_{\mathrm{F},\Delta}$. This discretization is therefore based on the value of the structural fields at the elements end sections only. This explains the subscript 2, *e.g.* $\mathrm{NL2}$ and $\mathrm{F2}$ in the expression above, for this approximate description, indicating the number of interpolation sections used.

Since the basic discrete fictitious force system must equilibrate the bending moments $\tilde{M}_{\mathrm{F}} = \tilde{M}_{\mathrm{F},\Delta}$, it is exclusively formed by moments and point forces at the element boundary sections, which are the moments of the differential description (3.97) and (3.98) plus the couple

$$Q_{\mathrm{F2},2} = -Q_{\mathrm{F2},1} = \frac{1}{L}\left(\tilde{M}_{\mathrm{F}}[L] - \tilde{M}_{\mathrm{F}}[0]\right) = \frac{1}{L}\left(\mathcal{M}_{\mathrm{F2},1} + \mathcal{M}_{\mathrm{F2},2}\right) \tag{3.111}$$

in equilibrium with them. This elemental system of forces is statically equivalent to that of the differential description, as proved in the following lines.

For the sake of simplicity, and as Figure 3.17c illustrates, let us consider that the fictitious force system has a single point force applied at the arbitrary section x^* inside the element, besides those at the boundaries. If the couple (3.111) is statically equivalent to the distributed load $\tilde{q}_{\mathrm{F}}$ and the point forces F_{F} then its forces are given by

$$\begin{aligned} Q_{\mathrm{F2},i} &= Q_{\mathrm{F},1}\,\tilde{n}_i[0] + Q_{\mathrm{F},2}\,\tilde{n}_i[L] + Q_{\mathrm{F},x^*}\,\tilde{n}_i[x^*] + \int_0^L \tilde{q}_{\mathrm{F}}\,\tilde{n}_i\,dx \\ &= Q_{\mathrm{F},i} + Q_{\mathrm{F},x^*}\,\tilde{n}_i[x^*] - \int_0^{x^*} \tilde{V}'_{\mathrm{F}}\,\tilde{n}_i\,dx - \int_{x^*}^L \tilde{V}'_{\mathrm{F}}\,\tilde{n}_i\,dx, \quad i = 1,2 \end{aligned} \tag{3.112}$$

Due to the transverse point force at x^*, the field $\tilde{V}_\mathrm{F}$ is not differentiable at this section and the integral $\int_0^L \tilde{V}_\mathrm{F}'\,\tilde{n}_i\,dx$ does not make sense: this explains the need to decompose the domain of integration at x^* in the above expression. Integrating by parts the last terms in the second member, and noting that $\tilde{n}_i' = (-1)^i / L$, see (3.103), gives

$$\begin{aligned}
-\int_0^{x^*} \tilde{V}_\mathrm{F}'\,\tilde{n}_i\,dx &= -\left[\tilde{V}_\mathrm{F}\,\tilde{n}_i\right]_0^{x^{*-}} + \int_0^{x^*} \tilde{V}_\mathrm{F}\,\tilde{n}_i'\,dx \\
&= -\tilde{V}_\mathrm{F}\left[x^{*-}\right]\tilde{n}_i\left[x^{*-}\right] + \tilde{V}_\mathrm{F}[0]\,\tilde{n}_i[0] + \frac{(-1)^i}{L}\int_0^{x^*} \tilde{V}_\mathrm{F}\,dx \qquad (3.113)\\
&= -\tilde{V}_\mathrm{F}\left[x^{*-}\right]\,\tilde{n}_i\left[x^{*-}\right] + \tilde{V}_\mathrm{F}[0]\,\tilde{n}_i[0] + \frac{(-1)^i}{L}\left(\tilde{M}_\mathrm{F}\left[x^*\right] - \tilde{M}_\mathrm{F}[0]\right)
\end{aligned}$$

and similarly

$$-\int_{x^*}^{L} \tilde{V}_\mathrm{F}'\,\tilde{n}_i\,dx = \tilde{V}_\mathrm{F}\left[x^{*+}\right]\tilde{n}_i\left[x^{*+}\right] - \tilde{V}_\mathrm{F}[L]\,\tilde{n}_i[L] + \frac{(-1)^i}{L}\left(\tilde{M}_\mathrm{F}[L] - \tilde{M}_\mathrm{F}\left[x^*\right]\right) \qquad (3.114)$$

Adding (3.113) to (3.114), recalling the jump discontinuity definition (3.86) and (3.95), (3.97), (3.98) and noting that $\tilde{n}_i\left[x^{*-}\right] = \tilde{n}_i\left[x^{*+}\right] = \tilde{n}_i\left[x^*\right]$, gives

$$\begin{aligned}
\int_0^L \tilde{q}_\mathrm{F}\,\tilde{n}_i\,dx &= \Delta\tilde{V}_\mathrm{F}\left[x^*\right]\tilde{n}_i\left[x^*\right] + \tilde{V}_\mathrm{F}[0]\,\tilde{n}_i[0] - \tilde{V}_\mathrm{F}[L]\,\tilde{n}_i[L] + \frac{(-1)^i}{L}\left(\tilde{M}_\mathrm{F}[L] - \tilde{M}_\mathrm{F}[0]\right) \\
&= -Q_{\mathrm{F},x^*}\,\tilde{n}_i\left[x^*\right] - Q_{\mathrm{F},1}\,\tilde{n}_i[0] - Q_{\mathrm{F},2}\,\tilde{n}_i[L] + \frac{(-1)^i}{L}\left(\tilde{M}_\mathrm{F}[L] - \tilde{M}_\mathrm{F}[0]\right) \qquad (3.115)\\
&= -Q_{\mathrm{F},x^*}\,\tilde{n}_i\left[x^*\right] - Q_{\mathrm{F},i} + \frac{(-1)^i}{L}\left(\tilde{M}_\mathrm{F}[L] - \tilde{M}_\mathrm{F}[0]\right)
\end{aligned}$$

Finally, substituting this result into (3.112), gives

$$Q_{\mathrm{F}2,i} = +\frac{(-1)^i}{L}\left(\tilde{M}_\mathrm{F}[L] - \tilde{M}_\mathrm{F}[0]\right) \qquad (3.116)$$

which proves (3.111). This force system is represented in Figure 3.18, which also illustrates how the error associated with the basic discrete fictitious force system decreases by progressive mesh refinement. The example presented in § 3.7 illustrates this issue.

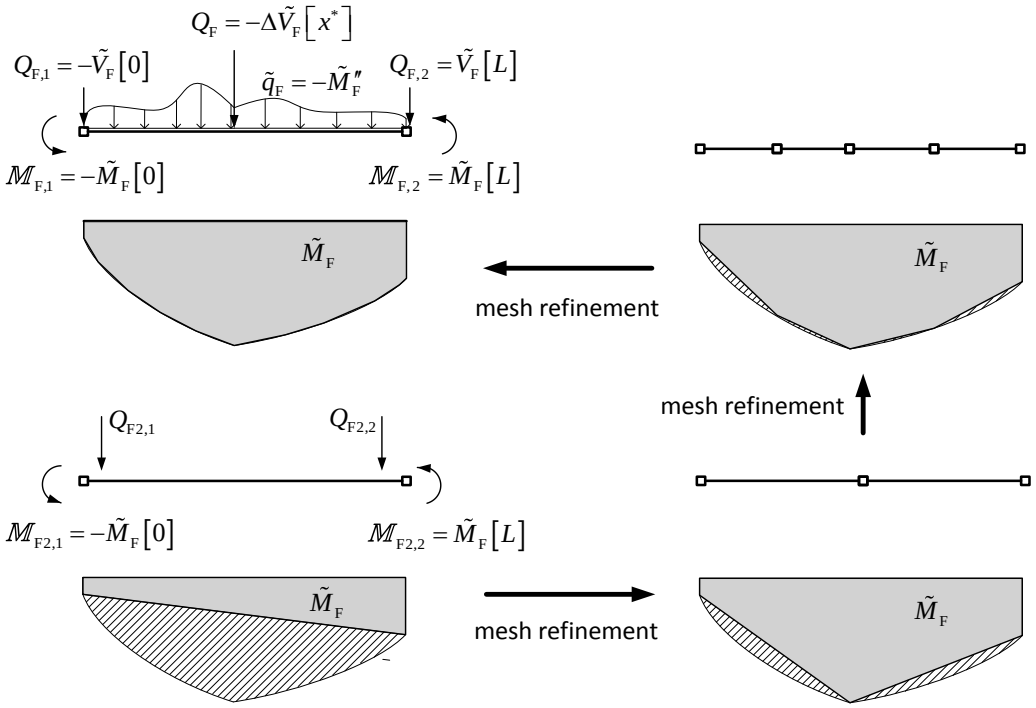

Figure 3.18. Differential and discrete components (basic description) of the elemental fictitious force system and error decrease with mesh refinement for the latter.

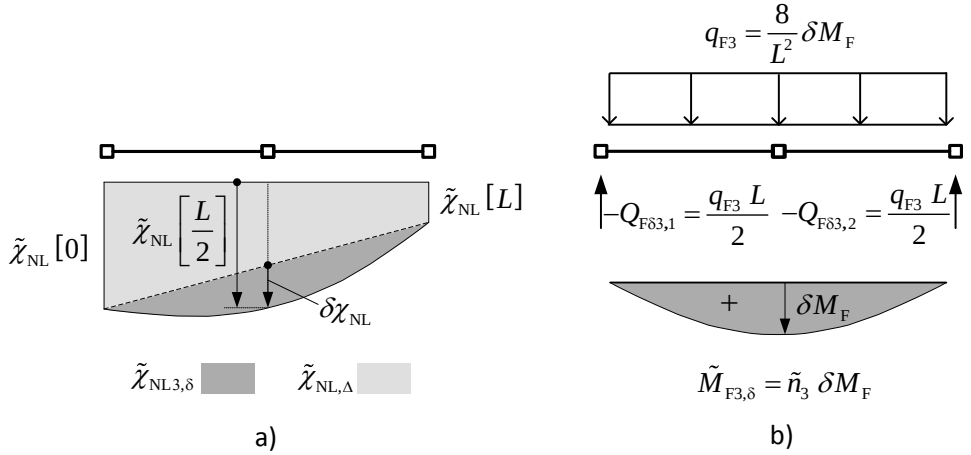

Figure 3.19. FFM_3: a) discretization and b) corresponding additional fictitious forces.

3.4.4.2. Improved discrete description of the elemental fictitious force system

In the improved discrete description of the elemental fictitious force system the corrective fields $\tilde{\chi}_{NL,\delta}$ and, therefore, $\tilde{M}_{F,\delta}$ are approximated by quadratic functions. This requires a third interpolation section which is the element midsection, see Figure 3.19a.

Thence, introducing the quadratic shape function with unit value at midspan and zero value at the element end sections,

$$\tilde{n}_3 \equiv 4\tilde{n}_1\,\tilde{n}_2 \tag{3.117}$$

the corrective nonlinear component of the curvatures $\tilde{\chi}_{\mathrm{NL},\delta}$ is approximated by

$$\tilde{\chi}_{\mathrm{NL3},\delta} = \tilde{n}_3\,\delta\chi_{\mathrm{NL}} \tag{3.118}$$

where the corrective nonlinear component of curvature at midspan is given by

$$\delta\chi_{\mathrm{NL}} \equiv \tilde{\chi}_{\mathrm{NL}}\left[\frac{L}{2}\right] - \tilde{\chi}_{\mathrm{NL},\Delta}\left[\frac{L}{2}\right] \tag{3.119}$$

Similarly, the corrective fictitious bending moments $\tilde{M}_{\mathrm{F},\delta}$ are approximated by

$$\tilde{M}_{\mathrm{F3},\delta} = \tilde{n}_3\,\delta M_{\mathrm{F}} \tag{3.120}$$

with

$$\delta M_{\mathrm{F}} = EI_{\mathrm{A}}\,\delta\chi_{\mathrm{NL}} \tag{3.121}$$

This approximate corrective fictitious bending moment field is in equilibrium with an *approximate* transverse uniformly distributed force

$$q_{\mathrm{F3}} = \frac{8}{L^2}\delta M_{\mathrm{F}} \tag{3.122}$$

and two *approximate* transverse point forces, see Figure 3.19b,

$$Q_{\mathrm{F3},\delta,1} = Q_{\mathrm{F3},\delta,2} = -\frac{q_{\mathrm{F3}}\,L}{2} \tag{3.123}$$

This improved description is denoted by the subscript 3 because three interpolation sections are used. Its fictitious force system results from adding the components (3.122) and (3.123) to the basic discrete fictitious force system, *i.e.*

$$Q_{\mathrm{F3},i} = Q_{\mathrm{F2},i} + Q_{\mathrm{F3},\delta,i} \tag{3.124}$$

It is easily proved that the substitution of the approximation $\tilde{\chi}_{\mathrm{NL3},\delta} = \tilde{n}_3\,\delta\chi_{\mathrm{NL}}$ (3.118) into the decomposition $\tilde{\chi}_{\mathrm{NL}} = \tilde{\chi}_{\mathrm{NL},\Delta} + \tilde{\chi}_{\mathrm{NL},\delta}$ (3.105) gives the quadratic approximation of the nonlinear component of the curvatures

$$\tilde{\chi}_{\mathrm{NL}} \approx \bar{\mathbf{n}}^{*,\mathrm{T}}\,\bar{\boldsymbol{\chi}}^{*}_{\mathrm{NL}} \tag{3.125}$$

where the vector

$$\overline{\boldsymbol{\chi}}_{\mathrm{NL}}^{*}=\left[\begin{array}{ccc}\tilde{\chi}_{\mathrm{NL}}[0] & \tilde{\chi}_{\mathrm{NL}}\left[\frac{L}{2}\right] & \tilde{\chi}_{\mathrm{NL}}[L]\end{array}\right]^{\mathrm{T}} \tag{3.126}$$

collects the values of the field $\tilde{\chi}_{\mathrm{NL}}$ at the nodal points and the vector

$$\overline{\mathbf{n}}^{*}=\left[\begin{array}{ccc}\tilde{n}_{1}^{*} & \tilde{n}_{2}^{*} & \tilde{n}_{3}^{*}\end{array}\right]^{\mathrm{T}} \tag{3.127}$$

contains the quadratic Lagrange polynomials,

$$\begin{cases}\tilde{n}_{1}^{*}=\tilde{n}_{1}\left(1-2\tilde{n}_{2}\right) \\ \tilde{n}_{2}^{*}=\tilde{n}_{3}=4\tilde{n}_{1}\,\tilde{n}_{2} \\ \tilde{n}_{3}^{*}=\tilde{n}_{2}\left(1-2\tilde{n}_{1}\right)\end{cases} \tag{3.128}$$

The error associated with the improved discrete fictitious force system can be decreased by progressive mesh refinement. However, in order to achieve a given accuracy, the required mesh refinement is obviously lesser than for the basic discrete fictitious force system. The example presented in § 3.7 illustrates this issue.

3.5. FFM discrete descriptions: matrix methods of structural analysis

This and the next sections present the application of FFM(*M*) in the context of matrix methods of structural analysis. Each one of the discrete descriptions of the fictitious force systems introduced in §§ 3.4.4.1 and 3.4.4.2 conducts to a particular discrete description of FFM(*M*). These discrete descriptions are therefore denoted accordingly: the basic discrete description is denoted FFM$(M)_2$, or simply FFM_2 while the improved discrete description is denoted FFM$(M)_3$, or simply FFM_3.

3.5.1. Elemental kinematics (end sections rotations-curvature)

The elemental kinematic relations will now be established in a generic format valid for both FFM_2 and FFM_3. According to the virtual force principle, the rotations at the end sections w.r.t. the element chord are given by

$$\phi_{i}=\int_{0}^{L}\tilde{n}_{i}\,\tilde{\chi}\,dx+\sum_{j}\tilde{n}_{i}\left[x_{j}\right]\Delta\tilde{w}'\left[x_{j}\right]+\sum_{j}\tilde{n}_{i}'\left[x_{j}\right]\Delta\tilde{w}\left[x_{j}\right],\quad i=1,2 \tag{3.129}$$

where $\Delta\tilde{w}\left[x_j\right]$ is a transverse jump discontinuity and $\Delta\tilde{w}'\left[x_j\right]$ a rotational jump discontinuity, at section x_j. One of the hypotheses assumed in § 3.1 is that there are no such discontinuities, *i.e.,* $\tilde{w}\left[x\right]$ and its derivative are continuous in the element. Thence, the above expression becomes simply

$$\phi_i = \int_0^L \tilde{n}_i \, \tilde{\chi} \, dx, \quad i = 1,2 \tag{3.130}$$

These two values are gathered in the elemental vector

$$\overline{\boldsymbol{\phi}} = \left[\phi_1 \quad \phi_2\right]^{\mathrm{T}} \tag{3.131}$$

Inserting the elemental decomposition (3.104) into the above integral gives

$$\phi_i = \phi_{\Delta,i} + \phi_{\delta,i}\,, \quad i = 1,2 \tag{3.132}$$

where the components of the end section rotations w.r.t. the element chord are given by

$$\phi_{\Delta,i} = \int_0^L \tilde{n}_i \, \tilde{\chi}_\Delta \, dx, \quad i = 1,2 \tag{3.133}$$

$$\phi_{\delta,i} = \int_0^L \tilde{n}_i \, \tilde{\chi}_\delta \, dx, \quad i = 1,2 \tag{3.134}$$

which are represented in Figure 3.20. Collecting these rotations in vectors, gives

$$\overline{\boldsymbol{\phi}} = \overline{\boldsymbol{\phi}}_\Delta + \overline{\boldsymbol{\phi}}_\delta \tag{3.135}$$

$$\overline{\boldsymbol{\phi}}_\Delta = \left[\phi_{\Delta,1} \quad \phi_{\Delta,2}\right]^{\mathrm{T}} \tag{3.136}$$

$$\overline{\boldsymbol{\phi}}_\delta = \left[\phi_{\delta,1} \quad \phi_{\delta,2}\right]^{\mathrm{T}} \tag{3.137}$$

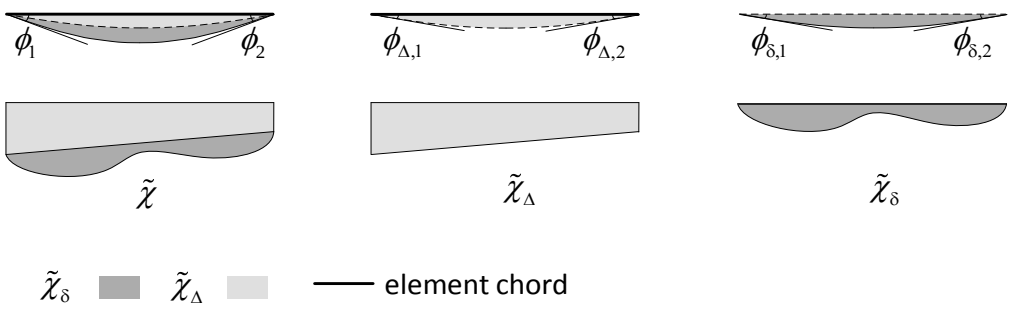

Figure 3.20. Decomposition of the end rotations w.r.t. element chord.

The expression (3.100) defines the linear component of the elemental curvature field,

$$\tilde{\chi}_{\Delta} = \overline{\mathbf{n}}^{\mathrm{T}}\, \overline{\boldsymbol{\chi}} \tag{3.138}$$

Substituting this into (3.133), gives

$$\overline{\boldsymbol{\phi}}_{\Delta} = \overline{\mathbf{F}}_0\, \overline{\boldsymbol{\chi}} \tag{3.139}$$

with

$$\overline{\mathbf{F}}_0 = \begin{bmatrix} \int_0^L \tilde{n}_1^2\, dx & \int_0^L \tilde{n}_1\, \tilde{n}_2\, dx \\ \int_0^L \tilde{n}_2\, \tilde{n}_1\, dx & \int_0^L \tilde{n}_2^2\, dx \end{bmatrix} = \frac{L}{6}\begin{bmatrix} 2 & 1 \\ 1 & 2 \end{bmatrix} \tag{3.140}$$

and substituting the previous expression into (3.135), gives

$$\overline{\boldsymbol{\phi}} = \overline{\mathbf{F}}_0\, \overline{\boldsymbol{\chi}} + \overline{\boldsymbol{\phi}}_{\delta} \tag{3.141}$$

According to (3.134), the rotations $\phi_{\delta,i}$ are determined by the field $\tilde{\chi}_{\delta}$, *i.e.*, they are determined solely by the actions applied between nodes[7]. However, there are many other curvature fields corresponding to the end sections rotations $\phi_{\delta,i}$, some of them not null at the end sections, contrary to what happens with $\tilde{\chi}_{\delta}$. The elemental equivalent curvature field $\tilde{\chi}_{\delta,\mathrm{eq}}$ is defined as the linear curvature field whose end sections rotations are equal to those of $\tilde{\chi}_{\delta}$, see Figure 3.21, *i.e.,*

$$\int_0^L \tilde{n}_i\, \tilde{\chi}_{\delta,\mathrm{eq}}\, dx = \phi_{\delta,i} = \int_0^L \tilde{n}_i\, \tilde{\chi}_{\delta}\, dx, \quad i = 1,2 \tag{3.142}$$

Since this equivalent curvature field is linear, it can be written as

$$\tilde{\chi}_{\delta,\mathrm{eq}} = \overline{\mathbf{n}}^{\mathrm{T}}\, \overline{\boldsymbol{\chi}}_{\delta,\mathrm{eq}} \tag{3.143}$$

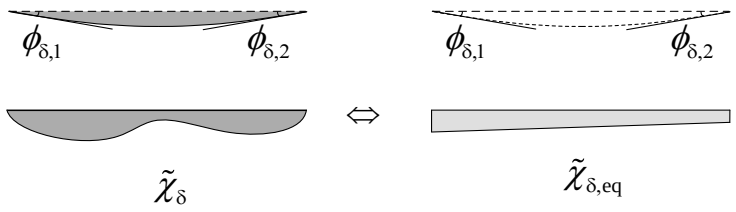

Figure 3.21. Kinematic equivalence of fields $\tilde{\chi}_{\delta}$ and $\tilde{\chi}_{\delta,\mathrm{eq}}$.

[7] But the converse is not true, *i.e.* the actions applied between nodes influence both $\phi_{\delta,i}$ and $\phi_{\Delta,i}$.

where

$$\bar{\boldsymbol{\chi}}_{\delta,\mathrm{eq}} = \left[\tilde{\chi}_{\delta,\mathrm{eq}}[0] \quad \tilde{\chi}_{\delta,\mathrm{eq}}[L] \right]^{\mathrm{T}} \tag{3.144}$$

gathers the values of $\tilde{\chi}_{\delta,\mathrm{eq}}$ at the end sections.

Left-multiplying both members of (3.139) by the inverse of (3.140),

$$\bar{\mathbf{K}}_0 = \bar{\mathbf{F}}_0^{-1} = \frac{2}{L}\begin{bmatrix} 2 & -1 \\ -1 & 2 \end{bmatrix} \tag{3.145}$$

gives

$$\bar{\boldsymbol{\chi}} = \bar{\boldsymbol{\chi}}_{\Delta} = \bar{\mathbf{K}}_0 \, \bar{\boldsymbol{\phi}}_{\Delta} \tag{3.146}$$

Replacing (3.143) into the left-hand side of (3.142), recalling the definition (3.140) and left-multiplying both members by $\bar{\mathbf{K}}_0$, gives

$$\bar{\boldsymbol{\chi}}_{\delta,\mathrm{eq}} = \bar{\mathbf{K}}_0 \, \bar{\boldsymbol{\phi}}_{\delta} \tag{3.147}$$

Adding these two expressions together and substituting the decomposition (3.135), gives

$$\bar{\boldsymbol{\chi}}_{\Delta} + \bar{\boldsymbol{\chi}}_{\delta,\mathrm{eq}} = \bar{\mathbf{K}}_0 \, \bar{\boldsymbol{\phi}} \tag{3.148}$$

It can also be noticed that, replacing expression (3.146) into (3.138), gives

$$\tilde{\chi}_{\Delta} = \bar{\mathbf{n}}^{\mathrm{T}} \, \bar{\mathbf{K}}_0 \, \bar{\boldsymbol{\phi}}_{\Delta} \tag{3.149}$$

which shows that the curvature field $\tilde{\chi}_{\Delta}$ is well characterized by the end sections rotations.

Consider now the curvature decomposition $\tilde{\chi}_{\mathrm{NL}} = \tilde{\chi} - \tilde{\chi}_{\mathrm{A}}$ (3.93). If it is inserted into (3.130), a similar decomposition of the end sections rotations is obtained

$$\phi_i = \phi_{\mathrm{A},i} + \phi_{\mathrm{NL},i} \,, \quad i = 1,2 \tag{3.150}$$

i.e.,

$$\bar{\boldsymbol{\phi}} = \bar{\boldsymbol{\phi}}_{\mathrm{A}} + \bar{\boldsymbol{\phi}}_{\mathrm{NL}} \tag{3.151}$$

Similarly, introducing into (3.134) the decomposition of $\tilde{\chi}_{\delta}$ into its linear and nonlinear components and using the equivalence (3.109), gives

$$\phi_{\delta,i} = \phi_{\mathrm{A},\delta,i} + \phi_{\mathrm{NL},\delta,i} = \phi_{\mathrm{L},\delta,i} + \phi_{\mathrm{NL},\delta,i} \,, \quad i = 1,2 \tag{3.152}$$

i.e.,

$$\bar{\boldsymbol{\phi}}_{\delta} = \bar{\boldsymbol{\phi}}_{\mathrm{A},\delta} + \bar{\boldsymbol{\phi}}_{\mathrm{NL},\delta} = \bar{\boldsymbol{\phi}}_{\mathrm{L},\delta} + \bar{\boldsymbol{\phi}}_{\mathrm{NL},\delta} \tag{3.153}$$

where $\phi_{\mathrm{NL},\delta,i}$ (resp. $\phi_{\mathrm{L},\delta,i} = \phi_{\mathrm{A},\delta,i}$) are the end sections rotations due to the part of the fictitious (resp. effective) force system applied between nodes.

Writing the kinematic relation (3.146) for the nonlinear component of the curvature and introducing the linear plus corrective term decomposition, gives

$$\bar{\boldsymbol{\chi}}_{\mathrm{NL}} = \bar{\boldsymbol{\chi}}_{\mathrm{NL},\Delta} = \bar{\mathbf{K}}_0 \, \bar{\boldsymbol{\phi}}_{\mathrm{NL},\Delta} = \bar{\mathbf{K}}_0 \, \bar{\boldsymbol{\phi}}_{\mathrm{NL}} - \bar{\mathbf{K}}_0 \, \bar{\boldsymbol{\phi}}_{\mathrm{NL},\delta} \tag{3.154}$$

It can also be defined a linear curvature field $\tilde{\chi}_{\mathrm{NL},\delta,\mathrm{eq}}$ kinematically equivalent to $\tilde{\chi}_{\mathrm{NL},\delta}$, *i.e.*, which corresponds to equal end sections rotations,

$$\bar{\boldsymbol{\chi}}_{\mathrm{NL},\delta,\mathrm{eq}} = \bar{\mathbf{K}}_0 \, \bar{\boldsymbol{\phi}}_{\mathrm{NL},\delta} \tag{3.155}$$

which is similar to (3.147). Substituting this expression into (3.154) gives

$$\bar{\boldsymbol{\chi}}_{\mathrm{NL},\Delta} + \bar{\boldsymbol{\chi}}_{\mathrm{NL},\delta,\mathrm{eq}} = \bar{\mathbf{K}}_0 \, \bar{\boldsymbol{\phi}}_{\mathrm{NL}} \tag{3.156}$$

In order to calculate $\bar{\boldsymbol{\chi}}_{\mathrm{NL},\delta,\mathrm{eq}}$ the end sections rotations $\bar{\boldsymbol{\phi}}_{\mathrm{NL},\delta}$ are required. Their calculation depends on the chosen discrete description of the fictitious force system. If the basic discrete description is adopted the approximation $\tilde{\chi}_{\mathrm{NL},\delta} = 0$ is assumed and therefore

$$\phi_{\mathrm{NL}2,\delta,i} = \int_0^L \tilde{n}_i \; \tilde{\chi}_{\mathrm{NL}2,\delta} \, dx = 0, \quad i = 1,2 \tag{3.157}$$

i.e.,

$$\bar{\boldsymbol{\phi}}_{\mathrm{NL}2,\delta} = \mathbf{0} \tag{3.158}$$

and

$$\bar{\boldsymbol{\chi}}_{\mathrm{NL}2,\delta,\mathrm{eq}} = \bar{\mathbf{K}}_0 \, \bar{\boldsymbol{\phi}}_{\mathrm{NL}2,\delta} = \mathbf{0} \tag{3.159}$$

Alternatively, if the improved discrete description, i.e. the symmetric parabolic approximation $\tilde{\chi}_{\mathrm{NL}3,\delta}$ (3.118) to $\tilde{\chi}_{\mathrm{NL},\delta}$ is adopted instead, expression (3.134) can be exactly evaluated by Simpson's rule

$$\phi_{\mathrm{NL}3,\delta,i} = \int_0^L \tilde{n}_i \; \tilde{\chi}_{\mathrm{NL}3,\delta} \, dx = \delta\chi_{\mathrm{NL}} \int_0^L \tilde{n}_i \; \tilde{n}_3 \, dx = \delta\chi_{\mathrm{NL}} \, \frac{L}{6} \times 4 \times \frac{1}{2} = \frac{1}{3} L \, \delta\chi_{\mathrm{NL}}, \quad i = 1,2 \tag{3.160}$$

i.e.,

$$\bar{\boldsymbol{\phi}}_{\mathrm{NL}3,\delta} = \frac{L}{3} \, \delta\chi_{\mathrm{NL}} \, \mathbf{1}_2 \tag{3.161}$$

Figure 3.22. FFM$_3$: kinematic equivalence between the curvature fields $\tilde{\chi}_{\mathrm{NL3},\delta}$ and $\tilde{\chi}_{\mathrm{NL3},\delta,\mathrm{eq}}$.

where $\mathbf{1}_2 \equiv \begin{bmatrix} 1 & 1 \end{bmatrix}^{\mathrm{T}}$. Introducing this expression into (3.155), gives the approximation to $\bar{\boldsymbol{\chi}}_{\mathrm{NL},\delta,\mathrm{eq}}$,

$$\bar{\boldsymbol{\chi}}_{\mathrm{NL3},\delta,\mathrm{eq}} = \bar{\mathbf{K}}_0\, \bar{\boldsymbol{\phi}}_{\mathrm{NL3},\delta} = \frac{2}{3}\delta\chi_{\mathrm{NL}}\mathbf{1}_2 \tag{3.162}$$

The left end and right end nodal values are equal because a symmetric approximation was used for $\tilde{\chi}_{\mathrm{NL},\delta}$. Hence, the approximated equivalent linear field of curvatures is constant,

$$\tilde{\chi}_{\mathrm{NL3},\delta,\mathrm{eq}} = \frac{2}{3}\delta\chi_{\mathrm{NL}} = \mathrm{const} \tag{3.163}$$

i.e., it is given by the average value of the parabola (3.118) over the element domain, see Figure 3.22.

Yet again, let $\tilde{\chi}_{\mathrm{L},\delta,\mathrm{eq}}$ be the linear curvature field kinematically equivalent to $\tilde{\chi}_{\mathrm{L},\delta}$, *i.e.* corresponding to the same end sections rotations. Thence, similarly to (3.147),

$$\bar{\boldsymbol{\chi}}_{\mathrm{L},\delta,\mathrm{eq}} = \bar{\mathbf{K}}_0\, \bar{\boldsymbol{\phi}}_{\mathrm{L},\delta} \tag{3.164}$$

Adding (3.155) to (3.164) and recalling (3.153) gives

$$\bar{\boldsymbol{\chi}}_{\delta,\mathrm{eq}} = \bar{\boldsymbol{\chi}}_{\mathrm{L},\delta,\mathrm{eq}} + \bar{\boldsymbol{\chi}}_{\mathrm{NL},\delta,\mathrm{eq}} = \bar{\mathbf{K}}_0\, \bar{\boldsymbol{\phi}}_{\delta} \tag{3.165}$$

Writing (3.146) for the auxiliary component, introducing the linear plus corrective term decomposition, and recalling that $\bar{\boldsymbol{\phi}}_{\mathrm{A},\delta} = \bar{\boldsymbol{\phi}}_{\mathrm{L},\delta}$, gives

$$\bar{\boldsymbol{\chi}}_{\mathrm{A}} = \bar{\boldsymbol{\chi}}_{\mathrm{A},\Delta} = \bar{\mathbf{K}}_0\, \bar{\boldsymbol{\phi}}_{\mathrm{A},\Delta} = \bar{\mathbf{K}}_0\, \bar{\boldsymbol{\phi}}_{\mathrm{A}} - \bar{\mathbf{K}}_0\, \bar{\boldsymbol{\phi}}_{\mathrm{A},\delta} = \bar{\mathbf{K}}_0\, \bar{\boldsymbol{\phi}}_{\mathrm{A}} - \bar{\mathbf{K}}_0\, \bar{\boldsymbol{\phi}}_{\mathrm{L},\delta} \tag{3.166}$$

Finally, introducing (3.164) into this expression, gives

$$\bar{\boldsymbol{\chi}}_{\mathrm{A},\Delta} + \bar{\boldsymbol{\chi}}_{\mathrm{L},\delta,\mathrm{eq}} = \bar{\mathbf{K}}_0\, \bar{\boldsymbol{\phi}}_{\mathrm{A}} \tag{3.167}$$

3.5.2. Auxiliary elemental constitutive relations

Since it was admitted (§ 3.4.2) that the auxiliary bending stiffness field is constant in each element, the cross-sectional constitutive relationship (3.9) can now be expressed at the element level by

$$\bar{\mathbf{M}}_{\mathrm{A}} = \bar{\mathbf{M}}_{\mathrm{A},\Delta} = \overline{\mathbf{EI}}_{\mathrm{A}}\, \bar{\boldsymbol{\chi}} = EI_{\mathrm{A}}\, \bar{\boldsymbol{\chi}} \tag{3.168}$$

with

$$\overline{\mathbf{EI}}_{\mathrm{A}} = EI_{\mathrm{A}} \mathbf{I}_2 \tag{3.169}$$

where $\mathbf{I}_i$ is the $i \times i$ unit matrix. Introducing the compatibility relation (3.146), gives

$$\bar{\mathbf{M}}_{\mathrm{A}} = \bar{\mathbf{M}}_{\mathrm{A},\Delta} = \bar{\mathbf{K}}_{\mathrm{A}}\, \bar{\boldsymbol{\phi}}_{\Delta} \tag{3.170}$$

where

$$\bar{\mathbf{K}}_{\mathrm{A}} = \overline{\mathbf{EI}}_{\mathrm{A}}\, \bar{\mathbf{K}}_0 = EI_{\mathrm{A}}\, \bar{\mathbf{K}}_0 \tag{3.171}$$

is the non-singular elemental stiffness matrix for the independent variables.

Similarly, the elemental constitutive relationships (3.21) and (3.154), give

$$\bar{\mathbf{M}}_{\mathrm{F}} = \bar{\mathbf{M}}_{\mathrm{F},\Delta} = \overline{\mathbf{EI}}_{\mathrm{A}}\, \bar{\boldsymbol{\chi}}_{\mathrm{NL}} = EI_{\mathrm{A}}\, \bar{\boldsymbol{\chi}}_{\mathrm{NL}} = \bar{\mathbf{K}}_{\mathrm{A}}\, \bar{\boldsymbol{\phi}}_{\mathrm{NL},\Delta} \tag{3.172}$$

The bending moments field corresponding to $\tilde{\chi}_{\delta,\mathrm{eq}}$ is given by

$$\tilde{M}_{\mathrm{A},\delta,\mathrm{eq}} = EI_{\mathrm{A}}\, \tilde{\chi}_{\delta,\mathrm{eq}} \tag{3.173}$$

The values of this field at the end sections are given by

$$\bar{\mathbf{M}}_{\mathrm{A},\delta,\mathrm{eq}} = \overline{\mathbf{EI}}_{\mathrm{A}}\, \bar{\boldsymbol{\chi}}_{\delta,\mathrm{eq}} = \bar{\mathbf{K}}_{\mathrm{A}}\, \bar{\boldsymbol{\phi}}_{\delta} \tag{3.174}$$

where the last equality is due to (3.165). Similarly,

$$\bar{\mathbf{M}}_{\mathrm{F},\delta,\mathrm{eq}} = \overline{\mathbf{EI}}_{\mathrm{A}}\, \bar{\boldsymbol{\chi}}_{\mathrm{NL},\delta,\mathrm{eq}} = \bar{\mathbf{K}}_{\mathrm{A}}\, \bar{\boldsymbol{\phi}}_{\mathrm{NL},\delta} \tag{3.175}$$

$$\bar{\mathbf{M}}_{\delta,\mathrm{eq}} = \overline{\mathbf{EI}}_{\mathrm{A}}\, \bar{\boldsymbol{\chi}}_{\mathrm{L},\delta,\mathrm{eq}} = \bar{\mathbf{K}}_{\mathrm{A}}\, \bar{\boldsymbol{\phi}}_{\mathrm{L},\delta} \tag{3.176}$$

Adding together the expressions (3.170) and (3.172) with, respectively, (3.174) and (3.175), and substituting the decomposition (3.135), gives

$$\bar{\mathbf{M}}_{\mathrm{A},\Delta} + \bar{\mathbf{M}}_{\mathrm{A},\delta,\mathrm{eq}} = \bar{\mathbf{K}}_{\mathrm{A}}\, \bar{\boldsymbol{\phi}} \tag{3.177}$$

$$\bar{\mathbf{M}}_{\mathrm{F},\Delta} + \bar{\mathbf{M}}_{\mathrm{F},\delta,\mathrm{eq}} = \bar{\mathbf{K}}_{\mathrm{A}}\, \bar{\boldsymbol{\phi}}_{\mathrm{NL}} \tag{3.178}$$

3.5.3. Elemental structural relations

Consider the system of nodal coordinates represented in Figure 3.23. According to Euler-Bernoulli hypothesis, the corresponding nodal displacements are

$$\bar{\mathbf{d}}^{\mathrm{el}} = \begin{bmatrix} d_1^{\mathrm{el}} & d_2^{\mathrm{el}} & d_3^{\mathrm{el}} & d_4^{\mathrm{el}} \end{bmatrix}^{\mathrm{T}} = \begin{bmatrix} -\tilde{w}'[0] & \tilde{w}[0] & -\tilde{w}'[L] & \tilde{w}[L] \end{bmatrix}^{\mathrm{T}} \tag{3.179}$$

This vector and the vector of rotations at the end sections w.r.t. the element chord $\bar{\boldsymbol{\phi}}$ satisfy the compatibility relation, see Figure 3.24a,

$$\bar{\boldsymbol{\phi}} = \bar{\mathbf{C}}^{\mathrm{el}} \bar{\mathbf{d}}^{\mathrm{el}} \tag{3.180}$$

where $\bar{\mathbf{C}}^{\mathrm{el}}$ is the elemental compatibility matrix associated to these local directions

$$\bar{\mathbf{C}}^{\mathrm{el}} = \begin{bmatrix} -1 & \dfrac{1}{L} & 0 & -\dfrac{1}{L} \\ 0 & -\dfrac{1}{L} & 1 & \dfrac{1}{L} \end{bmatrix} \tag{3.181}$$

The vector of nodal forces along these directions is

$$\bar{\mathbf{f}}^{\mathrm{el}} = \begin{bmatrix} f_1^{\mathrm{el}} & f_2^{\mathrm{el}} & f_3^{\mathrm{el}} & f_4^{\mathrm{el}} \end{bmatrix}^{\mathrm{T}} \tag{3.182}$$

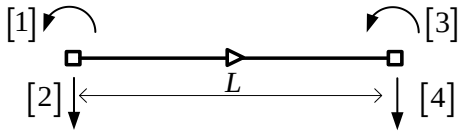

Figure 3.23. Elemental system of nodal coordinates.

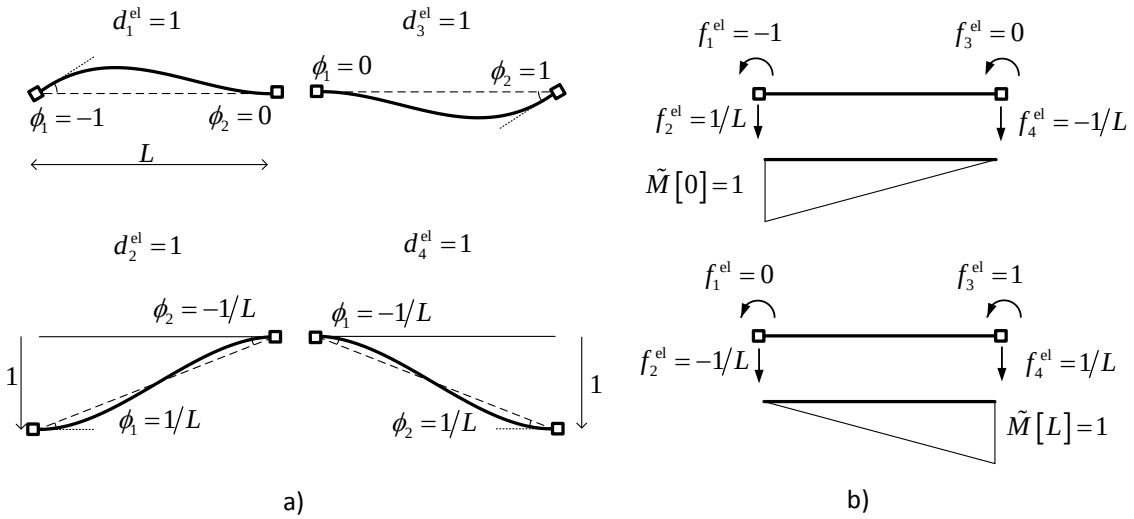

Figure 3.24. Elemental a) compatibility and b) equilibrium relations.

The dual equilibrium relation between the nodal force vector $\bar{\mathbf{f}}^{\text{el}}$ and the vector $\bar{\mathbf{M}}$ which gathers the values of the bending moment field $\tilde{M}$ at the element end sections, is given by

$$\bar{\mathbf{f}}^{\text{el}} = \bar{\mathbf{C}}^{\text{el,T}}\,\bar{\mathbf{M}} \tag{3.183}$$

where $\bar{\mathbf{C}}^{\text{el,T}}$ is the equilibrium matrix, see Figure 3.24b.

Left-multiplying both members of the constitutive relation (3.177) by $\bar{\mathbf{C}}^{\text{el,T}}$, the equilibrium relation (3.183) gives

$$\bar{\mathbf{f}}_{\text{A}}^{\text{el}} + \bar{\mathbf{f}}_{\text{A},\delta}^{\text{el}} = \bar{\mathbf{C}}^{\text{el,T}}\left(\bar{\mathbf{M}}_{\text{A},\Delta} + \bar{\mathbf{M}}_{\text{A},\delta,\text{eq}}\right) = \bar{\mathbf{C}}^{\text{el,T}}\,\bar{\mathbf{K}}_{\text{A}}\,\bar{\boldsymbol{\phi}} \tag{3.184}$$

Substituting (3.180) into the last expression gives

$$\bar{\mathbf{f}}_{\text{A}}^{\text{el}} + \bar{\mathbf{f}}_{\text{A},\delta}^{\text{el}} = \bar{\mathbf{K}}_{\text{A}}^{\text{el}}\,\bar{\mathbf{d}}^{\text{el}} \tag{3.185}$$

where $\bar{\mathbf{K}}_{\text{A}}^{\text{el}}$ is the elemental stiffness matrix in local directions,

$$\bar{\mathbf{K}}_{\text{A}}^{\text{el}} = \bar{\mathbf{C}}^{\text{el,T}}\,\bar{\mathbf{K}}_{\text{A}}\,\bar{\mathbf{C}}^{\text{el}} = EI_{\text{A}}\begin{pmatrix} \frac{4}{L} & -\frac{6}{L^2} & \frac{2}{L} & \frac{6}{L^2} \\ -\frac{6}{L^2} & \frac{12}{L^3} & -\frac{6}{L^2} & -\frac{12}{L^3} \\ \frac{2}{L} & -\frac{6}{L^2} & \frac{4}{L} & \frac{6}{L^2} \\ \frac{6}{L^2} & -\frac{12}{L^3} & \frac{6}{L^2} & \frac{12}{L^3} \end{pmatrix} \tag{3.186}$$

Since (3.183) is a generic equilibrium relation, the nodal force vector equivalent to the forces applied between nodes is given by

$$\bar{\mathbf{f}}_{\delta}^{\text{el}} = \bar{\mathbf{C}}^{\text{el,T}}\,\bar{\mathbf{M}}_{\delta,\text{eq}} \tag{3.187}$$

In the improved discrete description, multiplying both members of (3.163) by EI_{A}, gives

$$\tilde{M}_{\text{F3},\delta,\text{eq}} = \frac{2}{3}\delta M_{\text{F}} \quad \text{with} \quad \delta M_{\text{F}} = EI_{\text{A}}\,\delta\chi_{\text{NL}} \tag{3.188}$$

i.e.,

$$\bar{\mathbf{M}}_{\text{F3},\delta,\text{eq}} = \frac{2}{3}\delta M_{\text{F}}\mathbf{1}_2 \tag{3.189}$$

Thence, the corresponding nodal force vector is given by

$$\bar{\mathbf{f}}_{\text{F},\delta}^{\text{el}} = \frac{2}{3}\delta M_{\text{F}}\begin{bmatrix} -1 & 0 & 1 & 0 \end{bmatrix}^{\text{T}} \tag{3.190}$$

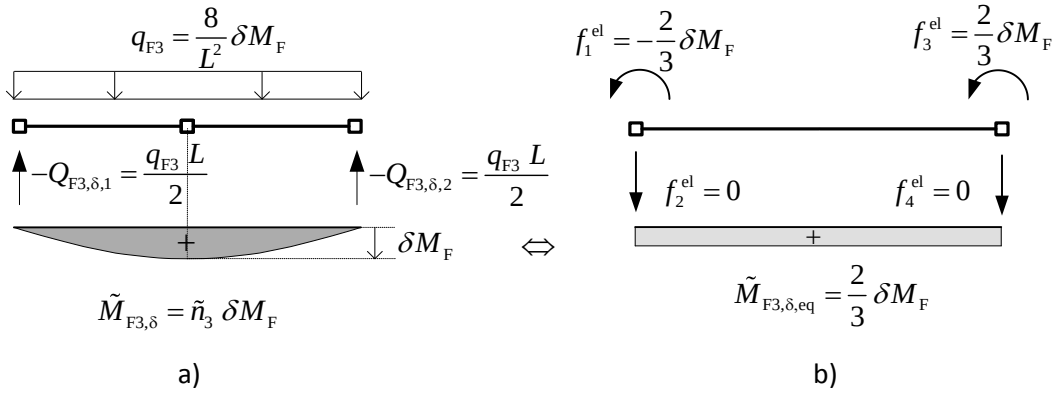

Figure 3.25. FFM_3: a) approximation of the fictitious forces applied between nodes and b) equivalent nodal fictitious forces.

This force vector, represented in Figure 3.25b, is kinematically equivalent to the approximation of the fictitious forces applied between nodes of FFM_3, Figure 3.25a.

3.5.4. Governing system of equations

3.5.4.1. Kinematics

Let us consider a decomposition of the beam in a mesh of *m* linear beam elements linked together at their nodes. Some displacements of these nodes are restrained by the beam supports. The remaining *n* nodal displacements, or generalized displacements, define a global system of coordinates. These displacements are grouped in the global vector $\mathbf{d}$.

The non-assembled global $4m$ vector $\mathbf{d}^{el}$ groups the *m* elemental vectors $\bar{\mathbf{d}}^{el}$,

$$\mathbf{d}^{el} = \left[\bar{\mathbf{d}}_1^{el,T} \quad \bar{\mathbf{d}}_2^{el,T} \quad \cdots \quad \bar{\mathbf{d}}_m^{el,T}\right]^T \tag{3.191}$$

This vector and the vector of assembled displacements $\mathbf{d}$ are related by

$$\mathbf{d}^{el} = \mathbf{D}\,\mathbf{d} \tag{3.192}$$

where $\mathbf{D}$ is a Boolean connectivity matrix (all its elements are 1 or 0), whose structure reflects (i) the connectivity of the beam elements and (ii) the supports kinematic constraints. This matrix groups the $4 \times n$ elemental connectivity matrices $\bar{\mathbf{D}}_i$, which link the four nodal displacements $\bar{\mathbf{d}}_i^{el}$ of element *i* to the *n* global displacements $\mathbf{d}$, *i.e.* $\bar{\mathbf{d}}_i^{el} = \bar{\mathbf{D}}_i\,\mathbf{d}$. Thus,

$$\mathbf{D} = \begin{bmatrix} \bar{\mathbf{D}}_1 \\ \bar{\mathbf{D}}_2 \\ \vdots \\ \bar{\mathbf{D}}_m \end{bmatrix} \tag{3.193}$$

Grouping the elemental compatibility relations (3.180), gives

$$\boldsymbol{\phi} = \mathbf{C}^{\mathrm{el}}\, \mathbf{d}^{\mathrm{el}} \tag{3.194}$$

where the $2m \times 4m$ block diagonal compatibility matrix $\mathbf{C}^{\mathrm{el}}$ collects the elemental matrices $\bar{\mathbf{C}}^{\mathrm{el}}$

$$\mathbf{C}^{\mathrm{el}} = \begin{bmatrix} \bar{\mathbf{C}}_1^{\mathrm{el}} & & & \\ & \bar{\mathbf{C}}_2^{\mathrm{el}} & & \\ & & \ddots & \\ & & & \bar{\mathbf{C}}_m^{\mathrm{el}} \end{bmatrix} \tag{3.195}$$

and the global $2m$ vector of rotations $\boldsymbol{\phi}$ is given by

$$\boldsymbol{\phi} = \begin{bmatrix} \bar{\boldsymbol{\phi}}_1^{\mathrm{T}} & \bar{\boldsymbol{\phi}}_2^{\mathrm{T}} & \ldots & \bar{\boldsymbol{\phi}}_m^{\mathrm{T}} \end{bmatrix}^{\mathrm{T}} \tag{3.196}$$

Substitution of (3.192) into (3.194) gives the global compatibility relation

$$\boldsymbol{\phi} = \mathbf{C}\,\mathbf{d} \tag{3.197}$$

where the $2m \times n$ global compatibility matrix $\mathbf{C}$ is given by

$$\mathbf{C} = \mathbf{C}^{\mathrm{el}}\, \mathbf{D} \tag{3.198}$$

or

$$\mathbf{C} = \begin{bmatrix} \bar{\mathbf{C}}_1 \\ \bar{\mathbf{C}}_2 \\ \vdots \\ \bar{\mathbf{C}}_m \end{bmatrix} \quad \text{with} \quad \bar{\mathbf{C}}_i = \bar{\mathbf{C}}_i^{\mathrm{el}}\, \bar{\mathbf{D}}_i \tag{3.199}$$

3.5.4.2. Statics

The non-assembled global force vector $\mathbf{f}^{\mathrm{el}}$ groups the m elemental vectors $\bar{\mathbf{f}}^{\mathrm{el}}$,

$$\mathbf{f}^{\mathrm{el}} = \begin{bmatrix} \bar{\mathbf{f}}_1^{\mathrm{el,T}} & \bar{\mathbf{f}}_2^{\mathrm{el,T}} & \ldots & \bar{\mathbf{f}}_m^{\mathrm{el,T}} \end{bmatrix}^{\mathrm{T}} \tag{3.200}$$

The static dual of (3.192) gives the assembled global force vector $\mathbf{f}$

$$\mathbf{f} = \mathbf{D}^{\mathrm{T}}\,\mathbf{f}^{\mathrm{el}} \tag{3.201}$$

The equilibrium relation grouping the elemental relations (3.183) is given by

$$\mathbf{f}^{\mathrm{el}} = \mathbf{C}^{\mathrm{el,T}}\,\mathbf{M} \tag{3.202}$$

where the global $2m$ vector of bending moments $\mathbf{M}$ is

$$\mathbf{M} = \left[\,\bar{\mathbf{M}}_1^{\mathrm{T}} \quad \bar{\mathbf{M}}_2^{\mathrm{T}} \quad \ldots \quad \bar{\mathbf{M}}_m^{\mathrm{T}}\,\right]^{\mathrm{T}} \tag{3.203}$$

Substitution of (3.202) into (3.201) gives the global equilibrium relation

$$\mathbf{f} = \mathbf{C}^{\mathrm{T}}\,\mathbf{M} \tag{3.204}$$

3.5.4.3. Auxiliary stiffness matrix

The non-assembled block diagonal $2m \times 2m$ global stiffness matrix is

$$\mathbf{K}_{\mathrm{A}}^{\mathrm{M}} = \mathbf{EI}_{\mathrm{A}}\,\mathbf{K}_0 = \begin{bmatrix} \bar{\mathbf{K}}_{\mathrm{A},1} & & & \\ & \bar{\mathbf{K}}_{\mathrm{A},2} & & \\ & & \ddots & \\ & & & \bar{\mathbf{K}}_{\mathrm{A},m} \end{bmatrix} \tag{3.205}$$

which aggregates the elemental stiffness matrices (3.171) and where the elasticity matrix is given by

$$\mathbf{EI}_{\mathrm{A}} = \begin{bmatrix} \overline{\mathbf{EI}}_{\mathrm{A},1} & & & \\ & \overline{\mathbf{EI}}_{\mathrm{A},2} & & \\ & & \ddots & \\ & & & \overline{\mathbf{EI}}_{\mathrm{A},m} \end{bmatrix} \tag{3.206}$$

and

$$\mathbf{K}_0 = \begin{bmatrix} \bar{\mathbf{K}}_{0,1} & & & \\ & \bar{\mathbf{K}}_{0,2} & & \\ & & \ddots & \\ & & & \bar{\mathbf{K}}_{0,m} \end{bmatrix} \tag{3.207}$$

3.5.4.4. Assemblage of equations

Collecting the m systems of equations (3.185), left-multiplying both members by $\mathbf{D}^{\mathrm{T}}$, substituting the connectivity relations (3.201) on the left-hand side and (3.192) on the right-hand side, gives the governing equation of FFM

$$\mathbf{f}_{\mathrm{A}} + \mathbf{f}_{\mathrm{A},\delta} = \mathbf{K}_{\mathrm{A}}\,\mathbf{d} \tag{3.208}$$

where the $n \times n$ linear assembled stiffness matrix is given by

$$\mathbf{K}_{\mathrm{A}} = \mathbf{D}^{\mathrm{T}}\,\mathbf{K}_{\mathrm{A}}^{\mathrm{el}}\,\mathbf{D} \tag{3.209}$$

and

$$\mathbf{K}_{\mathrm{A}}^{\mathrm{el}} = \begin{bmatrix} \bar{\mathbf{K}}_{\mathrm{A},1}^{\mathrm{el}} & & & \\ & \bar{\mathbf{K}}_{\mathrm{A},2}^{\mathrm{el}} & & \\ & & \ddots & \\ & & & \bar{\mathbf{K}}_{\mathrm{A},m}^{\mathrm{el}} \end{bmatrix} \tag{3.210}$$

is the block diagonal stiffness matrix which aggregates the elemental matrices (3.186). This stiffness matrix can also be written

$$\mathbf{K}_{\mathrm{A}}^{\mathrm{el}} = \mathbf{C}^{\mathrm{el,T}}\,\mathbf{K}_{\mathrm{A}}^{\mathrm{M}}\,\mathbf{C}^{\mathrm{el}} \tag{3.211}$$

that substituted into (3.209), and considering (3.198), allows rewriting $\mathbf{K}_{\mathrm{A}}$ as

$$\mathbf{K}_{\mathrm{A}} = \mathbf{C}^{\mathrm{T}}\,\mathbf{K}_{\mathrm{A}}^{\mathrm{M}}\,\mathbf{C} \tag{3.212}$$

The solution of equation (3.208) gives the displacement vector

$$\mathbf{d} = \mathbf{K}_{\mathrm{A}}^{-1}\left(\mathbf{f}_{\mathrm{A}} + \mathbf{f}_{\mathrm{A},\delta}\right) \tag{3.213}$$

Using the usual auxiliary force decomposition and the equilibrium relation (3.204), gives

$$\mathbf{f}_{\mathrm{A}} = \mathbf{f} + \mathbf{f}_{\mathrm{F}} \tag{3.214}$$

$$\mathbf{f}_{\mathrm{A},\delta} = \mathbf{f}_{\delta} + \mathbf{f}_{\mathrm{F},\delta} \tag{3.215}$$

Moreover, the displacement vector of the linear problem of the auxiliary structure is given by

$$\mathbf{d}_{\mathrm{L}} = \mathbf{K}_{\mathrm{A}}^{-1}\left(\mathbf{f} + \mathbf{f}_{\delta}\right) \tag{3.216}$$

Thence, subtracting the last expression from (3.213), the displacement increment due to the fictitious forces is given by

$$\mathbf{d}_{\text{incr}} \equiv \mathbf{d} - \mathbf{d}_{\text{L}} = \mathbf{K}_{\text{A}}^{-1}\left(\mathbf{f}_{\text{F}} + \mathbf{f}_{\text{F},\delta}\right) \tag{3.217}$$

which, in the iterative format, reads

$$\mathbf{d}^{(i+1)} = \mathbf{d}^{(1)} + \mathbf{K}_{\text{A}}^{-1}\left(\mathbf{f}_{\text{F}}^{(i)} + \mathbf{f}_{\text{F},\delta}^{(i)}\right) \tag{3.218}$$

with

$$\mathbf{d}^{(1)} \equiv \mathbf{d}_{\text{L}} \tag{3.219}$$

According to the previous expression in FFM discrete descriptions the fictitious force vectors $\mathbf{f}_{\text{F}}^{(i)}$ and $\mathbf{f}_{\text{F},\delta}^{(i)}$ are required to calculate the subsequent approximation of the displacement vector $\mathbf{d}^{(i+1)}$.

3.5.5. Implementation of FFM basic discrete description

In the basic discrete description of FFM the curvature $\tilde{\chi}_{\text{NL},\delta}$ is assumed to be zero ($\tilde{\chi}_{\text{NL2},\delta} = 0$) and thus, according to (3.175), the equivalent fictitious bending moments are also null $\mathbf{M}_{\text{F2},\delta,\text{eq}} = 0$. Thence, according to (3.204), $\mathbf{f}_{\text{F},\delta}^{(i)} = \mathbf{0}$ and equation (3.218) gets reduced to

$$\mathbf{d}^{(i+1)} = \mathbf{d}^{(1)} + \mathbf{K}_{\text{A}}^{-1}\,\mathbf{f}_{\text{F}}^{(i)} \tag{3.220}$$

On the other hand, according again to the equilibrium relation (3.204), the fictitious force vector $\mathbf{f}_{\text{F}}^{(i)}$ is determined by the fictitious bending moments at the end sections of the elements $\mathbf{M}_{\text{F}}^{(i)}$. As seen in § 3.2.2, there are two alternative ways to establish these fictitious bending moments, corresponding to FFM_{Def} and FFM_{S}.

Once the displacements $\mathbf{d}^{(i)}$ have been determined, the auxiliary solution, *i.e.* the curvatures $\boldsymbol{\chi}^{(i)}$ and the auxiliary bending moments $\mathbf{M}_{\text{A}}^{(i)}$, can be calculated as follows. Firstly, decomposing the corrective term in (3.148), noting that $\boldsymbol{\chi}_{\Delta} = \boldsymbol{\chi}$ and collecting the elemental relations gives

$$\boldsymbol{\chi} + \boldsymbol{\chi}_{\text{L},\delta,\text{eq}} + \boldsymbol{\chi}_{\text{NL},\delta,\text{eq}} = \mathbf{K}_0\,\boldsymbol{\phi} \tag{3.221}$$

Then, since $\tilde{\chi}_{\text{NL},\delta} = 0$, substituting the compatibility relation (3.197) on the right-hand side of the last expression and writing the result in the iterative format, gives

$$\boldsymbol{\chi}^{(i)} = \mathbf{K}_0\,\mathbf{C}\,\mathbf{d}^{(i)} - \boldsymbol{\chi}_{\text{L},\delta,\text{eq}} \tag{3.222}$$

and, left-multiplying both members by $\mathbf{EI}_{\text{A}}$,

$$\mathbf{M}_{\mathrm{A}}^{(i)} = \mathbf{K}_{\mathrm{A}}^{\mathrm{M}}\,\mathbf{C}\,\mathbf{d}^{(i)} - \mathbf{M}_{\delta,\mathrm{eq}} \tag{3.223}$$

Note that $\mathbf{M}_{\delta,\mathrm{eq}}$ and, therefore, $\boldsymbol{\chi}_{\mathrm{L},\delta,\mathrm{eq}}$ are easily determined because the linear solution is known.

The flowcharts in Figure 3.4 are adapted in Figure 3.26 to the basic discrete description of FFM. The vectors $\bar{\mathbf{M}}_j\left[\bar{\boldsymbol{\chi}}_j\right]$ and $\bar{\boldsymbol{\chi}}_j\left[\bar{\mathbf{M}}_j\right]$ are formed by the effective nonlinear constitutive relations at the end sections of element *j*, *i.e.*

$$\bar{\mathbf{M}}_j\left[\bar{\boldsymbol{\chi}}_j\right] = \left[\hat{M}_j\left[\tilde{\chi}[0]\right] \quad \hat{M}_j\left[\tilde{\chi}[L]\right]\right]^{\mathrm{T}} \tag{3.224}$$

$$\bar{\boldsymbol{\chi}}_j\left[\bar{\mathbf{M}}_j\right] = \left[\hat{\chi}_j\left[\tilde{M}[0]\right] \quad \hat{\chi}_j\left[\tilde{M}[L]\right]\right]^{\mathrm{T}} \tag{3.225}$$

3.5.6. Implementation of FFM improved discrete description

In the improved discrete description of FFM the equivalent curvatures $\boldsymbol{\chi}_{\mathrm{NL},\delta,\mathrm{eq}}$ are approximated in each element by $(2/3)\delta\chi_{\mathrm{NL}}\mathbf{1}_2$ (3.162). This means that the fictitious force vector $\mathbf{f}_{\mathrm{F},\delta}^{(i)}$ is determined by the equivalent fictitious bending moments approximated in each element by $\bar{\mathbf{M}}_{\mathrm{F3},\delta,\mathrm{eq}}^{(i)} = (2/3)\delta M_{\mathrm{F}}^{(i)}\mathbf{1}_2$ (3.189) with

$$\delta M_{\mathrm{F}}^{(i)} = \tilde{M}_{\mathrm{F}}^{(i)}\left[\frac{L}{2}\right] - \tilde{M}_{\mathrm{F},\Delta}^{(i)}\left[\frac{L}{2}\right] = \tilde{M}_{\mathrm{F}}^{(i)}\left[\frac{L}{2}\right] - \frac{1}{2}\bar{\mathbf{M}}_{\mathrm{F}}^{(i),\mathrm{T}}\mathbf{1}_2 \tag{3.226}$$

Since the fictitious bending moments depend on the effective nonlinear constitutive relations and on the auxiliary solution, see Figure 3.3, it is necessary to determine the curvatures and the auxiliary bending moments at the end sections and midsection. Thence, substituting expressions (3.162), (3.197) and (3.199) into (3.221) gives, in the iterative format,

$$\bar{\boldsymbol{\chi}}^{(i)} = \bar{\mathbf{K}}_0\,\bar{\mathbf{C}}\,\mathbf{d}^{(i)} - \bar{\boldsymbol{\chi}}_{\mathrm{L},\delta,\mathrm{eq}} - \frac{2}{3}\delta\chi_{\mathrm{NL}}^{(i)}\mathbf{1}_2 \simeq \bar{\mathbf{K}}_0\,\bar{\mathbf{C}}\,\mathbf{d}^{(i)} - \bar{\boldsymbol{\chi}}_{\mathrm{L},\delta,\mathrm{eq}} - \frac{2}{3}\delta\chi_{\mathrm{NL}}^{(i-1)}\mathbf{1}_2 \tag{3.227}$$

Left-multiplying both members of this expression by $\overline{\mathbf{EI}}_{\mathrm{A}}$ and introducing (3.168), (3.176) and (3.121), gives

$$\bar{\mathbf{M}}_{\mathrm{A}}^{(i)} = \bar{\mathbf{K}}_{\mathrm{A}}\,\bar{\mathbf{C}}\,\mathbf{d}^{(i)} - \bar{\mathbf{M}}_{\delta,\mathrm{eq}} - \frac{2}{3}\delta M_{\mathrm{F}}^{(i)}\mathbf{1}_2 \simeq \bar{\mathbf{K}}_{\mathrm{A}}\,\bar{\mathbf{C}}\,\mathbf{d}^{(i)} - \bar{\mathbf{M}}_{\delta,\mathrm{eq}} - \frac{2}{3}\delta M_{\mathrm{F}}^{(i-1)}\mathbf{1}_2 \tag{3.228}$$

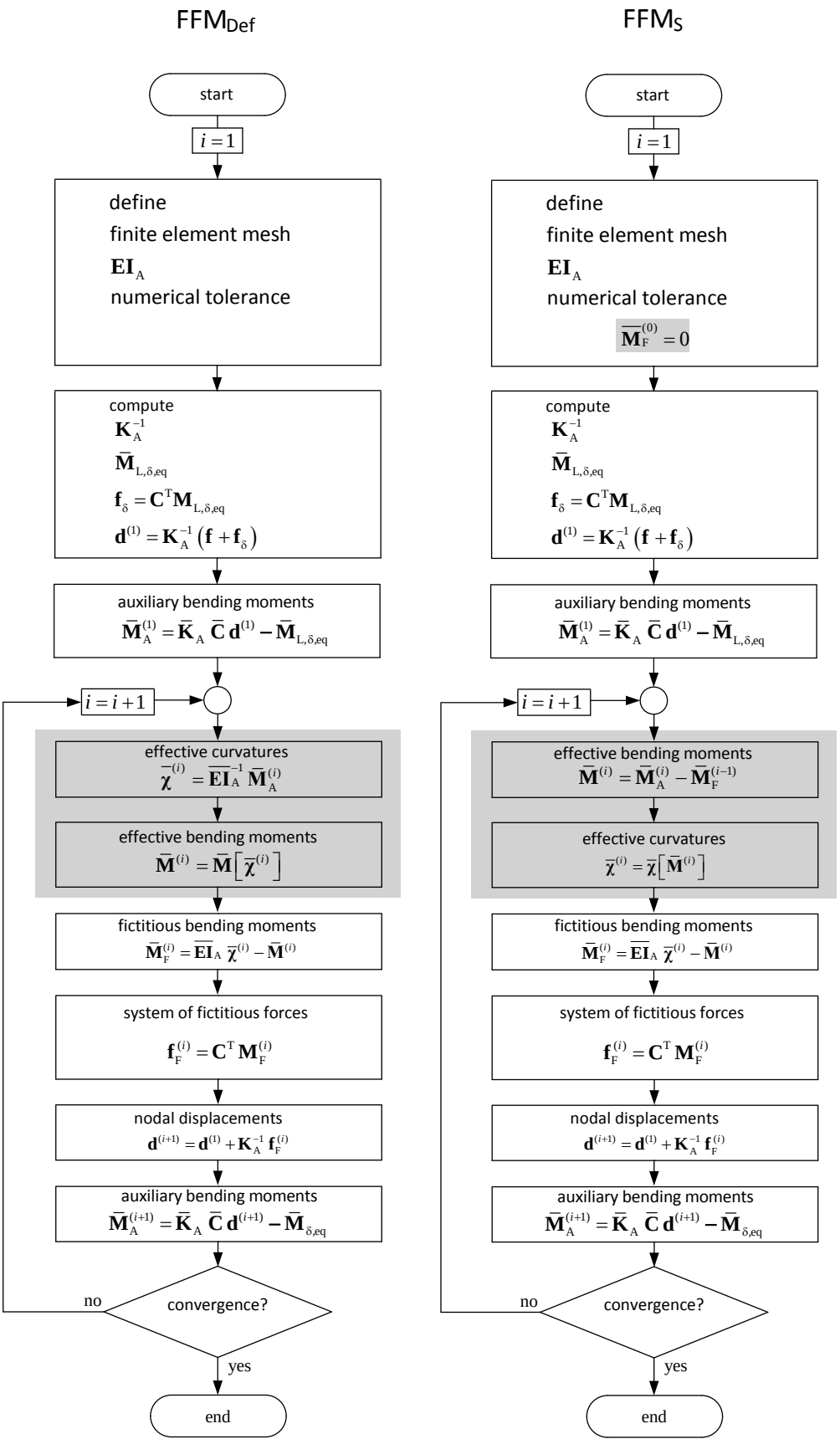

Figure 3.26. FFM$_2$: Basic discrete description of FFM(*M*) (shaded boxes identify the differences).

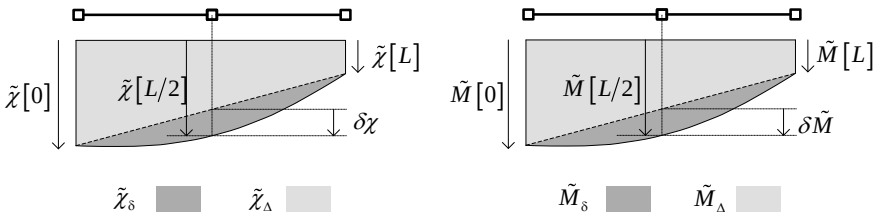

Figure 3.27. FFM_3: Curvature and bending moment deviations at the additional interpolation section.

The approximation $\delta M_{\mathrm{F}}^{(i)} \simeq \delta M_{\mathrm{F}}^{(i-1)}$ (resp. $\delta\chi_{\mathrm{NL}}^{(i)} \simeq \delta\chi_{\mathrm{NL}}^{(i-1)}$) used in (3.228) (resp. (3.227)) is needed because $\delta M_{\mathrm{F}}^{(i)}$ (resp. $\delta\chi_{\mathrm{NL}}^{(i)}$) depends on the values of the curvature field $\tilde{\chi}^{(i)}$ (resp. bending moment field $\tilde{M}^{(i)}$) which is not yet known.

The auxiliary solution at midsection, is given by

$$\tilde{M}_{\mathrm{A}}^{(i)}\left[\frac{L}{2}\right] = \frac{1}{2}\overline{\mathbf{M}}_{\mathrm{A}}^{(i),\mathrm{T}}\mathbf{1}_2 + \delta M_{\mathrm{A}}^{(i)} \simeq \frac{1}{2}\overline{\mathbf{M}}_{\mathrm{A}}^{(i),\mathrm{T}}\mathbf{1}_2 + \delta M + \delta M_{\mathrm{F}}^{(i-1)} \tag{3.229}$$

$$\tilde{\chi}^{(i)}\left[\frac{L}{2}\right] = \frac{1}{2}\overline{\boldsymbol{\chi}}^{(i)\mathrm{T}}\mathbf{1}_2 + \delta\chi^{(i)} \simeq \frac{1}{2}\overline{\boldsymbol{\chi}}^{(i)\mathrm{T}}\mathbf{1}_2 + \frac{\delta M + \delta M_{\mathrm{F}}^{(i-1)}}{EI_{\mathrm{A}}} \tag{3.230}$$

where the deviation of the auxiliary bending moment at midsection is written

$$\delta M_{\mathrm{A}}^{(i)} = \delta M + \delta M_{\mathrm{F}}^{(i)} \simeq \delta M + \delta M_{\mathrm{F}}^{(i-1)} \tag{3.231}$$

with δM remaining constant during the iterative procedure. Finally, note that the effective bending moment at the midsection can also be written

$$\tilde{M}^{(i)}\left[\frac{L}{2}\right] = \tilde{M}_{\Delta}^{(i)}\left[\frac{L}{2}\right] + \delta M = \frac{1}{2}\overline{\mathbf{M}}^{(i)\mathrm{T}}\mathbf{1}_2 + \delta M \tag{3.232}$$

Figure 3.27 illustrates expressions (3.230) and (3.232). The flowcharts in Figure 3.4 are adapted in Figure 3.28 to the improved discrete description of FFM.

3.6. Analysis of FFM basic discrete description

In this section the iteration formulas of FFM_{Def} and FFM_S are presented in the context of FFM basic discrete description. Their convergence conditions are then investigated, with a spectral analysis of the iteration matrices. Finally, sufficient convergence conditions of the basic discrete description are determined.

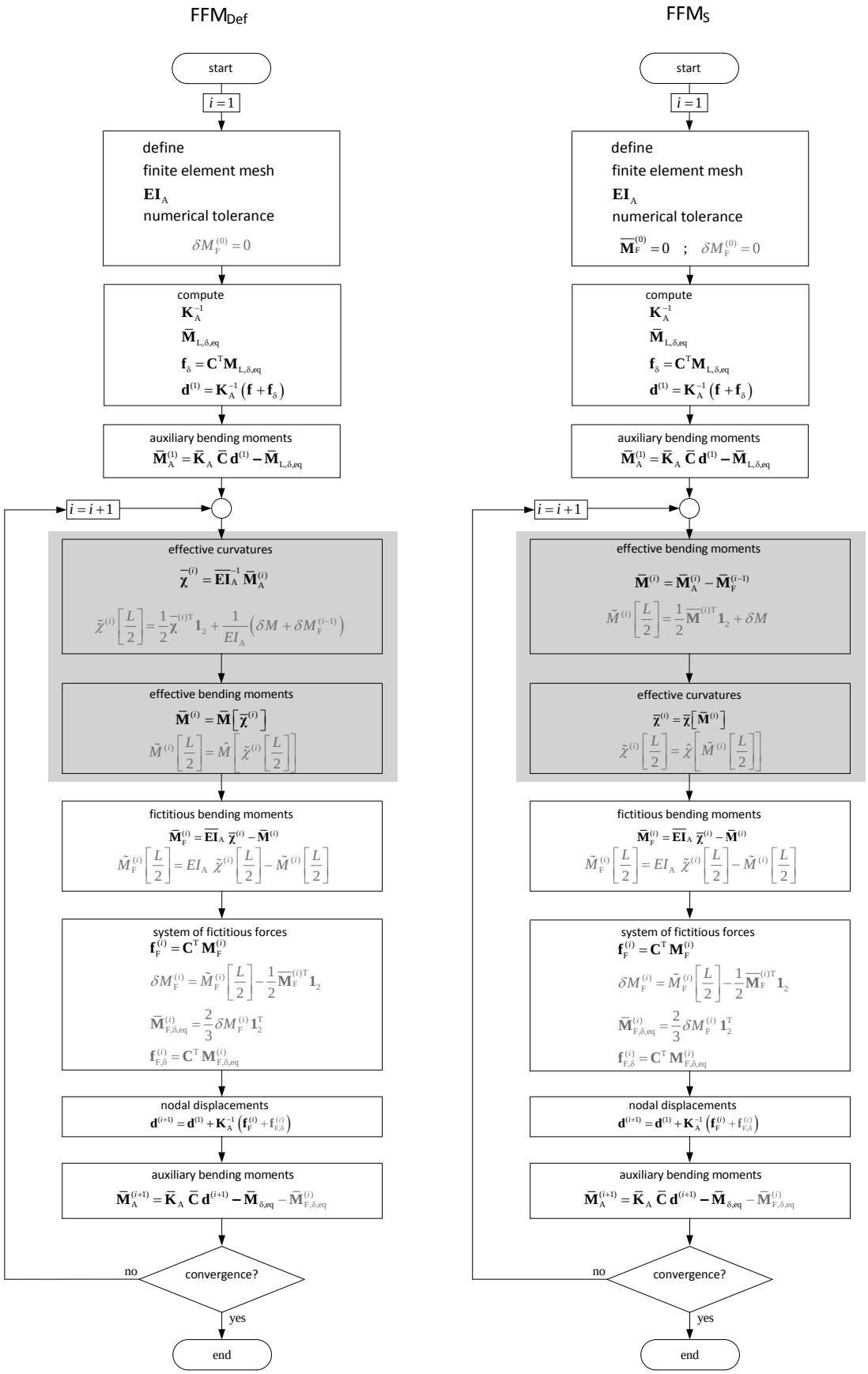

Figure 3.28. FFM$_3$: Improved discrete description of FFM(*M*) (differences identified by shaded boxes; expressions in grey are specific of FFM$_3$).

3.6.1. Iteration formulas of the basic discrete description

Substitution of (3.217) into the compatibility condition (3.197) gives the increment of rotations

$$\boldsymbol{\phi}_{\text{incr}} = \mathbf{C}\,\mathbf{d}_{\text{incr}} = \mathbf{C}\,\mathbf{K}_{\text{A}}^{-1}\left(\mathbf{f}_{\text{F}} + \mathbf{f}_{\text{F},\delta}\right) \tag{3.233}$$

Introducing the equilibrium condition (3.204) gives

$$\boldsymbol{\phi}_{\text{incr}} = \mathbf{C}\mathbf{K}_{\text{A}}^{-1}\mathbf{C}^{\text{T}}\left(\mathbf{M}_{\text{F}} + \mathbf{M}_{\text{F},\delta,\text{eq}}\right) \tag{3.234}$$

Finally, using also (3.178) gives

$$\boldsymbol{\phi}_{\text{incr}} = \mathbf{C}\mathbf{K}_{\text{A}}^{-1}\mathbf{C}^{\text{T}}\mathbf{K}_{\text{A}}^{\text{M}}\boldsymbol{\phi}_{\text{NL}} \tag{3.235}$$

or

$$\boldsymbol{\phi}_{\text{incr}} = \mathbf{T}_{\phi}\,\boldsymbol{\phi}_{\text{NL}} \tag{3.236}$$

with

$$\mathbf{T}_{\phi} = \mathbf{C}\mathbf{K}_{\text{A}}^{-1}\mathbf{C}^{\text{T}}\mathbf{K}_{\text{A}}^{\text{M}} \tag{3.237}$$

Substituting the global version of (3.141) in both members of (3.236) gives

$$\mathbf{F}_0\,\boldsymbol{\chi}_{\text{incr}} + \boldsymbol{\phi}_{\text{incr},\delta} = \mathbf{T}_{\phi}\left(\mathbf{F}_0\,\boldsymbol{\chi}_{\text{NL}} + \boldsymbol{\phi}_{\text{NL},\delta}\right) \tag{3.238}$$

Left-multiplying both members by $\mathbf{K}_0$ and recalling that $\boldsymbol{\phi}_{\text{incr},\delta} = \boldsymbol{\phi}_{\text{NL},\delta}$ (3.153) gives

$$\boldsymbol{\chi}_{\text{incr}} = \mathbf{T}_{\chi}\,\boldsymbol{\chi}_{\text{NL}} + \left(\mathbf{T}_{\chi} - \mathbf{I}_{2m}\right)\mathbf{K}_0\,\boldsymbol{\phi}_{\text{NL},\delta} \tag{3.239}$$

with

$$\mathbf{T}_{\chi} \equiv \mathbf{K}_0\,\mathbf{T}_{\phi}\,\mathbf{F}_0 \tag{3.240}$$

Introducing (3.155), the previous expression becomes

$$\boldsymbol{\chi}_{\text{incr}} = \mathbf{T}_{\chi}\,\boldsymbol{\chi}_{\text{NL}} + \left(\mathbf{T}_{\chi} - \mathbf{I}_{2m}\right)\boldsymbol{\chi}_{\text{NL},\delta,\text{eq}} \tag{3.241}$$

and finally, the hypothesis $\boldsymbol{\chi}_{\text{NL},\delta,\text{eq}} = \mathbf{0}$ of the basic discrete description of FFM, gives

$$\boldsymbol{\chi} = \mathbf{G}_{\chi}^{\text{I}}\left[\boldsymbol{\chi}_{\text{NL}}\right] = \boldsymbol{\chi}_{\text{L}} + \mathbf{T}_{\chi}\,\boldsymbol{\chi}_{\text{NL}} \tag{3.242}$$

which is similar to (3.31). Introducing the decomposition $\boldsymbol{\chi} = \boldsymbol{\chi}_{\text{A}} + \boldsymbol{\chi}_{\text{NL}}$, see (3.93), gives

$$\boldsymbol{\chi}_{\text{A}} = \boldsymbol{\chi}_{\text{L}} + \left(\mathbf{T}_{\chi} - \mathbf{I}_{2m}\right)\boldsymbol{\chi}_{\text{NL}} \tag{3.243}$$

or

$$\boldsymbol{\chi}_{\mathrm{A}} = \boldsymbol{\chi}_{\mathrm{L}} + \mathbf{T}_{\chi_{\mathrm{A}}}\, \boldsymbol{\chi}_{\mathrm{NL}} \tag{3.244}$$

with

$$\mathbf{T}_{\chi_{\mathrm{A}}} = \mathbf{T}_{\chi} - \mathbf{I}_{2m} \tag{3.245}$$

Left-multiplying both members by $\mathbf{EI}_{\mathrm{A}}$ gives

$$\mathbf{M} = \mathbf{G}_{\mathrm{M}}^{\mathrm{I}^*}\left[\boldsymbol{\chi}_{\mathrm{NL}}\right] = \mathbf{M}_{\mathrm{L}} + \mathbf{EI}_{\mathrm{A}}\, \mathbf{T}_{\chi_{\mathrm{A}}}\, \boldsymbol{\chi}_{\mathrm{NL}} \tag{3.246}$$

which is similar to (3.33). Introducing the relation $\boldsymbol{\chi}_{\mathrm{NL}} = \mathbf{EI}_{\mathrm{A}}^{-1}\mathbf{M}_{\mathrm{F}}$ into the last expression, gives

$$\mathbf{M} = \mathbf{G}_{\mathrm{M}}^{\mathrm{I}}\left[\mathbf{M}_{\mathrm{F}}\right] = \mathbf{M}_{\mathrm{L}} + \mathbf{T}_{\mathrm{M}}\, \mathbf{M}_{\mathrm{F}} \tag{3.247}$$

with

$$\mathbf{T}_{\mathrm{M}} = \mathbf{EI}_{\mathrm{A}}\, \mathbf{T}_{\chi_{\mathrm{A}}}\, \mathbf{EI}_{\mathrm{A}}^{-1} \tag{3.248}$$

Expressions (3.242) and (3.247) correspond to the more general expressions (3.31) and (3.35), in the context of FFM_2. In particular, to the operator T_{χ} (resp. T_{M}) in (3.31) (resp. (3.35)) corresponds matrix $\mathbf{T}_{\chi}$ (resp. $\mathbf{T}_{\mathrm{M}}$) in (3.242) (resp. (3.247)).

The matrix form of the iterative relation (3.16) is given by

$$\mathbf{M}_{\mathrm{F}}\left[\mathbf{M}^{(i)}\right] = \mathbf{G}_{\mathrm{M}}^{\mathrm{II}}\left[\mathbf{M}^{(i)}\right] = \mathbf{EI}_{\mathrm{A}}\, \boldsymbol{\chi}\left[\mathbf{M}^{(i)}\right] - \mathbf{M}^{(i)} \tag{3.249}$$

Similarly, substituting (3.15) into (3.21) gives, in the matrix format,

$$\boldsymbol{\chi}_{\mathrm{NL}}\left[\boldsymbol{\chi}^{(i)}\right] = \mathbf{G}_{\chi}^{\mathrm{II}}\left[\boldsymbol{\chi}^{(i)}\right] = \boldsymbol{\chi}^{(i)} - \mathbf{EI}_{\mathrm{A}}^{-1}\, \mathbf{M}\left[\boldsymbol{\chi}^{(i)}\right] \tag{3.250}$$

where the global vectors $\mathbf{M}[\boldsymbol{\chi}]$ and $\boldsymbol{\chi}[\mathbf{M}]$ collect the elemental constitutive relations (3.224) and (3.225).

Inserting these expressions into (3.242) and (3.247), respectively, and recalling (3.18), the iteration formulas of $\mathrm{FFM}_{\mathrm{Def}}$ and $\mathrm{FFM}_{\mathrm{S}}$ can be defined as

$$\boldsymbol{\chi}^{(i+1)} = \mathbf{G}_{\chi}\left[\boldsymbol{\chi}^{(i)}\right] = \mathbf{G}_{\chi}^{\mathrm{I}}\left[\mathbf{G}_{\chi}^{\mathrm{II}}\left[\boldsymbol{\chi}^{(i)}\right]\right] = \boldsymbol{\chi}^{(1)} + \mathbf{T}_{\chi}\, \boldsymbol{\chi}_{\mathrm{NL}}\left[\boldsymbol{\chi}^{(i)}\right] \tag{3.251}$$

$$\mathbf{M}^{(i+1)} = \mathbf{G}_{\mathrm{M}}\left[\mathbf{M}^{(i)}\right] = \mathbf{G}_{\mathrm{M}}^{\mathrm{I}}\left[\mathbf{G}_{\mathrm{M}}^{\mathrm{II}}\left[\mathbf{M}^{(i)}\right]\right] = \mathbf{M}^{(1)} + \mathbf{T}_{\mathrm{M}}\, \mathbf{M}_{\mathrm{F}}\left[\mathbf{M}^{(i)}\right] \tag{3.252}$$

These two expressions represent the more general expressions (3.38) and (3.39) in the discrete format, expressing the fixed point iteration method, see § 2.4.

FFM_2 can be implemented with these expressions instead of the procedures summarised in the flowchart in Figure 3.26. Similarly, the expression (3.241) can also be used to implement FFM_3 instead of the procedures summarised in the flowchart in Figure 3.28.

3.6.2. Convergence conditions of the basic discrete description

In § 3.2.6, it was explained that the iteration formulas (3.251) and (3.252) are convergent if the operators $\mathbf{G}_\chi$ and $\mathbf{G}_\mathrm{M}$ are contractive. Moreover, $\mathbf{G}_\chi$ is contractive if both $\mathbf{G}_\chi^\mathrm{I}$ and $\mathbf{G}_\chi^\mathrm{II}$ are non-expansive and at least one of them is contractive. The same happens with $\mathbf{G}_\mathrm{M}^\mathrm{I}$, $\mathbf{G}_\mathrm{M}^\mathrm{II}$ and $\mathbf{G}_\mathrm{M}$. The Jacobian matrices of $\mathbf{G}_\chi^\mathrm{I}$ and $\mathbf{G}_\mathrm{M}^\mathrm{I}$, are, respectively,

$$\mathbf{J}_\chi^\mathrm{I} = \mathbf{T}_\chi \tag{3.253}$$

$$\mathbf{J}_\mathrm{M}^\mathrm{I} = \mathbf{T}_\mathrm{M} \tag{3.254}$$

In the context of matrix methods of structural analysis, the non-expansiveness of $\mathbf{G}_\chi^\mathrm{I}$ (resp. $\mathbf{G}_\mathrm{M}^\mathrm{I}$) depends solely on the spectral proprieties of matrix $\mathbf{T}_\chi$ (resp. $\mathbf{T}_\mathrm{M}$). More precisely, $\mathbf{G}_\chi^\mathrm{I}$ (resp. $\mathbf{G}_\mathrm{M}^\mathrm{I}$) is non-expansive if the spectral radius $\rho\left[\mathbf{T}_\chi\right]$ (resp. $\rho\left[\mathbf{T}_\mathrm{M}\right]$) is less than or equal to one.

It was also proved in § 3.2.6 that $\mathbf{G}_\chi^\mathrm{II}$ and $\mathbf{G}_\mathrm{M}^\mathrm{II}$ are contractive if conditions (3.48) and (3.49) are satisfied at every section. In fact, the Jacobian matrices $\mathbf{J}_\chi^\mathrm{II}$ of $\mathbf{G}_\chi^\mathrm{II}$ and $\mathbf{J}_\mathrm{M}^\mathrm{II}$ of $\mathbf{G}_\mathrm{M}^\mathrm{II}$ are $2m \times 2m$ diagonal matrices containing the relative differences of bending stiffness at the two end sections of each element, which are written as

$$\mathbf{J}_\chi^\mathrm{II} = \boldsymbol{\beta}_\chi \equiv \begin{bmatrix} \overline{\boldsymbol{\beta}}_{\chi,1} & & & \\ & \overline{\boldsymbol{\beta}}_{\chi,2} & & \\ & & \ddots & \\ & & & \overline{\boldsymbol{\beta}}_{\chi,m} \end{bmatrix} \tag{3.255}$$

with

$$\overline{\boldsymbol{\beta}}_{\chi,j} \equiv \begin{bmatrix} \beta_{\chi,1} & 0 \\ 0 & \beta_{\chi,2} \end{bmatrix} \tag{3.256}$$

where, according to (3.42), $\beta_{\chi,1}$ and $\beta_{\chi,2}$ are given by

$$\beta_{\chi,1} = \frac{EI_\mathrm{A} - \widetilde{EI}[0]}{EI_\mathrm{A}} \tag{3.257}$$

$$\beta_{\chi,2} = \frac{EI_{\mathrm{A}} - \widetilde{EI}\left[L\right]}{EI_{\mathrm{A}}} \tag{3.258}$$

and

$$\mathbf{J}_{\mathrm{M}}^{\mathrm{II}} = \boldsymbol{\beta}_{\mathrm{M}} \equiv \begin{bmatrix} \overline{\boldsymbol{\beta}}_{\mathrm{M},1} & & & \\ & \overline{\boldsymbol{\beta}}_{\mathrm{M},2} & & \\ & & \ddots & \\ & & & \overline{\boldsymbol{\beta}}_{\mathrm{M},m} \end{bmatrix} \tag{3.259}$$

with

$$\overline{\boldsymbol{\beta}}_{\mathrm{M},j} \equiv \begin{bmatrix} \beta_{\mathrm{M},1} & 0 \\ 0 & \beta_{\mathrm{M},2} \end{bmatrix} \tag{3.260}$$

where, according to (3.43), $\beta_{\mathrm{M},1}$ and $\beta_{\mathrm{M},2}$ are given by

$$\beta_{\mathrm{M},1} = \frac{EI_{\mathrm{A}} - \widetilde{EI}\left[0\right]}{\widetilde{EI}\left[0\right]} \tag{3.261}$$

$$\beta_{\mathrm{M},2} = \frac{EI_{\mathrm{A}} - \widetilde{EI}\left[L\right]}{\widetilde{EI}\left[L\right]} \tag{3.262}$$

Thence, the Jacobian matrices of the transformations (3.251) and (3.252), can be written as

$$\mathbf{J}_{\chi} = \mathbf{J}_{\chi}^{\mathrm{I}}\,\mathbf{J}_{\chi}^{\mathrm{II}} = \mathbf{T}_{\chi}\,\boldsymbol{\beta}_{\chi} \tag{3.263}$$

$$\mathbf{J}_{\mathrm{M}} = \mathbf{J}_{\mathrm{M}}^{\mathrm{I}}\,\mathbf{J}_{\mathrm{M}}^{\mathrm{II}} = \mathbf{T}_{\mathrm{M}}\,\boldsymbol{\beta}_{\mathrm{M}} \tag{3.264}$$

3.6.3. Spectral analysis of the iteration matrices

In this section it is proved that the eigenvalues of the iteration matrix $\mathbf{T}_{\chi}$ (resp. $\mathbf{T}_{\mathrm{M}}$) belong to the set $\{0,1\}$ (resp. $\{-1,0\}$), which means that

$$\rho\left[\mathbf{T}_{\chi}\right] = \rho\left[\mathbf{T}_{\mathrm{M}}\right] = 1 \tag{3.265}$$

Firstly, according to (3.248), $\mathbf{T}_{\mathrm{M}}$ and $\mathbf{T}_{\chi_{\mathrm{A}}}$ are similar matrices and therefore have the same eigenvalues, *i.e.*

$$\rho\left[\mathbf{T}_{\mathrm{M}}\right] = \rho\left[\mathbf{T}_{\chi_{\mathrm{A}}}\right] \tag{3.266}$$

Similarly, according to (3.240), $\mathbf{T}_{\chi}$ and $\mathbf{T}_{\phi}$ are similar matrices and therefore

$$\rho\left[\mathbf{T}_{\chi}\right]=\rho\left[\mathbf{T}_{\phi}\right] \tag{3.267}$$

Secondly, since $\boldsymbol{\phi}^{(1)}=\boldsymbol{\phi}_{\mathrm{A}}^{(1)}$, then

$$\boldsymbol{\phi}_{\mathrm{A,incr}}=\boldsymbol{\phi}_{\mathrm{A}}-\boldsymbol{\phi}_{\mathrm{A}}^{(1)}=\boldsymbol{\phi}-\boldsymbol{\phi}_{\mathrm{NL}}-\boldsymbol{\phi}^{(1)}=\boldsymbol{\phi}_{\mathrm{incr}}-\boldsymbol{\phi}_{\mathrm{NL}} \tag{3.268}$$

Hence, according to (3.236), the matrix

$$\mathbf{T}_{\phi_{\mathrm{A}}}=\mathbf{T}_{\phi}-\mathbf{I}_{2m} \tag{3.269}$$

transforms the rotations $\boldsymbol{\phi}_{\mathrm{NL}}$ into the increment $\boldsymbol{\phi}_{\mathrm{A,incr}}$, *i.e.*

$$\boldsymbol{\phi}_{\mathrm{A,incr}}=\mathbf{T}_{\phi_{\mathrm{A}}}\,\boldsymbol{\phi}_{\mathrm{NL}} \tag{3.270}$$

Note that $\mathbf{T}_{\phi_{\mathrm{A}}}$ and $\mathbf{T}_{\chi_{\mathrm{A}}}$ (and therefore $\mathbf{T}_{\mathrm{M}}$) are similar matrices since, see (3.269) and (3.240),

$$\mathbf{K}_0\,\mathbf{T}_{\phi_{\mathrm{A}}}\,\mathbf{F}_0=\mathbf{K}_0\left(\mathbf{T}_{\phi}-\mathbf{I}_{2m}\right)\mathbf{F}_0=\mathbf{K}_0\,\mathbf{T}_{\phi}\,\mathbf{F}_0-\mathbf{K}_0\,\mathbf{F}_0=\mathbf{T}_{\chi}-\mathbf{I}_{2m}=\mathbf{T}_{\chi_{\mathrm{A}}} \tag{3.271}$$

Hence, according to (3.266),

$$\rho\left[\mathbf{T}_{\mathrm{M}}\right]=\rho\left[\mathbf{T}_{\chi_{\mathrm{A}}}\right]=\rho\left[\mathbf{T}_{\phi_{\mathrm{A}}}\right] \tag{3.272}$$

The spectral analysis of matrices $\mathbf{T}_{\phi}$ and $\mathbf{T}_{\phi_{\mathrm{A}}}$ is now addressed. Let ($\lambda_{\mathbf{T}_{\phi_{\mathrm{A}}}}$, $\widehat{\boldsymbol{\phi}}_{\mathrm{NL}}$) be an eigenpair of $\mathbf{T}_{\phi_{\mathrm{A}}}$, *i.e.*

$$\mathbf{T}_{\phi_{\mathrm{A}}}\,\widehat{\boldsymbol{\phi}}_{\mathrm{NL}}=\left(\mathbf{T}_{\phi}-\mathbf{I}_{2m}\right)\widehat{\boldsymbol{\phi}}_{\mathrm{NL}}=\lambda_{\mathbf{T}_{\phi_{\mathrm{A}}}}\,\widehat{\boldsymbol{\phi}}_{\mathrm{NL}} \tag{3.273}$$

This means that

$$\mathbf{T}_{\phi}\,\widehat{\boldsymbol{\phi}}_{\mathrm{NL}}=\lambda_{\mathbf{T}_{\phi_{\mathrm{A}}}}\,\widehat{\boldsymbol{\phi}}_{\mathrm{NL}}+\widehat{\boldsymbol{\phi}}_{\mathrm{NL}}=\left(\lambda_{\mathbf{T}_{\phi_{\mathrm{A}}}}+1\right)\widehat{\boldsymbol{\phi}}_{\mathrm{NL}} \tag{3.274}$$

which proves that every eigenvector of $\mathbf{T}_{\phi_{\mathrm{A}}}$ is also an eigenvector of $\mathbf{T}_{\phi}$ and that the corresponding eigenvalues are connected by the relation

$$\lambda_{\mathbf{T}_{\phi}}=\lambda_{\mathbf{T}_{\phi_{\mathrm{A}}}}+1 \tag{3.275}$$

Consider now an arbitrary vector of nodal displacements $\mathbf{d}_{\mathrm{C}}$ and the corresponding kinematically admissible vector of rotations

$$\boldsymbol{\phi}_{\mathrm{C}}=\mathbf{C}\mathbf{d}_{\mathrm{C}} \tag{3.276}$$

The matrix $\mathbf{T}_{\phi}$ (3.237) transforms $\boldsymbol{\phi}_{\mathrm{C}}$ into itself,

$$\mathbf{T}_{\phi}\,\boldsymbol{\phi}_{\mathrm{C}}=\mathbf{C}\mathbf{K}_{\mathrm{A}}^{-1}\mathbf{C}^{\mathrm{T}}\,\mathbf{K}_{\mathrm{A}}^{\mathrm{M}}\,\mathbf{C}\mathbf{d}_{\mathrm{C}}=\mathbf{C}\mathbf{K}_{\mathrm{A}}^{-1}\mathbf{K}_{\mathrm{A}}\,\mathbf{d}_{\mathrm{C}}=\mathbf{C}\mathbf{d}_{\mathrm{C}}=\boldsymbol{\phi}_{\mathrm{C}} \tag{3.277}$$

and, according to (3.269),

$$\mathbf{T}_{\phi_A}\,\boldsymbol{\phi}_C = \mathbf{0} \tag{3.278}$$

Hence, any vector $\boldsymbol{\phi}_C$ is an eigenvector of $\mathbf{T}_\phi$, with a unit eigenvalue, and of $\mathbf{T}_{\phi_A}$, with a null eigenvalue.

For a beam partition with *m* elements and *n* degrees of freedom, the degree of static indeterminacy is $2m - n$ and there are, according to definition (3.276), *n* linearly independent vectors $\boldsymbol{\phi}_C$.

If the beam is isostatic ($2m = n$), since $\mathbf{T}_{\phi_A}$ (resp. $\mathbf{T}_\phi$) is a $2m \times 2m$ matrix, all its eigenvalues are zero (resp. one). This means that, in the isostatic case, the *n* linearly independent eigenvectors defined by (3.276) span the eigenspace of the matrices $\mathbf{T}_{\phi_A}$ and $\mathbf{T}_\phi$.

However, in the hyperstatic case ($2m > n$), the remaining $2m - n$ eigenvalues of the matrices $\mathbf{T}_{\phi_A}$ and $\mathbf{T}_\phi$ still have to be determined. Having this objective in view the principle of virtual work is applied to the spectral analysis of $\mathbf{T}_{\phi_A}$ and $\mathbf{T}_\phi$.

Consider an arbitrary self-equilibrating statically admissible virtual bending moment field $\delta\tilde{M}$, which exists since the beam is hyperstatic, to which corresponds the vector $\delta\mathbf{M} \neq \mathbf{0}$. Consider also the rotations vectors $\boldsymbol{\phi}$ and $\boldsymbol{\phi}^{(1)}$ which correspond to compatible curvature fields. Then, according to the principle of virtual work

$$\delta\mathbf{M}\boldsymbol{\phi} = \mathbf{0} \tag{3.279}$$

$$\delta\mathbf{M}\boldsymbol{\phi}^{(1)} = \mathbf{0} \tag{3.280}$$

Substituting $\boldsymbol{\phi} = \boldsymbol{\phi}_{A,incr} + \boldsymbol{\phi}^{(1)} + \boldsymbol{\phi}_{NL}$, see (3.268), in (3.279) gives

$$\delta\mathbf{M}\boldsymbol{\phi}_{A,incr} = -\delta\mathbf{M}\boldsymbol{\phi}^{(1)} - \delta\mathbf{M}\boldsymbol{\phi}_{NL} \tag{3.281}$$

and summing (3.280) gives

$$\delta\mathbf{M}\boldsymbol{\phi}_{A,incr} = -\delta\mathbf{M}\boldsymbol{\phi}_{NL} \tag{3.282}$$

Consider again the eigenpair ($\lambda_{\mathbf{T}_{\phi_A}}$, $\hat{\boldsymbol{\phi}}_{NL}$) of $\mathbf{T}_{\phi_A}$. Introducing (3.273) into (3.270), gives

$$\hat{\boldsymbol{\phi}}_{A,incr} = \mathbf{T}_{\phi_A}\,\hat{\boldsymbol{\phi}}_{NL} = \lambda_{\mathbf{T}_{\phi_A}}\,\hat{\boldsymbol{\phi}}_{NL} \tag{3.283}$$

and substituting this expression into condition (3.282), gives

$$\delta\mathbf{M}\,\lambda_{\mathbf{T}_{\phi_A}}\,\hat{\boldsymbol{\phi}}_{NL} = -\delta\mathbf{M}\hat{\boldsymbol{\phi}}_{NL} \tag{3.284}$$

Since eigenvectors are non-null by definition and $\delta\mathbf{M} \neq \mathbf{0}$, the equation above can be satisfied only for $\lambda_{\mathbf{T}_{\phi_A}} = -1$.

In conclusion, the eigenvalues of $\mathbf{T}_{\phi_A}$ are 0, with multiplicity *n*, and -1 with multiplicity $2m - n$ and the corresponding eigenvalues of $\mathbf{T}_{\phi}$ are $0 + 1 = 1$, with multiplicity *n*, and $-1 + 1 = 0$, with multiplicity $2m - n$. Hence,

$$\rho\left[\mathbf{T}_{\phi}\right] = \rho\left[\mathbf{T}_{\phi_A}\right] = 1 \tag{3.285}$$

This result, together with (3.267) and (3.272) proves (3.265).

3.6.4. Sufficient convergence conditions of the basic discrete description

In the previous section it was proved that $\rho\left[\mathbf{T}_{\chi}\right] = \rho\left[\mathbf{T}_{\mathrm{M}}\right] = 1$. Hence, according to the Jacobian expressions (3.263) and (3.264), the iteration formulas of the basic discrete description of FFM are convergent if, respectively, $\mathbf{G}_{\chi}^{\mathrm{II}}$ and $\mathbf{G}_{\mathrm{M}}^{\mathrm{II}}$ are contractive, *i.e.* if conditions (3.48) and (3.49) are satisfied at every cross section. According to (3.42), the condition $\left|\beta_{\chi,i}\right| < 1$ is equivalent to

$$0 < \frac{EI_i}{EI_{\mathrm{A},i}} < 2 \tag{3.286}$$

at every end section, *i.e.* for $i = 1,2,\ldots,2m$. This condition implies that $EI_i \neq 0$ and that the algebraic sign of the auxiliary bending stiffness is equal to that of the effective bending stiffness. Since it is admitted that $EI_i > 0$ (3.8), the above conditions reduce to

$$EI_{\mathrm{A},i} > \frac{1}{2} EI_i > 0 \tag{3.287}$$

Hence, $\mathrm{FFM}_{\mathrm{Def}}$ converges if the auxiliary constitutive law verifies this condition at the end sections of the elements of the beam partition.

On the other hand, according to (3.43), the condition $\left|\beta_{\mathrm{M},i}\right| < 1$ is equivalent to

$$0 < \frac{EI_{\mathrm{A},i}}{EI_i} < 2 \tag{3.288}$$

at every end section. This condition is similar to (3.286). Once again, the auxiliary bending stiffness must have the algebraic sign of the effective bending stiffness. Hence, since it was admitted that $EI_i > 0$, the condition for convergence is

$$0 < EI_{\mathrm{A},i} < 2EI_i \tag{3.289}$$

at the end section of every element.

Expressions (3.264) and (3.263) shows that the closest the values of $EI_{\mathrm{A},i}$ are to the values of EI_i the closer is the Jacobian to zero and the fastest the convergence rate of $\mathrm{FFM_S}$ and $\mathrm{FFM_{Def}}$. However, since EI_i is nonlinear, the choice of these optimal values for the EI_{A} field may not be a trivial task. Finally, note that the numerical convergence of $\mathrm{FFM_{Def}}$ and $\mathrm{FFM_S}$ iterative procedures is achieved when the relative error of a certain norm, *e.g.* the Euclidian norm, of the curvatures or bending moments, is less than a given tolerance. When this condition gets satisfied, the relative error of other relevant variables, such as the deflections, is also less than a corresponding tolerance. Hence, in practical applications of FFM other convergence criteria may be used.

3.7. Second illustrative example

The next example illustrates the role played in $\mathrm{FFM_{Def}}$ and $\mathrm{FFM_S}$ iterative procedures by the chosen (i) mesh refinement and (ii) auxiliary bending stiffness field EI_{A}.

Consider the prismatic continuous beam with two spans of length $L = 1$, see Figure 3.29. The elastic bending constitutive relation is given by (3.52), which is bounded by $\pm M_{\mathrm{ref}} = 1$, see Figure 3.12. The beam carries a point load[8] with magnitude $Q = 4$ at midspan of its right span.

This structure has one degree of static indeterminacy. Hence, the bending moment field can be expressed in terms of Q and the bending moment at a single section, for instance M_{S2} at the

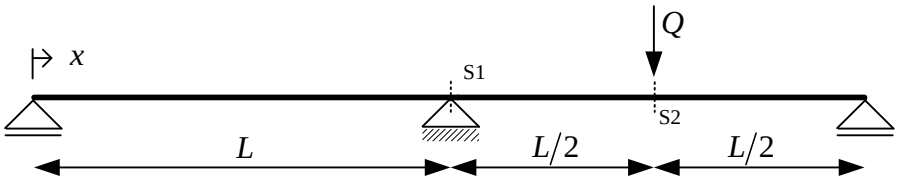

Figure 3.29. Example 3.2. Continuous beam: geometry, boundary conditions and loading.

[8] This load value has to be such that the maximum absolute bending moment in the beam is less than $M_{\mathrm{ref}} = 1$. For instance, when applying $\mathrm{MFF_S}$, if this condition is not fulfilled the curvature $\hat{\chi}[M]$ becomes undefined during the iterative procedure. A simple plastic analysis gives $QL/4 \le 1.5M_{\mathrm{ref}}$, *i.e.* $Q \le 6M_{\mathrm{ref}} = 6$.

loaded section. The equilibrium condition gives the bending moment at the middle support section $M_{S1} = 2M_{S2} - QL/2$. The exact solution can be calculated by the force method, with the primary structure defined by releasing the bending moment at the section over the middle support. The corresponding compatibility condition is given by

$$\int_0^{2L} \tilde{b}\,\hat{\chi}\left[\tilde{M}[x]\right] dx = 0 \tag{3.290}$$

where $\tilde{b}$ is a self-equilibrated bending moment distribution. This equation has a single real solution defined by $M_{S1} = -0.416$, $M_{S2} = 0.792$ and $\chi_{S2} = 1.29$ which was computed with the computer algebra system *Mathematica* (Wolfram, 2008). To the maximum bending moment at S2 corresponds a minimum of the tangent bending stiffness $EI_{S2} = 0.228$.

A constant auxiliary bending stiffness field EI_A along the beam was chosen. The corresponding linear solution is given by $M_{L,S2} = M_{S2}^{(1)} = 0.8125$.

A first uniform mesh with four elements, was consecutively refined by bisection, establishing a family of six uniform meshes with $2^{i+1} = 4, 8, \ldots, 128$ elements. Figure 3.30 and Table 3.3

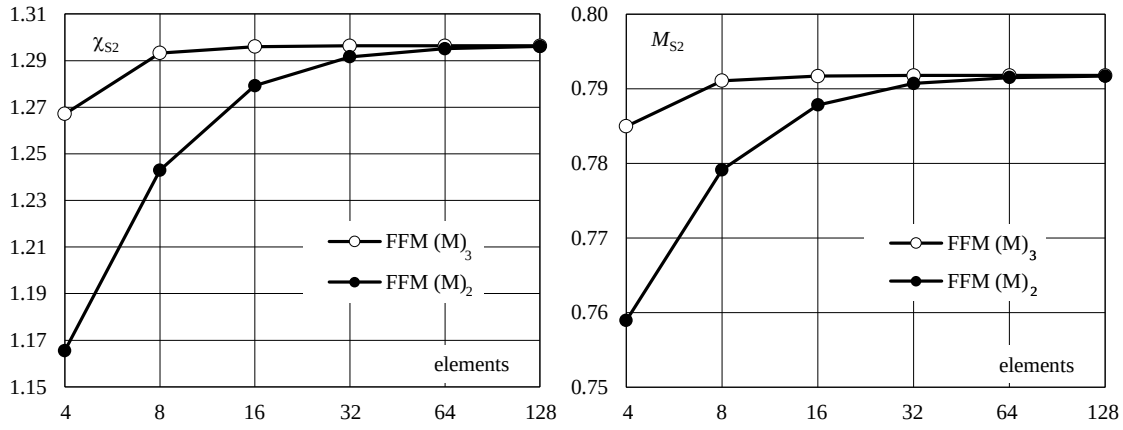

Figure 3.30. Example 3.2: Mesh-convergence of FFM_2 and FFM_3.

Table 3.3 – Example 3.2: MFF solutions and exact solution.

		number of elements (FFM)						exact solution
		4	8	16	32	64	128	
χ_{S2}	FFM(M)$_2$	1.166	1.243	1.279	1.292	1.295	1.296	1.296
	FFM(M)$_3$	1.267	1.293	1.296	1.296	1.296	1.296	
M_{S2}	FFM(M)$_2$	0.759	0.779	0.788	0.791	0.792	0.792	0.792
	FFM(M)$_3$	0.785	0.791	0.792	0.792	0.792	0.792	

present the values of the maxima curvature χ_{S2} and bending moment M_{S2} computed with FFM(M)$_2$ and FFM(M)$_3$.

A convergence analysis was performed with respect to (i) the mesh refinement (*mesh*-convergence) and (ii) FFM iterative procedure itself (*FFM*-convergence).

The convergence analyses are based on two measures of the relative errors of a given variable x. Relative error I compares the results of successive iterations

$$err_{\mathrm{I}}^{(i)} = \left| \frac{x^{(i)} - x^{(i-1)}}{x^{(i-1)}} \right| \tag{3.291}$$

or successive meshes

$$err_{\mathrm{I},j} = \left| \frac{x_j - x_{j-1}}{x_{j-1}} \right| \tag{3.292}$$

while relative error II compares the exact solution x_{ex} with the result of a given iteration

$$err_{\mathrm{II}}^{(i)} = \left| \frac{x^{(i)} - x_{\mathrm{ex}}}{x_{\mathrm{ex}}} \right| \tag{3.293}$$

or mesh

$$err_{\mathrm{II},j} = \left| \frac{x_j - x_{\mathrm{ex}}}{x_{\mathrm{ex}}} \right| \tag{3.294}$$

For a given mesh, the ith approximation of variable x is *FFM*-convergent if its relative error I is less than a fixed tolerance tol_{FFM},

$$err_{\mathrm{I}}^{(i)} < tol_{\mathrm{FFM}} \tag{3.295}$$

or its relative error II is inferior to tol_{FFM},

$$err_{\mathrm{II}}^{(i)} < tol_{\mathrm{FFM}} \tag{3.296}$$

Consider the set of meshes established above by successive bisection. Let x_j be the *FFM*-convergent approximation of x for the jth mesh and tolerance tol_{FFM}, *i.e.* satisfying (3.295). The value x_j is also *mesh*-convergent if its relative error I is inferior to tol_{mesh},

$$err_{\mathrm{I},j} < tol_{\mathrm{mesh}} \tag{3.297}$$

or its relative error II is inferior to tol_{mesh},

$$err_{\mathrm{II},\,j} < tol_{\mathrm{mesh}} \tag{3.298}$$

Thence, any *mesh*-convergent solution is also *FFM*-convergent, but the converse is not necessarily true.

Figure 3.31 presents the results of a *mesh*-convergence analysis with $tol_{\mathrm{FFM}} = 0.001$ and $tol_{\mathrm{mesh}} = 0.01$, *i.e.*, each solution in these graphics represents a *FFM*-convergent solution. Figure 3.32 presents the same results in a semi-log plot (or log-log if we think in terms of element length): the logarithm of the errors is seen to decrease almost linearly with the mesh refinement. Moreover, the higher slope of the curves defined by FFM_3 solutions reveals their faster convergence. These patterns are typical of the Finite Element Method, (Reddy, 1984, Becker *et al.*, 1981).

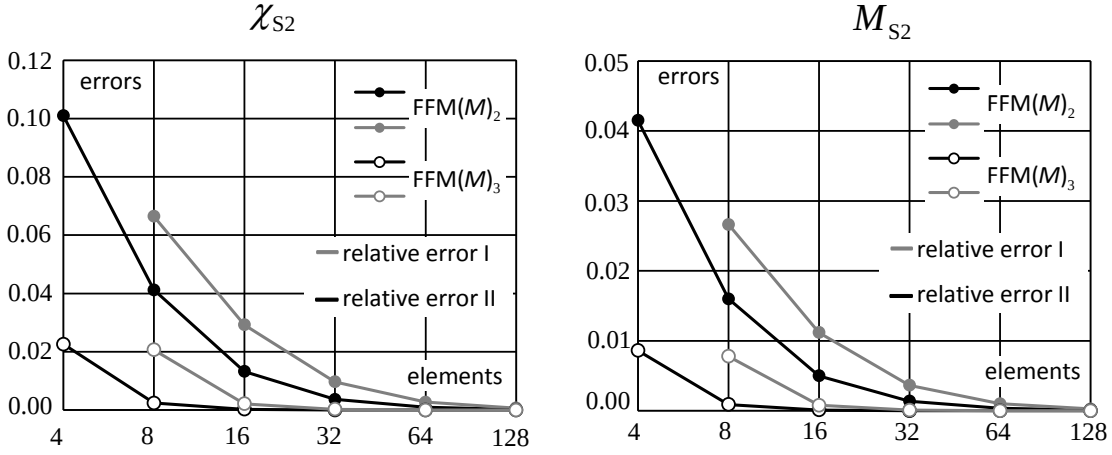

Figure 3.31. Example 3.2: Mesh-convergence of FFM_2 and FFM_3 (linear scale).

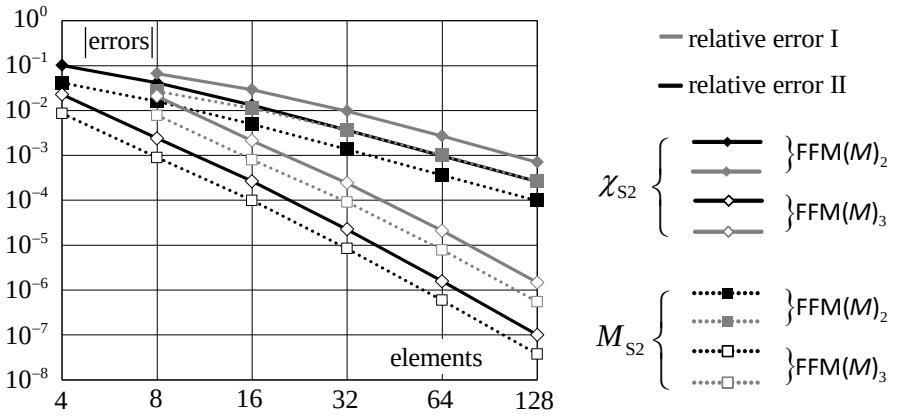

Figure 3.32. Example 3.2: Mesh-convergence of FFM_2 and FFM_3 (logarithmic scale).

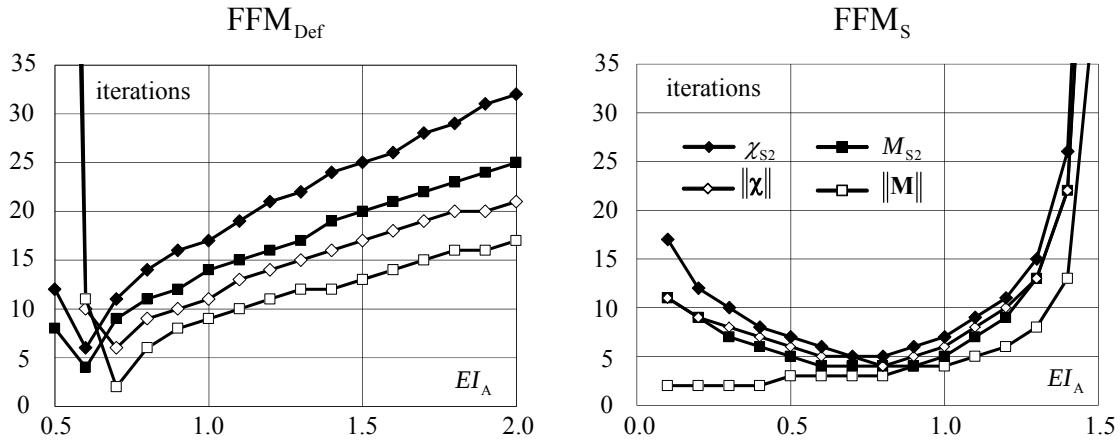

Figure 3.33. Example 3.2: Number of iterations required for FFM_2 to converge.

For the tolerance values given above, Figure 3.32 shows that *mesh*-convergence required 32 elements in the FFM_2 case while 16 elements sufficed for FFM_3.

In order to illustrate how the performance of FFM iterative procedures depends on the selected EI_{A} field, the *FFM*-convergence was investigated. For a mesh of 128 elements and EI_{A} fields of constant magnitude chosen in the interval $[0.1,2]$, Figure 3.33 represents the number of iterations required for convergence in terms of χ_{S2}, M_{S2}, $\|\boldsymbol{\chi}\|$ and $\|\mathbf{M}\|$, where $\|.\|$ represents the Euclidean norm.

There was no numerical convergence of FFM_{Def} for $EI_{\mathrm{A}} < 0.5$ and of FFM_S for $EI_{\mathrm{A}} > 1.6$.

Considering the cross-sectional constitutive relation (3.52), the sufficient condition for FFM_{Def} to converge (3.287) gives

$$EI_{\mathrm{A}} > \frac{1}{2}\max \widetilde{EI} = \frac{1}{2} EI_0 = 0.5 \tag{3.299}$$

and the sufficient condition for FFM_S to converge (3.289) gives

$$0 < EI_{\mathrm{A}} < 2\min \widetilde{EI} = 2\, EI_{\mathrm{S2}} = 0.456\, EI_0 = 0.456 \tag{3.300}$$

The results plotted in Figure 3.33 show that FFM_{Def} and FFM_S sufficient convergence conditions are satisfied. Actually, FFM_S converges for values of EI_{A} up to 1.6, well above the maximum defined by (3.300). Moreover, it can be observed that the convergence rate depends strongly on the value of EI_{A} and that the optimal interval is $EI_{\mathrm{A}} \in [0.6\,,\,0.8]$. In § 3.6.4, it was proved that the convergence rate increases when the value of EI_{A} is similar, at every cross section, to the tangent bending stiffness EI. This conclusion can be used to improve the convergence rate, for example, selecting a different value of EI_{A} for each element of the mesh, based on the

linear solution. The results in Figure 3.33 show also that the number of iterations needed to achieve convergence in terms of the value at S_2 of a specific variable is larger than with the Euclidian norm of the values of that variable along the beam.

3.8. Concluding remarks

The main results presented in this chapter are now summarised. The chapter covers all the fundamental aspects of FFM. *Model M* was chosen for this purpose because FFM was originally created with this model, see Gala (2007). The general ideas of FFM were presented in § 3.2.

FFM was shown to use the linear operator G_{χ}^{I} to treat nonlinear deformations as initial deformations and $G_{\mathrm{M}}^{\mathrm{I}}$ to treat fictitious stresses as initial stresses. These operators are similar to:

- the matrix operators $\mathbf{T}_{\mathrm{a}}$ and $\mathbf{T}_{\mathrm{b}}$ of Argyris's Initial Load Technique;
- the influence function $g\left[x,x'\right]$ of Lin;
- the influence function $g_{\mathrm{I}}\left[x,x'\right]$ of Aguado's Imposed Deformations Method.

The operators G_{χ}^{I} and $G_{\mathrm{M}}^{\mathrm{I}}$ are also related to the linear solver used in the Virtual Distortion Method, the Pseudo Distortion Method and the Pseudo Force Method of Deng and Ghosn (see chapter 2 for details and references).

FFM considers the nonlinear material behaviour by means of the cross-sectional operators G_{χ}^{II} and $G_{\mathrm{M}}^{\mathrm{II}}$ that also have correspondence in the Initial Strain and Initial Stress Methods presented in chapter 2. Hence, FFM general operators G_{χ} and G_{M} result of the composition of two operators, *i.e.* $G_{\chi}=G_{\chi}^{\mathrm{I}}\left[G_{\chi}^{\mathrm{II}}\right]$ and $G_{\mathrm{M}}=G_{\mathrm{M}}^{\mathrm{I}}\left[G_{\mathrm{M}}^{\mathrm{II}}\right]$; an analogous composition was identified in chapter 2 for the Initial Strain and Initial Stress Methods.

Sufficient conditions for the convergence of $\mathrm{FFM_{Def}}$ and $\mathrm{FFM_S}$ were derived, in a procedure similar to that followed by Argyris and Scharpf (1972), by taking advantage of the fact that G_{χ}^{I} and $G_{\mathrm{M}}^{\mathrm{I}}$ are non-expansive operators. These sufficient conditions are condensed in the expression $\left|\beta_{\chi}\right|<1$ for $\mathrm{FFM_{Def}}$ and $\left|\beta_{\mathrm{M}}\right|<1$ for $\mathrm{FFM_S}$. Since it is admitted that $EI>0$, these conditions are equivalent to $EI_{\mathrm{A}}>EI/2$ and $0<EI_{\mathrm{A}}<2EI$, respectively.

A comment must be made with respect to the practical application of these conditions. The $\mathrm{FFM_{Def}}$ seems to be more interesting, because it is easier to fulfil the convergence requirement $EI_{\mathrm{A}}>EI/2$. In fact, for constitutive laws without strain hardening branches, the choice of

values for EI_{A} corresponding to the initial tangent stiffness (or a larger value) guarantees the convergence of the iterative procedure. Moreover, $\mathrm{FFM_S}$ can have problems in dealing with constitutive laws with horizontal branches, or horizontal asymptotes, as seen in the first illustrative example presented in § 3.3.

However, FFM iterative procedures may converge even when the above sufficient conditions are not verified. This is clearly illustrated in the examples presented in this chapter and also in the examples presented in chapters 4 and 5. These examples show that the range of EI_{A} fields leading to convergent iterative procedures, but not fulfilling the convergence conditions, is very wide. It is therefore important to investigate what other factors affect the convergence of FFM.

It is worth noting that effective constitutive relations with horizontal branches or softening branches are not considered in this thesis. This is a severe limitation of FFM that might be surpassed, but requires further investigation.

Finally, let us present four important observations:

(i) One of the objectives of this work was to clarify the meaning of FFM iterative procedures from both physical and mathematical points of view. In this context, the explanation of the meaning of the operators G^{I} which transform initial deformations (resp. initial stresses) into effective generalized deformations (resp. effective generalized stresses) is a relevant achievement. However, two issues should still be investigated: (i) from the more general functional viewpoint, the operators G^{I} appear to be projection operators (Arantes e Oliveira, 1975); (ii) in the discrete case, there appears to be a close relation between matrices $\mathbf{T}$ and similar matrices established by Fellipa (1997, 2001).

(ii) The framework presented in § 3.2 and § 3.3 can be easily extended to cover nonlinear point elements; such an extension was used by Costa (2013).

(iii) Instead of following the flowcharts presented in § 3.6 to program FFM procedure, the implementation of the method can be based on the given discrete iteration formulas (3.251) and (3.252) for $\mathrm{FFM_2}$ and (3.241) for $\mathrm{FFM_3}$.

(iv) One of the initial reasons for the creation of FFM was the need for an analysis method of skeletal structures able to model the material nonlinearity like the Equivalent Force Method models the geometric nonlinearity. Now that this project revealed to be

feasible, the possible combination of the two methods might be able to tackle nonlinear geometrical and material problems. In practical terms, the combination of FFM with the equivalent force method is easy to implement, see Gala (2007) and Costa (2013). However the convergence of this combined method still has to be studied, and particularly, it should be investigated if the convergence criterion of each of these two methods is still valid when they are combined.

The last observation raises another question: what are the convergence conditions of the Equivalent Force Method? It appears that this question was never formulated or investigated, not to say solved. Our study of this topic appears to show that the equivalent force method always converges when an admissible solution exists, i.e. whenever at least one equilibrium configuration exists. A possible explanation for this result is that the equivalent force method is an application of Picard method, whose convergence bounds correspond to the cases were the equilibrium of the skeletal structure is possible (Bailey *et al.* 1968).

Chapter 4
The Fictitious Force Method – *model N*

In this chapter, the application of FFM with the rod *model N*, *i.e.* FFM(*N*), is presented. This model may be used in the analysis of trusses whose elements satisfy a nonlinear elastic constitutive relationship.

The fundamental concepts of FFM, previously presented in § 3.2, are first reviewed in the light of *model N*. Next, a discrete description of the elemental fictitious force system of FFM(*N*) is presented, which has the features needed for its combination with the fictitious force system of FFM(M)$_2$ to form the fictitious force system of FFM(*MN*) presented in the next chapter. In a third stage, the application of FFM(*N*) in the context of the matrix methods of structural analysis is presented and the convergence of FFM iterative procedure is reviewed. The chapter is concluded with an illustrative example.

In this chapter, the effective structure is a rod whose constitutive law is described, at each cross section, by

$$N \equiv \hat{N}\left[\varepsilon\right] \quad \text{or} \quad \varepsilon \equiv \hat{\varepsilon}\left[N\right] \tag{4.1}$$

The cross-sectional axial stiffness is given by

$$\widehat{EA} = \frac{d\hat{N}}{d\varepsilon} \tag{4.2}$$

This function of ε (or N) is discontinuous at every point with different right and left derivatives. Its inverse, the cross-sectional axial flexibility, is denoted $\widehat{EA}^{-1}$.

4.1. FFM with rod *model N*

4.1.1. The auxiliary problem

FFM(*N*) considers an *auxiliary structure* similar to the effective rod but whose cross sections follow a linear elastic auxiliary constitutive relation, given by

$$N_{\mathrm{A}} \equiv \hat{N}_{\mathrm{A}}\left[\varepsilon\right] = EA_{\mathrm{A}}\ \varepsilon \quad \text{or} \quad \varepsilon_{\mathrm{A}} \equiv \hat{\varepsilon}_{\mathrm{A}}\left[N\right] = \frac{N}{EA_{\mathrm{A}}} \tag{4.3}$$

In the auxiliary rod, the combination of the fictitious loading system F_{F} with the effective loading system F defines the auxiliary loading system F_{A}, which originates a deformation field that is equal to the deformation field produced in the effective rod by F only. To the loading system F_{F} corresponds now the fictitious axial force N_{F} that, together with the effective axial force N, defines the auxiliary axial force N_{A}

$$N_{\mathrm{A}} = N_{\mathrm{F}} + N \tag{4.4}$$

which expresses the auxiliary decomposition of the axial force. This is illustrated in Figure 4.1, where S denotes a generic section and S' and S'' its displaced configurations:

(i) Due to the action of loading system F on the auxiliary rod, section S moves to position S'. The displacement $\overline{\mathrm{SS}'}$ corresponds to the axial strain ε_{L}, point 2 in the figure;

(ii) When the loading system F_{A} acts on the auxiliary rod, section S moves to position S''. The displacement $\overline{\mathrm{SS}''}$ corresponds to the axial strain ε, represented by point 3 in the figure.

4.1.2. FFM(*N*) *by deformations* and FFM(*N*) *by stresses*

Introducing the auxiliary (4.3) and the effective (4.1) constitutive relations into the fictitious axial force definition (4.4), gives

$$N_{\mathrm{F}}\left[\varepsilon\right] = EA_{\mathrm{A}}\ \varepsilon - \hat{N}\left[\varepsilon\right] \tag{4.5}$$

and

$$N_{\mathrm{F}}\left[N\right] = EA_{\mathrm{A}}\ \hat{\varepsilon}\left[N\right] - N \tag{4.6}$$

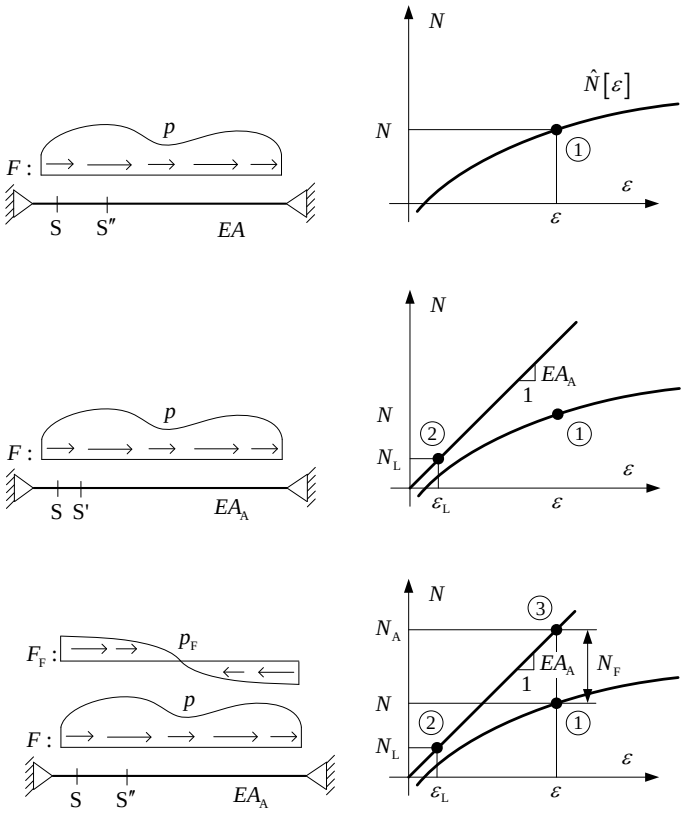

Figure 4.1. Illustration of the auxiliary problem of FFM(*N*).

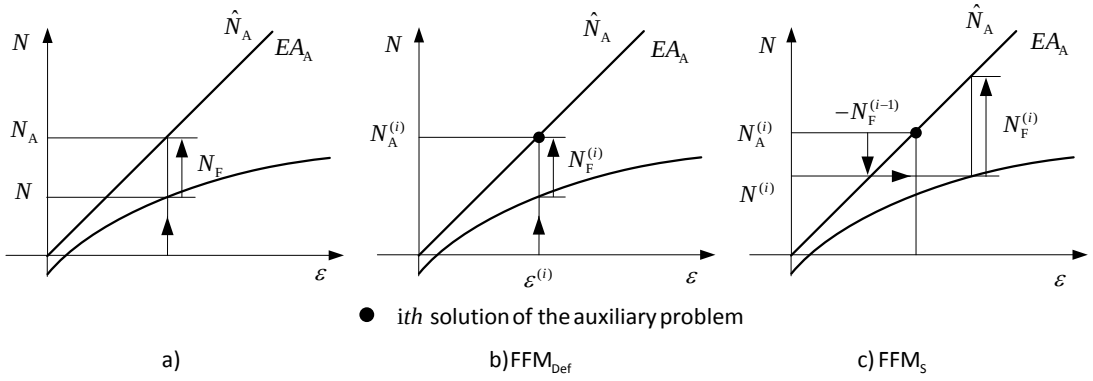

Figure 4.2. Calculation of fictitious axial force: a) non-iterative format, b) FFM_{Def} and c) FFM_S.

If neither ε nor N are known *a priori*, it may be helpful to write both these expressions in the iterative format

$$N_F^{(i)} = EA_A\ \varepsilon^{(i)} - \hat{N}\left[\varepsilon^{(i)}\right] \tag{4.7}$$

$$N_F^{(i)} = EA_A\ \hat{\varepsilon}\left[N^{(i)}\right] - N^{(i)} \tag{4.8}$$

which Figure 4.2 depicts schematically.

The iterative version of the auxiliary decomposition of the axial force (4.4), reads

$$N^{(i)} = N_{\mathrm{A}}^{(i)} - N_{\mathrm{F}}^{(i-1)} \tag{4.9}$$

This expression is used in both FFM(N)$_{\mathrm{S}}$ and FFM(N)$_{\mathrm{Def}}$. Expressions (4.8) and (4.9) are both deduced from (4.4) but they present a slight difference: in a given iteration N_{F} is calculated with the current value of N, but N is calculated with the previous value of N_{F}.

The initial guess required to start the iterative procedure is calculated for a null fictitious loading system and therefore

$$\begin{cases} \varepsilon^{(1)} \equiv \varepsilon_{\mathrm{L}} \\ N^{(1)} \equiv N_{\mathrm{L}} \end{cases} \tag{4.10}$$

where the pair $(\varepsilon_{\mathrm{L}}, N_{\mathrm{L}})$ represents a linear solution to the effective problem, *i.e.* the solution associated with the effective loading system F in the auxiliary rod. The flowchart in Figure 4.3, illustrates the application of the iterative procedures of FFM in the context of *model N*.

4.1.3. Fictitious forces and initial deformations

From the viewpoint of kinematics the effective axial strain can be decomposed in the auxiliary component ε_{A} and the remaining component

$$\varepsilon_{\mathrm{NL}} = \varepsilon - \varepsilon_{\mathrm{A}} \tag{4.11}$$

This relation, which expresses the auxiliary decomposition of the axial strain, is dual of (4.4) and corresponds to (3.19). Substituting in expression (4.4) the auxiliary constitutive relation (4.3) and, afterwards, the nonlinear component of the axial strain defined above, gives

$$N_{\mathrm{F}} = EA_{\mathrm{A}}\, \varepsilon_{\mathrm{NL}} \tag{4.12}$$

The axial strain field $\varepsilon_{\mathrm{NL}}$ can be regarded as an initial generalized strain field whose effect on the auxiliary rod, combined with that of the effective loading system, gives the auxiliary solution $(\varepsilon, N_{\mathrm{A}})$, see Figure 4.4. Alternatively, this auxiliary solution can be obtained combining the effect on the auxiliary rod of the axial force N_{F}, which can be regarded as an initial generalized stress field, with that of the effective loading system.

Actually, besides its iterative character, the auxiliary problem tackled by FFM(N) is similar to the problem of a rod with a linear constitutive law of the type (4.3) subjected to a uniform

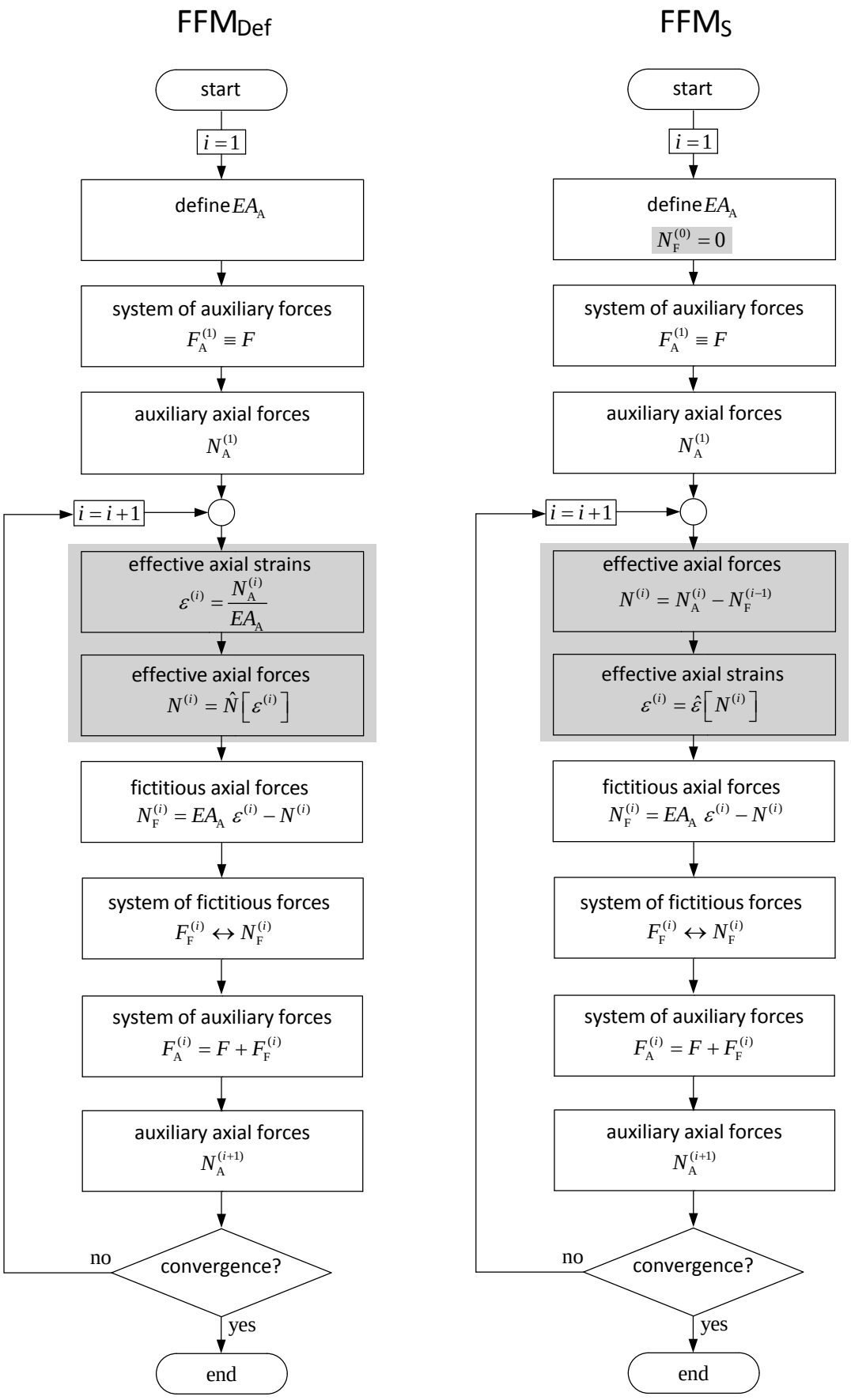

Figure 4.3. FFM(*N*) iterative procedures (differences identified with shaded boxes).

(in the cross section) temperature variation corresponding to the initial axial strain ε_{I}. Hence, Duhamel's method can be used to analyse this problem and to determine the fields of elastic axial strain ε_{E} and axial force N, as illustrated in Figure 4.5. In this case, the elastic strain ε_{E} in the thermal problem corresponds to $\varepsilon_{\mathrm{A}}-\varepsilon_{\mathrm{L}}$ in the auxiliary problem, as represented in Table 4.1.

4.1.4. Iteration formulas of FFM(*N*)

An operator T can now be defined for the auxiliary rod which transforms the generic action $\left(\varepsilon_{\mathrm{NL}},F\right)$ into the effective axial strain field ε,

$$\varepsilon = T\left[\varepsilon_{\mathrm{NL}},F\right] \tag{4.13}$$

Moreover, since, as shown in chapter 3, this operator T is linear in the pair $\left(\varepsilon_{\mathrm{NL}},F\right)$,

$$\varepsilon = T\left[\varepsilon_{\mathrm{NL}},F\right] = T\left[\varepsilon_{\mathrm{NL}},0\right] + T\left[0,F\right] = T_{\varepsilon}\left[\varepsilon_{\mathrm{NL}}\right] + \varepsilon_{\mathrm{L}} \tag{4.14}$$

where $T_{\varepsilon}\left[\varepsilon_{\mathrm{NL}}\right] = T\left[\varepsilon_{\mathrm{NL}},0\right]$ is a linear operator and $\varepsilon_{\mathrm{L}} = T\left[0,F\right]$. Hence, (4.14) defines the operator $G_{\varepsilon}^{\mathrm{I}}$ transforming (initial) axial strains $\varepsilon_{\mathrm{NL}}$ into the effective strains,

$$\varepsilon = G_{\varepsilon}^{\mathrm{I}}\left[\varepsilon_{\mathrm{NL}}\right] \equiv \varepsilon_{\mathrm{L}} + T_{\varepsilon}\left[\varepsilon_{\mathrm{NL}}\right] \tag{4.15}$$

Subtracting $\varepsilon_{\mathrm{NL}}$ to both members of this expression and recalling that $\varepsilon_{\mathrm{A}} \equiv \varepsilon - \varepsilon_{\mathrm{NL}}$, gives

$$\varepsilon_{\mathrm{A}} = \varepsilon_{\mathrm{L}} + T_{\varepsilon}\left[\varepsilon_{\mathrm{NL}}\right] - \varepsilon_{\mathrm{NL}} \tag{4.16}$$

Multiplying both members by EA_{A} and recalling that $N = EA_{\mathrm{A}}\ \varepsilon_{\mathrm{A}}$ and $N_{\mathrm{L}} = EA_{\mathrm{A}}\ \varepsilon_{\mathrm{L}}$, gives

$$N = N_{\mathrm{L}} + EA_{\mathrm{A}}\ T_{\mathrm{N}}\left[\varepsilon_{\mathrm{NL}}\right] \tag{4.17}$$

where one more linear operator, $T_{\mathrm{N}} \equiv T_{\varepsilon} - I$, was introduced. Since $N_{\mathrm{F}} = EA_{\mathrm{A}}\ \varepsilon_{\mathrm{NL}}$, the right hand member of the above expression is an operator $G_{\mathrm{N}}^{\mathrm{I}}$ which transforms fictitious axial forces into the effective axial forces,

$$N = G_{\mathrm{N}}^{\mathrm{I}}\left[N_{\mathrm{F}}\right] \equiv N_{\mathrm{L}} + T_{\mathrm{N}}\left[N_{\mathrm{F}}\right] \tag{4.18}$$

The operators $G_{\varepsilon}^{\mathrm{I}}$ and $G_{\mathrm{N}}^{\mathrm{I}}$ defined in (4.15) and (4.18), correspond to the operators G_{χ}^{I} and $G_{\mathrm{M}}^{\mathrm{I}}$ presented for *model M* in chapter 3.

Since $\varepsilon_{\mathrm{NL}}$ and N_{F} are usually not known in advance, they can be defined in terms of an estimative of (i) the effective axial strains ε, using (4.12) and (4.7),

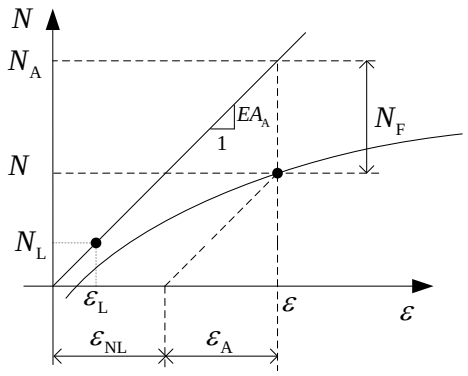

Figure 4.4. Fictitious axial force and nonlinear component of axial strain.

Table 4.1 – FFM(*N*): Duhamel's *vs.* FFM approaches.

Duhamel	ε_{I}	N_{I}	F_{R}	N_{R}	ε_{E}
FFM	$\varepsilon_{\mathrm{NL}}$	$-N_{\mathrm{F}}$	$-F_{\mathrm{F}}$	N_{A}	$\varepsilon_{\mathrm{A}}-\varepsilon_{\mathrm{L}}$

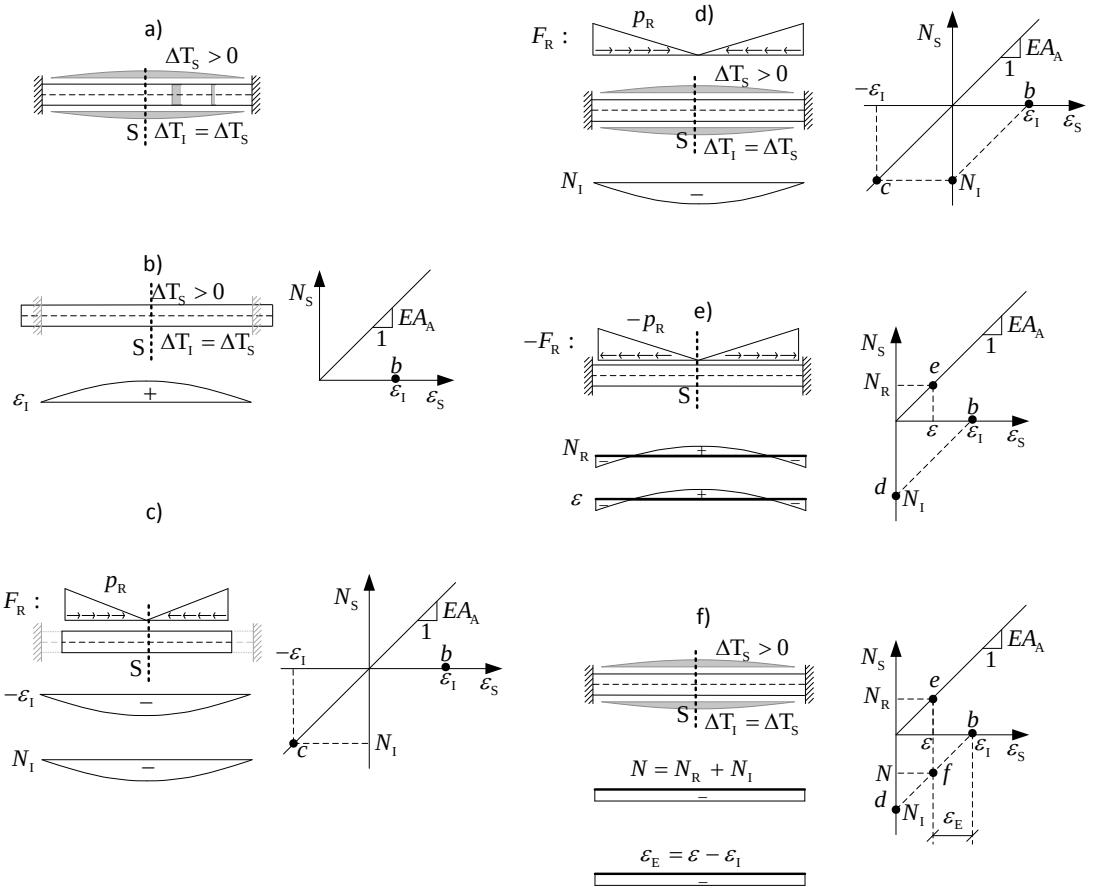

Figure 4.5. FFM(*N*): Duhamel's method applied to the analysis of a rod subjected to a thermal action.

$$\varepsilon_{\mathrm{NL}}^{(i)} = G_{\varepsilon}^{\mathrm{II}}\left[\varepsilon^{(i)}\right] \equiv \frac{N_{\mathrm{F}}\left[\varepsilon^{(i)}\right]}{EA_{\mathrm{A}}} \tag{4.19}$$

or (ii) the effective axial forces N, using (4.8),

$$N_{\mathrm{F}}^{(i)} = G_{\mathrm{N}}^{\mathrm{II}}\left[N^{(i)}\right] \equiv N_{\mathrm{F}}\left[N^{(i)}\right] \tag{4.20}$$

Introducing the last but one expression into (4.15), and recalling that $\varepsilon^{(1)} \equiv \varepsilon_{\mathrm{L}}$, gives the iterative formula of $\mathrm{FFM}_{\mathrm{Def}}$

$$\varepsilon^{(i+1)} = G_{\varepsilon}\left[\varepsilon^{(i)}\right] \equiv G_{\varepsilon}^{\mathrm{I}}\left[G_{\varepsilon}^{\mathrm{II}}\left[\varepsilon^{(i)}\right]\right] = \varepsilon^{(1)} + T_{\varepsilon}\left[\varepsilon_{\mathrm{NL}}\left[\varepsilon^{(i)}\right]\right] \tag{4.21}$$

Similarly, introducing the last but one expression in the iterative version of (4.18), and recalling that $N^{(1)} \equiv N_{\mathrm{L}}$, gives the iterative formula of $\mathrm{FFM}_{\mathrm{S}}$,

$$N^{(i+1)} = G_{\mathrm{N}}\left[N^{(i)}\right] \equiv G_{\mathrm{N}}^{\mathrm{I}}\left[G_{\mathrm{N}}^{\mathrm{II}}\left[N^{(i)}\right]\right] = N^{(1)} + T_{\mathrm{N}}\left[N_{\mathrm{F}}\left[N^{(i)}\right]\right] \tag{4.22}$$

Recall that in axially isostatic structures the iterative procedure of $\mathrm{FFM}_{\mathrm{S}}$ gets reduced to a unique "iteration", after the initialization, since in this case the axial force is independent of the material nonlinearities, *i.e.* $N^{(1)} \equiv N$.

4.1.5. Convergence conditions of FFM(*N*)

According to the composition $G_{\varepsilon} \equiv G_{\varepsilon}^{\mathrm{I}}\left[G_{\varepsilon}^{\mathrm{II}}\right]$ in (4.21) (resp. $G_{\mathrm{N}} \equiv G_{\mathrm{N}}^{\mathrm{I}}\left[G_{\mathrm{N}}^{\mathrm{II}}\right]$ in (4.22)), $\mathrm{FFM}(N)_{\mathrm{Def}}$ (resp. $\mathrm{FFM}(N)_{\mathrm{S}}$) iteration formula converges if (i) both operators in this composition are non-expansive and (ii) at least one of them is contractive. On the other hand, deriving (4.19) with respect to ε and recalling (4.5) gives

$$\frac{d\varepsilon_{\mathrm{NL}}\left[\varepsilon\right]}{d\varepsilon} = \beta_{\varepsilon} \equiv \frac{EA_{\mathrm{A}} - \widehat{EA}}{EA_{\mathrm{A}}} \tag{4.23}$$

Deriving (4.20), which repeats (4.6), with respect to N gives

$$\frac{dN_{\mathrm{F}}\left[N\right]}{dN} = \beta_{\mathrm{N}} \equiv \frac{EA_{\mathrm{A}} - \widehat{EA}}{\widehat{EA}} = \frac{\beta_{\varepsilon}}{1-\beta_{\varepsilon}} \tag{4.24}$$

Thence, $G_{\varepsilon}^{\mathrm{II}}$ is contractive if

$$\left|\beta_{\varepsilon}\right| < 1 \tag{4.25}$$

and $G_{\mathrm{N}}^{\mathrm{II}}$ is contractive if

$$\left|\beta_{\mathrm{N}}\right|<1 \tag{4.26}$$

In §§ 4.4.1 and 4.4.2, it is explained that the operators $G_{\varepsilon}^{\mathrm{I}}$ and $G_{\mathrm{N}}^{\mathrm{I}}$, when established in the context of the discrete description of FFM(*N*), are non-expansive. Therefore, the two last expressions are sufficient convergence conditions for FFM(*N*).

4.2. Elemental fictitious force system for rod *model N*

This section presents the fictitious force system of FFM(*N*) for a rod element. The definition of a mesh of rod elements (domain partition) and the description of the rod element are presented in § 4.2.1. The differential description of the fictitious force system is then presented in § 4.2.2. A decomposition of the elemental fields is presented in § 4.2.3 and, finally, the discrete description of the fictitious force system is presented in § 4.2.4

4.2.1. Domain partition

Figure 4.6 illustrates part of a rod under a generic loading composed of (i) a distributed axial load $\tilde{p}$ and (ii) one axial point load P[9]. The axial force and axial strain fields in the element are

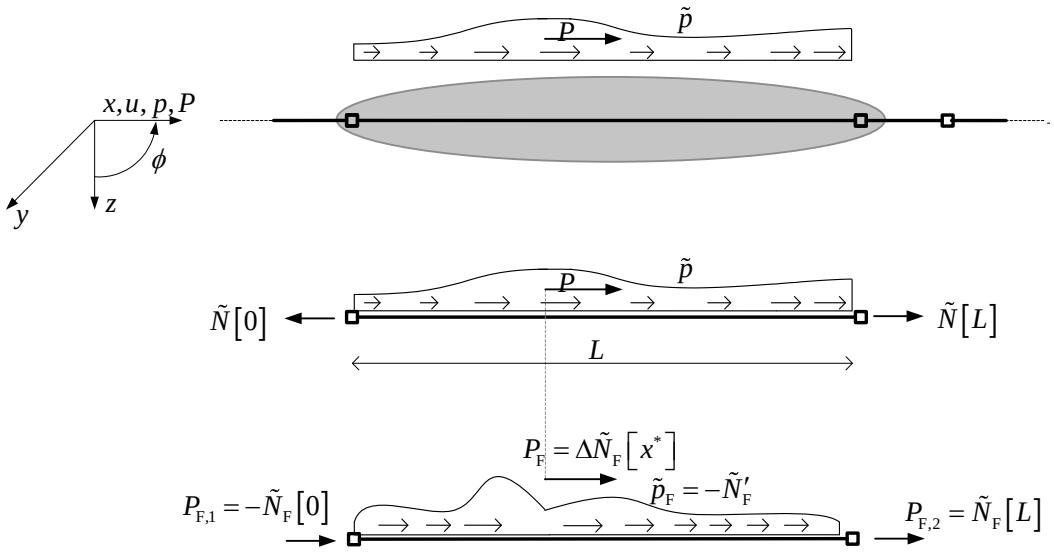

Figure 4.6. Rod partition (top), effective (middle) and fictitious (bottom) elemental force systems and corresponding internal forces at rod ends.

[9] One load for illustrative matters but any number would do.

linked together by the relationship

$$\tilde{N} = \hat{N}\left[\tilde{\varepsilon}\right] \quad \text{or} \quad \tilde{\varepsilon} = \hat{\varepsilon}\left[\tilde{N}\right] \tag{4.27}$$

An eligible partition of the rod must comply with its geometry – each element is prismatic – and supports – there is a mandatory or natural node next to each support. The axial stiffness field is given by

$$\widetilde{EA} = \widehat{EA}\left[\tilde{\varepsilon}\right] \quad \text{or} \quad \widetilde{EA} = \widehat{EA}\left[\tilde{N}\right] \tag{4.28}$$

According to the elemental system of coordinates introduced in § 3.4.1, the element end sections correspond to $x = 0$ and $x = L$.

4.2.2. Differential description of the elemental fictitious force system

The simplifying assumption of a constant auxiliary stiffness in each element, will be adopted once more (see § 3.4.2),

$$\widetilde{EA}_{\mathrm{A}}\left[x\right] = EA_{\mathrm{A}} = \mathrm{const} \tag{4.29}$$

Since expression (4.5) is valid for each elemental cross section, the fictitious axial force field can be established in terms of the axial strains, as required by FFM(N)$_{\mathrm{Def}}$,

$$\tilde{N}_{\mathrm{F}} = \hat{N}_{\mathrm{A}}\left[\tilde{\varepsilon}\right] - \hat{N}\left[\tilde{\varepsilon}\right] \tag{4.30}$$

Alternatively, according to (4.6) the fictitious axial force can be written in terms of the effective axial forces, as required by FFM(N)$_{\mathrm{S}}$,

$$\tilde{N}_{\mathrm{F}} = EA_{\mathrm{A}}\,\hat{\varepsilon}\left[\tilde{N}\right] - \tilde{N} \tag{4.31}$$

Similarly, recalling the second expression (4.3) and (4.11), the auxiliary and nonlinear components of the axial strain field are given by

$$\tilde{\varepsilon}_{\mathrm{A}} = \frac{\tilde{N}}{EA_{\mathrm{A}}} \tag{4.32}$$

$$\tilde{\varepsilon}_{\mathrm{NL}} = \tilde{\varepsilon} - \tilde{\varepsilon}_{\mathrm{A}} \tag{4.33}$$

The elemental fictitious force system F_{F} is in equilibrium with the fictitious axial force field $\tilde{N}_{\mathrm{F}}$ in the rod element. Thence, it has two types of forces acting along the axial direction:

(i) a distributed force,

$$\tilde{p}_{\mathrm{F}} = -\tilde{N}'_{\mathrm{F}} \tag{4.34}$$

(ii) axial point forces at the fictitious axial force discontinuity sections,

$$P_{\mathrm{F},i} = -\Delta\tilde{N}_{\mathrm{F}}\left[x_i\right] \tag{4.35}$$

The latter sections include those with applied effective point loads P and the element boundaries where

$$P_{\mathrm{F},1} = -\tilde{N}_{\mathrm{F}}\left[0\right] \tag{4.36}$$

$$P_{\mathrm{F},2} = \tilde{N}_{\mathrm{F}}\left[L\right] \tag{4.37}$$

4.2.3. Decomposition of the elemental fields

Let us consider again the decomposition of the generic elemental field $\tilde{g}\left[x\right]$ introduced in chapter 3, and which shall be called the elemental fields decomposition,

$$\tilde{g} = \tilde{g}_{\Delta} + \tilde{g}_{\delta} \tag{4.38}$$

In that chapter, $\tilde{g}_{\Delta}$ was defined as a linear function because the curvature $\tilde{\chi}_{\Delta}$ is well characterized by the two elemental end sections rotations, which are the independent parameters characterizing the bending deformation of *model M*. However, since the deformation of the rod *model N* element is well characterized by a single parameter, the elemental elongation, $\tilde{g}_{\Delta}$ in the expression above can now be defined as a constant function.

Thence, the element right end section was chosen to be the unique interpolation section of the discretized field $\tilde{g}_{\Delta}$, *i.e.*

$$\tilde{g}_{\Delta}\left[x\right] = \tilde{g}\left[L\right] \tag{4.39}$$

The boundary values of the corrective term $\tilde{g}_{\delta}$ are now, see Figure 4.7,

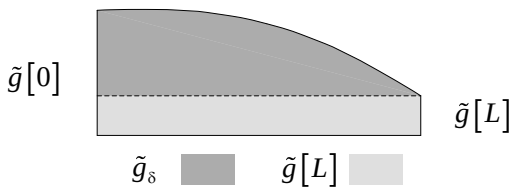

Figure 4.7. Decomposition of the elemental field $\tilde{g}\left[x\right]$.

$$\tilde{g}_{\delta}[L]=0 \tag{4.40}$$

$$\tilde{g}_{\delta}[0]=\tilde{g}[0]-\tilde{g}[L] \tag{4.41}$$

This decomposition can be applied to the axial strain field and its auxiliary and nonlinear components

$$\tilde{\varepsilon}[x]=\tilde{\varepsilon}_{\Delta}[x]+\tilde{\varepsilon}_{\delta}[x]=\tilde{\varepsilon}[L]+\tilde{\varepsilon}_{\delta}[x] \tag{4.42}$$

$$\tilde{\varepsilon}_{\mathrm{A}}[x]=\tilde{\varepsilon}_{\mathrm{A},\Delta}[x]+\tilde{\varepsilon}_{\mathrm{A},\delta}[x]=\tilde{\varepsilon}_{\mathrm{A}}[L]+\tilde{\varepsilon}_{\mathrm{A},\delta}[x] \tag{4.43}$$

$$\tilde{\varepsilon}_{\mathrm{NL}}[x]=\tilde{\varepsilon}_{\mathrm{NL},\Delta}[x]+\tilde{\varepsilon}_{\mathrm{NL},\delta}[x]=\tilde{\varepsilon}_{\mathrm{NL}}[L]+\tilde{\varepsilon}_{\mathrm{NL},\delta}[x] \tag{4.44}$$

and to the auxiliary, fictitious and effective axial force fields

$$\tilde{N}_{\mathrm{A}}[x]=\tilde{N}_{\mathrm{A},\Delta}[x]+\tilde{N}_{\mathrm{A},\delta}[x]=\tilde{N}_{\mathrm{A}}[L]+\tilde{N}_{\mathrm{A},\delta}[x] \tag{4.45}$$

$$\tilde{N}_{\mathrm{F}}[x]=\tilde{N}_{\mathrm{F},\Delta}[x]+\tilde{N}_{\mathrm{F},\delta}[x]=\tilde{N}_{\mathrm{F}}[L]+\tilde{N}_{\mathrm{F},\delta}[x] \tag{4.46}$$

$$\tilde{N}[x]=\tilde{N}_{\Delta}[x]+\tilde{N}_{\delta}[x]=\tilde{N}[L]+\tilde{N}_{\delta}[x] \tag{4.47}$$

The last but one expression shows that the fictitious axial force field $\tilde{N}_{\mathrm{F}}[x]$ can be decomposed in a constant term $\tilde{N}_{\mathrm{F},\Delta}[x]=\tilde{N}_{\mathrm{F}}[L]$ plus a corrective term $\tilde{N}_{\mathrm{F},\delta}[x]$. These axial force fields are in equilibrium with the element fictitious force system represented in Figure 4.8, *i.e.* the constant field $\tilde{N}_{\mathrm{F},\Delta}[x]=\tilde{N}_{\mathrm{F}}[L]$ is in equilibrium with two axial point forces

$$P^{\mathrm{a}}_{\mathrm{F},2}=-P^{\mathrm{a}}_{\mathrm{F},1}=\tilde{N}_{\mathrm{F}}[L] \tag{4.48}$$

and the corrective field $\tilde{N}_{\mathrm{F},\delta}[x]$ is in equilibrium with a distributed axial force $\tilde{p}_{\mathrm{F}}$,

$$\tilde{p}_{\mathrm{F}}=-\tilde{N}'_{\mathrm{F},\delta} \tag{4.49}$$

and an axial point force at $x = 0$,

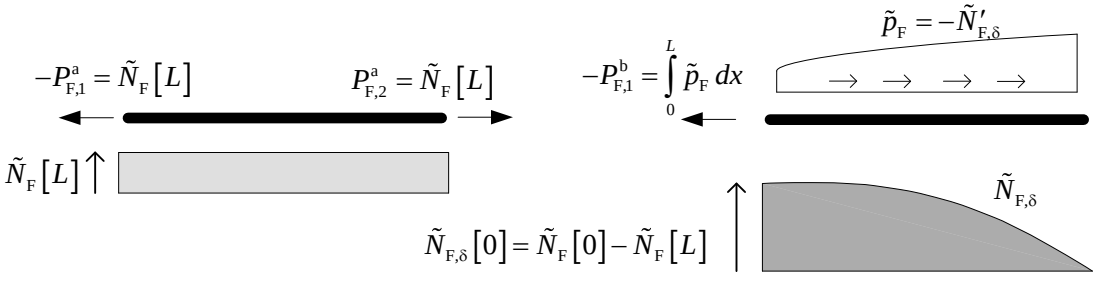

Figure 4.8. Elemental fictitious forces of FFM(*N*).

$$P_{\mathrm{F},1}^{\mathrm{b}} = -\int_0^L \tilde{p}_{\mathrm{F}}\, dx \tag{4.50}$$

Multiplying both members of (4.42) by EA_{A} it is easily concluded, according to (4.3), that there is a direct correspondence between each term of the resulting expression and (4.45). For instance, the corrective fields $\tilde{\varepsilon}_{\delta}[x]$ and $\tilde{N}_{\mathrm{A},\delta}[x]$ are proportional to each other

$$\tilde{N}_{\mathrm{A},\delta}[x] = EA_{\mathrm{A}}\ \tilde{\varepsilon}_{\delta}[x] \tag{4.51}$$

Similarly,

$$\tilde{N}_{\mathrm{A},\Delta} = EA_{\mathrm{A}}\ \tilde{\varepsilon}_{\Delta} \tag{4.52}$$

$$\tilde{N}_{\delta}[x] = EA_{\mathrm{A}}\ \tilde{\varepsilon}_{\mathrm{A},\delta}[x] \tag{4.53}$$

(Note that we have to consider both the auxiliary decomposition and the elemental fields decomposition.) The corrective field $\tilde{N}_{\delta}[x]$ equilibrates the part of the loading applied between the end sections in an isostatic element supported on the left side only, *i.e.* this field is fully defined by equilibrium considerations and is independent of the constitutive law. Hence, it is equal to the corresponding field in the linear solution,

$$\tilde{N}_{\delta}[x] = \tilde{N}_{\mathrm{L},\delta}[x] \tag{4.54}$$

and, therefore, the auxiliary decomposition (4.4) of the corrective fields is given by

$$\tilde{N}_{\mathrm{A},\delta}[x] = \tilde{N}_{\delta}[x] + \tilde{N}_{\mathrm{F},\delta}[x] = \tilde{N}_{\mathrm{L},\delta}[x] + \tilde{N}_{\mathrm{F},\delta}[x] \tag{4.55}$$

Dividing both members of (4.54) by EA_{A} and recalling (4.53), gives the corresponding kinematical relation,

$$\tilde{\varepsilon}_{\mathrm{A},\delta}[x] = \tilde{\varepsilon}_{\mathrm{L},\delta}[x] \tag{4.56}$$

4.2.4. Discrete description of the elemental fictitious force system

As already mentioned in § 3.4.4 for FFM(*M*) discrete descriptions, in order to write the corrective terms $\tilde{N}_{\mathrm{F},\delta}$ (resp. $\tilde{\varepsilon}_{\mathrm{NL},\delta}$) and $\tilde{N}_{\delta}$ (resp. $\tilde{\varepsilon}_{\mathrm{A},\delta}$) in a discrete form, the part of the force system which is applied between nodes should be known in advance. This means that the discrete description of $\tilde{N}_{\delta}$ and $\tilde{\varepsilon}_{\mathrm{A},\delta}$ is a trivial task, but the same cannot be said of $\tilde{N}_{\mathrm{F},\delta}$ and $\tilde{\varepsilon}_{\mathrm{NL},\delta}$, since the fictitious force system is not known in advance. This difficulty is overcome by imposing the form of that force system, *i.e.*, the shape of the nonlinear component of the axial

strains $\tilde{\varepsilon}_{\mathrm{NL},\delta}$ or of the effective axial stiffness $\widetilde{EA}$, since $\tilde{\varepsilon}_{\mathrm{NL},\delta}$ emulates $\widetilde{EA}$, in the auxiliary problem.

Before presenting the simplifying assumption which lays the basis of the discrete description of the fictitious force system proposed for FFM(*N*), let us clarify the option taken. This discrete description will be combined with that of FFM$(M)_2$ to form a discrete description of the fictitious force system of FFM(*MN*), presented in next chapter. To combine the discrete descriptions of FFM(*N*) and FFM(*M*) and, therefore, the discrete descriptions of their fictitious force systems, they should share the same interpolation sections, *i.e.* the fields $\tilde{\varepsilon}_{\mathrm{NL}}$ and $\tilde{\chi}_{\mathrm{NL}}$ must be approximated by functions of the same degree. The justification to this requirement is presented next chapter in § 5.3.1.1.

Thence, in the proposed discrete description of the fictitious force system of FFM(*N*), the fields $\tilde{\varepsilon}_{\mathrm{NL},\delta}$ and $\tilde{N}_{\mathrm{F},\delta}$ are admitted to be linear in *x*. This means that a second interpolation section is required, which was chosen to be the element left end section. Thence, see Figure 4.9, the approximation of the fictitious axial force field $\tilde{N}_{\mathrm{F},\delta}[x]$ is given by

$$\tilde{N}_{\mathrm{F2},\delta}[x] = \tilde{n}_{\mathrm{l}}[x]\left(\tilde{N}_{\mathrm{F}}[0] - \tilde{N}_{\mathrm{F}}[L]\right) \tag{4.57}$$

Dividing both members by EA_{A} gives the corresponding approximation of $\tilde{\varepsilon}_{\mathrm{NL},\delta}[x]$,

$$\tilde{\varepsilon}_{\mathrm{NL2},\delta}[x] = \tilde{n}_{\mathrm{l}}[x]\left(\tilde{\varepsilon}_{\mathrm{NL}}[0] - \tilde{\varepsilon}_{\mathrm{NL}}[L]\right) \tag{4.58}$$

The components of the fictitious force system (4.49) and (4.50) become

$$p_{\mathrm{F2}} = -\tilde{N}'_{\mathrm{F2},\delta} = \frac{1}{L}\left(\tilde{N}_{\mathrm{F}}[0] - \tilde{N}_{\mathrm{F}}[L]\right) \tag{4.59}$$

$$P^{\mathrm{b}}_{\mathrm{F2},1} = -\int_0^L p_{\mathrm{F2}}\, dx = \tilde{N}_{\mathrm{F}}[L] - \tilde{N}_{\mathrm{F}}[0] \tag{4.60}$$

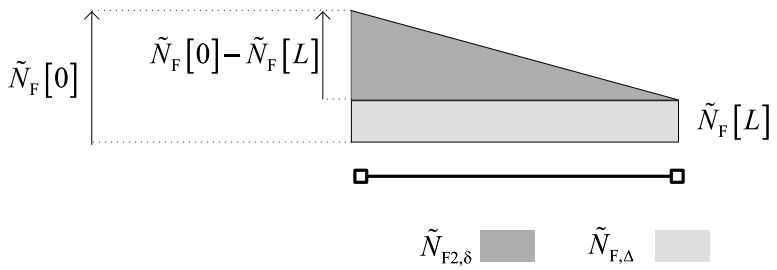

Figure 4.9. Discretization of the fictitious axial force field.

Note that the fictitious distributed force is approximated by a uniform load. The fictitious force system of the discrete description of FFM(*N*) is therefore given by the sum of forces (4.59) and (4.60) with forces (4.48), *i.e.* it is composed of the two concentrated axial forces (4.36) at the element end sections and the uniformly distributed force (4.59), see Figure 4.10.

Note that the error introduced by the adoption of this discrete fictitious force system decreases when the element mesh is refined. The example presented in § 4.5 illustrates this issue.

Finally, substituting (4.58) into (4.44), and recalling (3.101) and (3.102), yields the approximation for $\tilde{\varepsilon}_{\mathrm{NL}}$,

$$\tilde{\varepsilon}_{\mathrm{NL2}} = \overline{\mathbf{n}}^{\mathrm{T}}\, \overline{\boldsymbol{\varepsilon}}_{\mathrm{NL}} \tag{4.61}$$

with

$$\overline{\boldsymbol{\varepsilon}}_{\mathrm{NL}} = \left[\tilde{\varepsilon}_{\mathrm{NL}}[0] \quad \tilde{\varepsilon}_{\mathrm{NL}}[L] \right]^{\mathrm{T}} \tag{4.62}$$

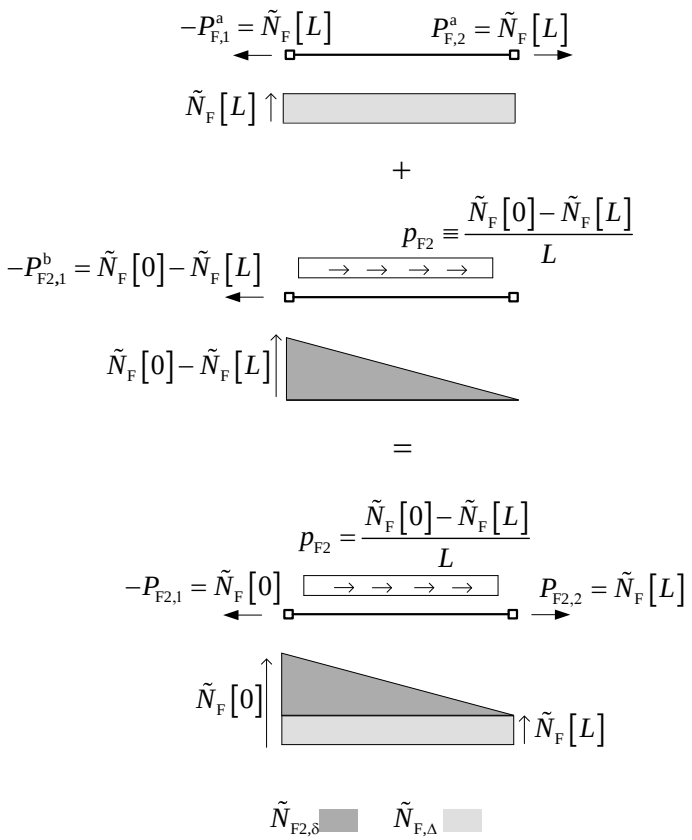

Figure 4.10. Discrete components of the fictitious force system.

4.3. FFM(*N*) discrete description: matrix methods of structural analysis

This and the next sections present the application of the discrete description of FFM(*N*) in the context of matrix methods of structural analysis. This discrete description is hereinafter denoted FFM$(N)_2$ or simply FFM_2 if it is obvious that the *model N* is being employed. This exposition follows as close as possible the discrete description of FFM(*M*) presented in § 3.5, which explains why some expressions are alike.

4.3.1. Elemental kinematics

The elemental kinematic relations are established in this section. Assuming that the displacement field $\tilde{u}[x]$ is continuous in the element, the elemental elongation is given by

$$\varphi \equiv \tilde{u}[L] - \tilde{u}[0] = \int_0^L \tilde{\varepsilon}\, dx \tag{4.63}$$

Substituting the strain decomposition (4.42) into the last expression, yields, see Figure 4.11,

$$\varphi = \varphi_\Delta + \varphi_\delta \tag{4.64}$$

with (recall that $\tilde{\varepsilon}_\Delta = \tilde{\varepsilon}[L]$ (4.39))

$$\varphi_\Delta = \int_0^L \tilde{\varepsilon}_\Delta\, dx = \tilde{\varepsilon}_\Delta \int_0^L dx = F_0^{\mathrm{N}}\ \tilde{\varepsilon}_\Delta \tag{4.65}$$

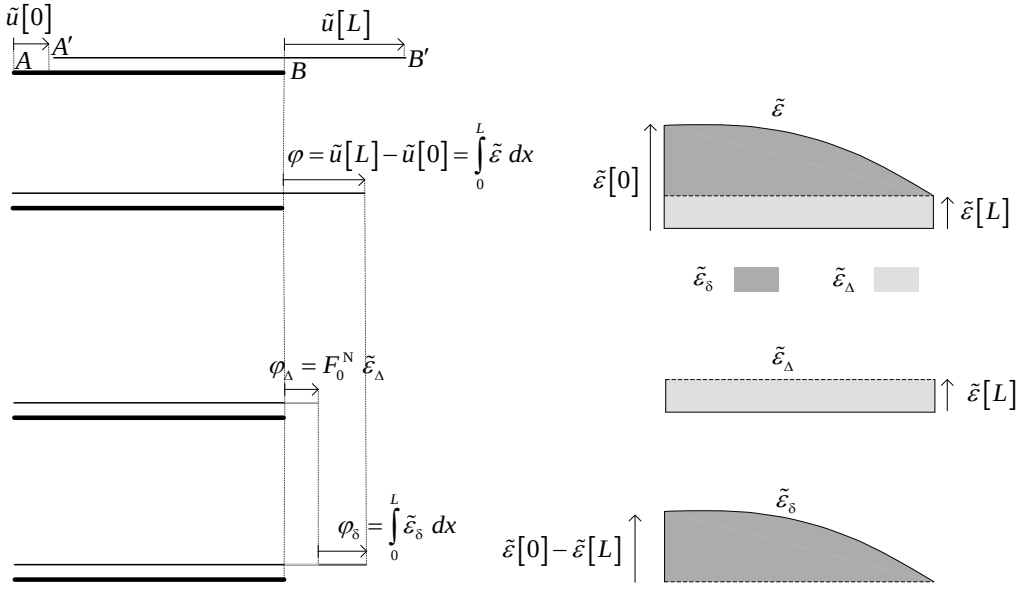

Figure 4.11. Element elongation and its decomposition.

where

$$F_0^{\mathrm{N}} = L \tag{4.66}$$

and

$$\varphi_\delta = \int_0^L \tilde{\varepsilon}_\delta \, dx \tag{4.67}$$

Thence

$$\tilde{\varepsilon}_\Delta = K_0^{\mathrm{N}} \left(\varphi - \varphi_\delta \right) \tag{4.68}$$

with

$$K_0^{\mathrm{N}} = \frac{1}{F_0^{\mathrm{N}}} = \frac{1}{L} \tag{4.69}$$

The equivalent axial strain field $\tilde{\varepsilon}_{\delta,\mathrm{eq}}$ is defined as the constant strain field to which corresponds an elemental elongation equal to that for $\tilde{\varepsilon}_\delta$, see Figure 4.12,

$$\varphi_\delta = \int_0^L \tilde{\varepsilon}_{\delta,\mathrm{eq}} \, dx = \tilde{\varepsilon}_{\delta,\mathrm{eq}} \int_0^L dx = \tilde{\varepsilon}_{\delta,\mathrm{eq}} \, L = F_0^{\mathrm{N}} \; \tilde{\varepsilon}_{\delta,\mathrm{eq}} \tag{4.70}$$

Introducing this expression into (4.68) gives

$$\tilde{\varepsilon}_\Delta + \tilde{\varepsilon}_{\delta,\mathrm{eq}} = K_0^{\mathrm{N}} \; \varphi \tag{4.71}$$

Introducing the auxiliary strain decomposition (4.33) into (4.63), gives a similar decomposition of the elongations

$$\varphi = \varphi_{\mathrm{A}} + \varphi_{\mathrm{NL}} \tag{4.72}$$

Similarly, the element elongations φ_δ are decomposed according to

$$\varphi_\delta = \varphi_{\mathrm{A},\delta} + \varphi_{\mathrm{NL},\delta} = \varphi_{\mathrm{L},\delta} + \varphi_{\mathrm{NL},\delta} \tag{4.73}$$

where the equivalence (4.56) was used.

Figure 4.12. Equivalence between the fields $\tilde{\varepsilon}_\delta$ and $\tilde{\varepsilon}_{\delta,\mathrm{eq}}$.

According to the kinematic relation (4.68),

$$\tilde{\varepsilon}_{\mathrm{NL},\Delta} = K_0^{\mathrm{N}} \left(\varphi_{\mathrm{NL}} - \varphi_{\mathrm{NL},\delta} \right) \tag{4.74}$$

with

$$\varphi_{\mathrm{NL},\delta} = \int_0^L \tilde{\varepsilon}_{\mathrm{NL},\delta} \, dx \tag{4.75}$$

A constant axial strain field $\tilde{\varepsilon}_{\mathrm{NL},\delta,\mathrm{eq}}$ kinematically equivalent to $\tilde{\varepsilon}_{\mathrm{NL},\delta}$ can be defined, *i.e.* which corresponds to the same elongation $\varphi_{\mathrm{NL},\delta}$ by an expression similar to (4.70),

$$\varphi_{\mathrm{NL},\delta} = \int_0^L \tilde{\varepsilon}_{\mathrm{NL},\delta,\mathrm{eq}} \, dx = F_0^{\mathrm{N}} \; \tilde{\varepsilon}_{\mathrm{NL},\delta,\mathrm{eq}} \tag{4.76}$$

Substituting this expression in (4.74) gives

$$\tilde{\varepsilon}_{\mathrm{NL},\Delta} + \tilde{\varepsilon}_{\mathrm{NL},\delta,\mathrm{eq}} = K_0^{\mathrm{N}} \; \varphi_{\mathrm{NL}} \tag{4.77}$$

and it can be concluded that (4.71) is a generic result valid not only for the effective strains but also for their nonlinear and auxiliary components. In the case of the approximation (4.58) to $\tilde{\varepsilon}_{\mathrm{NL},\delta}$,

$$\varphi_{\mathrm{NL2},\delta} = \int_0^L \tilde{n}_1[x] \left(\tilde{\varepsilon}_{\mathrm{NL}}[0] - \tilde{\varepsilon}_{\mathrm{NL}}[L] \right) dx = \frac{F_0^{\mathrm{N}}}{2} \left(\tilde{\varepsilon}_{\mathrm{NL}}[0] - \tilde{\varepsilon}_{\mathrm{NL}}[L] \right) \tag{4.78}$$

Thence, equating this to (4.76), gives this equivalent strain field for the basic discrete description,

$$\tilde{\varepsilon}_{\mathrm{NL2},\delta,\mathrm{eq}} = \frac{1}{2} \left(\tilde{\varepsilon}_{\mathrm{NL}}[0] - \tilde{\varepsilon}_{\mathrm{NL}}[L] \right) \tag{4.79}$$

see Figure 4.13.

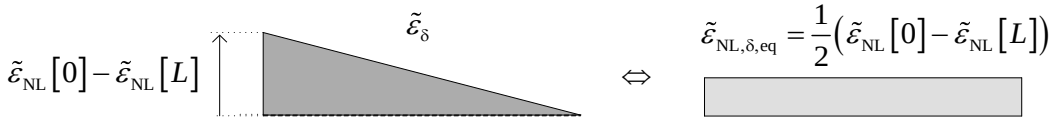

Figure 4.13. Equivalence between the fields $\tilde{\varepsilon}_{\delta}$ and $\tilde{\varepsilon}_{\delta,\mathrm{eq}}$ in the context of the approximation of FFM(*N*) discrete description.

Substituting $\tilde{\varepsilon}_{\Delta}$ by $\tilde{\varepsilon}_{\mathrm{A},\Delta}$ in (4.68), and recalling that $\varphi_{\mathrm{A},\delta} = \varphi_{\mathrm{L},\delta}$, see (4.73), gives

$$\tilde{\varepsilon}_{\mathrm{A},\Delta} = K_0^{\mathrm{N}} \left(\varphi_{\mathrm{A}} - \varphi_{\mathrm{L},\delta} \right) \tag{4.80}$$

Let $\tilde{\varepsilon}_{\mathrm{L},\delta,\mathrm{eq}}$ be the constant field kinematically equivalent to $\tilde{\varepsilon}_{\mathrm{L},\delta}$, *i.e.* corresponding to the same elongation. Thence, similarly to (4.70),

$$\varphi_{\mathrm{L},\delta} = \int_0^L \tilde{\varepsilon}_{\mathrm{L},\delta,\mathrm{eq}} \, dx = F_0^{\mathrm{N}} \; \tilde{\varepsilon}_{\mathrm{L},\delta,\mathrm{eq}} \tag{4.81}$$

Introducing this relation into (4.80) gives

$$\tilde{\varepsilon}_{\mathrm{A},\Delta} + \tilde{\varepsilon}_{\mathrm{L},\delta,\mathrm{eq}} = K_0^{\mathrm{N}} \; \varphi_{\mathrm{A}} \tag{4.82}$$

Note that it is also possible to write

$$\tilde{\varepsilon}_{\delta,\mathrm{eq}} = \tilde{\varepsilon}_{\mathrm{L},\delta,\mathrm{eq}} + \tilde{\varepsilon}_{\mathrm{NL},\delta,\mathrm{eq}} = K_0^{\mathrm{N}} \; \varphi_{\delta} \tag{4.83}$$

4.3.2. Auxiliary elemental constitutive relations

Substituting (4.68) on the right-hand side of (4.52), gives

$$\tilde{N}_{\mathrm{A},\Delta} = K_{\mathrm{A}}^{\mathrm{N}} \; \varphi_{\Delta} \tag{4.84}$$

with

$$K_{\mathrm{A}}^{\mathrm{N}} = EA_{\mathrm{A}} \;\; K_0^{\mathrm{N}} = \frac{EA_{\mathrm{A}}}{L} \tag{4.85}$$

Similarly,

$$\tilde{N}_{\mathrm{F},\Delta} = EA_{\mathrm{A}} \; \tilde{\varepsilon}_{\mathrm{NL},\Delta} = K_{\mathrm{A}}^{\mathrm{N}} \; \varphi_{\mathrm{NL},\Delta} \tag{4.86}$$

$$\tilde{N}_{\Delta} = EA_{\mathrm{A}} \; \tilde{\varepsilon}_{\mathrm{A},\Delta} = K_{\mathrm{A}}^{\mathrm{N}} \; \varphi_{\mathrm{A},\Delta} \tag{4.87}$$

The axial force field corresponding to $\tilde{\varepsilon}_{\delta,\mathrm{eq}}$ (4.83) is given by

$$\tilde{N}_{\mathrm{A},\delta,\mathrm{eq}} = EA_{\mathrm{A}} \; \tilde{\varepsilon}_{\delta,\mathrm{eq}} = K_{\mathrm{A}}^{\mathrm{N}} \; \varphi_{\delta} \tag{4.88}$$

and similarly,

$$\tilde{N}_{\mathrm{F},\delta,\mathrm{eq}} = EA_{\mathrm{A}} \; \tilde{\varepsilon}_{\mathrm{NL},\delta,\mathrm{eq}} = K_{\mathrm{A}}^{\mathrm{N}} \; \varphi_{\mathrm{NL},\delta} \tag{4.89}$$

$$\tilde{N}_{\delta,\mathrm{eq}} = EA_{\mathrm{A}} \; \tilde{\varepsilon}_{\mathrm{A},\delta,\mathrm{eq}} = K_{\mathrm{A}}^{\mathrm{N}} \; \varphi_{\mathrm{A},\delta} \tag{4.90}$$

In the discrete description of FFM(*N*), introducing (4.79) into (4.89), gives the approximation of $\tilde{N}_{\mathrm{F},\delta,\mathrm{eq}}$,

$$\tilde{N}_{\mathrm{F2},\delta,\mathrm{eq}} = \frac{EA_{\mathrm{A}}}{2}\left(\tilde{\varepsilon}_{\mathrm{NL}}\left[0\right]-\tilde{\varepsilon}_{\mathrm{NL}}\left[L\right]\right)=\frac{1}{2}\left(\tilde{N}_{\mathrm{F}}\left[0\right]-\tilde{N}_{\mathrm{F}}\left[L\right]\right) \tag{4.91}$$

Finally, adding together the expressions (4.84), (4.86) and (4.87) with, respectively, (4.88) to (4.90), and substituting the decomposition (4.71), gives

$$\tilde{N}_{\mathrm{A},\Delta}+\tilde{N}_{\mathrm{A},\delta,\mathrm{eq}} = K_{\mathrm{A}}^{\mathrm{N}}\,\varphi \tag{4.92}$$

$$\tilde{N}_{\mathrm{F},\Delta}+\tilde{N}_{\mathrm{F},\delta,\mathrm{eq}} = K_{\mathrm{A}}^{\mathrm{N}}\,\varphi_{\mathrm{NL}} \tag{4.93}$$

$$\tilde{N}_{\Delta}+\tilde{N}_{\delta,\mathrm{eq}} = K_{\mathrm{A}}^{\mathrm{N}}\,\varphi_{\mathrm{A}} \tag{4.94}$$

4.3.3. Elemental structural relations

Consider the elemental local coordinates (*i.e.* along the element axis direction) represented in Figure 4.14, to which correspond the nodal displacements

$$\bar{\mathbf{d}}^{\mathrm{el}} = \left[\begin{array}{cc} d_1^{\mathrm{el}} & d_2^{\mathrm{el}} \end{array}\right]^{\mathrm{T}} = \left[\begin{array}{cc} \tilde{u}\left[0\right] & \tilde{u}\left[L\right] \end{array}\right]^{\mathrm{T}} \tag{4.95}$$

The elongation φ is given by the compatibility relation, see Figure 4.15,

$$\varphi = \bar{\mathbf{C}}^{\mathrm{el}}\,\bar{\mathbf{d}}^{\mathrm{el}} \tag{4.96}$$

where $\bar{\mathbf{C}}^{\mathrm{el}}$ is the elemental local compatibility matrix

$$\bar{\mathbf{C}}^{\mathrm{el}} = \left[\begin{array}{cc} -1 & 1 \end{array}\right] \tag{4.97}$$

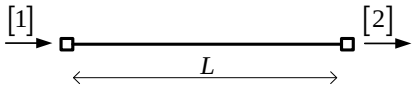

Figure 4.14. Local nodal coordinates of rod element.

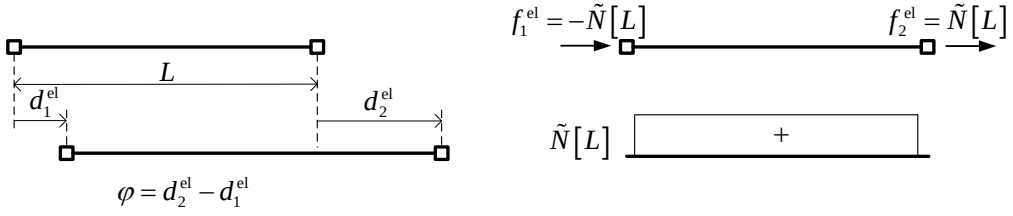

Figure 4.15. Illustration of elemental compatibility and equilibrium relations.

The elemental vector of nodal forces along these local directions is

$$\bar{\mathbf{f}}^{\mathrm{el}} = \begin{bmatrix} f_1^{\mathrm{el}} & f_2^{\mathrm{el}} \end{bmatrix}^{\mathrm{T}} \tag{4.98}$$

The elemental equilibrium relation, dual of (4.96), is given by

$$\bar{\mathbf{f}}^{\mathrm{el}} = \bar{\mathbf{C}}^{\mathrm{el,T}}\, \tilde{N}_{\Delta} \tag{4.99}$$

where $\bar{\mathbf{C}}^{\mathrm{el,T}}$ is the elemental equilibrium matrix. This means that, as represented in the right hand side of Figure 4.15,

$$-f_1^{\mathrm{el}} = +f_2^{\mathrm{el}} = +\tilde{N}_{\Delta} \tag{4.100}$$

According to the equilibrium relation (4.99), the elemental force vector equivalent to the forces applied between nodes is given by

$$\bar{\mathbf{f}}_{\delta}^{\mathrm{el}} = \bar{\mathbf{C}}^{\mathrm{el,T}}\, \tilde{N}_{\delta,\mathrm{eq}} \tag{4.101}$$

Left-multiplying both members of (4.92) by $\bar{\mathbf{C}}^{\mathrm{el,T}}$ and considering the equilibrium relation (4.99), gives

$$\bar{\mathbf{f}}_{\mathrm{A}}^{\mathrm{el}} + \bar{\mathbf{f}}_{\mathrm{A},\delta}^{\mathrm{el}} = \bar{\mathbf{C}}^{\mathrm{el,T}} \left(\tilde{N}_{\mathrm{A},\Delta} + \tilde{N}_{\mathrm{A},\delta,\mathrm{eq}} \right) = \bar{\mathbf{C}}^{\mathrm{el,T}}\, K_{\mathrm{A}}^{\mathrm{N}}\, \varphi \tag{4.102}$$

Substituting (4.96) into the last expression, gives

$$\bar{\mathbf{f}}_{\mathrm{A}}^{\mathrm{el}} + \bar{\mathbf{f}}_{\mathrm{A},\delta}^{\mathrm{el}} = \bar{\mathbf{K}}_{\mathrm{A}}^{\mathrm{el}}\, \bar{\mathbf{d}}^{\mathrm{el}} \tag{4.103}$$

where

$$\bar{\mathbf{K}}_{\mathrm{A}}^{\mathrm{el}} = K_{\mathrm{A}}^{\mathrm{N}}\, \bar{\mathbf{C}}^{\mathrm{el,T}}\, \bar{\mathbf{C}}^{\mathrm{el}} = \frac{EA_{\mathrm{A}}}{L} \begin{pmatrix} 1 & -1 \\ -1 & 1 \end{pmatrix} \tag{4.104}$$

is the auxiliary element local axial stiffness matrix.

4.3.4. Governing system of equations

4.3.4.1. Kinematics

Let us consider a decomposition of the rod into a mesh of *m* linear rod elements linked together at their nodes. Some displacements of these nodes are restrained by the rod

supports. The remaining n generalized displacements of these nodes define a global system of coordinates. These displacements are grouped in the global vectors $\mathbf{d}$. The global vector $\mathbf{d}^{\mathrm{el}}$, grouping the elemental vectors $\bar{\mathbf{d}}^{\mathrm{el}}$, is related to $\mathbf{d}$ by

$$\mathbf{d}^{\mathrm{el}} = \mathbf{D}\,\mathbf{d} \tag{4.105}$$

where $\mathbf{D}$ is a Boolean matrix, whose structure reflects the connectivity of the elements and the kinematic constraints due to supports.

Grouping the elemental compatibility relations (4.96), gives

$$\boldsymbol{\varphi} = \mathbf{C}^{\mathrm{el}}\,\mathbf{d}^{\mathrm{el}} \tag{4.106}$$

where the $m \times 2m$ $\mathbf{C}^{\mathrm{el}}$ block diagonal matrix collects the elemental compatibility matrices (4.97) and $\boldsymbol{\varphi}$ is the global vector of axial elongations

$$\boldsymbol{\varphi} = \begin{bmatrix} \varphi_1 & \varphi_2 & \cdots & \varphi_m \end{bmatrix}^{\mathrm{T}} \tag{4.107}$$

Substitution of (4.105) into (4.106) gives the global compatibility relation

$$\boldsymbol{\varphi} = \mathbf{C}\,\mathbf{d} \tag{4.108}$$

where $\mathbf{C}$ is the $m \times n$ compatibility matrix

$$\mathbf{C} = \mathbf{C}^{\mathrm{el}}\,\mathbf{D} \tag{4.109}$$

with

$$\mathbf{C}^{\mathrm{el}} = \begin{bmatrix} \bar{\mathbf{C}}_1^{\mathrm{el}} & & & \\ & \bar{\mathbf{C}}_2^{\mathrm{el}} & & \\ & & \ddots & \\ & & & \bar{\mathbf{C}}_m^{\mathrm{el}} \end{bmatrix} \tag{4.110}$$

or

$$\mathbf{C} = \begin{bmatrix} \bar{\mathbf{C}}_1 \\ \bar{\mathbf{C}}_2 \\ \vdots \\ \bar{\mathbf{C}}_m \end{bmatrix} \tag{4.111}$$

with

$$\bar{\mathbf{C}}_i = \bar{\mathbf{C}}_i^{\mathrm{el}}\,\bar{\mathbf{D}}_i \tag{4.112}$$

4.3.4.2. Statics

The static dual of (4.105) gives the assembled global force vector $\mathbf{f}$,

$$\mathbf{f} = \mathbf{D}^{\mathrm{T}}\,\mathbf{f}^{\mathrm{el}} \tag{4.113}$$

where $\mathbf{f}^{\mathrm{el}}$ is the non-assembled global force vector, dual of $\mathbf{d}^{\mathrm{el}}$, grouping the elemental vectors $\overline{\mathbf{f}}^{\mathrm{el}}$. The equilibrium relation grouping the elemental relations (4.99) is

$$\mathbf{f}^{\mathrm{el}} = \mathbf{C}^{\mathrm{el,T}}\,\mathbf{N}_{\Delta} \tag{4.114}$$

where the global vector of axial forces $\mathbf{N}_{\Delta}$ is

$$\mathbf{N}_{\Delta} = \begin{bmatrix} \tilde{N}_1[L] & \tilde{N}_2[L] & \cdots & \tilde{N}_m[L] \end{bmatrix}^{\mathrm{T}} \tag{4.115}$$

Substitution of (4.114) into (4.113) gives the equilibrium relation, dual of (4.108),

$$\mathbf{f} = \mathbf{C}^{\mathrm{T}}\,\mathbf{N}_{\Delta} \tag{4.116}$$

According to the equilibrium relations (4.116),

$$\mathbf{f}_{\delta} = \mathbf{C}^{\mathrm{T}}\,\mathbf{N}_{\delta,\mathrm{eq}} \tag{4.117}$$

where the global vector of axial forces $\mathbf{N}_{\delta,\mathrm{eq}}$ is

$$\mathbf{N}_{\delta,\mathrm{eq}} = \begin{bmatrix} \tilde{N}_{\delta,\mathrm{eq},1} & \tilde{N}_{\delta,\mathrm{eq},2} & \cdots & \tilde{N}_{\delta,\mathrm{eq},m} \end{bmatrix}^{\mathrm{T}} \tag{4.118}$$

4.3.4.3. Auxiliary constitutive relationship

The collection of the elemental constitutive relations (4.92), is given by

$$\mathbf{N}_{\mathrm{A},\Delta} + \mathbf{N}_{\mathrm{A},\delta,\mathrm{eq}} = \mathbf{K}_{\mathrm{A}}^{\mathrm{N}}\,\boldsymbol{\varphi} \tag{4.119}$$

where the non-assembled block diagonal $m \times m$ global stiffness matrix, which groups the elemental matrices (4.85), is given by

$$\mathbf{K}_{\mathrm{A}}^{\mathrm{N}} = \mathbf{E}\mathbf{A}_{\mathrm{A}}\,\mathbf{K}_{0}^{\mathrm{N}} = \begin{bmatrix} K_{\mathrm{A},1}^{\mathrm{N}} & & & \\ & K_{\mathrm{A},2}^{\mathrm{N}} & & \\ & & \ddots & \\ & & & K_{\mathrm{A},m}^{\mathrm{N}} \end{bmatrix} = \begin{bmatrix} \dfrac{EA_{\mathrm{A},1}}{L_1} & & & \\ & \dfrac{EA_{\mathrm{A},2}}{L_2} & & \\ & & \ddots & \\ & & & \dfrac{EA_{\mathrm{A},m}}{L_m} \end{bmatrix} \tag{4.120}$$

the elasticity matrix is given by

$$\mathbf{EA}_{\mathrm{A}} = \begin{bmatrix} EA_{\mathrm{A},1} & & & \\ & EA_{\mathrm{A},2} & & \\ & & \ddots & \\ & & & EA_{\mathrm{A},m} \end{bmatrix} \tag{4.121}$$

and

$$\mathbf{K}_0^{\mathrm{N}} = \begin{bmatrix} K_{0,1}^{\mathrm{N}} & & & \\ & K_{0,2}^{\mathrm{N}} & & \\ & & \ddots & \\ & & & K_{0,m}^{\mathrm{N}} \end{bmatrix} = \begin{bmatrix} \dfrac{1}{L_1} & & & \\ & \dfrac{1}{L_2} & & \\ & & \ddots & \\ & & & \dfrac{1}{L_m} \end{bmatrix} \tag{4.122}$$

The elemental constitutive relations (4.52) are collected in the global constitutive relation

$$\mathbf{N}_{\mathrm{A},\Delta} = \mathbf{EA}_{\mathrm{A}}\, \boldsymbol{\varepsilon}_{\Delta} \tag{4.123}$$

where the global vector gathering the axial strains at $x = 0$ is

$$\boldsymbol{\varepsilon}_{\Delta} = \begin{bmatrix} \tilde{\varepsilon}_1[L] & \tilde{\varepsilon}_2[L] & \cdots & \tilde{\varepsilon}_m[L] \end{bmatrix}^{\mathrm{T}} \tag{4.124}$$

Considering the vector $\mathbf{N}_0$ which collects the axial forces at the elements left end section

$$\mathbf{N}_0 = \begin{bmatrix} \tilde{N}_1[0] & \tilde{N}_2[0] & \cdots & \tilde{N}_m[0] \end{bmatrix}^{\mathrm{T}} \tag{4.125}$$

and the dual global vector gathering the axial strains at that section,

$$\boldsymbol{\varepsilon}_0 = \begin{bmatrix} \tilde{\varepsilon}_1[0] & \tilde{\varepsilon}_2[0] & \cdots & \tilde{\varepsilon}_m[0] \end{bmatrix}^{\mathrm{T}} \tag{4.126}$$

it is possible to write, similarly to (4.123), the global constitutive relation

$$\mathbf{N}_{\mathrm{A},0} = \mathbf{EA}_{\mathrm{A}}\, \boldsymbol{\varepsilon}_0 \tag{4.127}$$

Let $\mathbf{N}$ be the generic global axial force vector collecting $\mathbf{N}_0$ and $\mathbf{N}_{\Delta}$, *i.e.*

$$\mathbf{N} = \begin{bmatrix} \mathbf{N}_0 \\ \mathbf{N}_{\Delta} \end{bmatrix} \tag{4.128}$$

and $\boldsymbol{\varepsilon}$ the global axial strain vector, dual of $\mathbf{N}$, collecting $\boldsymbol{\varepsilon}_0$ and $\boldsymbol{\varepsilon}_{\Delta}$,

$$\boldsymbol{\varepsilon} = \begin{bmatrix} \boldsymbol{\varepsilon}_0 \\ \boldsymbol{\varepsilon}_\Delta \end{bmatrix} \tag{4.129}$$

Thence, the constitutive relations (4.123) and (4.127) can be gathered into

$$\mathbf{N}_\mathrm{A} = \mathbf{E}\mathbf{A}_\mathrm{A}^* \boldsymbol{\varepsilon} \tag{4.130}$$

where the elasticity matrix $\mathbf{E}\mathbf{A}_\mathrm{A}^*$ is

$$\mathbf{E}\mathbf{A}_\mathrm{A}^* = \begin{bmatrix} \mathbf{E}\mathbf{A}_\mathrm{A} & \mathbf{0}_m \\ \mathbf{0}_m & \mathbf{E}\mathbf{A}_\mathrm{A} \end{bmatrix} \tag{4.131}$$

The constitutive relations (4.127) and (4.130) are used in § 4.3.5.

4.3.4.4. Assembling the equations

Collecting the m equations (4.103), left-multiplying both members by $\mathbf{D}^\mathrm{T}$, substituting the connectivity relations (4.113) on the left-hand side and (4.105) on the right-hand side, gives FFM governing equation

$$\mathbf{f}_\mathrm{A} + \mathbf{f}_{\mathrm{A},\delta} = \mathbf{K}_\mathrm{A}\,\mathbf{d} \tag{4.132}$$

where the $m \times m$ assembled linear stiffness matrix is given by

$$\mathbf{K}_\mathrm{A} = \mathbf{D}^\mathrm{T}\,\mathbf{K}_\mathrm{A}^\mathrm{el}\,\mathbf{D} \tag{4.133}$$

and

$$\mathbf{K}_\mathrm{A}^\mathrm{el} = \begin{bmatrix} \bar{\mathbf{K}}_{\mathrm{A},1}^\mathrm{el} & & & \\ & \bar{\mathbf{K}}_{\mathrm{A},2}^\mathrm{el} & & \\ & & \ddots & \\ & & & \bar{\mathbf{K}}_{\mathrm{A},m}^\mathrm{el} \end{bmatrix} \tag{4.134}$$

is the block diagonal stiffness matrix which aggregates the elemental stiffness matrices (4.104). Note that $\mathbf{K}_\mathrm{A}^\mathrm{el}$ can also be written

$$\mathbf{K}_\mathrm{A}^\mathrm{el} = \mathbf{C}^{\mathrm{el},\mathrm{T}}\,\mathbf{K}_\mathrm{A}^\mathrm{N}\,\mathbf{C}^\mathrm{el} \tag{4.135}$$

Thence, substituting (4.135) into (4.133) and considering (4.109) gives

$$\mathbf{K}_\mathrm{A} = \mathbf{C}^\mathrm{T}\,\mathbf{K}_\mathrm{A}^\mathrm{N}\,\mathbf{C} \tag{4.136}$$

Solution of equation (4.132) gives

$$\mathbf{d} = \mathbf{K}_{\mathrm{A}}^{-1}\left(\mathbf{f}_{\mathrm{A}} + \mathbf{f}_{\mathrm{A},\delta}\right) \tag{4.137}$$

The auxiliary forces in this expression are given by the superposition of their effective and fictitious components

$$\mathbf{f}_{\mathrm{A}} = \mathbf{f} + \mathbf{f}_{\mathrm{F}} \tag{4.138}$$

$$\mathbf{f}_{\mathrm{A},\delta} = \mathbf{f}_{\delta} + \mathbf{f}_{\mathrm{F},\delta} \tag{4.139}$$

Substituting these expressions in the last expression and noting that

$$\mathbf{d}_{\mathrm{L}} = \mathbf{K}_{\mathrm{A}}^{-1}\left(\mathbf{f} + \mathbf{f}_{\delta}\right) \tag{4.140}$$

gives

$$\mathbf{d} = \mathbf{d}_{\mathrm{L}} + \mathbf{K}_{\mathrm{A}}^{-1}\left(\mathbf{f}_{\mathrm{F}} + \mathbf{f}_{\mathrm{F},\delta}\right) \tag{4.141}$$

Recalling that $\mathbf{d}^{(1)} = \mathbf{d}_{\mathrm{L}}$, this expression can be written in the iterative form

$$\mathbf{d}^{(i+1)} = \mathbf{d}^{(i)} + \mathbf{K}_{\mathrm{A}}^{-1}\left(\mathbf{f}_{\mathrm{F}}^{(i)} + \mathbf{f}_{\mathrm{F},\delta}^{(i)}\right) \tag{4.142}$$

4.3.5. Implementation of FFM(*N*) discrete description

As seen in chapter 3, the implementation of FFM discrete description consists in determining the fictitious force vectors $\mathbf{f}_{\mathrm{F}}^{(i)}$ and $\mathbf{f}_{\mathrm{F},\delta}^{(i)}$ which, according to (4.142), are required to calculate the next approximation of the displacement vector $\mathbf{d}^{(i+1)}$. In FFM(*N*), the force vector $\mathbf{f}_{\mathrm{F}}^{(i)}$ is determined by the fictitious axial force at the right end section of the elements,

$$\mathbf{f}_{\mathrm{F}} = \mathbf{C}^{\mathrm{T}}\mathbf{N}_{\mathrm{F},\Delta} \tag{4.143}$$

On the other hand, according to (4.91) and (4.117), $\mathbf{f}_{\mathrm{F},\delta}$ is approximated by the difference between the fictitious axial forces at the end sections

$$\mathbf{f}_{\mathrm{F},\delta} = \mathbf{C}^{\mathrm{T}}\mathbf{N}_{\mathrm{F},\delta,\mathrm{eq}} \tag{4.144}$$

In the case of $\mathrm{FFM}_{\mathrm{Def}}$ (resp. $\mathrm{FFM}_{\mathrm{S}}$) these fictitious axial forces are written in terms of the axial strains (4.5) (resp. axial forces (4.6)).

Once $\mathbf{d}^{(i+1)}$ is known, and bearing in mind that the linear solution is also known, particularly $\tilde{N}_{\mathrm{L}}$ and $\tilde{N}_{\mathrm{L},\delta,\mathrm{eq}}$, it is possible to establish the auxiliary axial forces at the element end sections, as explained next.

Let us start by establishing the vector $\mathbf{N}_{\mathrm{A},\Delta}^{(i)}$ gathering the auxiliary forces at $x = L$. Thence, let us write the field $\tilde{N}_{\mathrm{A},\delta,\mathrm{eq}}$, according to (4.9), (4.91) and (4.54), as

$$\tilde{N}_{\mathrm{A},\delta,\mathrm{eq}}^{(i)} = \tilde{N}_{\delta,\mathrm{eq}} + \tilde{N}_{\mathrm{F},\delta,\mathrm{eq}}^{(i-1)} \simeq \tilde{N}_{\mathrm{L},\delta,\mathrm{eq}} + \frac{\tilde{N}_{\mathrm{F}}^{(i-1)}[0] - \tilde{N}_{\mathrm{F}}^{(i-1)}[L]}{2} \tag{4.145}$$

Collecting these elemental relations gives in the global format

$$\mathbf{N}_{\mathrm{A},\delta,\mathrm{eq}}^{(i)} = \mathbf{N}_{\delta,\mathrm{eq}} + \mathbf{N}_{\mathrm{F},\delta,\mathrm{eq}}^{(i-1)} \simeq \mathbf{N}_{\mathrm{L},\delta,\mathrm{eq}} + \frac{1}{2}\mathbf{N}_{\mathrm{F},0}^{(i-1)} - \frac{1}{2}\mathbf{N}_{\mathrm{F},\Delta}^{(i-1)} \tag{4.146}$$

Substituting (4.108) and (4.146) into the global constitutive relation (4.119) gives

$$\mathbf{N}_{\mathrm{A},\Delta}^{(i)} = \mathbf{K}_{\mathrm{A}}^{\mathrm{N}}\mathbf{C}\mathbf{d}^{(i)} - \mathbf{N}_{\mathrm{L},\delta,\mathrm{eq}} + \frac{1}{2}\left(\mathbf{N}_{\mathrm{F},\Delta}^{(i-1)} - \mathbf{N}_{\mathrm{F},0}^{(i-1)}\right) \tag{4.147}$$

Let us now establish the axial force vector $\mathbf{N}_{\mathrm{A},0}^{(i)}$ gathering the auxiliary axial forces at $x = 0$. Firstly, take (4.55) at $x = 0$. Since $\tilde{N}^{(1)} = \tilde{N}_{\mathrm{L}}$, this expression can be written in the iterative format, according to (4.9), as

$$\tilde{N}_{\mathrm{A},\delta}^{(i)}[0] = \tilde{N}_{\delta}^{(1)}[0] + \tilde{N}_{\mathrm{F},\delta}^{(i-1)}[0] \tag{4.148}$$

According to (4.41), the terms on the right-hand side of this expression can be written as

$$\tilde{N}_{\delta}^{(1)}[0] = \tilde{N}^{(1)}[0] - \tilde{N}^{(1)}[L] \tag{4.149}$$

$$\tilde{N}_{\mathrm{F},\delta}^{(i-1)}[0] = \tilde{N}_{\mathrm{F}}^{(i-1)}[0] - \tilde{N}_{\mathrm{F}}^{(i-1)}[L] \tag{4.150}$$

and according to (4.41),

$$\tilde{N}_{\mathrm{A}}^{(i)}[0] = \tilde{N}_{\mathrm{A}}^{(i)}[L] + \tilde{N}_{\mathrm{A},\delta}^{(i)}[0] \tag{4.151}$$

Substituting (4.149) and (4.150) into (4.148) and the result into the last expression gives

$$\tilde{N}_{\mathrm{A}}^{(i)}[0] = \tilde{N}_{\mathrm{A}}^{(i)}[L] + \tilde{N}^{(1)}[0] - \tilde{N}^{(1)}[L] + \tilde{N}_{\mathrm{F}}^{(i-1)}[0] - \tilde{N}_{\mathrm{F}}^{(i-1)}[L] \tag{4.152}$$

Collecting these elemental axial forces gives in the global format

$$\mathbf{N}_{\mathrm{A},0}^{(i)} = \mathbf{N}_{\mathrm{A},\Delta}^{(i)} + \mathbf{N}_{0}^{(1)} - \mathbf{N}_{\Delta}^{(1)} + \mathbf{N}_{\mathrm{F},0}^{(i-1)} - \mathbf{N}_{\mathrm{F},\Delta}^{(i-1)} \tag{4.153}$$

Finally, substituting (4.147) into the last expression, gives

$$\mathbf{N}_{\mathrm{A},0}^{(i)} = \mathbf{K}_{\mathrm{A}}^{\mathrm{N}}\mathbf{C}\mathbf{d}^{(i)} - \mathbf{N}_{\mathrm{L},\delta,\mathrm{eq}} - \mathbf{N}_{\Delta}^{(1)} + \mathbf{N}_{0}^{(1)} - \frac{1}{2}\left(\mathbf{N}_{\mathrm{F},\Delta}^{(i-1)} - \mathbf{N}_{\mathrm{F},0}^{(i-1)}\right) \tag{4.154}$$

It is then possible to group (4.147) and (4.154) as

$$\mathbf{N}_{\mathrm{A}}^{(i)}=\begin{bmatrix}\mathbf{I}_m\\ \mathbf{I}_m\end{bmatrix}\left(\mathbf{K}_{\mathrm{A}}^{\mathrm{N}}\mathbf{C}\mathbf{d}^{(i)}-\mathbf{N}_{\mathrm{L},\delta,\mathrm{eq}}\right)+\begin{bmatrix}\mathbf{N}_0^{(1)}-\mathbf{N}_{\Delta}^{(1)}\\ \mathbf{0}_{m\times 1}\end{bmatrix}+\frac{1}{2}\begin{bmatrix}\mathbf{I}_m & -\mathbf{I}_m\\ -\mathbf{I}_m & \mathbf{I}_m\end{bmatrix}\mathbf{N}_{\mathrm{F}}^{(i-1)} \tag{4.155}$$

This expression and the constitutive relation (4.130) give the axial strains $\boldsymbol{\varepsilon}^{(i)}=\left(\mathbf{E}\mathbf{A}_{\mathrm{A}}^{*}\right)^{-1}\mathbf{N}_{\mathrm{A}}^{(i)}$.

Defining the vectors $\mathbf{N}\left[\boldsymbol{\varepsilon}\right]$ and $\boldsymbol{\varepsilon}\left[\mathbf{N}\right]$ which gather the effective constitutive relations at the element end sections,

$$\mathbf{N}\left[\boldsymbol{\varepsilon}\right]=\begin{bmatrix}\mathbf{N}_0\left[\boldsymbol{\varepsilon}_0\right]\\ \mathbf{N}_{\Delta}\left[\boldsymbol{\varepsilon}_{\Delta}\right]\end{bmatrix}=\begin{bmatrix}\hat{N}_1\left[\tilde{\varepsilon}_1\left[0\right]\right]\\ \hat{N}_2\left[\tilde{\varepsilon}_2\left[0\right]\right]\\ \vdots\\ \hat{N}_m\left[\tilde{\varepsilon}_m\left[0\right]\right]\\ \hat{N}_1\left[\tilde{\varepsilon}_1\left[L_m\right]\right]\\ \hat{N}_2\left[\tilde{\varepsilon}_2\left[L_m\right]\right]\\ \vdots\\ \hat{N}_m\left[\tilde{\varepsilon}_m\left[L_m\right]\right]\end{bmatrix} \tag{4.156}$$

$$\boldsymbol{\varepsilon}\left[\mathbf{N}\right]=\begin{bmatrix}\boldsymbol{\varepsilon}_0\left[\mathbf{N}_0\right]\\ \boldsymbol{\varepsilon}_{\Delta}\left[\mathbf{N}_{\Delta}\right]\end{bmatrix}=\begin{bmatrix}\hat{\varepsilon}_1\left[\tilde{N}_1\left[0\right]\right]\\ \hat{\varepsilon}_2\left[\tilde{N}_2\left[0\right]\right]\\ \vdots\\ \hat{\varepsilon}_m\left[\tilde{N}_m\left[0\right]\right]\\ \hat{\varepsilon}_1\left[\tilde{N}_1\left[L_1\right]\right]\\ \hat{\varepsilon}_2\left[\tilde{N}_2\left[L_2\right]\right]\\ \vdots\\ \hat{\varepsilon}_m\left[\tilde{N}_m\left[L_m\right]\right]\end{bmatrix} \tag{4.157}$$

it is finally possible to produce the flowchart in Figure 4.16, which updates the flowchart in Figure 4.3, describing the implementation of the discrete description of FFM(*N*).

4.4. Iteration formulas of FFM(*N*) discrete description

The iteration formulas for the discrete description of FFM(*N*) will now be developed. Substituting the global displacements (4.141) into the compatibility relation (4.108) gives

$$\boldsymbol{\varphi}=\boldsymbol{\varphi}_{\mathrm{L}}+\mathbf{C}\mathbf{K}_{\mathrm{A}}^{-1}\left(\mathbf{f}_{\mathrm{F}}+\mathbf{f}_{\mathrm{F},\delta}\right) \tag{4.158}$$

with

$$\boldsymbol{\varphi}_{\mathrm{L}}=\mathbf{C}\mathbf{d}_{\mathrm{L}} \tag{4.159}$$

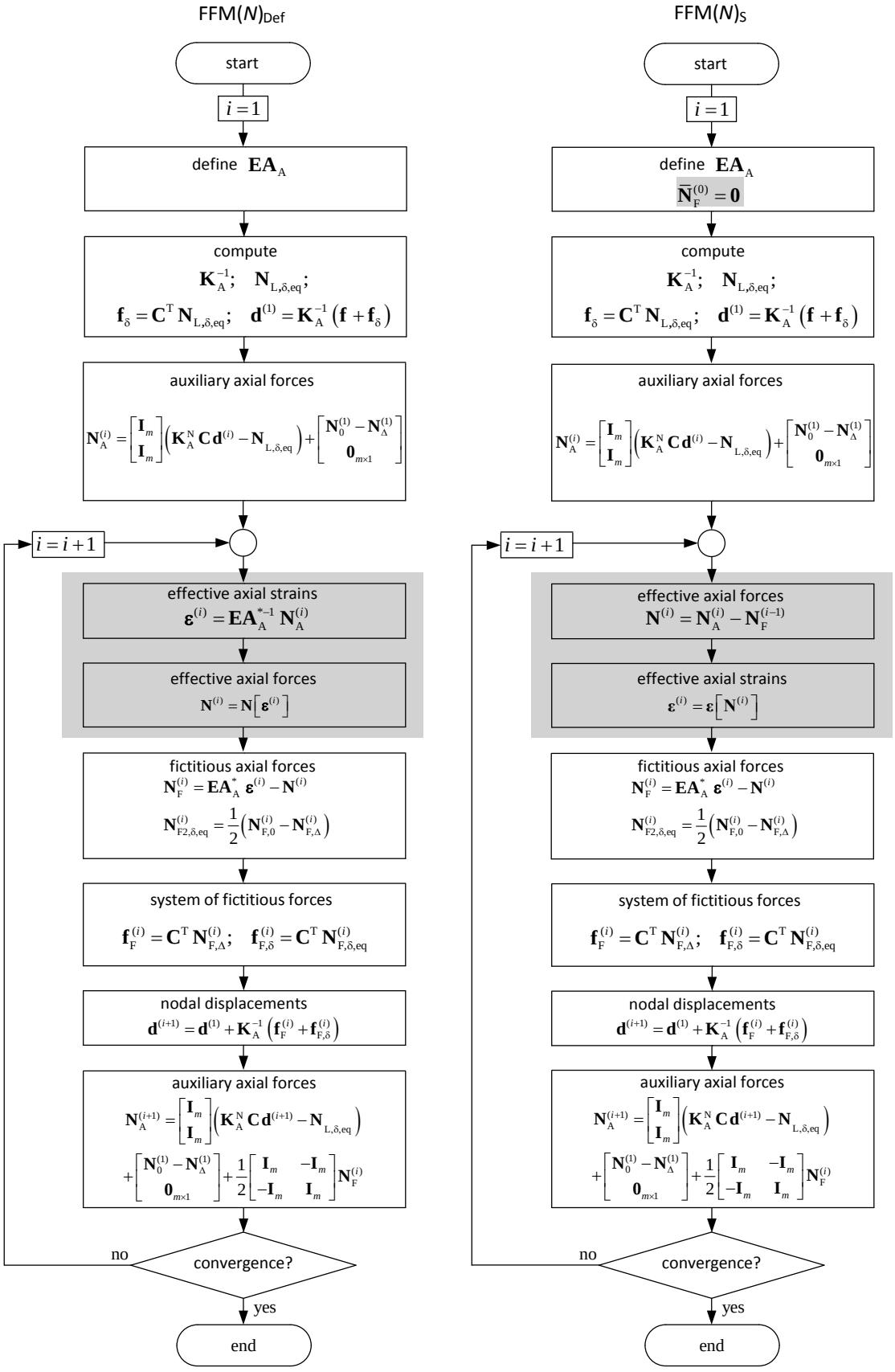

Figure 4.16. Discrete description of FFM(*N*).

Introducing (4.143) and (4.144) into (4.158) gives

$$\boldsymbol{\varphi} = \boldsymbol{\varphi}_{\mathrm{L}} + \mathbf{C}\mathbf{K}_{\mathrm{A}}^{-1}\mathbf{C}^{\mathrm{T}}\left(\mathbf{N}_{\mathrm{F},\Delta} + \mathbf{N}_{\mathrm{F},\delta,\mathrm{eq}}\right) \tag{4.160}$$

Grouping the elemental relations (4.93) gives, similarly to (4.119),

$$\mathbf{N}_{\mathrm{F},\Delta} + \mathbf{N}_{\mathrm{F},\delta,\mathrm{eq}} = \mathbf{K}_{\mathrm{A}}^{\mathrm{N}}\,\boldsymbol{\varphi}_{\mathrm{NL}} \tag{4.161}$$

Substituting this expression into (4.160) gives

$$\boldsymbol{\varphi} = \boldsymbol{\varphi}_{\mathrm{L}} + \mathbf{C}\mathbf{K}_{\mathrm{A}}^{-1}\mathbf{C}^{\mathrm{T}}\mathbf{K}_{\mathrm{A}}^{\mathrm{N}}\boldsymbol{\varphi}_{\mathrm{NL}} \tag{4.162}$$

or

$$\boldsymbol{\varphi}_{\mathrm{incr}} \equiv \boldsymbol{\varphi} - \boldsymbol{\varphi}_{\mathrm{L}} = \mathbf{T}_{\varphi}\,\boldsymbol{\varphi}_{\mathrm{NL}} \tag{4.163}$$

with

$$\mathbf{T}_{\varphi} \equiv \mathbf{C}\mathbf{K}_{\mathrm{A}}^{-1}\mathbf{C}^{\mathrm{T}}\mathbf{K}_{\mathrm{A}}^{\mathrm{N}} \tag{4.164}$$

In order to convert the previous expression into a similar relation between axial strains $\boldsymbol{\varepsilon}_{\mathrm{NL}}$ and $\boldsymbol{\varepsilon}_{\mathrm{incr}}$, let us start by collecting the generic elemental kinematic relations (4.68),

$$\boldsymbol{\varepsilon}_{\Delta} = \mathbf{K}_{0}^{\mathrm{N}}\left(\boldsymbol{\varphi} - \boldsymbol{\varphi}_{\delta}\right) \tag{4.165}$$

that can be inverted to give

$$\boldsymbol{\varphi} = \mathbf{F}_{0}^{\mathrm{N}}\,\boldsymbol{\varepsilon}_{\Delta} + \boldsymbol{\varphi}_{\delta} \tag{4.166}$$

where $\mathbf{F}_{0}^{\mathrm{N}} = \left(\mathbf{K}_{0}^{\mathrm{N}}\right)^{-1}$. Since this kinematic relation is generic one also has

$$\boldsymbol{\varphi}_{\mathrm{L}} = \mathbf{F}_{0}^{\mathrm{N}}\,\boldsymbol{\varepsilon}_{\mathrm{L},\Delta} + \boldsymbol{\varphi}_{\mathrm{L},\delta} \tag{4.167}$$

$$\boldsymbol{\varphi}_{\mathrm{NL}} = \mathbf{F}_{0}^{\mathrm{N}}\,\boldsymbol{\varepsilon}_{\mathrm{NL},\Delta} + \boldsymbol{\varphi}_{\mathrm{NL},\delta} \tag{4.168}$$

Subtracting (4.167) from (4.166) and recalling that, according to (4.73), $\boldsymbol{\varphi}_{\delta} - \boldsymbol{\varphi}_{\mathrm{L},\delta} = \boldsymbol{\varphi}_{\mathrm{NL},\delta}$, gives

$$\boldsymbol{\varphi}_{\mathrm{incr}} \equiv \boldsymbol{\varphi} - \boldsymbol{\varphi}_{\mathrm{L}} = \mathbf{F}_{0}^{\mathrm{N}}\left(\boldsymbol{\varepsilon}_{\Delta} - \boldsymbol{\varepsilon}_{\mathrm{L},\Delta}\right) + \boldsymbol{\varphi}_{\mathrm{NL},\delta} \tag{4.169}$$

According to (4.78),

$$\boldsymbol{\varphi}_{\mathrm{NL},\delta} \simeq \boldsymbol{\varphi}_{\mathrm{NL2},\delta} = \frac{1}{2}\mathbf{F}_{0}^{\mathrm{N}}\left(\boldsymbol{\varepsilon}_{\mathrm{NL},0} - \boldsymbol{\varepsilon}_{\mathrm{NL},\Delta}\right) \tag{4.170}$$

and introducing this relation into (4.169) and (4.168) gives, respectively,

$$\boldsymbol{\varphi}_{\text{incr}} = \mathbf{F}_0^{\text{N}} \left(\boldsymbol{\varepsilon}_{\Delta} - \boldsymbol{\varepsilon}_{\text{L},\Delta} + \frac{1}{2}\boldsymbol{\varepsilon}_{\text{NL},0} - \frac{1}{2}\boldsymbol{\varepsilon}_{\text{NL},\Delta} \right) \tag{4.171}$$

$$\boldsymbol{\varphi}_{\text{NL}} = \frac{1}{2}\mathbf{F}_0^{\text{N}} \left(\boldsymbol{\varepsilon}_{\text{NL},0} + \boldsymbol{\varepsilon}_{\text{NL},\Delta} \right) \tag{4.172}$$

Substituting these two relations into (4.163) gives,

$$\boldsymbol{\varepsilon}_{\text{incr},\Delta} \equiv \boldsymbol{\varepsilon}_{\Delta} - \boldsymbol{\varepsilon}_{\text{L},\Delta} = \frac{1}{2}\left(-\boldsymbol{\varepsilon}_{\text{NL},0} + \boldsymbol{\varepsilon}_{\text{NL},\Delta} \right) + \frac{1}{2}\mathbf{K}_0^{\text{N}}\,\mathbf{T}_{\varphi}\,\mathbf{F}_0^{\text{N}} \left(\boldsymbol{\varepsilon}_{\text{NL},0} + \boldsymbol{\varepsilon}_{\text{NL},\Delta} \right) \tag{4.173}$$

or

$$\boldsymbol{\varepsilon}_{\text{incr},\Delta} = \frac{1}{2}\left(\mathbf{T}_{\varepsilon} - \mathbf{I}_m \right)\boldsymbol{\varepsilon}_{\text{NL},0} + \frac{1}{2}\left(\mathbf{T}_{\varepsilon} + \mathbf{I}_m \right)\boldsymbol{\varepsilon}_{\text{NL},\Delta} \tag{4.174}$$

with

$$\mathbf{T}_{\varepsilon} = \mathbf{K}_0^{\text{N}}\,\mathbf{T}_{\varphi}\,\mathbf{F}_0^{\text{N}} \tag{4.175}$$

To derive an expression for $\boldsymbol{\varepsilon}_{\text{incr},0}$ similar to (4.174), let us start by noting that according to (4.42) and (4.56),

$$\tilde{\varepsilon}[0] = \tilde{\varepsilon}[L] + \tilde{\varepsilon}_{\delta}[0] = \tilde{\varepsilon}[L] + \tilde{\varepsilon}_{\text{L},\delta}[0] + \tilde{\varepsilon}_{\text{NL},\delta}[0] \tag{4.176}$$

and recalling the definition (4.41),

$$\tilde{\varepsilon}[0] = \tilde{\varepsilon}[L] + \tilde{\varepsilon}_{\text{L}}[0] - \tilde{\varepsilon}_{\text{L}}[L] + \tilde{\varepsilon}_{\text{NL}}[0] - \tilde{\varepsilon}_{\text{NL}}[L] \tag{4.177}$$

Grouping these elemental relations, gives

$$\boldsymbol{\varepsilon}_{\text{incr},0} = \boldsymbol{\varepsilon}_0 - \boldsymbol{\varepsilon}_{\text{L},0} = \boldsymbol{\varepsilon}_{\text{incr},\Delta} + \boldsymbol{\varepsilon}_{\text{NL},0} - \boldsymbol{\varepsilon}_{\text{NL},\Delta} \tag{4.178}$$

Substituting (4.174) into this relation gives

$$\boldsymbol{\varepsilon}_{\text{incr},0} = \frac{1}{2}\left(\mathbf{T}_{\varepsilon} + \mathbf{I}_m \right)\boldsymbol{\varepsilon}_{\text{NL},0} + \frac{1}{2}\left(\mathbf{T}_{\varepsilon} - \mathbf{I}_m \right)\boldsymbol{\varepsilon}_{\text{NL},\Delta} \tag{4.179}$$

Finally, collecting (4.174) and (4.179) gives

$$\boldsymbol{\varepsilon} = \mathbf{G}_{\varepsilon}^{\text{I}}\left[\boldsymbol{\varepsilon}_{\text{NL}} \right] = \boldsymbol{\varepsilon}_{\text{L}} + \mathbf{T}_{\varepsilon}^{*}\,\boldsymbol{\varepsilon}_{\text{NL}} \tag{4.180}$$

with

$$\mathbf{T}_{\varepsilon}^{*} \equiv \frac{1}{2}\mathbf{T}_{\varepsilon}\begin{bmatrix} \mathbf{I}_m & \mathbf{I}_m \\ \mathbf{I}_m & \mathbf{I}_m \end{bmatrix} + \begin{bmatrix} \mathbf{I}_m & -\mathbf{I}_m \\ -\mathbf{I}_m & \mathbf{I}_m \end{bmatrix} \tag{4.181}$$

Since $\boldsymbol{\varepsilon} = \boldsymbol{\varepsilon}_{\mathrm{A}} + \boldsymbol{\varepsilon}_{\mathrm{NL}}$, the above expression gives

$$\boldsymbol{\varepsilon}_{\mathrm{A}} = \boldsymbol{\varepsilon}_{\mathrm{L}} + \mathbf{T}_{\varepsilon_{\mathrm{A}}}\, \boldsymbol{\varepsilon}_{\mathrm{NL}} \tag{4.182}$$

with

$$\mathbf{T}_{\varepsilon_{\mathrm{A}}} \equiv \mathbf{T}_{\varepsilon}^{*} - \mathbf{I}_{2m} = \frac{1}{2}\mathbf{T}_{\varepsilon}\begin{bmatrix} \mathbf{I}_m & \mathbf{I}_m \\ \mathbf{I}_m & \mathbf{I}_m \end{bmatrix} - 2\begin{bmatrix} \mathbf{0}_m & -\mathbf{I}_m \\ -\mathbf{I}_m & \mathbf{0}_m \end{bmatrix} \tag{4.183}$$

and, similarly to (4.130), $\mathbf{N} = \mathbf{E}\mathbf{A}_{\mathrm{A}}^{*}\, \boldsymbol{\varepsilon}_{\mathrm{A}}$,

$$\mathbf{N} = \mathbf{N}_{\mathrm{L}} + \mathbf{E}\mathbf{A}_{\mathrm{A}}^{*}\, \mathbf{T}_{\varepsilon_{\mathrm{A}}}\, \boldsymbol{\varepsilon}_{\mathrm{NL}} \tag{4.184}$$

Substituting $\boldsymbol{\varepsilon}_{\mathrm{NL}} = \left(\mathbf{E}\mathbf{A}_{\mathrm{A}}^{*}\right)^{-1} \mathbf{N}_{\mathrm{F}}$ in the last expression yields

$$\mathbf{N} = \mathbf{G}_{\mathrm{N}}^{\mathrm{I}}\left[\mathbf{N}_{\mathrm{F}}\right] = \mathbf{N}_{\mathrm{L}} + \mathbf{T}_{\mathrm{N}}\, \mathbf{N}_{\mathrm{F}} \tag{4.185}$$

with

$$\mathbf{T}_{\mathrm{N}} = \mathbf{E}\mathbf{A}_{\mathrm{A}}^{*}\, \mathbf{T}_{\varepsilon_{\mathrm{A}}} \left(\mathbf{E}\mathbf{A}_{\mathrm{A}}^{*}\right)^{-1} \tag{4.186}$$

(*i.e.*, $\mathbf{T}_{\mathrm{N}}$ and $\mathbf{T}_{\varepsilon_{\mathrm{A}}}$ are similar matrices). Expressions (4.180) and (4.185) are the discrete versions of the general expressions (4.15) and (4.18). For example, the operator T_{ε} in (4.15) corresponds to matrix $\mathbf{T}_{\varepsilon}^{*}$ in (4.180) and T_{N} in (4.18) to matrix $\mathbf{T}_{\mathrm{N}}$ in (4.185).

The matrix format of (4.20) is given by

$$\mathbf{N}_{\mathrm{F}}^{(i)} = \mathbf{G}_{\mathrm{N}}^{\mathrm{II}}\left[\mathbf{N}^{(i)}\right] = \mathbf{E}\mathbf{A}_{\mathrm{A}}^{*}\, \boldsymbol{\varepsilon}\left[\mathbf{N}^{(i)}\right] - \mathbf{N}^{(i)} \tag{4.187}$$

and the matrix format of (4.19) is given by

$$\boldsymbol{\varepsilon}_{\mathrm{NL}}^{(i)} = \mathbf{G}_{\varepsilon}^{\mathrm{II}}\left[\boldsymbol{\varepsilon}^{(i)}\right] = \boldsymbol{\varepsilon}^{(i)} - \left(\mathbf{E}\mathbf{A}_{\mathrm{A}}^{*}\right)^{-1} \mathbf{N}\left[\boldsymbol{\varepsilon}^{(i)}\right] \tag{4.188}$$

Inserting these expressions into (4.180) and (4.185), and bearing in mind that $\boldsymbol{\varepsilon}^{(1)} = \boldsymbol{\varepsilon}_{\mathrm{L}}$ and $\mathbf{N}^{(1)} = \mathbf{N}_{\mathrm{L}}$, gives the iteration formulas of FFM(N)$_{\mathrm{Def}}$

$$\boldsymbol{\varepsilon}^{(i+1)} = \mathbf{G}_{\varepsilon}\left[\boldsymbol{\varepsilon}^{(i)}\right] = \mathbf{G}_{\varepsilon}^{\mathrm{I}}\left[\mathbf{G}_{\varepsilon}^{\mathrm{II}}\left[\boldsymbol{\varepsilon}^{(i)}\right]\right] = \boldsymbol{\varepsilon}^{(1)} + \mathbf{T}_{\varepsilon}^{*}\, \boldsymbol{\varepsilon}_{\mathrm{NL}}\left[\boldsymbol{\varepsilon}^{(i)}\right] \tag{4.189}$$

and FFM(N)$_{\mathrm{S}}$

$$\mathbf{N}^{(i+1)} = \mathbf{G}_{\mathrm{N}}\left[\mathbf{N}^{(i)}\right] = \mathbf{G}_{\mathrm{N}}^{\mathrm{I}}\left[\mathbf{G}_{\mathrm{N}}^{\mathrm{II}}\left[\mathbf{N}^{(i)}\right]\right] = \mathbf{N}^{(1)} + \mathbf{T}_{\mathrm{N}}\, \mathbf{N}_{\mathrm{F}}\left[\mathbf{N}^{(i)}\right] \tag{4.190}$$

which are discrete versions of the more general (4.21) and (4.22).

4.4.1. Convergence conditions of FFM(*N*) discrete description

As already explained in § 4.1.5, the iteration formulas (4.189) and (4.190) converge if the operators $\mathbf{G}_\varepsilon$ and $\mathbf{G}_\mathrm{N}$ are contractive. On the other hand, $\mathbf{G}_\varepsilon$ is contractive if both $\mathbf{G}_\varepsilon^\mathrm{I}$ and $\mathbf{G}_\varepsilon^\mathrm{II}$ are non-expansive and at least one of them is contractive. A similar reasoning applies to $\mathbf{G}_\mathrm{N}$, $\mathbf{G}_\mathrm{N}^\mathrm{I}$ and $\mathbf{G}_\mathrm{N}^\mathrm{II}$. The Jacobian matrices of $\mathbf{G}_\varepsilon^\mathrm{I}$ and $\mathbf{G}_\mathrm{N}^\mathrm{I}$ are

$$\mathbf{J}_\varepsilon^\mathrm{I} = \mathbf{T}_\varepsilon^* \tag{4.191}$$

$$\mathbf{J}_\mathrm{N}^\mathrm{I} = \mathbf{T}_\mathrm{N} \tag{4.192}$$

Hence, $\mathbf{G}_\varepsilon^\mathrm{I}$ (resp. $\mathbf{G}_\mathrm{N}^\mathrm{I}$) is non-expansive if $\rho\left[\mathbf{T}_\varepsilon^*\right]$ (resp. $\rho\left[\mathbf{T}_\mathrm{N}\right]$), the spectral radius of $\mathbf{T}_\varepsilon^*$ (resp. $\mathbf{T}_\mathrm{N}$), is less than or equal to 1. In § 4.1.5, it was proved that $\mathbf{G}_\varepsilon^\mathrm{II}$ (resp. $\mathbf{G}_\mathrm{N}^\mathrm{II}$) is contractive if the relative auxiliary axial stiffness field satisfies condition (4.25) (resp. (4.26)) at every cross section of the structure. The $2m \times 2m$ diagonal Jacobian matrices $\mathbf{J}_\varepsilon^\mathrm{II}$ of $\mathbf{G}_\varepsilon^\mathrm{II}$ and $\mathbf{J}_\mathrm{N}^\mathrm{II}$ of $\mathbf{G}_\mathrm{N}^\mathrm{II}$ contain the relative differences of axial stiffness at the end cross sections of each element and are written as

$$\mathbf{J}_\varepsilon^\mathrm{II} = \boldsymbol{\beta}_\varepsilon \equiv \begin{bmatrix} \overline{\boldsymbol{\beta}}_{\varepsilon,1} & & & \\ & \overline{\boldsymbol{\beta}}_{\varepsilon,2} & & \\ & & \ddots & \\ & & & \overline{\boldsymbol{\beta}}_{\varepsilon,m} \end{bmatrix} \tag{4.193}$$

with

$$\overline{\boldsymbol{\beta}}_{\varepsilon,j} \equiv \begin{bmatrix} \beta_{\varepsilon,1} & 0 \\ 0 & \beta_{\varepsilon,2} \end{bmatrix} \tag{4.194}$$

where, according to (4.23), $\beta_{\varepsilon,1}$ and $\beta_{\varepsilon,2}$ are given by

$$\beta_{\varepsilon,1} = \frac{EA_\mathrm{A} - \widetilde{EA}[0]}{EA_\mathrm{A}} \tag{4.195}$$

$$\beta_{\varepsilon,2} = \frac{EA_\mathrm{A} - \widetilde{EA}[L]}{EA_\mathrm{A}} \tag{4.196}$$

and

$$\mathbf{J}_\mathrm{N}^\mathrm{II} = \boldsymbol{\beta}_\mathrm{N} \equiv \begin{bmatrix} \overline{\boldsymbol{\beta}}_{\mathrm{N},1} & & & \\ & \overline{\boldsymbol{\beta}}_{\mathrm{N},2} & & \\ & & \ddots & \\ & & & \overline{\boldsymbol{\beta}}_{\mathrm{N},m} \end{bmatrix} \tag{4.197}$$

with

$$\overline{\boldsymbol{\beta}}_{\mathrm{N},j} \equiv \begin{bmatrix} \beta_{\mathrm{N},1} & 0 \\ 0 & \beta_{\mathrm{N},2} \end{bmatrix} \tag{4.198}$$

where, according to (4.24), $\beta_{\mathrm{N},1}$ and $\beta_{\mathrm{N},2}$ are given by

$$\beta_{\mathrm{N},1} = \frac{EA_{\mathrm{A}} - \widetilde{EA}[0]}{\widetilde{EA}[0]} \tag{4.199}$$

$$\beta_{\mathrm{N},2} = \frac{EA_{\mathrm{A}} - \widetilde{EA}[L]}{\widetilde{EA}[L]} \tag{4.200}$$

Hence, the Jacobian matrices of $\mathbf{G}_{\varepsilon}$ and $\mathbf{G}_{\mathrm{N}}$ can be written as

$$\mathbf{J}_{\varepsilon} = \mathbf{J}_{\varepsilon}^{\mathrm{I}} \mathbf{J}_{\varepsilon}^{\mathrm{II}} = \mathbf{T}_{\varepsilon} \boldsymbol{\beta}_{\varepsilon} \tag{4.201}$$

$$\mathbf{J}_{\mathrm{N}} = \mathbf{J}_{\mathrm{N}}^{\mathrm{I}} \mathbf{J}_{\mathrm{N}}^{\mathrm{II}} = \mathbf{T}_{\mathrm{N}} \boldsymbol{\beta}_{\mathrm{N}} \tag{4.202}$$

The first (resp. second) of these expressions shows that $\mathbf{G}_{\varepsilon}$ (resp. $\mathbf{G}_{\mathrm{N}}$) is contractive if both $\mathbf{G}_{\varepsilon}^{\mathrm{I}}$ and $\mathbf{G}_{\varepsilon}^{\mathrm{II}}$ (resp. $\mathbf{G}_{\mathrm{N}}^{\mathrm{I}}$ and $\mathbf{G}_{\mathrm{N}}^{\mathrm{II}}$) are non-expansive and at least one of them is contractive.

4.4.2. Sufficient convergence conditions of FFM(*N*) discrete description

In order to derive the sufficient convergence conditions, let us start by noting that

$$\rho\left[\mathbf{T}_{\varepsilon}^{*}\right] = \rho\left[\mathbf{T}_{\mathrm{N}}\right] = 1 \tag{4.203}$$

The demonstration of this identity is omitted in this thesis. Such proof is similar to that performed in chapter 3 to demonstrate that $\rho\left[\mathbf{T}_{\chi}\right] = \rho\left[\mathbf{T}_{\mathrm{M}}\right] = 1$.

Hence, the iteration formulas of FFM(*N*), in the context of the discrete description, converge if $\mathbf{G}_{\varepsilon}^{\mathrm{II}}$ and $\mathbf{G}_{\mathrm{N}}^{\mathrm{II}}$ are contractive, *i.e.* if (4.25) and (4.26) are verified at every cross section. According to (4.195), the condition $\left|\tilde{\beta}_{\varepsilon}\right| < 1$ is verified if the following relation is verified at every cross section

$$0 < \frac{\widetilde{EA}_i}{EA_{\mathrm{A},i}} < 2, \quad i = 1, 2, \cdots, m \tag{4.204}$$

This condition implies that $\widetilde{EA}_i \neq 0$ and that the auxiliary constant axial stiffness has the same sign as the effective axial stiffness. If $\widetilde{EA}_i > 0$ the above conditions reduce to

$$EA_{\mathrm{A},i} > \frac{1}{2}\widetilde{EA}_i, \quad i = 1,2,\cdots,m \tag{4.205}$$

Thence, in the context of the discrete description with $\widetilde{EA}_i > 0$, $\mathrm{FFM_{Def}}$ converges if the auxiliary constitutive law satisfies condition (4.205).

On the other hand, according to (4.199), the condition $\left|\tilde{\beta}_{\mathrm{N}}\right| < 1$ is equivalent to

$$0 < \frac{EA_{\mathrm{A},i}}{\widetilde{EA}_i} < 2, \quad i = 1,2,\cdots,m \tag{4.206}$$

Note the similarity between conditions (4.206) and (4.204). Once again, the sign of the auxiliary constant axial stiffness must be equal to the sign of the effective axial stiffness. Hence, if $\widetilde{EA}_i > 0$ everywhere, the convergence condition is

$$0 < EA_{\mathrm{A},i} < 2\widetilde{EA}_i, \quad i = 1,2,\cdots,m \tag{4.207}$$

Conditions (4.204) to (4.207) correspond to the conditions developed in chapter 3 in the context of FFM(*M*). Expression (4.202) also shows that the closest the values of $EA_{\mathrm{A},i}$ and $\widetilde{EA}_i$ the fastest the convergence rate of $\mathrm{FFM_S}$, a conclusion shared with $\mathrm{FFM_{Def}}$.

4.5. Illustrative example

This example illustrates the role of the mesh refinement in FFM(*N*) discrete description. It also illustrates the role played by the chosen auxiliary axial stiffness in $\mathrm{FFM_{Def}}$ and $\mathrm{FFM_S}$ iterative procedures. Let us consider the rod represented in Figure 4.17a, formed by two prismatic parts of equal length $L = 1/2$ and constant constitutive relations. The left hand half of the rod has a linear constitutive relation

$$\hat{N}\left[\varepsilon\right] = EA_1\ \varepsilon = \varepsilon \tag{4.208}$$

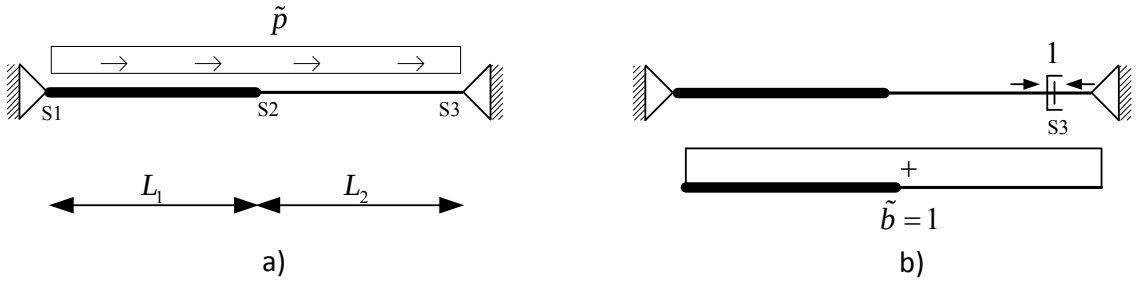

Figure 4.17. Example 4: a) Rod and axial loading; b) primary structure.

with EA_1=1. The right hand rod half has the nonlinear constitutive relation already used in the examples presented in chapter 3 (Richard and Abbott, 1975)

$$\hat{N}\left[\varepsilon\right]=\frac{EA_0\,\varepsilon}{\sqrt{1+\left(\dfrac{EA_0\,\varepsilon}{N_{\text{ref}}}\right)^2}}=\frac{\varepsilon}{\sqrt{1+\varepsilon^2}}\quad\text{or}\quad\hat{\varepsilon}\left[N\right]=\frac{\dfrac{N}{EA_0}}{\sqrt{1-\left(\dfrac{N}{N_{\text{ref}}}\right)^2}}=\frac{N}{\sqrt{1-N^2}}\tag{4.209}$$

where $EA_0=\widehat{EA}_2\left[0\right]=1$ and $N_{\text{ref}}=1$. The rod carries an axial uniformly distributed load $p=1$, see Figure 4.17a.

This structure has one degree of static indeterminacy and, therefore, the axial force field can be expressed in terms of the axial force at a single section, for instance, N_{S3} at the right end section S_3. In order to establish the exact solution, the problem is analysed by the force method, considering the primary structure defined by releasing the normal force at S_3. The corresponding compatibility condition is given by

$$\int_0^{2L}\tilde{b}\,\hat{\varepsilon}\left[\tilde{N}\left[x\right]\right]dx=\int_0^{2L}\hat{\varepsilon}\left[\tilde{N}\left[x\right]\right]dx=0\tag{4.210}$$

where $\tilde{b}=1$ is the self-equilibrated axial force field represented in Figure 4.17b. Equation (4.210) has a single solution defined by $N_{\text{S3}}=-0.492$. The corresponding axial strain is $\varepsilon_{\text{S3}}=-0.565$.

In the FFM analysis of the problem, the auxiliary constant axial stiffness EA_{A} was chosen to be constant along the rod with value 1, which means that the effective and auxiliary constitutive relations are the same in left half of the rod, corresponding to null fictitious normal forces.

At first, a uniform mesh with two elements corresponding to the two rod halves was considered. Other meshes were defined by consecutive bisection of the nonlinear second half establishing a family of non-uniform meshes with $m=1+2^{i-1}=2,3,5,9,17,33$ and 65 elements, 2^{i-1} of which have equal length. There is no point in refining the linear left half of the rod because the corresponding fictitious normal force is zero due to the choice of EA_{A}.

A convergence analysis was performed (i) with respect to the mesh refinement (*mesh*-convergence) and (ii) with respect to FFM iterative procedure itself (*FFM*-convergence). Both convergence analyses are based on relative error I (err_{I}) and relative error II (err_{II}) defined in § 3.7. For a given mesh, the ith approximation of x is *FFM*-convergent if $err_{\text{I}}^{(i)}<tol_{\text{FFM}}=0.001$

while the *FFM*-convergent approximation of x, for the jth mesh, is *mesh*-convergent if $\{err_{\mathrm{I},j}, err_{\mathrm{II},j}\} < tol_{\mathrm{mesh}} = 0.01$.

Figure 4.18 and Table 4.2 present the results of the *mesh*-convergence analysis. Each solution in this plot represents an *FFM*-convergent solution. For the tolerance values given above, Figure 4.18 shows that *mesh*-convergence requires 33 elements.

In order to illustrate that the performance of FFM(*N*) iterative procedures depends on the selected EA_{A} field, the number of iterations needed for *FFM*-convergence with 33 elements in terms of $\varepsilon_{\mathrm{S3}}$, N_{S3}, $\|\boldsymbol{\varepsilon}\|$ and $\|\mathbf{N}\|$ ($\|.\|$ is the Euclidean norm) for constant fields $EA_{\mathrm{A}} \in [0.1, 2]$ was investigated, see Figure 4.19.

Considering the cross-sectional constitutive relation (4.209), the sufficient condition for convergence of FFM(N)$_{\mathrm{Def}}$ (4.205) gives

$$EA_{\mathrm{A}} > \frac{1}{2}\max \widetilde{EA} = \frac{1}{2} EA_0 = 0.5 \tag{4.211}$$

and the sufficient condition for convergence of FFM(N)$_{\mathrm{S}}$ (4.207) gives

$$0 < EA_{\mathrm{A}} < 2\min \widetilde{EA} = 2\, EA_{\mathrm{S3}} = 1.33\, EA_0 = 1.33 \tag{4.212}$$

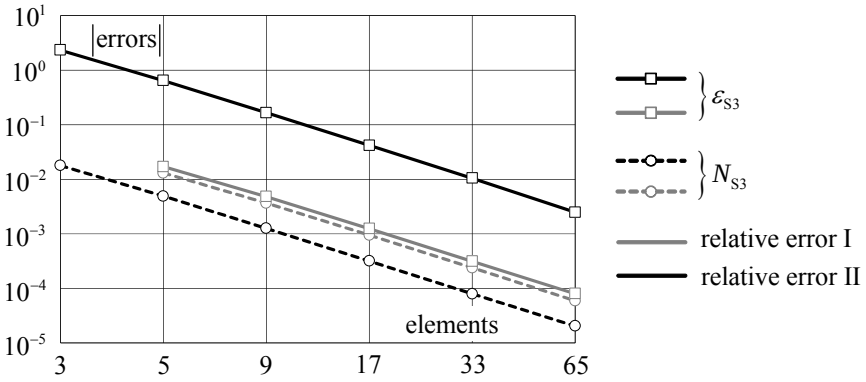

Figure 4.18. Example 4: Mesh-convergence (logarithmic scale).

Table 4.2 – Example 4: Numerical FFM solutions vs. exact solution.

	number of elements (FFM)						exact solution
	1+1	1+2	1+4	1+8	1+16	1+32	
$\varepsilon_{\mathrm{S3}}$	-0.551	-0.561	-0.564	-0.564	-0.565	-0.565	-0.565
N_{S3}	-0.483	-0.489	-0.491	-0.491	-0.492	-0.492	-0.492

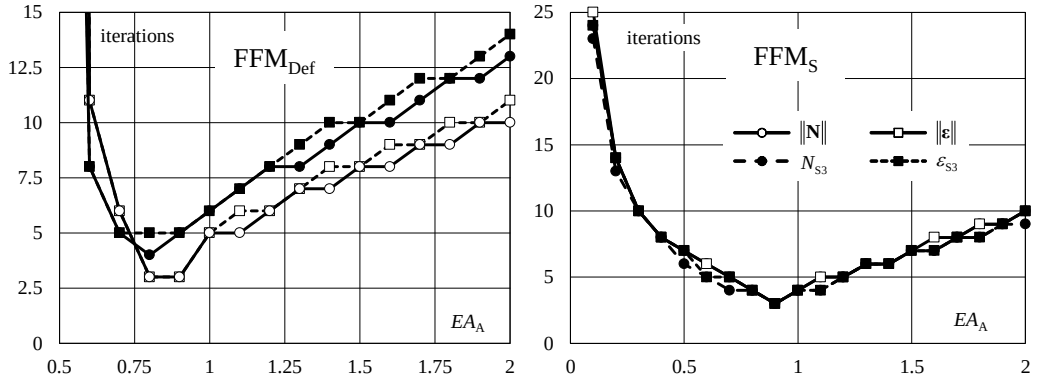

Figure 4.19. Example 4: FFM(*N*) – number of iterations required by for convergence.

The results in Figure 4.19 show that the above sufficient convergence conditions are satisfied. Actually, there was no numerical convergence of FFM$(N)_{\text{Def}}$ for $EA_{\text{A}} \le 0.5$ and of FFM$(N)_{\text{S}}$ for $EA_{\text{A}} \ge 10.8$. In the latter case, the normal force becomes larger than N_{ref} during the iterative procedure, but the upper limit of the convergence domain, 10.8, is well above the maximum defined by (4.212). It can also be observed that the convergence rate depends strongly on the value of EA_{A} and that the optimal interval is $EA_{\text{A}} \in [0.7\,, 1.0]$.

Figure 4.19 shows that the number of iterations required by FFM$(N)_{\text{Def}}$ for convergence in terms of N_{S3} or ε_{S3} is almost always larger than in terms of the Euclidian norm of the axial force or strain. The same figure shows, however, that FFM$(N)_{\text{S}}$ requires almost the same number of iterations for convergence in terms of N_{S3} or ε_{S3} or in terms of the Euclidian norm.

Chapter 5
The Fictitious Force Method – *model MN*

In this chapter, the particularization of FFM to the beam *model MN* is presented and applied to the analysis of generic skeletal structures. The chapter starts with an improved description of the considered effective nonlinear constitutive relationships. Then, FFM is reviewed in the light of *model MN* and the sufficient convergence conditions of FFM(MN)$_{\text{Def}}$ are derived. Next, the discrete description of the elemental fictitious force system of FFM(MN) is presented. In a fourth stage, the application of FFM(MN) in the context of the matrix methods of structural analysis is presented and the convergence of the FFM iterative procedure is reviewed. The chapter concludes with an example which illustrates the application of FFM(MN)$_{\text{Def}}$.

5.1. Effective nonlinear constitutive relationship

The formulation presented in this chapter applies to skeletal structures whose cross-sectional nonlinear constitutive relations between internal forces (M,N) and generalized strains (χ,ε) are elastic and continuous. These relations are generically denoted[10]

$$M = \hat{M}\left[\chi,\varepsilon\right] \tag{5.1}$$

$$N = \hat{N}\left[\chi,\varepsilon\right] \tag{5.2}$$

[10] Recall that the circumflex accent stands for a cross-sectional function.

or

$$\chi = \hat{\chi}\left[M, N\right] \tag{5.3}$$

$$\varepsilon = \hat{\varepsilon}\left[M, N\right] \tag{5.4}$$

The cross-sectional tangent properties are given by

$$EI \equiv \widehat{EI}\left[\chi, \varepsilon\right] = \frac{\partial \hat{M}\left[\chi, \varepsilon\right]}{\partial \chi} \tag{5.5}$$

$$EA \equiv \widehat{EA}\left[\chi, \varepsilon\right] = \frac{\partial \hat{N}\left[\chi, \varepsilon\right]}{\partial \varepsilon} \tag{5.6}$$

$$ES \equiv \widehat{ES}\left[\chi, \varepsilon\right] = \frac{\partial \hat{M}\left[\chi, \varepsilon\right]}{\partial \varepsilon} = \frac{\partial \hat{N}\left[\chi, \varepsilon\right]}{\partial \chi} \tag{5.7}$$

e.g., $\widehat{EI}\left[\chi, \varepsilon\right]$ is the bending stiffness and $\widehat{EA}\left[\chi, \varepsilon\right]$ the axial stiffness. These properties may be discontinuous. Thence, the constitutive relation incremental format is given by

$$\begin{bmatrix} dM \\ dN \end{bmatrix} = \begin{bmatrix} \widehat{EI} & \widehat{ES} \\ \widehat{ES} & \widehat{EA} \end{bmatrix} \begin{bmatrix} d\chi \\ d\varepsilon \end{bmatrix} \tag{5.8}$$

In this general case of Euler-Bernoulli beam, each internal force (bending moment and axial force) depends on both generalized strains (curvature and axial strain). In other words, a variation of the curvature changes both internal forces, the same happening with a variation of the axial strain. This coupling is due to the third stiffness coefficient $\widehat{ES}$, which is a generalized static moment.

In order to determine the cross-sectional proprieties (5.5) to (5.7), the original 3D problem must be recalled, *i.e.* the local nonlinear elastic constitutive relationship

$$\widehat{\sigma}\left[e\right] \tag{5.9}$$

or

$$\widehat{e}\left[\sigma\right] \tag{5.10}$$

between the longitudinal normal strain *e* and stress σ for each material of the cross section must be considered. The symbol $\widehat{\ }$ on top of a variable stands for a constitutive relation established at the point or local level. The longitudinal stiffness at a given point of the cross section is given by

$$E = \widehat{E}[e] = \frac{d\widehat{\sigma}[e]}{de} \tag{5.11}$$

and obviously depends on the material at that location. The hypothesis presented in § 3.1 will now be extended so that only materials with $E > 0$ are considered in this chapter. This excludes stress-strain curves with either horizontal or post-peak descending branches[11]. In practise, the nonlinear constitutive relations are only known at the point level, *i.e.* defined by relations (5.9) or (5.10). The cross-sectional relations (5.1) to (5.4) are computed with these local constitutive relations and the cross-sectional geometry.

Let D be the region of the surface corresponding to the cross section and dD a differential element of that region. The bending moment and axial force are given by

$$M = \int_D \sigma\, z\, dD \tag{5.12}$$

$$N = \int_D \sigma\, dD \tag{5.13}$$

According to Euler-Bernoulli hypothesis, the longitudinal normal strain at each point of a cross section with generalized stresses ε and χ is given by

$$e = \varepsilon + \chi\, z \tag{5.14}$$

Thence,

$$M = \hat{M} = \int_D \widehat{\sigma}[\varepsilon + \chi\, z]\, z\, dD \tag{5.15}$$

$$N = \hat{N} = \int_D \widehat{\sigma}[\varepsilon + \chi\, z]\, dD \tag{5.16}$$

and

$$EI = \frac{\partial M}{\partial \chi} = \frac{\partial}{\partial \chi}\left(\int_D \sigma\, z\, dD\right) = \int_D \frac{\partial \sigma}{\partial \chi}\, z\, dD = \int_D \frac{d\sigma}{de}\frac{\partial e}{\partial \chi}\, z\, dD = \int_D E\, z^2\, dD \tag{5.17}$$

$$EA = \frac{\partial N}{\partial \varepsilon} = \frac{\partial}{\partial \varepsilon}\left(\int_D \sigma\, dD\right) = \int_D \frac{\partial \sigma}{\partial \varepsilon}\, dD = \int_D \frac{d\sigma}{de}\frac{\partial e}{\partial \varepsilon}\, dD = \int_D E\, dD \tag{5.18}$$

[11] However, note that even though there are no theoretical results for these possibilities ($E = 0$ or $E < 0$), FFM has already been applied with success to RC problems where some points in the section do not present a positive stiffness, see (Costa,2013).

$$\frac{\partial M}{\partial \varepsilon} = \frac{\partial}{\partial \varepsilon}\left(\int_D \sigma \, z \, dD \right) = \int_D \frac{\partial \sigma}{\partial \varepsilon} z \, dD = \int_D \frac{d\sigma}{de} \frac{\partial e}{\partial \varepsilon} z \, dD = \int_D E \, z \, dD \tag{5.19}$$

$$\frac{\partial N}{\partial \chi} = \frac{\partial}{\partial \chi}\left(\int_D \sigma \, dD \right) = \int_D \frac{\partial \sigma}{\partial \chi} dD = \int_D \frac{d\sigma}{de} \frac{\partial e}{\partial \chi} dD = \int_D E \, z \, dD = \frac{\partial M}{\partial \varepsilon} \tag{5.20}$$

and, therefore,

$$ES = \frac{\partial N}{\partial \chi} = \frac{\partial M}{\partial \varepsilon} = \int_D E \, z \, dD \tag{5.21}$$

This means that a differential variation of the axial strain ε causes a differential variation of the bending moment M which is equal to the differential variation of the normal force N caused by a differential variation of the curvature χ.

In general, for nonlinear materials or non-prismatic elements there is no elemental coordinate system for which ES is null at every section.

5.2. FFM with beam *model MN*

5.2.1. Auxiliary linear constitutive relationship

The auxiliary linear constitutive relation for this general case combines the axial component established for the *rod model N* and the flexural component established for the beam *model M*. It can be written in the following matrix form

$$\begin{bmatrix} M_{\mathrm{A}} \\ N_{\mathrm{A}} \end{bmatrix} = \begin{bmatrix} EI_{\mathrm{A}} & 0 \\ 0 & EA_{\mathrm{A}} \end{bmatrix} \begin{bmatrix} \chi \\ \varepsilon \end{bmatrix} \tag{5.22}$$

or

$$\begin{bmatrix} \chi_{\mathrm{A}} \\ \varepsilon_{\mathrm{A}} \end{bmatrix} = \begin{bmatrix} 1/EI_{\mathrm{A}} & 0 \\ 0 & 1/EA_{\mathrm{A}} \end{bmatrix} \begin{bmatrix} M \\ N \end{bmatrix} \tag{5.23}$$

This is a particular case of (5.8) for the case where (i) every point in the cross section has the same linear constitutive relation determined by Young modulus E_{A}

$$\sigma_{\mathrm{A}} \equiv \widehat{\sigma}_{\mathrm{A}}[e] = E_{\mathrm{A}} \, e \tag{5.24}$$

and (ii) the cross-sectional coordinate system is barycentric. If these two simplifying assumptions are satisfied, the bending and axial stiffnesses are given by

$$EI_{\mathrm{A}} = E_{\mathrm{A}} I_y \tag{5.25}$$

$$EA_{\mathrm{A}} = E_{\mathrm{A}} A \tag{5.26}$$

while the auxiliary generalized static moment is

$$ES_{\mathrm{A}} = E_{\mathrm{A}} S = 0 \tag{5.27}$$

The geometric proprieties in the above expressions are

$$I_y = \int_D z^2 \, dD \tag{5.28}$$

which is the second moment of area of the cross section with respect to the barycentric *y*-axis,

$$A = \int_D dD \tag{5.29}$$

which is the cross-sectional area, and

$$S = \int_D z \, dD = 0 \tag{5.30}$$

which is the first moment of area of the cross section with respect to the *y*-axis, which is null because the coordinate system is barycentric, see § 3.1. This is why ES_{A} is also null. This auxiliary constitutive relation replaces the effective relation in the auxiliary structure.

5.2.2. FFM(*MN*) *by deformations* and FFM(*MN*) *by stresses*

The fictitious internal forces, given by the difference between auxiliary and effective internal forces, *i.e.*, $M_{\mathrm{F}} = M_{\mathrm{A}} - M$ and $N_{\mathrm{F}} = N_{\mathrm{A}} - N$, can be written in terms of the pair of generalized strains

$$M_{\mathrm{F}} \equiv M_{\mathrm{F}}\left[\chi, \varepsilon\right] = EI_{\mathrm{A}} \, \chi - \hat{M}\left[\chi, \varepsilon\right] \tag{5.31}$$

$$N_{\mathrm{F}} \equiv N_{\mathrm{F}}\left[\chi, \varepsilon\right] = EA_{\mathrm{A}} \, \varepsilon - \hat{N}\left[\chi, \varepsilon\right] \tag{5.32}$$

i.e.,

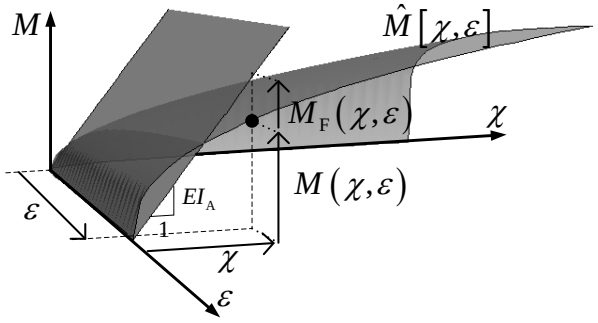

Figure 5.1. Computation of the fictitious bending moment in FFM(*MN*).

$$\begin{bmatrix} M_F \\ N_F \end{bmatrix} = \begin{bmatrix} EI_A & 0 \\ 0 & EA_A \end{bmatrix} \begin{bmatrix} \chi \\ \varepsilon \end{bmatrix} - \begin{bmatrix} \hat{M}[\chi,\varepsilon] \\ \hat{N}[\chi,\varepsilon] \end{bmatrix} \tag{5.33}$$

Since, usually, the generalized strains (χ, ε) (and the internal forces (M , N)) are not known *a priori,* it is necessary to establish iteration formulas. FFM_{Def} estimates the fictitious internal forces in terms of the estimative of the effective generalized strains,

$$M_F^{(i)} = EI_A \, \chi^{(i)} - \hat{M}\left[\chi^{(i)}, \varepsilon^{(i)}\right] \tag{5.34}$$

$$N_F^{(i)} = EA_A \, \varepsilon^{(i)} - \hat{N}\left[\chi^{(i)}, \varepsilon^{(i)}\right] \tag{5.35}$$

see Figure 5.1, and recalling (5.15) and (5.16),

$$M_F^{(i)} = EI_A \, \chi^{(i)} - \int_D \widehat{\sigma}\left[\varepsilon^{(i)} + \chi^{(i)} \, z\right] z \, dD \tag{5.36}$$

$$N_F^{(i)} = EA_A \, \varepsilon^{(i)} - \int_D \widehat{\sigma}\left[\varepsilon^{(i)} + \chi^{(i)} \, z\right] dD \tag{5.37}$$

Recalling (5.8), the incremental form of expression (5.33) is given by

$$\begin{bmatrix} dM_F \\ dN_F \end{bmatrix} = \left(\begin{bmatrix} EI_A & 0 \\ 0 & EA_A \end{bmatrix} - \begin{bmatrix} EI & ES \\ ES & EA \end{bmatrix} \right) \begin{bmatrix} d\chi \\ d\varepsilon \end{bmatrix} \tag{5.38}$$

Hence, the increment of the fictitious internal forces is a function of the difference between the uncoupled auxiliary cross-sectional stiffness and the coupled effective cross-sectional stiffness.

The fictitious internal forces can also be established in terms of the pair of internal forces

$$M_F \equiv M_F[M, N] = EI_A \, \hat{\chi}[M, N] - M \tag{5.39}$$

$$N_F \equiv N_F[M, N] = EA_A \, \hat{\varepsilon}[M, N] - N \tag{5.40}$$

corresponding to FFM_S which estimates the fictitious internal forces in terms of the estimative of the effective internal forces,

$$M_{\mathrm{F}}^{(i)} = EI_{\mathrm{A}}\,\hat{\chi}\left[M^{(i)}, N^{(i)}\right] - M^{(i)} \tag{5.41}$$

$$N_{\mathrm{F}}^{(i)} = EA_{\mathrm{A}}\,\hat{\varepsilon}\left[M^{(i)}, N^{(i)}\right] - N^{(i)} \tag{5.42}$$

Since a null fictitious force system is used to compute the initial guess, $\chi^{(1)} \equiv \chi_{\mathrm{L}}$, $\varepsilon^{(1)} \equiv \varepsilon_{\mathrm{L}}$, $M^{(1)} \equiv M_{\mathrm{L}}$ and $N^{(1)} \equiv N_{\mathrm{L}}$. The flowcharts represented in Figure 5.2 illustrate the application of FFM in the context of the beam *model MN*. These flowcharts can be seen as a generalization of the flowcharts in Figure 3.4 and Figure 4.3.

5.2.3. Iteration formula of FFM(*MN*) *by deformations*

Let us define the vectors of cross-sectional generalized strains

$$\boldsymbol{\eta} = \begin{bmatrix} \chi \\ \varepsilon \end{bmatrix} \tag{5.43}$$

and generalized stresses

$$\mathbf{R} = \begin{bmatrix} M \\ N \end{bmatrix} \tag{5.44}$$

The auxiliary generalized stresses are decomposed according to

$$\mathbf{R}_{\mathrm{A}} = \mathbf{R} + \mathbf{R}_{\mathrm{F}} \tag{5.45}$$

and the generalized strains are decomposed according to

$$\boldsymbol{\eta} = \boldsymbol{\eta}_{\mathrm{A}} + \boldsymbol{\eta}_{\mathrm{NL}} \tag{5.46}$$

The nonlinear components χ_{NL} and $\varepsilon_{\mathrm{NL}}$ (resp. M_{F} and N_{F}) gathered in $\boldsymbol{\eta}_{\mathrm{NL}}$ (resp. $\mathbf{R}_{\mathrm{F}}$) can still be regarded as initial generalized deformations (resp. initial internal forces), whose effect on the auxiliary structure, combined with that of the effective force system, gives the auxiliary solution, now characterized by the pair of vectors ($\boldsymbol{\eta}$, $\mathbf{R}_{\mathrm{A}}$).

For a given structure subjected to an arbitrary force system F, let the linear operator $\mathbf{T}$, associated to the corresponding auxiliary problem, represent the transformation of the generic action formed by F and an arbitrary initial deformation field

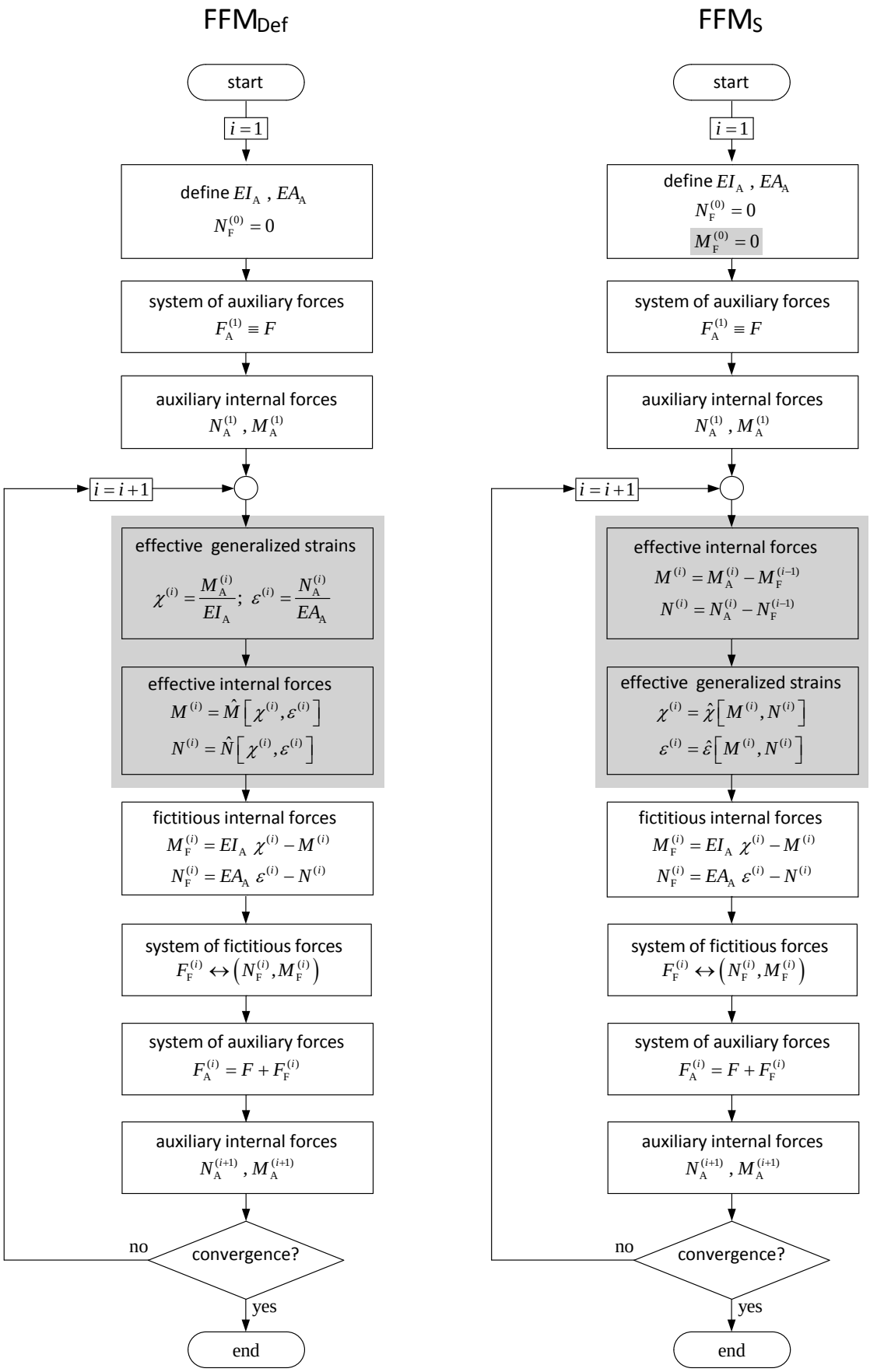

Figure 5.2. FMM(*MN*) iterative procedures.

$$\tilde{\boldsymbol{\eta}}_{\mathrm{NL}} = \begin{bmatrix} \tilde{\chi}_{\mathrm{NL}} \\ \tilde{\varepsilon}_{\mathrm{NL}} \end{bmatrix} \tag{5.47}$$

into the effective deformation fields grouped in $\boldsymbol{\eta}$,

$$\tilde{\boldsymbol{\eta}} = \mathbf{T}\left[\tilde{\boldsymbol{\eta}}_{\mathrm{NL}}\,,\, F\right] \tag{5.48}$$

Since $\mathbf{T}$ is linear,

$$\tilde{\boldsymbol{\eta}} = \mathbf{T}\left[\tilde{\boldsymbol{\eta}}_{\mathrm{NL}}\,,\, 0\right] + \mathbf{T}\left[0\,,\, F\right] = \mathbf{T}_{\eta}\left[\tilde{\boldsymbol{\eta}}_{\mathrm{NL}}\right] + \tilde{\boldsymbol{\eta}}_{\mathrm{L}} \tag{5.49}$$

where

$$\tilde{\boldsymbol{\eta}}_{\mathrm{L}} = \mathbf{T}\left[0\,,\, F\right] \tag{5.50}$$

is the linear solution to the effective problem and

$$\mathbf{T}_{\eta}\left[\tilde{\boldsymbol{\eta}}_{\mathrm{NL}}\right] \equiv \mathbf{T}\left[\tilde{\boldsymbol{\eta}}_{\mathrm{NL}}\,,\, 0\right] \tag{5.51}$$

is a linear operator in $\tilde{\boldsymbol{\eta}}_{\mathrm{NL}}$. Hence, the operator $\mathbf{G}_{\eta}^{\mathrm{I}}$ which maps (initial) deformations $\tilde{\boldsymbol{\eta}}_{\mathrm{NL}}$ into the effective deformations is given by

$$\tilde{\boldsymbol{\eta}} = \mathbf{G}_{\eta}^{\mathrm{I}}\left[\tilde{\boldsymbol{\eta}}_{\mathrm{NL}}\right] \equiv \tilde{\boldsymbol{\eta}}_{\mathrm{L}} + \mathbf{T}_{\eta}\left[\tilde{\boldsymbol{\eta}}_{\mathrm{NL}}\right] \tag{5.52}$$

Since $\tilde{\boldsymbol{\eta}}_{\mathrm{NL}}$ is not known in advance, it must be approximated in terms of the (approximation of the) effective generalized strains. Thence, for a given cross section,

$$\chi_{\mathrm{NL}}^{(i)} = G_{\chi}^{\mathrm{II}}\left[\chi^{(i)}\,,\, \varepsilon^{(i)}\right] = \frac{M_{\mathrm{F}}\left[\chi^{(i)}\,,\, \varepsilon^{(i)}\right]}{EI_{\mathrm{A}}} = \chi^{(i)} - \frac{\hat{M}\left[\chi^{(i)}\,,\, \varepsilon^{(i)}\right]}{EI_{\mathrm{A}}} \tag{5.53}$$

$$\varepsilon_{\mathrm{NL}}^{(i)} = G_{\varepsilon}^{\mathrm{II}}\left[\chi^{(i)}\,,\, \varepsilon^{(i)}\right] = \frac{N_{\mathrm{F}}\left[\chi^{(i)}\,,\, \varepsilon^{(i)}\right]}{EA_{\mathrm{A}}} = \varepsilon^{(i)} - \frac{\hat{N}\left[\chi^{(i)}\,,\, \varepsilon^{(i)}\right]}{EA_{\mathrm{A}}} \tag{5.54}$$

and, thence

$$\boldsymbol{\eta}_{\mathrm{NL}}^{(i)} = \mathbf{G}_{\eta}^{\mathrm{II}}\left[\boldsymbol{\eta}^{(i)}\right] = \begin{bmatrix} \chi_{\mathrm{NL}}\left[\chi^{(i)}\,,\, \varepsilon^{(i)}\right] \\ \varepsilon_{\mathrm{NL}}\left[\chi^{(i)}\,,\, \varepsilon^{(i)}\right] \end{bmatrix} = \begin{bmatrix} \chi^{(i)} \\ \varepsilon^{(i)} \end{bmatrix} - \begin{bmatrix} EI_{\mathrm{A}}^{-1} & 0 \\ 0 & EA_{\mathrm{A}}^{-1} \end{bmatrix} \begin{bmatrix} \hat{M}\left[\chi^{(i)}\,,\, \varepsilon^{(i)}\right] \\ \hat{N}\left[\chi^{(i)}\,,\, \varepsilon^{(i)}\right] \end{bmatrix} \tag{5.55}$$

Substituting this expression into (5.52) gives the FFM(MN)$_{\mathrm{Def}}$ fixed point iteration formula

$$\tilde{\boldsymbol{\eta}}^{(i+1)} = \mathbf{G}_{\eta}^{\mathrm{I}}\left[\mathbf{G}_{\eta}^{\mathrm{II}}\left[\tilde{\boldsymbol{\eta}}^{(i)}\right]\right] = \mathbf{G}_{\eta}\left[\tilde{\boldsymbol{\eta}}^{(i)}\right] \tag{5.56}$$

with $\tilde{\boldsymbol{\eta}}^{(1)} = \tilde{\boldsymbol{\eta}}_{\mathrm{L}}$, because a null fictitious force system is used to compute the initial guess of the iterative procedures of FFM.

5.2.4. Convergence conditions of FFM(*MN*) *by deformations*

5.2.4.1. Jacobian matrix

According to the composition (5.56), FFM(MN)$_{\text{Def}}$ iteration formula converges if (i) both operators $\mathbf{G}_{\eta}^{\text{I}}$ and $\mathbf{G}_{\eta}^{\text{II}}$ are non-expansive and (ii) at least one of them is contractive. Similarly to what happens with G_{χ}^{I} and $G_{\varepsilon}^{\text{I}}$, see § 3.2.6 and § 4.1.5, $\mathbf{G}_{\eta}^{\text{I}}$ is a non-expansive operator. In these conditions, the operator $\mathbf{G}_{\eta}$ is contractive if $\mathbf{G}_{\eta}^{\text{II}}$ is also contractive. Furthermore, $\mathbf{G}_{\eta}^{\text{II}}$ will be contractive if the Jacobian matrix $\mathbf{J}_{\eta}^{\text{II}}$ of the transformation (5.55) has spectral radius less than one, *i.e.* $\rho\left[\mathbf{J}_{\eta}^{\text{II}}\right]<1$. Thence, this condition is a sufficient convergence condition of FFM(MN)$_{\text{Def}}$. For a given cross section, this Jacobian matrix is written

$$\mathbf{J}_{\eta}^{\text{II}}=\frac{\partial\mathbf{G}_{\eta}^{\text{II}}}{\partial\boldsymbol{\eta}}=\begin{bmatrix}\dfrac{\partial\chi_{\text{NL}}}{\partial\chi} & \dfrac{\partial\chi_{\text{NL}}}{\partial\varepsilon}\\ \dfrac{\partial\varepsilon_{\text{NL}}}{\partial\chi} & \dfrac{\partial\varepsilon_{\text{NL}}}{\partial\varepsilon}\end{bmatrix} \tag{5.57}$$

Recalling that $\partial\chi_{\text{NL}}/\partial\chi=\beta_{\chi}$, $\partial\varepsilon_{\text{NL}}/\partial\varepsilon=\beta_{\varepsilon}$, $\chi_{\text{NL}}=\chi-\chi_{\text{A}}$, $\varepsilon_{\text{NL}}=\varepsilon-\varepsilon_{\text{A}}$ and also (5.23) and (5.21), gives

$$\frac{\partial\chi_{\text{NL}}}{\partial\varepsilon}=-\frac{1}{EI_{\text{A}}}\frac{\partial\hat{M}}{\partial\varepsilon}=-\frac{ES}{EI_{\text{A}}}\equiv-\gamma_{\text{EI}} \tag{5.58}$$

$$\frac{\partial\varepsilon_{\text{NL}}}{\partial\chi}=-\frac{1}{EA_{\text{A}}}\frac{\partial\hat{N}}{\partial\chi}=-\frac{ES}{EA_{\text{A}}}\equiv-\gamma_{\text{EA}} \tag{5.59}$$

where γ_{EI} and γ_{EA} are different measures of the cross-sectional static moment. Thence, the above Jacobian matrix is non-symmetric,

$$\mathbf{J}_{\eta}^{\text{II}}=\begin{bmatrix}\beta_{\chi} & -\gamma_{\text{EI}}\\ -\gamma_{\text{EA}} & \beta_{\varepsilon}\end{bmatrix} \tag{5.60}$$

In order to derive the convergence condition, let us first establish a symmetric matrix $\mathbf{J}_{\eta,\text{P}}^{\text{II}}$ similar to $\mathbf{J}_{\eta}^{\text{II}}$, *i.e.* with the same eigenvalues, $\rho\left[\mathbf{J}_{\eta}^{\text{II}}\right]=\rho\left[\mathbf{J}_{\eta,\text{P}}^{\text{II}}\right]$. The advantage of the symmetry will be seen in § 5.2.4.2. Two square similar matrices are related by a generic transformation of the type

$$\mathbf{J}_{\eta,\text{P}}^{\text{II}}=\mathbf{P}\,\mathbf{J}_{\eta}^{\text{II}}\,\mathbf{P}^{-1} \tag{5.61}$$

where the square matrix $\mathbf{P}$ is non-singular. Choosing a real diagonal matrix with non-null entries P_{11} and P_{22}, the above expression gives

$$\mathbf{J}_{\eta,\mathrm{P}}^{\mathrm{II}} = \begin{bmatrix} \beta_{\chi} & -\dfrac{P_{11}}{P_{22}}\gamma_{\mathrm{EI}} \\ -\dfrac{P_{22}}{P_{11}}\gamma_{\mathrm{EA}} & \beta_{\varepsilon} \end{bmatrix} \tag{5.62}$$

Thence, the symmetry condition is

$$\frac{P_{11}}{P_{22}}\gamma_{\mathrm{EI}} = \frac{P_{22}}{P_{11}}\gamma_{\mathrm{EA}} \tag{5.63}$$

i.e., recalling the definitions (5.58) of γ_{EI} and (5.59) of γ_{EA},

$$\frac{P_{11}}{P_{22}} = \sqrt{\frac{\gamma_{\mathrm{EA}}}{\gamma_{\mathrm{EI}}}} = \sqrt{\frac{EI_{\mathrm{A}}}{EA_{\mathrm{A}}}} \equiv i_{\mathrm{A}} \tag{5.64}$$

Introducing the expressions (5.25) and (5.26) into the above definition gives

$$i_{\mathrm{A}} = \sqrt{\frac{I_y}{A}} \equiv i_y \tag{5.65}$$

where i_y is the usual cross-sectional radius of gyration with respect to the barycentric axis *y*. Finally, substituting (5.64) into expression (5.62), gives

$$\mathbf{J}_{\eta,\mathrm{P}}^{\mathrm{II}} = \begin{bmatrix} \beta_{\chi} & -\sqrt{\gamma_{\mathrm{EI}}\,\gamma_{\mathrm{EA}}} \\ -\sqrt{\gamma_{\mathrm{EI}}\,\gamma_{\mathrm{EA}}} & \beta_{\varepsilon} \end{bmatrix} = \begin{bmatrix} \beta_{\chi} & -\dfrac{ES}{\sqrt{EI_{\mathrm{A}}\,EA_{\mathrm{A}}}} \\ -\dfrac{ES}{\sqrt{EI_{\mathrm{A}}\,EA_{\mathrm{A}}}} & \beta_{\varepsilon} \end{bmatrix} \tag{5.66}$$

where all the entries are now dimensionless.

5.2.4.2. Minimum value of E_{A}

In this section sufficient convergence conditions for FFM(*MN*)$_{\mathrm{Def}}$ are derived by imposing that $\left|\rho\left[\mathbf{J}_{\eta,\mathrm{P}}^{\mathrm{II}}\right]\right| < 1$. These conditions will be established at the cross-sectional level. This means that a range of values of the auxiliary stiffness E_{A} should be determined at each section of the structure which guarantees the convergence of the iterative procedure.

Substituting the auxiliary cross-sectional stiffness (5.25) into (3.41), gives

$$\beta_{\chi} = \frac{EI_{\mathrm{A}} - EI}{EI_{\mathrm{A}}} = 1 - \frac{EI}{E_{\mathrm{A}}\, I_y} = 1 - \frac{E_{\mathrm{EI}}}{E_{\mathrm{A}}} \tag{5.67}$$

with the mean Young's modulus weighted by the cross-sectional second moment of area distribution

$$E_{\mathrm{EI}} \equiv \frac{EI}{I_y} \tag{5.68}$$

Similarly, substituting (5.26) into the axial stiffness relative difference β_{ε}, gives

$$\beta_{\varepsilon} = \frac{EA_{\mathrm{A}} - EA}{EA_{\mathrm{A}}} = 1 - \frac{EA}{E_{\mathrm{A}} A} = 1 - \frac{E_{\mathrm{EA}}}{E_{\mathrm{A}}} \tag{5.69}$$

with the mean Young's modulus weighted by cross-sectional area distribution

$$E_{\mathrm{EA}} \equiv \frac{EA}{A} \tag{5.70}$$

In the same way,

$$i_{\mathrm{A}}\, \gamma_{\mathrm{EI}} = \frac{ES}{\sqrt{EI_{\mathrm{A}}\, EA_{\mathrm{A}}}} = \frac{ES}{\sqrt{E_{\mathrm{A}} I_y\, E_{\mathrm{A}} A}} = \frac{E_{\mathrm{ES}}}{E_{\mathrm{A}}} \tag{5.71}$$

where

$$E_{\mathrm{ES}} \equiv \frac{ES}{\sqrt{I_y\, A}} \tag{5.72}$$

which, perhaps abusively, may be considered yet another weighted mean of the Young's modulus, that can be negative even if E is positive at every fibre. Substituting the above expressions into the Jacobian matrix $\mathbf{J}^{\mathrm{II}}_{\eta,\mathrm{P}}$ (5.66) gives

$$\mathbf{J}^{\mathrm{II}}_{\eta,\mathrm{P}} = \mathbf{I}_2 - \frac{1}{E_{\mathrm{A}}} \mathbf{E} \tag{5.73}$$

with

$$\mathbf{E} \equiv \begin{bmatrix} E_{\mathrm{EI}} & E_{\mathrm{ES}} \\ E_{\mathrm{ES}} & E_{\mathrm{EA}} \end{bmatrix} \tag{5.74}$$

The result (5.73) could only be obtained because the symmetric Jacobian $\mathbf{J}^{\mathrm{II}}_{\eta,\mathrm{P}}$ was used instead of $\mathbf{J}^{\mathrm{II}}_{\eta}$.

Let λ_{E} denote a generic eigenvalue of $\mathbf{E}$ and let λ_{J} denote the corresponding eigenvalue of $\mathbf{J}^{\mathrm{II}}_{\eta,\mathrm{P}}$. According to (5.73), these two eigenvalues are related by

$$\lambda_{\mathrm{J}} = 1 - \frac{\lambda_{\mathrm{E}}}{E_{\mathrm{A}}} \tag{5.75}$$

The condition $\left|\rho\left[\mathbf{J}^{\mathrm{II}}_{\eta,\mathrm{P}}\right]\right| < 1$ is satisfied if $\left|\lambda_{\mathrm{J}}\right| < 1$, *i.e.*

$$\left|1 - \frac{\lambda_{\mathrm{E}}}{E_{\mathrm{A}}}\right| < 1 \tag{5.76}$$

The simplifying hypothesis $E > 0$ introduced in § 5.1 determines that $\lambda_{\mathrm{E}} > 0$, as it will be proven in § 5.2.4.4. This result and (5.76) determine the sufficient convergence condition

$$E_{\mathrm{A}} > \frac{\lambda_{\mathrm{E}}}{2} > 0 \tag{5.77}$$

According to Gershgorin's circle theorem (Jennings and McKeown, 1992), the absolute value of the eigenvalues λ_{E} is bounded by

$$\left|\lambda_{\mathrm{E}}\right| < \max\left\{E_{\mathrm{EI}}, E_{\mathrm{EA}}\right\} + \left|E_{\mathrm{ES}}\right| \tag{5.78}$$

Note that E_{EI} and E_{EA} are positive. Let $E_{\max}$ be the maximum value of the cross-sectional effective tangent Young moduli of the nonlinear constitutive relations

$$E_{\max} = \max E \tag{5.79}$$

Since E_{EI}, E_{EA} and $\left|E_{\mathrm{ES}}\right|$ are weighed by means of E, it is fairly evident that

$$\left\{E_{\mathrm{EI}}, E_{\mathrm{EA}}, \left|E_{\mathrm{ES}}\right|\right\} < E_{\max} \tag{5.80}$$

Nevertheless these bounding relations are formally proven in the next section. Thence, according to (5.78) a new bound for $\left|\lambda_{\mathrm{E}}\right|$ can be established

$$\left|\lambda_{\mathrm{E}}\right| < \underbrace{\max\left\{E_{\mathrm{EI}}, E_{\mathrm{EA}}\right\}}_{\leq E_{\max}} + \underbrace{\left|E_{\mathrm{ES}}\right|}_{< E_{\max}} < 2E_{\max} \tag{5.81}$$

This means that if E_{A} is chosen so that

$$E_{\mathrm{A}} > E_{\max} \tag{5.82}$$

then, according to (5.81),

$$E_{\mathrm{A}} > E_{\max} > \frac{\left|\lambda_{\mathrm{E}}\right|}{2} \tag{5.83}$$

and the sufficient convergence condition (5.77) is also satisfied. Hence, (5.83) is a sufficient convergence condition of FFM(MN)$_{\text{Def}}$.

5.2.4.3. Bounds of the average stiffness coefficients

In this section, the upper bounding inequalities (5.80) are proven. Recall that if f and g are integrable functions in a domain $\Omega \subset \mathbb{R}^2$, and if $f \le g$ at every point of Ω, *i.e.* if g is a majorant of f, then $\int_\Omega f\, d\Omega \le \int_\Omega g\, d\Omega$ (Lang, 2010). Hence, recalling definitions (5.17) and (5.18), the following upper bounds of EI and EA can be established

$$EA = \int_D E\, dD \le \int_D E_{\max}\, dD = E_{\max} A \tag{5.84}$$

$$EI = \int_D E\, z^2\, dD \le \int_D E_{\max}\, z^2\, dD = E_{\max} I_y \tag{5.85}$$

Introducing these expressions into the definitions of E_{EI} (5.68) and E_{EA} (5.70), gives

$$\left\{E_{\text{EI}}, E_{\text{EA}}\right\} \le E_{\max} \tag{5.86}$$

Next, it is proved that $\left|E_{\text{ES}}\right| < E_{\max}$. Consider the subdivision of the cross section D into the regions D^+ and D^-, according to the sign of the z-coordinate of their points, Figure 5.3. To these regions correspond the areas

$$A^+ = \int_{D^+} dD > 0 \tag{5.87}$$

$$A^- = \int_{D^-} dD > 0 \tag{5.88}$$

Thence, ES (5.21) can be expressed as

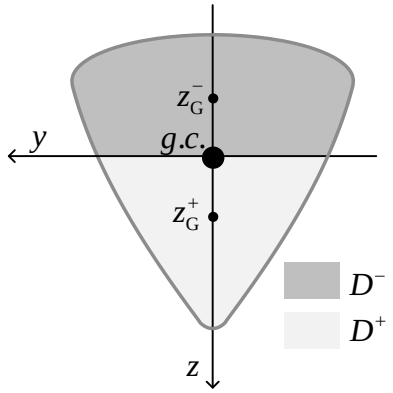

Figure 5.3. Cross section subdivision into the regions D^+ and D^-.

$$ES = \int_{D^-} E\,z\,dD + \int_{D^+} E\,z\,dD \tag{5.89}$$

Since E is always positive, the first (resp. second) term on the right-hand side of this expression is negative (resp. positive), and therefore

$$\int_{D^-} E\,z\,dD < ES < \int_{D^+} E\,z\,dD \tag{5.90}$$

According to (5.79), $E_{\max}$ is a majorant of E and, therefore, since $E\,z \le E_{\max}\,z$ for every point in D^+,

$$\int_{D^+} E\,z\,dD \le \int_{D^+} E_{\max}\,z\,dD = E_{\max} \int_{D^+} z\,dD = E_{\max}\,S^+ \tag{5.91}$$

where

$$S^+ \equiv \int_{D^+} z\,dD \tag{5.92}$$

Note that, since the system of coordinates is barycentric,

$$S = \int_{D} z\,dD = 0 \quad \Leftrightarrow \quad \int_{D^-} z\,dD = -\int_{D^+} z\,dD = -S^+ \tag{5.93}$$

Hence, since $E\,z \ge E_{\max}\,z$ for every point in D^-,

$$\int_{D^-} E\,z\,dD \ge \int_{D^-} E_{\max}\,z\,dD = E_{\max} \int_{D^-} z\,dD = -E_{\max}\,S^+ \tag{5.94}$$

Substituting this expression and (5.91) into (5.90) gives

$$-E_{\max}\,S^+ < ES < E_{\max}\,S^+ \tag{5.95}$$

or

$$-E_{\max} < E_{\mathrm{ES}}^+ < E_{\max} \tag{5.96}$$

with

$$E_{\mathrm{ES}}^+ \equiv \frac{ES}{S^+} \tag{5.97}$$

Recalling the definition of E_{ES} (5.72),

$$E_{\mathrm{ES}} = \frac{ES}{\sqrt{I_y A}} = \frac{ES}{S^+}\frac{S^+}{\sqrt{I_y A}} = E_{\mathrm{ES}}^+\,f_{\mathrm{ES}} \tag{5.98}$$

with

$$f_{\mathrm{ES}} \equiv \frac{S^+}{\sqrt{I_y\, A}} = \frac{S^+}{i_y\, A} > 0 \tag{5.99}$$

and thence, substituting (5.98) into (5.96),

$$-f_{\mathrm{ES}} < \frac{E_{\mathrm{ES}}}{E_{\max}} < f_{\mathrm{ES}} \tag{5.100}$$

Let z_{G}^+ and z_{G}^- denote the *z*-coordinate of the barycentre of D^+ and D^-, respectively (Figure 5.3), *i.e.*

$$S^+ = \int_{D^+} z\, dD = z_{\mathrm{G}}^+\, A^+ = -z_{\mathrm{G}}^-\, A^- \tag{5.101}$$

Introducing this relation in the above definition of f_{ES} gives

$$f_{\mathrm{ES}} = \frac{z_{\mathrm{G}}^+}{i_y}\frac{A^+}{A} \tag{5.102}$$

Consider now the z_{G}^+/i_y factor in this expression. If I_y^+ and I_y^- are the second moment of area of D^+ and D^- with respect to the *y*-axis, then

$$\frac{1}{i_y^2} = \frac{A}{I_y} = \frac{A^+}{I_y^+ + I_y^-} + \frac{A^-}{I_y^+ + I_y^-} \tag{5.103}$$

and, according to the triangular inequality, easily proved if Pythagoras theorem (Lang, 2010) is considered,

$$\frac{1}{i_y} < \sqrt{\frac{A^+}{I_y^+ + I_y^-}} + \sqrt{\frac{A^-}{I_y^+ + I_y^-}} < \sqrt{\frac{A^+}{I_y^+}} + \sqrt{\frac{A^-}{I_y^-}} = \frac{1}{i_y^+} + \frac{1}{i_y^-} \tag{5.104}$$

where

$$i_y^+ \equiv \sqrt{\frac{I_y^+}{A^+}} \quad ; \quad i_y^- \equiv \sqrt{\frac{I_y^-}{A^-}} \tag{5.105}$$

Let y_1 be the axis parallel to *y* passing through the barycentre of D^+ and let I_{y1}^+ denote the second moment of area of the sub-region D^+ relatively to y_1. Let us also introduce

$$i_{y1}^{+2} \equiv \frac{I_{y1}^+}{A^+} \tag{5.106}$$

According to Steiner's theorem (Beer *et al.*, 2005),

$$I_y^+ = I_{y1}^+ + A^+ z_G^{+2} \tag{5.107}$$

Dividing both members of this expression by A^+ and introducing the first expression (5.105) and (5.106), gives

$$i_y^{+2} = i_{y1}^{+2} + z_G^{+2} \tag{5.108}$$

and thence

$$i_y^+ > z_G^+ \tag{5.109}$$

The demonstration that

$$i_y^- > -z_G^- \tag{5.110}$$

is similar. Multiplying both members of (5.104) by z_G^+ gives

$$\frac{z_G^+}{i_y} < \frac{z_G^+}{i_y^+} + \frac{z_G^+}{i_y^-} \tag{5.111}$$

According to (5.101)

$$z_G^+ = -z_G^- \frac{A^-}{A^+} \tag{5.112}$$

Substituting this into the second term of the right-hand side of the previous expression and recalling (5.109) and (5.110) gives

$$\frac{z_G^+}{i_y} < \frac{z_G^+}{i_y^+} + \frac{z_G^+}{i_y^-} = \frac{z_G^+}{i_y^+} - \frac{z_G^-}{i_y^-}\frac{A^-}{A^+} < 1 + \frac{A^-}{A^+} = \frac{A}{A^+} \tag{5.113}$$

Finally, replacing this inequality into (5.102) gives

$$f_{ES} = \frac{z_G^+}{i_y}\frac{A^+}{A} < \frac{A}{A^+}\frac{A^+}{A} = 1 \tag{5.114}$$

and then, inserting this bounding inequality into (5.100), gives

$$-1 < \frac{E_{ES}}{E_{max}} < 1 \quad \Leftrightarrow \quad \left|E_{ES}\right| < E_{max} \tag{5.115}$$

which concludes this rather long proof.

5.2.4.4. Spectral analysis of the cross-sectional stiffness matrix

In this section, it is proved that the simplifying hypothesis $E > 0$ stated in § 5.1, is a sufficient condition for the positivity of the eigenvalues λ_{E} of $\mathbf{E}$ (5.74), *i.e.* if $E > 0$ then

$$\lambda_{\mathrm{E}} > 0 \tag{5.116}$$

Let us start by noting that the minimum eigenvalue of $\mathbf{E}$ is given by

$$\lambda_{\mathrm{E,min}} = \frac{E_{\mathrm{EI}} + E_{\mathrm{EA}}}{2} - \sqrt{\left(\frac{E_{\mathrm{EI}} - E_{\mathrm{EA}}}{2}\right)^2 + E_{\mathrm{ES}}^2} \tag{5.117}$$

Thence, the two eigenvalues λ_{E} are positive if,

$$\left(\frac{E_{\mathrm{EI}} + E_{\mathrm{EA}}}{2}\right)^2 > \left(\frac{E_{\mathrm{EI}} - E_{\mathrm{EA}}}{2}\right)^2 + E_{\mathrm{ES}}^2 \tag{5.118}$$

which is equivalent to

$$E_{\mathrm{EI}}\, E_{\mathrm{EA}} > E_{\mathrm{ES}}^2 \tag{5.119}$$

or, according to the definitions (5.68), (5.70) and (5.72) of these parameters,

$$EI\ EA > ES^2 \tag{5.120}$$

It is next proven that this condition is true if $E > 0$. Consider the scalar field representing the value of E at any point f_* in the cross section. According to the definition (5.18) of EA, the elemental axial stiffness is given by

$$dEA \equiv E\, dD \tag{5.121}$$

where dD is a cross-sectional element in the neighbourhood of f_*. Introducing this expression in the cross-sectional stiffnesses (5.17), (5.21) to (5.18) gives

$$EI = \int_D z^2\, dEA \tag{5.122}$$

$$ES = \int_D z\, dEA \tag{5.123}$$

$$EA = \int_D dEA \tag{5.124}$$

According to these expressions the cross-sectional stiffnesses EI, ES and EA can be seen as the second moment of area, the static moment and the total area of a cross-sectional geometry

"deformed" by the distribution of E. Note, however, that this distribution is a function of the internal forces at the section. Let us introduce a new cross-sectional Cartesian system of coordinates *o'y'z'*, resulting from the affine transformation of *oyz*, whose *z'*-axis is parallel to the *z*-axis and is contained in the plane *oxz* and whose *y'*-axis is parallel to the *y*-axis and its location, defined by the *z*-coordinate $z_{y'}$, is such that the static moment with respect to it[12] is null, *i.e.*

$$ES_{y'} = \int_D z'\, dEA = 0 \tag{5.125}$$

In consequence, the new system of coordinates is said to be E-centric. The moment of inertia of the deformed geometry with respect to the *y'* axis is

$$EI_{y'} = \int_D y'^2\, dEA \tag{5.126}$$

Then, see Figure 5.4

$$ES = z_{y'}\, EA \tag{5.127}$$

The "radius of gyration" of the E-deformed cross-sectional geometry w.r.t the *y*-axis is given by

$$i_{y,\mathrm{E}} = \sqrt{\frac{EI}{EA}} \tag{5.128}$$

In other words, $i_{y,\mathrm{E}}$ is the distance along *z* from the geometric centre *o* to a point where EA, *i.e.* the area of the E-deformed geometry, is concentrated in such way that the corresponding

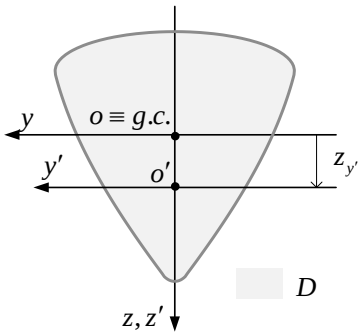

Figure 5.4. Systems of coordinates *oyz* (barycentric) and *o'y'z'* (E-centric).

[12] Since the origin *o* of *oxyz* is located at the left end section of the element, *o'y'z'* refers to that cross section. For simplicity, however, this reference system is admitted valid for all cross sections.

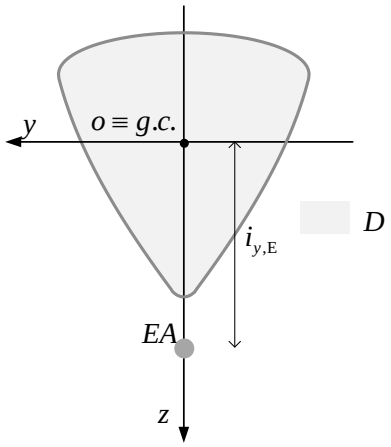

Figure 5.5. Radius of gyration $i_{y,\mathrm{E}}$.

moment of inertia is equal to the moment of inertia EI, see Figure 5.5. Similarly, the radius of gyration of the E-deformed cross-sectional geometry, *i.e.* w.r.t. the y'-axis is given by

$$i_{y',\mathrm{E}} = \sqrt{\frac{EI_{y'}}{EA}} \tag{5.129}$$

Recalling again Steiner's theorem,

$$EI = EI_{y'} + EA\, z_{y'}^2 \tag{5.130}$$

Dividing both members of this equation by EA and substituting (5.128) and (5.129) gives

$$i_{y,\mathrm{E}}^2 = i_{y',\mathrm{E}}^2 + z_{y'}^2 > z_{y'}^2 \tag{5.131}$$

Multiplying both members by EA^2 and substituting (5.127) and (5.128) gives (5.120). This concludes the proof of (5.116).

5.3. Elemental fictitious force system for beam *model MN*

5.3.1. Discrete description of the elemental fictitious force system

Adding together the terms of FFM(*M*) and FFM(*N*) force systems presented in the last two chapters gives the fictitious force system of FFM(*MN*). The discrete description of this system is now established for a generic beam element.

5.3.1.1. General considerations

As mentioned in § 4.2.4, two discrete descriptions of FFM(*M*) and FFM(*N*) can be combined to form a discrete description of FFM(*MN*) if they share the same interpolation sections. This requirement will now be justified.

Let us start by noting that the fictitious force system simulates the coupled effective nonlinear stiffness in the uncoupled auxiliary problem. In other words, if $\tilde{\chi}_{\mathrm{NL}}$ (resp. $\tilde{M}_{\mathrm{F}}$) and $\tilde{\varepsilon}_{\mathrm{NL}}$ (resp. $\tilde{N}_{\mathrm{F}}$) are taken as arbitrary initial deformations (resp. initial forces), the FFM auxiliary problem appears to be uncoupled. However, these initial deformations (resp. fictitious internal forces) are coupled since, in the case of $\mathrm{FFM}_{\mathrm{Def}}$, they are function of the effective generalized strains (resp. effective generalized stresses, in the case of $\mathrm{FFM}_{\mathrm{S}}$) which are coupled as seen in § 5.1. In order to evaluate this coupling accurately the same interpolation sections are required in FFM(*M*) and FFM(*N*) discrete descriptions. This is next explained.

Consider the linear element represented in Figure 5.6, having a nonlinear constitutive law of the type described in § 5.1 and subjected to the state of stress characterized by the depicted internal forces, with $\tilde{N}[0]=\tilde{N}[L]$ and $\tilde{V}[0]=\tilde{V}[L]$, *i.e.* there are no loads applied between nodes.

Suppose that this element is part of a structure that is to be analysed with a discrete description of FFM(*MN*) resulting from the combination of $\mathrm{FFM}(M)_2$ (*i.e.* 2 interpolation points) with $\mathrm{FFM}(N)_1$ (*i.e.* 1 interpolation point – basic discrete description), *i.e.* considering $\tilde{\varepsilon}_{\mathrm{NL},\delta}=0$. Since there are no loads applied between nodes, $\tilde{\varepsilon}_{\mathrm{L},\delta}=\tilde{\varepsilon}_{\mathrm{A},\delta}=0$, and therefore $\tilde{\varepsilon}_{\delta}=0$ or

$$\tilde{\varepsilon}[0]=\tilde{\varepsilon}[L] \tag{5.132}$$

On the other hand, since the effective constitutive law $\hat{\varepsilon}[M,N]$ is coupled

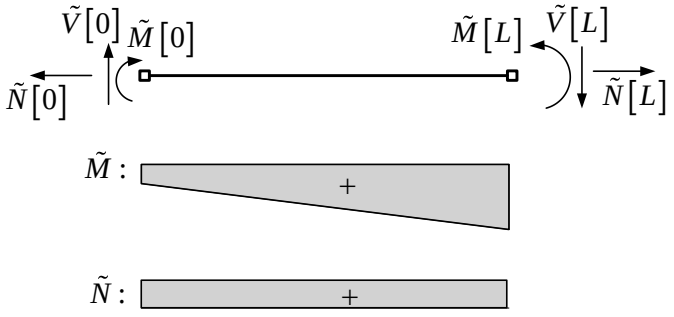

Figure 5.6. Linear element with constant axial force field.

$$\tilde{\varepsilon}[0]=\hat{\varepsilon}\left[\tilde{M}[0],\tilde{N}[0]\right] \tag{5.133}$$

$$\tilde{\varepsilon}[L]=\hat{\varepsilon}\left[\tilde{M}[L],\tilde{N}[L]\right] \tag{5.134}$$

Thus, since, see Figure 5.6,

$$\tilde{N}[0]=\tilde{N}[L] \tag{5.135}$$

$$\tilde{M}[0]\neq\tilde{M}[L] \tag{5.136}$$

then, in general,

$$\tilde{\varepsilon}[0]\neq\tilde{\varepsilon}[L] \tag{5.137}$$

which contradicts (5.132). This paradox vanishes if a second interpolation point for FFM(*N*) is adopted.

In what follows, the fictitious force systems of FFM(M)$_2$ and FFM(N)$_2$ are combined to form the discrete description of the fictitious force system for the *Model MN*.

5.3.1.2. Discrete description of the fictitious force system for *model MN*

The discrete description of the elemental fictitious force system of FFM(*MN*) is formed by the following terms, see Figure 5.7:

(i) a moment and an axial point force at each end section of the elements, corresponding to the fictitious internal forces,

$$\begin{cases}\mathcal{M}_{\mathrm{F2,1}}=-\tilde{M}_{\mathrm{F}}[0]\\ P_{\mathrm{F2,1}}=-\tilde{N}_{\mathrm{F}}[0]\end{cases}\quad\text{and}\quad\begin{cases}\mathcal{M}_{\mathrm{F2,2}}=\tilde{M}_{\mathrm{F}}[L]\\ P_{\mathrm{F2,2}}=\tilde{N}_{\mathrm{F}}[L]\end{cases} \tag{5.138}$$

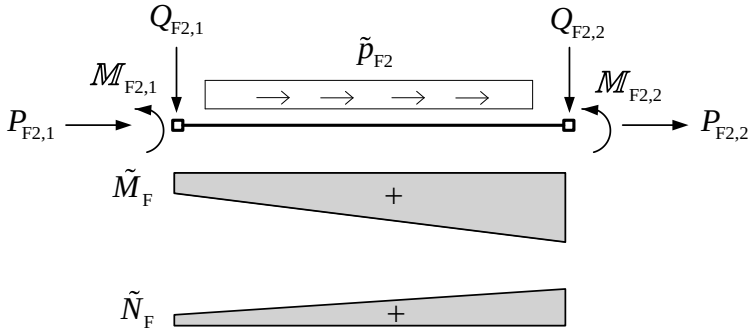

Figure 5.7. Fictitious force system of FFM(MN)$_2$.

(ii) a couple of transverse point forces at the end sections of the elements

$$Q_{\mathrm{F2},2} = -Q_{\mathrm{F2},1} = \frac{\mathscr{M}_{\mathrm{F2},1} + \mathscr{M}_{\mathrm{F2},2}}{L} \tag{5.139}$$

(iii) a uniformly distributed axial force

$$\tilde{p}_{\mathrm{F2}} = -\frac{P_{\mathrm{F2},1} + P_{\mathrm{F2},2}}{L} \tag{5.140}$$

This is a self-equilibrated system of forces which, as mentioned before, combines the systems of fictitious forces of FFM(M)$_2$ and FFM(N)$_2$ developed in chapters 3 and 4. Note that the auxiliary fields $\widetilde{EI}_{\mathrm{A}}$ and $\widetilde{EA}_{\mathrm{A}}$ are constant in each element, similarly to what happens with the discrete descriptions of FFM(M) and FFM(N).

5.4. FFM(*MN*) discrete description: matrix methods of structural analysis

This section presents the application of FFM(MN) discrete description, denoted FFM(MN)$_2$, in the context of matrix methods of structural analysis. Such presentation is general and therefore applicable to a generic skeletal structure.

Note that FFM(MN)$_2$ fulfils, in the framework of a linear analysis, the requirement identified by Blaauwendraad (1972) of simulating a quadratic axial displacement field, *i.e.* the component related to $\varepsilon_{\mathrm{NL}}$.

This exposition follows as close as possible the implementation of FFM(M)$_2$ and FFM(N)$_2$ presented in the last two chapters. This explains some repetitions and the omissions.

5.4.1. Elemental kinematics

Let $\overline{\boldsymbol{\eta}}_{\Delta}$ be the generic vector containing the independent generalized strains of an element

$$\overline{\boldsymbol{\eta}}_{\Delta} \equiv \begin{bmatrix} \overline{\boldsymbol{\chi}} \\ \tilde{\varepsilon}_{\Delta} \end{bmatrix} = \begin{bmatrix} \tilde{\chi}[0] \\ \tilde{\chi}[L] \\ \tilde{\varepsilon}[L] \end{bmatrix} \tag{5.141}$$

and let $\boldsymbol{\Phi}$ be the elemental vector collecting the strain resultants,

$$\bar{\mathbf{\Phi}} \equiv \begin{bmatrix} \bar{\boldsymbol{\phi}} \\ \varphi \end{bmatrix} = \begin{bmatrix} \phi_1 \\ \phi_2 \\ \varphi \end{bmatrix} \tag{5.142}$$

Gathering the kinematic relation $\bar{\boldsymbol{\chi}}_{\Delta} + \bar{\boldsymbol{\chi}}_{\delta,\mathrm{eq}} = \bar{\mathbf{K}}_0 \bar{\boldsymbol{\phi}}$ of *model M* and $\tilde{\varepsilon}_{\Delta} + \tilde{\varepsilon}_{\delta,\mathrm{eq}} = K_0^{\mathrm{N}} \varphi$ of *model N* gives, for *model MN*

$$\bar{\boldsymbol{\eta}}_{\Delta} + \bar{\boldsymbol{\eta}}_{\delta,\mathrm{eq}} = \bar{\mathbf{K}}_0^{\mathrm{MN}} \bar{\mathbf{\Phi}} \tag{5.143}$$

where

$$\bar{\mathbf{K}}_0^{\mathrm{MN}} = \begin{bmatrix} \bar{\mathbf{K}}_0 & \mathbf{0}_{2\times 1} \\ \mathbf{0}_{1\times 2} & K_0^{\mathrm{N}} \end{bmatrix} = \frac{1}{L} \begin{bmatrix} 4 & -2 & 0 \\ -2 & 4 & 0 \\ 0 & 0 & 1 \end{bmatrix} \tag{5.144}$$

and

$$\bar{\boldsymbol{\eta}}_{\delta,\mathrm{eq}} \equiv \begin{bmatrix} \bar{\boldsymbol{\chi}}_{\delta,\mathrm{eq}} \\ \tilde{\varepsilon}_{\delta,\mathrm{eq}} \end{bmatrix} \tag{5.145}$$

5.4.2. Auxiliary elemental constitutive relations

The vector, dual of $\bar{\boldsymbol{\eta}}_{\Delta}$, containing the generic independent generalized stresses, is given by

$$\bar{\mathbf{R}}_{\Delta} \equiv \begin{bmatrix} \bar{\mathbf{M}} \\ \tilde{N}_{\Delta} \end{bmatrix} = \begin{bmatrix} \tilde{M}[0] \\ \tilde{M}[L] \\ \tilde{N}[L] \end{bmatrix} \tag{5.146}$$

The elemental auxiliary constitutive relations for this *model MN* results from collecting $\bar{\mathbf{M}}_{\mathrm{A},\Delta} = \overline{\mathbf{EI}}_{\mathrm{A}} \bar{\boldsymbol{\chi}}$ (3.167), with $\tilde{N}_{\mathrm{A},\Delta} = EA_{\mathrm{A}} \tilde{\varepsilon}_{\Delta}$ (4.52), giving

$$\bar{\mathbf{R}}_{\mathrm{A},\Delta} = \bar{\mathbf{s}}_{\mathrm{A}} \bar{\boldsymbol{\eta}}_{\Delta} \tag{5.147}$$

where

$$\bar{\mathbf{s}}_{\mathrm{A}} = \begin{bmatrix} EI_{\mathrm{A}} & & \\ & EI_{\mathrm{A}} & \\ & & EA_{\mathrm{A}} \end{bmatrix} \tag{5.148}$$

is the elemental auxiliary matrix of cross-sectional stiffnesses.

Substituting (5.143) into (5.147) gives

$$\bar{\mathbf{R}}_{\mathrm{A},\Delta} + \bar{\mathbf{R}}_{\mathrm{A},\delta,\mathrm{eq}} = \bar{\mathbf{K}}_{\mathrm{A}}^{\mathrm{MN}}\,\bar{\mathbf{\Phi}} \tag{5.149}$$

where the non-singular elemental auxiliary stiffness matrix for the independent variables is

$$\bar{\mathbf{K}}_{\mathrm{A}}^{\mathrm{MN}} = \bar{\mathbf{s}}_{\mathrm{A}}\,\bar{\mathbf{K}}_{0}^{\mathrm{MN}} = \begin{bmatrix} \dfrac{4EI_{\mathrm{A}}}{L} & -\dfrac{2EI_{\mathrm{A}}}{L} & 0 \\ -\dfrac{2EI_{\mathrm{A}}}{L} & \dfrac{4EI_{\mathrm{A}}}{L} & 0 \\ 0 & 0 & \dfrac{EA_{\mathrm{A}}}{L} \end{bmatrix} \tag{5.150}$$

and

$$\bar{\mathbf{R}}_{\mathrm{A},\delta,\mathrm{eq}} = \bar{\mathbf{s}}_{\mathrm{A}}\,\bar{\boldsymbol{\eta}}_{\delta,\mathrm{eq}} = \bar{\mathbf{K}}_{\mathrm{A}}^{\mathrm{MN}}\,\bar{\mathbf{\Phi}}_{\delta} \tag{5.151}$$

with

$$\bar{\boldsymbol{\eta}}_{\delta,\mathrm{eq}} = \bar{\mathbf{K}}_{0}^{\mathrm{MN}}\,\bar{\mathbf{\Phi}}_{\delta} \tag{5.152}$$

Note that (5.151) aggregates $\bar{\mathbf{M}}_{\mathrm{A},\delta,\mathrm{eq}} = \overline{\mathbf{EI}}_{\mathrm{A}}\,\bar{\boldsymbol{\chi}}_{\delta,\mathrm{eq}}$ (3.173) and $\tilde{N}_{\mathrm{A},\delta,\mathrm{eq}} = EA_{\mathrm{A}}\,\varepsilon_{\delta,\mathrm{eq}}$ (4.90).

5.4.3. Elemental structural relations

Consider the local system of nodal coordinates represented in Figure 5.8. According to Euler-Bernoulli hypothesis, the corresponding nodal displacements are

$$\begin{aligned} \bar{\mathbf{d}}^{\mathrm{el}} &= \begin{bmatrix} d_1^{\mathrm{el}} & d_2^{\mathrm{el}} & d_3^{\mathrm{el}} & d_4^{\mathrm{el}} & d_5^{\mathrm{el}} & d_6^{\mathrm{el}} \end{bmatrix}^{\mathrm{T}} \\ &= \begin{bmatrix} -\tilde{w}'[0] & \tilde{w}[0] & \tilde{u}[0] & -\tilde{w}'[L] & \tilde{w}[L] & \tilde{u}[L] \end{bmatrix}^{\mathrm{T}} \end{aligned} \tag{5.153}$$

This vector and the vector of strain resultants $\bar{\mathbf{\Phi}}$ verify the compatibility relation

$$\bar{\mathbf{\Phi}} = \bar{\mathbf{C}}^{\mathrm{el}}\,\bar{\mathbf{d}}^{\mathrm{el}} \tag{5.154}$$

where $\bar{\mathbf{C}}^{\mathrm{el}}$ is the elemental compatibility matrix associated to these local directions

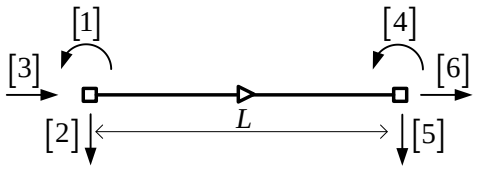

Figure 5.8. Elemental system of local nodal coordinates.

$$\bar{\mathbf{C}}^{\mathrm{el}} = \begin{bmatrix} -1 & \dfrac{1}{L} & 0 & 0 & -\dfrac{1}{L} & 0 \\ 0 & -\dfrac{1}{L} & 0 & 1 & \dfrac{1}{L} & 0 \\ 0 & 0 & -1 & 0 & 0 & 1 \end{bmatrix} \tag{5.155}$$

This compatibility matrix gathers the entries of the compatibility matrices for *models M* and *N*.

The elemental vector of nodal forces along these local directions is

$$\bar{\mathbf{f}}^{\mathrm{el}} = \begin{bmatrix} f_1^{\mathrm{el}} & f_2^{\mathrm{el}} & f_3^{\mathrm{el}} & f_4^{\mathrm{el}} & f_5^{\mathrm{el}} & f_6^{\mathrm{el}} \end{bmatrix}^{\mathrm{T}} \tag{5.156}$$

The equilibrium relation, dual of (5.154), is given by

$$\bar{\mathbf{f}}^{\mathrm{el}} = \bar{\mathbf{C}}^{\mathrm{el,T}}\, \bar{\mathbf{R}}_{\Delta} \tag{5.157}$$

Left-multiplying both members of the constitutive relation (5.149) by $\bar{\mathbf{C}}^{\mathrm{elT}}$ and substituting (5.154) gives

$$\bar{\mathbf{f}}_{\mathrm{A}}^{\mathrm{el}} + \bar{\mathbf{f}}_{\mathrm{A},\delta}^{\mathrm{el}} = \bar{\mathbf{K}}_{\mathrm{A}}^{\mathrm{el}}\, \bar{\mathbf{d}}^{\mathrm{el}} \tag{5.158}$$

where $\bar{\mathbf{K}}_{\mathrm{A}}^{\mathrm{el}}$ is the elemental stiffness matrix in local directions,

$$\bar{\mathbf{K}}_{\mathrm{A}}^{\mathrm{el}} = \bar{\mathbf{C}}^{\mathrm{el,T}}\, \bar{\mathbf{K}}_{\mathrm{A}}^{\mathrm{MN}}\, \bar{\mathbf{C}}^{\mathrm{el}} = \begin{bmatrix} \dfrac{4EI_{\mathrm{A}}}{L} & -\dfrac{6EI_{\mathrm{A}}}{L^2} & 0 & \dfrac{2EI_{\mathrm{A}}}{L} & \dfrac{6EI_{\mathrm{A}}}{L^2} & 0 \\ -\dfrac{6EI_{\mathrm{A}}}{L^2} & \dfrac{12EI_{\mathrm{A}}}{L^3} & 0 & -\dfrac{6EI_{\mathrm{A}}}{L^2} & -\dfrac{12EI_{\mathrm{A}}}{L^3} & 0 \\ 0 & 0 & \dfrac{EA_{\mathrm{A}}}{L} & 0 & 0 & -\dfrac{EA_{\mathrm{A}}}{L} \\ \dfrac{2EI_{\mathrm{A}}}{L} & -\dfrac{6EI_{\mathrm{A}}}{L^2} & 0 & \dfrac{4EI_{\mathrm{A}}}{L} & \dfrac{6EI_{\mathrm{A}}}{L^2} & 0 \\ \dfrac{6EI_{\mathrm{A}}}{L^2} & -\dfrac{12EI_{\mathrm{A}}}{L^3} & 0 & \dfrac{6EI_{\mathrm{A}}}{L^2} & \dfrac{12EI_{\mathrm{A}}}{L^3} & 0 \\ 0 & 0 & -\dfrac{EA_{\mathrm{A}}}{L} & 0 & 0 & \dfrac{EA_{\mathrm{A}}}{L} \end{bmatrix} \tag{5.159}$$

This matrix gathers the entries of the corresponding stiffness matrices for *models M* and *N*.

5.4.4. Transformation to global directions

The elemental structural relations established for local directions, presented in the last section, are now converted to a system of coordinates along global directions, Figure 5.9a.

Let $\bar{\mathbf{d}}^{\mathrm{gl}}$ denote the vector of elemental nodal displacements along global directions.

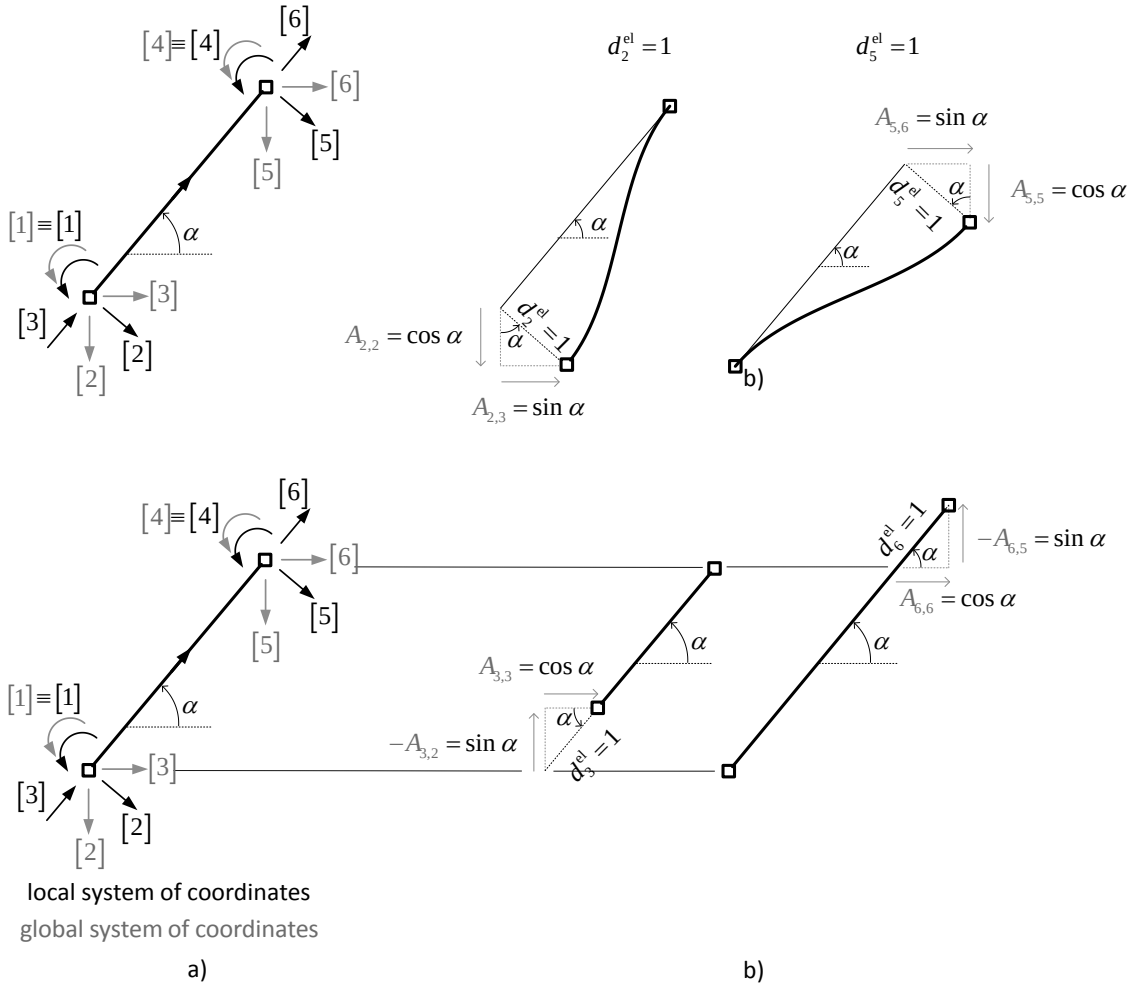

Figure 5.9. a) Elemental coordinate systems along global and local directions; b) elements of matrix $\bar{\mathbf{A}}$.

The relation between $\bar{\mathbf{d}}^{gl}$ and $\bar{\mathbf{d}}^{el}$ is given by, see Figure 5.9b,

$$\bar{\mathbf{d}}^{gl}=\bar{\mathbf{A}}^{T}\,\bar{\mathbf{d}}^{el} \quad \text{or} \quad \bar{\mathbf{d}}^{el}=\bar{\mathbf{A}}\,\bar{\mathbf{d}}^{gl} \tag{5.160}$$

where the block diagonal rotation matrix is,

$$\bar{\mathbf{A}}=\begin{bmatrix} 1 & 0 & 0 & 0 & 0 & 0 \\ 0 & \cos\alpha & \sin\alpha & 0 & 0 & 0 \\ 0 & -\sin\alpha & \cos\alpha & 0 & 0 & 0 \\ 0 & 0 & 0 & 1 & 0 & 0 \\ 0 & 0 & 0 & 0 & \cos\alpha & \sin\alpha \\ 0 & 0 & 0 & 0 & -\sin\alpha & \cos\alpha \end{bmatrix} \tag{5.161}$$

This rotation of coordinates is similarly applied to the nodal forces

$$\bar{\mathbf{f}}^{gl}=\bar{\mathbf{A}}^{T}\,\bar{\mathbf{f}}^{el} \quad \text{or} \quad \bar{\mathbf{f}}^{el}=\bar{\mathbf{A}}\,\bar{\mathbf{f}}^{gl} \tag{5.162}$$

Substitution of the second expression in (5.160) into (5.158), left-multiplication by $\bar{\mathbf{A}}^{\mathrm{T}}$ and, finally, substitution of the first expression in (5.162), gives

$$\bar{\mathbf{f}}_{\mathrm{A}}^{\mathrm{gl}} + \bar{\mathbf{f}}_{\mathrm{A},\delta}^{\mathrm{gl}} = \bar{\mathbf{K}}_{\mathrm{A}}^{\mathrm{gl}}\, \bar{\mathbf{d}}^{\mathrm{gl}} \tag{5.163}$$

where

$$\bar{\mathbf{K}}_{\mathrm{A}}^{\mathrm{gl}} = \bar{\mathbf{A}}^{\mathrm{T}}\, \bar{\mathbf{K}}_{\mathrm{A}}^{\mathrm{el}}\, \bar{\mathbf{A}} \tag{5.164}$$

is the elemental stiffness matrix relative to coordinates along global directions. Substituting (5.159) into (5.164), gives

$$\bar{\mathbf{K}}_{\mathrm{A}}^{\mathrm{gl}} = \bar{\mathbf{C}}^{\mathrm{gl,T}}\, \bar{\mathbf{K}}_{\mathrm{A}}^{\mathrm{MN}}\, \bar{\mathbf{C}}^{\mathrm{gl}} \tag{5.165}$$

where the elemental compatibility matrix associated to global directions is given by

$$\bar{\mathbf{C}}^{\mathrm{gl}} \equiv \bar{\mathbf{C}}^{\mathrm{el}}\, \bar{\mathbf{A}} \tag{5.166}$$

5.4.5. Governing system of equations

5.4.5.1. Kinematics

Let us consider a generic skeletal structure and a corresponding mesh of *m* linear elements linked together at their nodes. Some displacements of these nodes are restrained by the structure supports and the remaining *n* nodal displacements, or generalized displacements, define a global system of coordinates grouped in the global displacement vector $\mathbf{d}$.

The non-assembled global $6m$ vector $\mathbf{d}^{\mathrm{gl}}$ groups the *m* elemental vectors $\bar{\mathbf{d}}^{\mathrm{gl}}$,

$$\mathbf{d}^{\mathrm{gl}} = \left[\bar{\mathbf{d}}_1^{\mathrm{gl,T}} \quad \bar{\mathbf{d}}_2^{\mathrm{gl,T}} \quad \ldots \quad \bar{\mathbf{d}}_m^{\mathrm{gl,T}} \right]^{\mathrm{T}} \tag{5.167}$$

This vector is related to the vector of assembled displacements $\mathbf{d}$ by

$$\mathbf{d}^{\mathrm{gl}} = \mathbf{D}\, \mathbf{d} \tag{5.168}$$

where $\mathbf{D}$ is a Boolean matrix which reflects the connectivity of the beam elements and the supports kinematic constraints. This connectivity matrix $\mathbf{D}$ groups the $6 \times n$ elemental matrices $\bar{\mathbf{D}}_i$ which link the nodal displacements of element *i* to the *n* global displacements, $\bar{\mathbf{d}}_i^{\mathrm{gl}} = \bar{\mathbf{D}}_i\, \mathbf{d}$.

Substituting the second elemental relation (5.160) into the compatibility relation (5.154), and recalling (5.166) gives $\bar{\boldsymbol{\Phi}} = \bar{\mathbf{C}}^{\mathrm{gl}}\, \bar{\mathbf{d}}^{\mathrm{gl}}$. Grouping these elemental relations, gives

$$\boldsymbol{\Phi} = \mathbf{C}^{\mathrm{gl}}\, \mathbf{d}^{\mathrm{gl}} \tag{5.169}$$

where the $3m \times 6m$ block diagonal compatibility matrix $\mathbf{C}^{\mathrm{gl}}$ collects the elemental matrices $\bar{\mathbf{C}}^{\mathrm{gl}}$,

$$\mathbf{C}^{\mathrm{gl}} = \begin{bmatrix} \bar{\mathbf{C}}_1^{\mathrm{gl}} & & & \\ & \bar{\mathbf{C}}_2^{\mathrm{gl}} & & \\ & & \ddots & \\ & & & \bar{\mathbf{C}}_m^{\mathrm{gl}} \end{bmatrix} \tag{5.170}$$

and the global $3m$ vector of strain resultants $\boldsymbol{\Phi}$ is given by

$$\boldsymbol{\Phi} = \begin{bmatrix} \bar{\boldsymbol{\Phi}}_1^{\mathrm{T}} & \bar{\boldsymbol{\Phi}}_2^{\mathrm{T}} & \ldots & \bar{\boldsymbol{\Phi}}_m^{\mathrm{T}} \end{bmatrix}^{\mathrm{T}} \tag{5.171}$$

Finally, substitution of (5.168) into (5.169) gives the global compatibility relation

$$\boldsymbol{\Phi} = \mathbf{C}\mathbf{d} \tag{5.172}$$

where the $3m \times n$ global compatibility matrix $\mathbf{C}$ is given by

$$\mathbf{C} = \mathbf{C}^{\mathrm{gl}}\, \mathbf{D} \tag{5.173}$$

5.4.5.2. Statics

The static dual of (5.168) gives the assembled force vector $\mathbf{f}$

$$\mathbf{f} = \mathbf{D}^{\mathrm{T}}\, \mathbf{f}^{\mathrm{gl}} \tag{5.174}$$

where $\mathbf{f}^{\mathrm{gl}}$ is the non-assembled global force vector grouping the m elemental vectors $\bar{\mathbf{f}}^{\mathrm{gl}}$.

Left-multiplying (5.157) by $\bar{\mathbf{A}}^{\mathrm{T}}$ and recalling the first relation (5.162) and (5.166) gives $\bar{\mathbf{f}}^{\mathrm{gl}} = \bar{\mathbf{C}}^{\mathrm{gl,T}}\, \bar{\mathbf{R}}_{\Delta}$. Grouping these elemental relations, gives

$$\mathbf{f}^{\mathrm{gl}} = \mathbf{C}^{\mathrm{gl,T}}\, \mathbf{R}_{\Delta} \tag{5.175}$$

where the global $3m$ vector of independent generalized stresses $\mathbf{R}_{\Delta}$ is

$$\mathbf{R}_{\Delta} = \begin{bmatrix} \bar{\mathbf{R}}_{\Delta,1}^{\mathrm{T}} & \bar{\mathbf{R}}_{\Delta,2}^{\mathrm{T}} & \ldots & \bar{\mathbf{R}}_{\Delta,m}^{\mathrm{T}} \end{bmatrix}^{\mathrm{T}} \tag{5.176}$$

Substituting (5.175) into (5.174) and recalling (5.173) gives the global equilibrium relation

$$\mathbf{f} = \mathbf{C}^{\mathrm{T}}\,\mathbf{R}_{\Delta} \tag{5.177}$$

5.4.5.3. Auxiliary constitutive relationship

Grouping of the elemental constitutive equations (5.147) gives

$$\mathbf{R}_{\mathrm{A},\Delta} = \mathbf{s}_{\mathrm{A}}\,\boldsymbol{\eta}_{\Delta} \tag{5.178}$$

where the global $3m$ vector of generalized strains $\boldsymbol{\eta}_{\Delta}$ is given by

$$\boldsymbol{\eta}_{\Delta} = \left[\begin{array}{cccc} \bar{\boldsymbol{\eta}}_{\Delta,1}^{\mathrm{T}} & \bar{\boldsymbol{\eta}}_{\Delta,2}^{\mathrm{T}} & \cdots & \bar{\boldsymbol{\eta}}_{\Delta,m}^{\mathrm{T}} \end{array}\right]^{\mathrm{T}} \tag{5.179}$$

and the global $3m \times 3m$ elasticity matrix $\mathbf{s}_{\mathrm{A}}$ is given by

$$\mathbf{s}_{\mathrm{A}} = \left[\begin{array}{cccc} \bar{\mathbf{s}}_{\mathrm{A},1} & & & \\ & \bar{\mathbf{s}}_{\mathrm{A},2} & & \\ & & \ddots & \\ & & & \bar{\mathbf{s}}_{\mathrm{A},m} \end{array}\right] \tag{5.180}$$

Grouping of the elemental constitutive equations (5.149) gives

$$\mathbf{R}_{\mathrm{A},\Delta} + \mathbf{R}_{\mathrm{A},\delta,\mathrm{eq}} = \mathbf{K}_{\mathrm{A}}^{\mathrm{MN}}\,\boldsymbol{\Phi} \tag{5.181}$$

where the $3m \times 3m$ global stiffness matrix $\mathbf{K}_{\mathrm{A}}^{\mathrm{MN}}$ is

$$\mathbf{K}_{\mathrm{A}}^{\mathrm{MN}} = \mathbf{s}_{\mathrm{A}}\,\mathbf{K}_{0}^{\mathrm{MN}} = \left[\begin{array}{cccc} \bar{\mathbf{K}}_{\mathrm{A},1}^{\mathrm{MN}} & & & \\ & \bar{\mathbf{K}}_{\mathrm{A},2}^{\mathrm{MN}} & & \\ & & \ddots & \\ & & & \bar{\mathbf{K}}_{\mathrm{A},m}^{\mathrm{MN}} \end{array}\right] \tag{5.182}$$

where $\mathbf{K}_{0}^{\mathrm{MN}}$ is the block diagonal matrix grouping the elemental matrices $\bar{\mathbf{K}}_{0}^{\mathrm{MN}}$. The global vectors $\boldsymbol{\eta}_{\delta,\mathrm{eq}}$ and $\mathbf{R}_{\delta,\mathrm{eq}} = \mathbf{s}_{\mathrm{A}}\,\boldsymbol{\eta}_{\delta,\mathrm{eq}}$ collect the elemental vectors $\bar{\boldsymbol{\eta}}_{\delta,\mathrm{eq}}$ and $\bar{\mathbf{R}}_{\delta,\mathrm{eq},i}$ as usual.

5.4.5.4. Assemblage of equations

Collecting the m systems of equations (5.163), left-multiplying both members by $\mathbf{D}^{\mathrm{T}}$, substituting the connectivity relations (5.174) on the left-hand side and considering (5.168) on the right-hand side, gives the governing equation of FFM

$$\mathbf{f}_{\mathrm{A}} + \mathbf{f}_{\mathrm{A},\delta} = \mathbf{K}_{\mathrm{A}}\,\mathbf{d} \tag{5.183}$$

where the $n \times n$ assembled linear stiffness matrix is given by

$$\mathbf{K}_{\mathrm{A}} = \mathbf{D}^{\mathrm{T}} \mathbf{K}_{\mathrm{A}}^{\mathrm{gl}} \mathbf{D} \tag{5.184}$$

and $\mathbf{K}_{\mathrm{A}}^{\mathrm{gl}}$ is the block diagonal stiffness matrix which aggregates the elemental stiffness matrices in global directions (5.164) as usual. Introducing (5.165) and (5.173) into (5.184) gives

$$\mathbf{K}_{\mathrm{A}} = \mathbf{C}^{\mathrm{T}} \mathbf{K}_{\mathrm{A}}^{\mathrm{MN}} \mathbf{C} \tag{5.185}$$

Introducing the auxiliary force decompositions

$$\mathbf{f}_{\mathrm{A}} = \mathbf{f} + \mathbf{f}_{\mathrm{F}} \tag{5.186}$$

$$\mathbf{f}_{\mathrm{A},\delta} = \mathbf{f}_{\delta} + \mathbf{f}_{\mathrm{F},\delta} \tag{5.187}$$

into (5.183), gives the displacement increment due to the fictitious forces

$$\mathbf{d}_{\mathrm{incr}} \equiv \mathbf{d} - \mathbf{d}_{\mathrm{L}} = \mathbf{K}_{\mathrm{A}}^{-1} \left(\mathbf{f}_{\mathrm{F}} + \mathbf{f}_{\mathrm{F},\delta} \right) \tag{5.188}$$

Finally, since $\mathbf{d}^{(1)} \equiv \mathbf{d}_{\mathrm{L}}$, the iterative format of FFM is obtained,

$$\mathbf{d}^{(i+1)} = \mathbf{d}^{(1)} + \mathbf{K}_{\mathrm{A}}^{-1} \left(\mathbf{f}_{\mathrm{F}}^{(i)} + \mathbf{f}_{\mathrm{F},\delta}^{(i)} \right) \tag{5.189}$$

5.4.6. Implementation of FFM(*MN*) *by deformations* discrete description

5.4.6.1. General considerations

Similarly to what was seen in chapters 3 and 4, the implementation of FFM$(MN)_2$ *by deformations* consists in determining the fictitious force vectors $\mathbf{f}_{\mathrm{F}}^{(i)}$ and $\mathbf{f}_{\mathrm{F},\delta}^{(i)}$ which, according to (5.189), determine the displacement vector $\mathbf{d}^{(i+1)}$. According to the generic equilibrium relation (5.177), these fictitious force vectors are given by

$$\mathbf{f}_{\mathrm{F}}^{(i)} = \mathbf{C}^{\mathrm{T}} \mathbf{R}_{\mathrm{F},\Delta}^{(i)} \tag{5.190}$$

$$\mathbf{f}_{\mathrm{F},\delta}^{(i)} = \mathbf{C}^{\mathrm{T}} \mathbf{R}_{\mathrm{F},\delta,\mathrm{eq}}^{(i)} \tag{5.191}$$

where the global vector of fictitious internal forces $\mathbf{R}_{\mathrm{F},\Delta}^{(i)}$ collects m elemental vectors $\bar{\mathbf{R}}_{\mathrm{F},\Delta}^{(i)}$ with the structure of $\bar{\mathbf{R}}_{\Delta}$ (5.146) and similarly the global vector of fictitious internal forces $\mathbf{R}_{\mathrm{F},\delta,\mathrm{eq}}^{(i)}$ collects m elemental vectors

$$\bar{\mathbf{R}}^{(i)}_{\mathrm{F},\delta,\mathrm{eq}} = \begin{bmatrix} \tilde{M}^{(i)}_{\mathrm{F},\delta,\mathrm{eq}} \\ \tilde{M}^{(i)}_{\mathrm{F},\delta,\mathrm{eq}} \\ \tilde{N}^{(i)}_{\mathrm{F},\delta,\mathrm{eq}} \end{bmatrix} = \begin{bmatrix} 0 \\ 0 \\ \frac{1}{2}\left(\tilde{N}^{(i)}_{\mathrm{F}}[0] - \tilde{N}^{(i)}_{\mathrm{F}}[L] \right) \end{bmatrix} \tag{5.192}$$

where the terms on the right-hand side are the approximations of FFM(MN)$_2$, which are common to FFM(M)$_2$ and FFM(N)$_2$.

Note that the fictitious internal forces in $\bar{\mathbf{R}}^{(i)}_{\mathrm{F},\mathrm{A}}$ and $\bar{\mathbf{R}}^{(i)}_{\mathrm{F},\delta,\mathrm{eq}}$ depend on the four generalized strains at the element end sections and, according to FFM$_{\mathrm{Def}}$, they are computed by expressions (5.34) and (5.35) or (5.36) and (5.37). Recall that, as reflected in these expressions, the fictitious internal force $\tilde{M}^{(i)}_{\mathrm{F}}$ (resp. $\tilde{N}^{(i)}_{\mathrm{F}}$) depends on both fields of generalized strains $\tilde{\chi}^{(i)}$ and $\tilde{\varepsilon}^{(i)}$ because the effective nonlinear constitutive law is coupled.

As mentioned in § 3.1, it is possible to use *model M* for the analysis of plane skeletal structures if some simplifying assumptions are considered which uncouple the nonlinear constitutive relation. In that section, it was also mentioned that such assumptions usually correspond to consider simultaneously (i) a linear axial relation $N = EA\varepsilon$ and (ii) a nonlinear flexure relation $\hat{M}[\chi]$ approximately valid for a specific value, or range of values, of the axial force N, supposedly known in advance. Consider a mesh of prismatic elements and suppose that the linear axial stiffness EA is constant in each element. Thence, if the auxiliary axial stiffness is chosen to be $\widetilde{EA}_{\mathrm{A}} = EA = \mathrm{const}$, the fictitious axial forces are null. Moreover, in this case, the fictitious bending moments are independent of axial strains $\tilde{\varepsilon}^{(i)}$, *i.e.*, axial and bending behaviours are uncoupled ($\widetilde{ES} = 0$). This simplified model is used for the analysis of reinforced concrete structures presented in next chapter.

In order to compute the fictitious forces, either in the exact coupled format or in the approximated uncoupled format, it is necessary to know the auxiliary solution and the exact coupled (or approximated uncoupled) effective nonlinear constitutive relation.

5.4.6.2. FFM(MN) implementation: matrix format

In order to present the implementation of FFM(MN)$_2$ in a format close to that used in the FFM(N)$_2$ and FFM(M)$_2$, the global vectors of generalized strains and stresses and the global governing equations must be reordered. Consider the following rearranging $\underline{\mathbf{\Phi}}$ of the global vector $\mathbf{\Phi}$

$$\underline{\mathbf{\Phi}} \equiv \underline{\mathbf{P}}\,\mathbf{\Phi} = \begin{bmatrix} \bar{\boldsymbol{\phi}} \\ \boldsymbol{\varphi} \end{bmatrix} = \begin{bmatrix} \bar{\boldsymbol{\phi}}_1 \\ \bar{\boldsymbol{\phi}}_2 \\ \vdots \\ \bar{\boldsymbol{\phi}}_m \\ \varphi_1 \\ \varphi_2 \\ \vdots \\ \varphi_m \end{bmatrix} = \begin{bmatrix} \phi_{1,1} \\ \phi_{1,2} \\ \phi_{2,1} \\ \phi_{2,2} \\ \vdots \\ \phi_{m,1} \\ \underline{\phi_{m,2}} \\ \varphi_1 \\ \varphi_2 \\ \vdots \\ \varphi_m \end{bmatrix} \tag{5.193}$$

whose first 2*m* entries are the end sections rotations of all elements and last *m* entries the elemental elongations and $\underline{\mathbf{P}}$ is a square permutation matrix[13] which, when (left) applied to other vectors, will produce the same reordering. Thence,

(iii) Left-multiplication of the generic stress vector $\mathbf{R}_\Delta$ by $\underline{\mathbf{P}}$ gives

$$\underline{\mathbf{R}}_\Delta \equiv \underline{\mathbf{P}}\,\mathbf{R}_\Delta = \begin{bmatrix} \mathbf{M} \\ \mathbf{N}_\Delta \end{bmatrix} = \begin{bmatrix} \bar{\mathbf{M}}_1 \\ \bar{\mathbf{M}}_2 \\ \vdots \\ \bar{\mathbf{M}}_m \\ \tilde{N}_{\Delta,1} \\ \tilde{N}_{\Delta,2} \\ \vdots \\ \tilde{N}_{\Delta,m} \end{bmatrix} = \begin{bmatrix} \tilde{M}_1[0] \\ \tilde{M}_1[L_1] \\ \tilde{M}_2[0] \\ \tilde{M}_2[L_2] \\ \vdots \\ \tilde{M}_m[0] \\ \underline{\tilde{M}_m[L_m]} \\ \tilde{N}_1[L_1] \\ \tilde{N}_2[L_2] \\ \vdots \\ \tilde{N}_m[L_m] \end{bmatrix} \tag{5.194}$$

and similarly for $\mathbf{R}_{\delta,\mathrm{eq}}$.

(iv) Left-multiplication of strain vector $\boldsymbol{\eta}_\Delta$ by $\underline{\mathbf{P}}$ gives

[13] A bar under a symbol denotes this new ordering.

$$\underline{\boldsymbol{\eta}}_{\Delta} \equiv \underline{\mathbf{P}}\,\boldsymbol{\eta}_{\Delta} = \begin{bmatrix} \boldsymbol{\chi} \\ \boldsymbol{\varepsilon}_{\Delta} \end{bmatrix} = \begin{bmatrix} \overline{\boldsymbol{\chi}}_1 \\ \overline{\boldsymbol{\chi}}_2 \\ \vdots \\ \overline{\boldsymbol{\chi}}_m \\ \tilde{\varepsilon}_{\Delta,1} \\ \tilde{\varepsilon}_{\Delta,2} \\ \vdots \\ \tilde{\varepsilon}_{\Delta,m} \end{bmatrix} = \begin{bmatrix} \tilde{\chi}_1[0] \\ \tilde{\chi}_1[L_1] \\ \tilde{\chi}_2[0] \\ \tilde{\chi}_2[L_2] \\ \vdots \\ \tilde{\chi}_m[0] \\ \underline{\tilde{\chi}_m[L_m]} \\ \tilde{\varepsilon}_1[L_1] \\ \tilde{\varepsilon}_2[L_2] \\ \vdots \\ \tilde{\varepsilon}_m[L_m] \end{bmatrix} \tag{5.195}$$

and similarly for $\boldsymbol{\eta}_{\delta,\mathrm{eq}}$.

Left-multiplication of the global compatibility relation (5.172) by $\underline{\mathbf{P}}$ gives

$$\underline{\boldsymbol{\Phi}} = \underline{\mathbf{C}}\,\mathbf{d} \tag{5.196}$$

where $\underline{\mathbf{C}}$ is the new compatibility matrix

$$\underline{\mathbf{C}} = \underline{\mathbf{P}}\,\mathbf{C} = \begin{bmatrix} \mathbf{C}^{\mathrm{M}} \\ \mathbf{C}^{\mathrm{N}} \end{bmatrix} \tag{5.197}$$

were $\mathbf{C}^{\mathrm{M}}$ and $\mathbf{C}^{\mathrm{N}}$ are the compatibility matrices respectively of *model M* and *model N* previously introduced in the chapters 3 and 4. Since the matrix $\underline{\mathbf{P}}$ is orthogonal, *i.e.* $\underline{\mathbf{P}}^{-1} = \underline{\mathbf{P}}^{\mathrm{T}}$, it is possible to write $\mathbf{R}_{\Delta} = \underline{\mathbf{P}}^{-1}\underline{\mathbf{P}}\,\mathbf{R}_{\Delta} = \underline{\mathbf{P}}^{\mathrm{T}}\underline{\mathbf{R}}_{\Delta}$, and thence the generic equilibrium relation (5.177) can be rewritten as

$$\mathbf{f} = \underline{\mathbf{C}}^{\mathrm{T}}\,\underline{\mathbf{R}}_{\Delta} \tag{5.198}$$

Hence, the fictitious force vectors (5.190) and (5.191) can be given by

$$\mathbf{f}_{\mathrm{F}}^{(i)} = \underline{\mathbf{C}}^{\mathrm{T}}\,\underline{\mathbf{R}}_{\mathrm{F},\Delta}^{(i)} = \underline{\mathbf{C}}^{\mathrm{T}} \begin{bmatrix} \mathbf{M}_{\mathrm{F}}^{(i)} \\ \mathbf{N}_{\mathrm{F},\Delta}^{(i)} \end{bmatrix} \tag{5.199}$$

$$\mathbf{f}_{\mathrm{F},\delta}^{(i)} = \underline{\mathbf{C}}^{\mathrm{T}}\,\underline{\mathbf{R}}_{\mathrm{F},\delta,\mathrm{eq}}^{(i)} = \underline{\mathbf{C}}^{\mathrm{T}} \begin{bmatrix} \mathbf{0}_{2m} \\ \mathbf{N}_{\mathrm{F},\delta,\mathrm{eq}}^{(i)} \end{bmatrix} = \frac{1}{2}\underline{\mathbf{C}}^{\mathrm{T}} \begin{bmatrix} \mathbf{0}_{2m} \\ \mathbf{N}_{\mathrm{F},0}^{(i)} - \mathbf{N}_{\mathrm{F},\Delta}^{(i)} \end{bmatrix} \tag{5.200}$$

Left-multiplying the global constitutive equation (5.181) by $\underline{\mathbf{P}}$ gives

$$\underline{\mathbf{R}}_{\mathrm{A},\Delta} + \underline{\mathbf{R}}_{\mathrm{A},\delta,\mathrm{eq}} = \underline{\mathbf{K}}_{\mathrm{A}}^{\mathrm{MN}}\,\underline{\boldsymbol{\Phi}} \tag{5.201}$$

where the $3m \times 3m$ global stiffness matrix $\underline{\mathbf{K}}_{\mathrm{A}}^{\mathrm{MN}}$ is now block diagonal,

$$\underline{\mathbf{K}}_{\mathrm{A}}^{\mathrm{MN}} = \begin{bmatrix} \mathbf{K}_{\mathrm{A}}^{\mathrm{M}} & \\ & \mathbf{K}_{\mathrm{A}}^{\mathrm{N}} \end{bmatrix} \tag{5.202}$$

Thence, (5.201) can be rewritten as

$$\begin{bmatrix} \mathbf{M}_{\mathrm{A}} \\ \mathbf{N}_{\mathrm{A},\Delta} \end{bmatrix} + \begin{bmatrix} \mathbf{M}_{\mathrm{A},\delta,\mathrm{eq}} \\ \mathbf{N}_{\mathrm{A},\delta,\mathrm{eq}} \end{bmatrix} = \begin{bmatrix} \mathbf{K}_{\mathrm{A}}^{\mathrm{M}} & \\ & \mathbf{K}_{\mathrm{A}}^{\mathrm{N}} \end{bmatrix} \begin{bmatrix} \boldsymbol{\phi} \\ \boldsymbol{\varphi} \end{bmatrix} \tag{5.203}$$

which simply gathers the constitutive equation of *model M*

$$\mathbf{M}_{\mathrm{A}} + \mathbf{M}_{\mathrm{A},\delta,\mathrm{eq}} = \mathbf{K}_{\mathrm{A}}^{\mathrm{M}} \boldsymbol{\phi} \tag{5.204}$$

with the constitutive equation of *model N*

$$\mathbf{N}_{\mathrm{A},\Delta} + \mathbf{N}_{\mathrm{A},\delta,\mathrm{eq}} = \mathbf{K}_{\mathrm{A}}^{\mathrm{N}} \boldsymbol{\varphi} \tag{5.205}$$

Let us now compute the auxiliary solution in terms of the displacement vector $\mathbf{d}^{(i)}$. Substitution of the compatibility relation (3.197), which forms the first *2m* lines of (5.196), into the constitutive equation (5.204) and, according to FFM(*MN*)$_2$, recalling that $\mathbf{M}_{\mathrm{F},\delta,\mathrm{eq}} = 0$, *i.e.* $\mathbf{M}_{\mathrm{A},\delta,\mathrm{eq}} = \mathbf{M}_{\delta,\mathrm{eq}} = \mathbf{M}_{\mathrm{L},\delta,\mathrm{eq}}$, gives

$$\mathbf{M}_{\mathrm{A}}^{(i)} = \mathbf{K}_{\mathrm{A}}^{\mathrm{M}} \mathbf{C}^{\mathrm{M}} \mathbf{d}^{(i)} - \mathbf{M}_{\mathrm{L},\delta,\mathrm{eq}} \tag{5.206}$$

which had already been established in chapter 3 in the context of FFM(*M*)$_2$. Consider now the constitutive equation (5.205). Recalling that $\mathbf{N}_{\mathrm{A},\delta,\mathrm{eq}}^{(i)} = \mathbf{N}_{\mathrm{L},\delta,\mathrm{eq}} + \left(\mathbf{N}_{\mathrm{F},0}^{(i-1)} - \mathbf{N}_{\mathrm{F},\Delta}^{(i-1)}\right)/2$ (4.146) and substituting this and the compatibility relation (4.108), which forms the last *m* lines of (5.196) into (5.205), gives

$$\mathbf{N}_{\mathrm{A},\Delta}^{(i)} = \mathbf{K}_{\mathrm{A}}^{\mathrm{N}} \mathbf{C}^{\mathrm{N}} \mathbf{d}^{(i)} - \mathbf{N}_{\mathrm{L},\delta,\mathrm{eq}} + \frac{1}{2}\left(\mathbf{N}_{\mathrm{F},\Delta}^{(i-1)} - \mathbf{N}_{\mathrm{F},0}^{(i-1)}\right) \tag{5.207}$$

Recalling also that $\mathbf{N}_{\mathrm{A},0}^{(i)} = \mathbf{N}_{\mathrm{A},\Delta}^{(i)} + \mathbf{N}_{0}^{(1)} - \mathbf{N}_{\Delta}^{(1)} + \mathbf{N}_{\mathrm{F},0}^{(i-1)} - \mathbf{N}_{\mathrm{F},\Delta}^{(i-1)}$ (4.153) and substituting (5.207) into this equation gives

$$\mathbf{N}_{\mathrm{A},0}^{(i)} = \mathbf{K}_{\mathrm{A}}^{\mathrm{N}} \mathbf{C}^{\mathrm{N}} \mathbf{d}^{(i)} - \mathbf{N}_{\mathrm{L},\delta,\mathrm{eq}} - \mathbf{N}_{\Delta}^{(1)} + \mathbf{N}_{0}^{(1)} - \frac{1}{2}\left(\mathbf{N}_{\mathrm{F},\Delta}^{(i-1)} - \mathbf{N}_{\mathrm{F},0}^{(i-1)}\right) \tag{5.208}$$

Finally, grouping equations (5.207) and (5.208) gives

$$\mathbf{N}_{\mathrm{A}}^{(i)} = \begin{bmatrix} \mathbf{I}_m \\ \mathbf{I}_m \end{bmatrix} \left(\mathbf{K}_{\mathrm{A}}^{\mathrm{N}} \mathbf{C}^{\mathrm{N}} \mathbf{d}^{(i)} - \mathbf{N}_{\mathrm{L},\delta,\mathrm{eq}}\right) + \begin{bmatrix} \mathbf{N}_{0}^{(1)} - \mathbf{N}_{\Delta}^{(1)} \\ \mathbf{0}_{m\times 1} \end{bmatrix} + \frac{1}{2} \begin{bmatrix} \mathbf{I}_m & -\mathbf{I}_m \\ -\mathbf{I}_m & \mathbf{I}_m \end{bmatrix} \mathbf{N}_{\mathrm{F}}^{(i-1)} \tag{5.209}$$

Note that the expressions (5.207), (5.208) and (5.209) had already been established in chapter 4 in the context of FFM(N)$_2$. The auxiliary internal forces (5.206) and (5.209), together with the global constitutive relations $\mathbf{M}_{\mathrm{A}} = \mathbf{E}\mathbf{I}_{\mathrm{A}}\boldsymbol{\chi}$ (3.168) and $\mathbf{N}_{\mathrm{A}} = \mathbf{E}\mathbf{A}^{*}_{\mathrm{A}}\boldsymbol{\varepsilon}$ (4.130), determine the auxiliary approximation. This auxiliary solution and the nonlinear constitutive relations determine the fictitious internal forces and, thus, the fictitious forces (5.190) and (5.191), which in turn, according to (5.189), determine the displacement vector $\mathbf{d}^{(i+1)}$. The flowcharts in Figure 5.10 summarise this FFM implementation for both the exact coupled format of the constitutive law and the approximated uncoupled format.

5.5. Iteration formula of FFM(*MN*)

Substituting the generic equilibrium conditions (5.190) and (5.191) into (5.188) and the constitutive relation $\bar{\mathbf{R}}_{\mathrm{F},\Delta} + \bar{\mathbf{R}}_{\mathrm{F},\delta,\mathrm{eq}} = \bar{\mathbf{K}}^{\mathrm{MN}}_{\mathrm{A}}\bar{\boldsymbol{\Phi}}_{\mathrm{NL}}$, see (5.149), into the resulting expression, and finally left-multiplying the result by $\mathbf{C}$ and considering $\boldsymbol{\Phi} = \mathbf{C}\mathbf{d}$ (5.172) on the left-hand side, gives

$$\boldsymbol{\Phi}_{\mathrm{incr}} = \mathbf{T}\boldsymbol{\Phi}_{\mathrm{NL}} \tag{5.210}$$

with

$$\mathbf{T} = \mathbf{C}\mathbf{K}^{-1}_{\mathrm{A}}\mathbf{C}^{\mathrm{T}}\mathbf{K}^{\mathrm{MN}}_{\mathrm{A}} \tag{5.211}$$

Left-multiplication of (5.210) by $\underline{\mathbf{P}}$, and consideration of (5.193), gives

$$\underline{\boldsymbol{\Phi}}_{\mathrm{incr}} = \underline{\mathbf{T}}\,\underline{\boldsymbol{\Phi}}_{\mathrm{NL}} \tag{5.212}$$

with

$$\underline{\mathbf{T}} \equiv \underline{\mathbf{P}}\,\mathbf{T}\,\underline{\mathbf{P}}^{-1} = \begin{bmatrix} \underline{\mathbf{T}}_{1,1} & \underline{\mathbf{T}}_{1,2} \\ \underline{\mathbf{T}}_{2,1} & \underline{\mathbf{T}}_{2,2} \end{bmatrix} \tag{5.213}$$

where the submatrices correspond to the partition of (5.212) into

$$\boldsymbol{\phi}_{\mathrm{incr}} = \underline{\mathbf{T}}_{1,1}\boldsymbol{\phi}_{\mathrm{NL}} + \underline{\mathbf{T}}_{1,2}\boldsymbol{\varphi}_{\mathrm{NL}} \tag{5.214}$$

$$\boldsymbol{\varphi}_{\mathrm{incr}} = \underline{\mathbf{T}}_{2,1}\boldsymbol{\phi}_{\mathrm{NL}} + \underline{\mathbf{T}}_{2,2}\boldsymbol{\varphi}_{\mathrm{NL}} \tag{5.215}$$

These relations between strain resultants can now be converted into similar relations between generalized strains. First, recall the global kinematic relation for *model M*

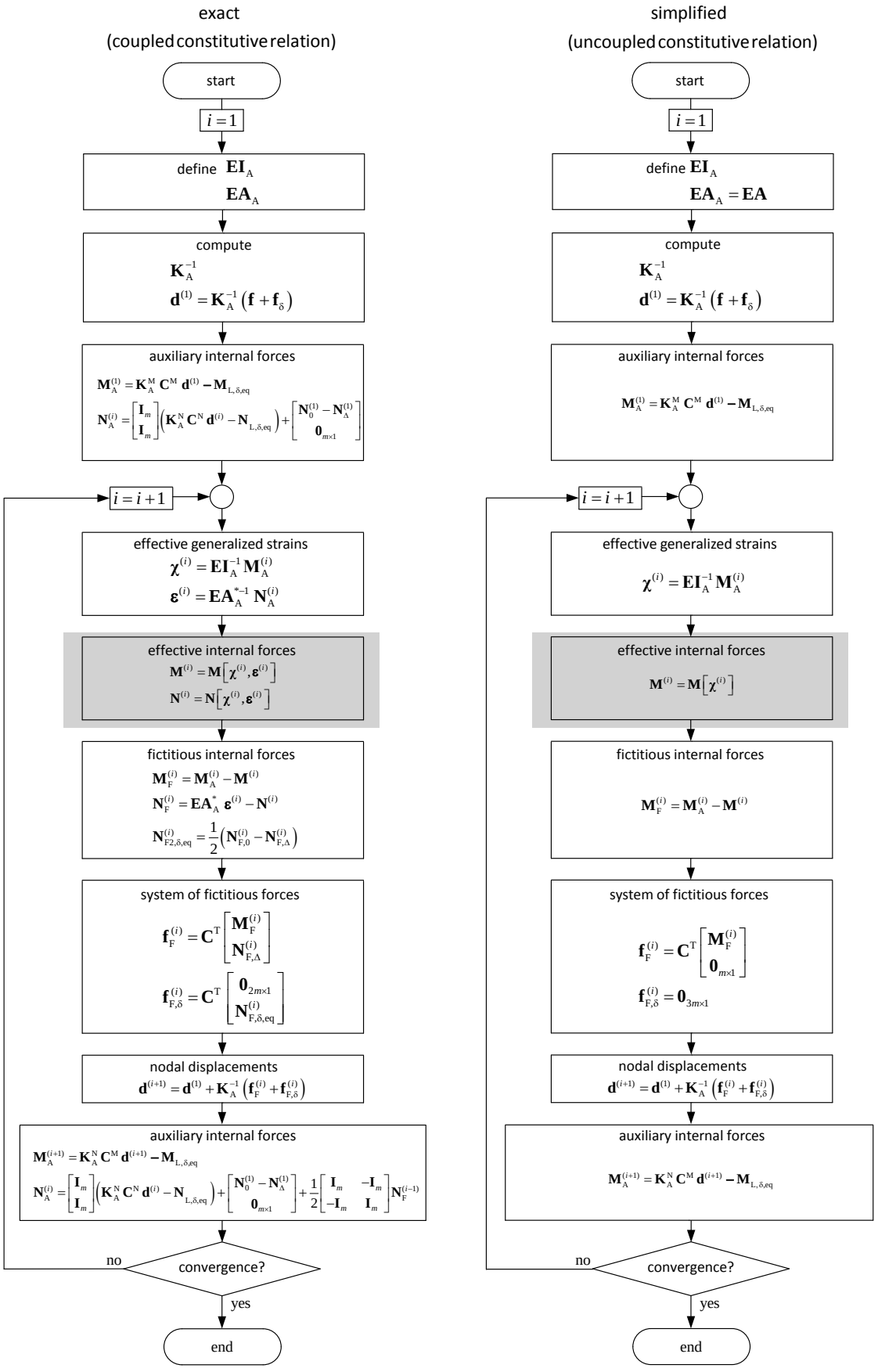

Figure 5.10. FMM(MN)$_2$ *by deformations* (shaded boxes identify differences).

$$\boldsymbol{\chi} + \boldsymbol{\chi}_{\delta,\mathrm{eq}} = \mathbf{K}_0 \, \boldsymbol{\phi} \tag{5.216}$$

and the global kinematic relation of *model N*

$$\boldsymbol{\varepsilon}_{\Delta} + \boldsymbol{\varepsilon}_{\delta,\mathrm{eq}} = \mathbf{K}_0^{\mathrm{N}} \, \boldsymbol{\varphi} \tag{5.217}$$

Second, note that:

(i) according to the generic kinematic relation (5.216), and recalling that $\boldsymbol{\chi}_{\mathrm{NL},\delta,\mathrm{eq}} \simeq \mathbf{0}$,

$$\boldsymbol{\phi}_{\mathrm{NL}} = \mathbf{F}_0 \, \boldsymbol{\chi}_{\mathrm{NL}} \quad \text{with} \quad \mathbf{F}_0 = \left(\mathbf{K}_0 \right)^{-1} \tag{5.218}$$

(ii) according to the generic kinematic relation (5.217) and recalling that $\boldsymbol{\varepsilon}_{\mathrm{NL},\delta,\mathrm{eq}} \simeq (1/2)\left(\boldsymbol{\varepsilon}_{\mathrm{NL},0} - \boldsymbol{\varepsilon}_{\mathrm{NL},\Delta} \right)$,

$$\boldsymbol{\varphi}_{\mathrm{NL}} = \frac{1}{2} \mathbf{F}_0^{\mathrm{N}} \left(\boldsymbol{\varepsilon}_{\mathrm{NL},\Delta} + \boldsymbol{\varepsilon}_{\mathrm{NL},0} \right) \quad \text{with} \quad \mathbf{F}_0^{\mathrm{N}} = \left(\mathbf{K}_0^{\mathrm{N}} \right)^{-1} \tag{5.219}$$

Thence, substituting these two expressions into relations (5.214) and (5.215), gives

$$\boldsymbol{\phi}_{\mathrm{incr}} = \underline{\mathbf{T}}_{1,1} \mathbf{F}_0 \, \boldsymbol{\chi}_{\mathrm{NL}} + \frac{1}{2} \underline{\mathbf{T}}_{1,2} \, \mathbf{F}_0^{\mathrm{N}} \, \boldsymbol{\varepsilon}_{\mathrm{NL},\Delta} + \frac{1}{2} \underline{\mathbf{T}}_{1,2} \, \mathbf{F}_0^{\mathrm{N}} \, \boldsymbol{\varepsilon}_{\mathrm{NL},0} \tag{5.220}$$

$$\boldsymbol{\varphi}_{\mathrm{incr}} = \underline{\mathbf{T}}_{2,1} \mathbf{F}_0 \, \boldsymbol{\chi}_{\mathrm{NL}} + \frac{1}{2} \underline{\mathbf{T}}_{2,2} \, \mathbf{F}_0^{\mathrm{N}} \boldsymbol{\varepsilon}_{\mathrm{NL},\Delta} + \frac{1}{2} \underline{\mathbf{T}}_{2,2} \, \mathbf{F}_0^{\mathrm{N}} \, \boldsymbol{\varepsilon}_{\mathrm{NL},0} \tag{5.221}$$

Third, note that

(i) inverting (5.216), *i.e.* writing $\boldsymbol{\phi} = \mathbf{F}_0 \boldsymbol{\chi} + \boldsymbol{\phi}_{\delta}$ with $\boldsymbol{\phi}_{\delta} = \mathbf{F}_0 \, \boldsymbol{\chi}_{\delta,\mathrm{eq}}$, and noting that $\phi_{\mathrm{incr},\delta} = \phi_{\mathrm{NL},\delta} = 0$, gives

$$\boldsymbol{\phi}_{\mathrm{incr}} = \mathbf{F}_0 \boldsymbol{\chi}_{\mathrm{incr}} \tag{5.222}$$

(ii) inverting (5.217), *i.e.* writing $\boldsymbol{\varphi} = \mathbf{F}_0^{\mathrm{N}} \boldsymbol{\varepsilon}_{\Delta} + \boldsymbol{\varphi}_{\delta}$ with $\boldsymbol{\varphi}_{\delta} = \mathbf{F}_0^{\mathrm{N}} \boldsymbol{\varepsilon}_{\delta,\mathrm{eq}}$, and recalling that $\varphi_{\delta} = \varphi_{\mathrm{L},\delta} + \varphi_{\mathrm{NL},\delta}$ (4.73) and thence that $\boldsymbol{\varphi}_{\mathrm{incr},\delta} = \boldsymbol{\varphi}_{\mathrm{NL},\delta} \simeq \mathbf{F}_0^{\mathrm{N}} \left(\boldsymbol{\varepsilon}_{\mathrm{NL},0} - \boldsymbol{\varepsilon}_{\mathrm{NL},\Delta} \right) / 2$, see (4.170), gives

$$\boldsymbol{\varphi}_{\mathrm{incr}} = \mathbf{F}_0^{\mathrm{N}} \, \boldsymbol{\varepsilon}_{\mathrm{incr},\Delta} + \frac{1}{2} \mathbf{F}_0^{\mathrm{N}} \boldsymbol{\varepsilon}_{\mathrm{NL},0} - \frac{1}{2} \mathbf{F}_0^{\mathrm{N}} \boldsymbol{\varepsilon}_{\mathrm{NL},\Delta} \tag{5.223}$$

Thence, substituting these two expressions into relations (5.220) and (5.221), and left-multiplying them by $\mathbf{K}_0$ and $\mathbf{K}_0^{\mathrm{N}}$ gives

$$\boldsymbol{\chi}_{\mathrm{incr}} = \left(\mathbf{K}_0 \, \underline{\mathbf{T}}_{1,1} \, \mathbf{F}_0 \right) \boldsymbol{\chi}_{\mathrm{NL}} + \frac{1}{2} \left(\mathbf{K}_0 \, \underline{\mathbf{T}}_{1,2} \, \mathbf{F}_0^{\mathrm{N}} \right) \boldsymbol{\varepsilon}_{\mathrm{NL},\Delta} + \frac{1}{2} \left(\mathbf{K}_0 \, \underline{\mathbf{T}}_{1,2} \, \mathbf{F}_0^{\mathrm{N}} \right) \boldsymbol{\varepsilon}_{\mathrm{NL},0} \tag{5.224}$$

$$\boldsymbol{\varepsilon}_{\text{incr},\Delta} = \left(\mathbf{K}_0^{\text{N}}\,\underline{\mathbf{T}}_{2,1}\,\mathbf{F}_0\right)\boldsymbol{\chi}_{\text{NL}} + \frac{1}{2}\left(\mathbf{K}_0^{\text{N}}\,\underline{\mathbf{T}}_{2,2}\,\mathbf{F}_0^{\text{N}} + \mathbf{I}_m\right)\boldsymbol{\varepsilon}_{\text{NL},\Delta} + \frac{1}{2}\left(\mathbf{K}_0^{\text{N}}\,\underline{\mathbf{T}}_{2,2}\,\mathbf{F}_0^{\text{N}} - \mathbf{I}_m\right)\boldsymbol{\varepsilon}_{\text{NL},0} \tag{5.225}$$

Last, recall that $\tilde{\varepsilon}[0] = \tilde{\varepsilon}[L] + \tilde{\varepsilon}_{\text{L}}[0] - \tilde{\varepsilon}_{\text{L}}[L] + \tilde{\varepsilon}_{\text{NL}}[0] - \tilde{\varepsilon}_{\text{NL}}[L]$ (4.177), or, in the global format,

$$\boldsymbol{\varepsilon}_0 = \boldsymbol{\varepsilon}_\Delta + \boldsymbol{\varepsilon}_{\text{L},0} - \boldsymbol{\varepsilon}_{\text{L},\Delta} + \boldsymbol{\varepsilon}_{\text{NL},0} - \boldsymbol{\varepsilon}_{\text{NL},\Delta} \tag{5.226}$$

giving

$$\boldsymbol{\varepsilon}_{\text{incr},0} = \boldsymbol{\varepsilon}_{\text{incr},\Delta} + \boldsymbol{\varepsilon}_{\text{NL},0} - \boldsymbol{\varepsilon}_{\text{NL},\Delta} \tag{5.227}$$

Substituting (5.225) into the last expression, gives

$$\boldsymbol{\varepsilon}_{\text{incr},0} = \left(\mathbf{K}_0^{\text{N}}\,\underline{\mathbf{T}}_{2,1}\,\mathbf{F}_0\right)\boldsymbol{\chi}_{\text{NL}} + \frac{1}{2}\left(\mathbf{K}_0^{\text{N}}\,\underline{\mathbf{T}}_{2,2}\,\mathbf{F}_0^{\text{N}} - \mathbf{I}_m\right)\boldsymbol{\varepsilon}_{\text{NL},\Delta} + \frac{1}{2}\left(\mathbf{K}_0^{\text{N}}\,\underline{\mathbf{T}}_{2,2}\,\mathbf{F}_0^{\text{N}} + \mathbf{I}_m\right)\boldsymbol{\varepsilon}_{\text{NL},0} \tag{5.228}$$

Let us define the generic global strain vector

$$\underline{\boldsymbol{\eta}} = \begin{bmatrix} \underline{\boldsymbol{\eta}}_\Delta \\ \boldsymbol{\varepsilon}_0 \end{bmatrix} = \begin{bmatrix} \boldsymbol{\chi} \\ \boldsymbol{\varepsilon}_\Delta \\ \boldsymbol{\varepsilon}_0 \end{bmatrix} \tag{5.229}$$

It is then possible to group the global relations (5.224), (5.225) and (5.228),

$$\underline{\boldsymbol{\eta}}_{\text{incr}} = \underline{\mathbf{T}}_\eta\,\underline{\boldsymbol{\eta}}_{\text{NL}} \tag{5.230}$$

with

$$\underline{\mathbf{T}}_\eta \equiv \begin{bmatrix} \underline{\mathbf{T}}_{\eta 1,1} & \underline{\mathbf{T}}_{\eta 1,2} & \underline{\mathbf{T}}_{\eta 1,3} \\ \underline{\mathbf{T}}_{\eta 2,1} & \underline{\mathbf{T}}_{\eta 2,2} & \underline{\mathbf{T}}_{\eta 2,3} \\ \underline{\mathbf{T}}_{\eta 3,1} & \underline{\mathbf{T}}_{\eta 3,2} & \underline{\mathbf{T}}_{\eta 3,3} \end{bmatrix} \tag{5.231}$$

where

$$\underline{\mathbf{T}}_{\eta 1,1} = \mathbf{K}_0\,\underline{\mathbf{T}}_{1,1}\,\mathbf{F}_0 \tag{5.232}$$

$$\underline{\mathbf{T}}_{\eta 2,1} = \underline{\mathbf{T}}_{\eta 3,1} = \mathbf{K}_0^{\text{N}}\,\underline{\mathbf{T}}_{2,1}\,\mathbf{F}_0 \tag{5.233}$$

$$\underline{\mathbf{T}}_{\eta 1,2} = \underline{\mathbf{T}}_{\eta 1,3} = \frac{1}{2}\mathbf{K}_0\,\underline{\mathbf{T}}_{1,2}\,\mathbf{F}_0^{\text{N}} \tag{5.234}$$

$$\underline{\mathbf{T}}_{\eta 2,2} = \underline{\mathbf{T}}_{\eta 3,3} = \frac{1}{2}\left(\mathbf{K}_0^{\text{N}}\,\underline{\mathbf{T}}_{2,2}\,\mathbf{F}_0^{\text{N}} + \mathbf{I}_m\right) \tag{5.235}$$

$$\underline{\mathbf{T}}_{\eta 2,3} = \underline{\mathbf{T}}_{\eta 3,2} = \frac{1}{2}\left(\mathbf{K}_0^{\text{N}}\,\underline{\mathbf{T}}_{2,2}\,\mathbf{F}_0^{\text{N}} - \mathbf{I}_m\right) \tag{5.236}$$

Consider now a new square permutation matrix $\mathbf{P}$ reordering the entries of the generic global strain vector $\boldsymbol{\eta}$ according to

$$\boldsymbol{\eta} = \mathbf{P}\,\underline{\boldsymbol{\eta}} = \begin{bmatrix} \overline{\boldsymbol{\eta}}_1 \\ \overline{\boldsymbol{\eta}}_2 \\ \vdots \\ \overline{\boldsymbol{\eta}}_m \end{bmatrix} \tag{5.237}$$

with

$$\overline{\boldsymbol{\eta}}_j = \begin{bmatrix} \tilde{\chi}_j[0] \\ \tilde{\varepsilon}_j[0] \\ \tilde{\chi}_j[L_j] \\ \tilde{\varepsilon}_j[L_j] \end{bmatrix} \tag{5.238}$$

Thence, left-multiplying (5.230) by $\mathbf{P}$ gives

$$\boldsymbol{\eta}_{\text{incr}} = \mathbf{T}_\eta\,\boldsymbol{\eta}_{\text{NL}} \tag{5.239}$$

or

$$\boldsymbol{\eta} = \mathbf{G}_\eta^{\text{I}}[\boldsymbol{\eta}_{\text{NL}}] = \boldsymbol{\eta}_{\text{L}} + \mathbf{T}_\eta\,\boldsymbol{\eta}_{\text{NL}} \tag{5.240}$$

with

$$\mathbf{T}_\eta = \mathbf{P}\,\underline{\mathbf{T}}_\eta\,\mathbf{P}^{-1} \tag{5.241}$$

Hence, (5.240) is a discrete version of the more general expression (5.52). On the other hand, the global relation corresponding to (5.53) and (5.54) is given by

$$\boldsymbol{\eta}_{\text{NL}}^{(i)} = \mathbf{G}_\eta^{\text{II}}[\boldsymbol{\eta}^{(i)}] = \boldsymbol{\eta}^{(i)} - \left(\mathbf{s}_{\text{A}}^*\right)^{-1}\mathbf{R}[\boldsymbol{\eta}^{(i)}] \tag{5.242}$$

where $\mathbf{s}_{\text{A}}^*$ is the block diagonal global $4m \times 4m$ stiffness matrix,

$$\mathbf{s}_{\text{A}}^* = \begin{bmatrix} \overline{\mathbf{s}}_{\text{A},1}^* & & & \\ & \overline{\mathbf{s}}_{\text{A},2}^* & & \\ & & \ddots & \\ & & & \overline{\mathbf{s}}_{\text{A},m}^* \end{bmatrix} \tag{5.243}$$

where $\overline{\mathbf{s}}_{\text{A}}^*$ is the auxiliary elemental 4×4 matrix which collects cross-sectional stiffnesses

$$\overline{\mathbf{s}}_{\text{A}}^* = \begin{bmatrix} EI_{\text{A},j} & & & \\ & EA_{\text{A},j} & & \\ & & EI_{\text{A},j} & \\ & & & EA_{\text{A},j} \end{bmatrix} \tag{5.244}$$

and

$$\mathbf{R}\left[\boldsymbol{\eta}^{(i)}\right]=\begin{bmatrix}\bar{\mathbf{R}}_1\left[\bar{\boldsymbol{\eta}}_1^{(i)}\right]\\ \bar{\mathbf{R}}_2\left[\bar{\boldsymbol{\eta}}_2^{(i)}\right]\\ \vdots\\ \bar{\mathbf{R}}_m\left[\bar{\boldsymbol{\eta}}_m^{(i)}\right]\end{bmatrix} \tag{5.245}$$

is the global vector grouping the elemental constitutive relations at the end sections

$$\bar{\mathbf{R}}\left[\bar{\boldsymbol{\eta}}^{(i)}\right]=\begin{bmatrix}\hat{M}\left[\tilde{\chi}^{(i)}[0],\tilde{\varepsilon}^{(i)}[0]\right]\\ \hat{N}\left[\tilde{\chi}^{(i)}[0],\tilde{\varepsilon}^{(i)}[0]\right]\\ \hat{M}\left[\tilde{\chi}^{(i)}[L],\tilde{\varepsilon}^{(i)}[L]\right]\\ \hat{N}\left[\tilde{\chi}^{(i)}[L],\tilde{\varepsilon}^{(i)}[L]\right]\end{bmatrix} \tag{5.246}$$

Substitution of (5.242) into (5.240) gives the iteration formula of FFM(*MN*)$_{\text{Def}}$

$$\boldsymbol{\eta}^{(i+1)}=\mathbf{G}_\eta\left[\boldsymbol{\eta}^{(i)}\right]=\mathbf{G}_\eta^{\mathrm{I}}\left[\mathbf{G}_\eta^{\mathrm{II}}\left[\boldsymbol{\eta}^{(i)}\right]\right] \tag{5.247}$$

which is a discrete version of the more general iteration formula (5.56).

5.5.1. Convergence conditions

As explained in section § 5.2.4, the iteration formula (5.247) is contractive if both operators $\mathbf{G}_\eta^{\mathrm{I}}$ and $\mathbf{G}_\eta^{\mathrm{II}}$ are non-expansive and at least one of them is a contraction. However, it is possible to prove that

$$\rho\left[\mathbf{T}_\eta\right]=\rho\left[\underline{\mathbf{T}}_\eta\right]=\rho\left[\underline{\mathbf{T}}\right]=\rho\left[\mathbf{T}\right]=1 \tag{5.248}$$

following the steps presented in chapter 3 to prove that $\rho\left[\mathbf{T}_\chi\right]=1$. This means that $\mathbf{G}_\chi^{\mathrm{I}}$ is a non-expansive operator.

Next, it will be proved that if the condition $E_{\mathrm{A}}>E_{\max}$ is satisfied by the auxiliary constitutive relation at each point of every cross section, then $\mathbf{G}_\eta^{\mathrm{II}}$ is a contraction and, therefore, $\mathbf{G}_\eta$ is also a contraction. This will prove that FFM(*MN*)$_{\text{Def}}$ discrete description converges when the condition $E_{\mathrm{A}}>E_{\max}$ is satisfied.

Let us start by writing the Jacobian matrix of $\mathbf{G}_\eta^{\mathrm{II}}$ as

$$\mathbf{J}_\eta^{\mathrm{II}}\equiv\mathbf{I}_{4m}-\left(\mathbf{s}_{\mathrm{A}}^{*}\right)^{-1}\mathbf{s} \tag{5.249}$$

where $\mathbf{s}_{\mathrm{A}}^{*}$ is the auxiliary stiffness matrix (5.243) and $\mathbf{s}$ is the effective stiffness matrix

$$\mathbf{s}=\begin{bmatrix}\overline{\mathbf{s}}_1 & & & \\ & \overline{\mathbf{s}}_2 & & \\ & & \ddots & \\ & & & \overline{\mathbf{s}}_m\end{bmatrix} \tag{5.250}$$

with

$$\overline{\mathbf{s}}\equiv\begin{bmatrix}\dfrac{\partial\tilde{M}[0]}{\partial\tilde{\chi}[0]} & \dfrac{\partial\tilde{M}[0]}{\partial\tilde{\varepsilon}[0]} & \dfrac{\partial\tilde{M}[0]}{\partial\tilde{\chi}[L]} & \dfrac{\partial\tilde{M}[0]}{\partial\tilde{\varepsilon}[L]} \\ \dfrac{\partial\tilde{N}[0]}{\partial\tilde{\chi}[0]} & \dfrac{\partial\tilde{N}[0]}{\partial\tilde{\varepsilon}[0]} & \dfrac{\partial\tilde{N}[0]}{\partial\tilde{\chi}[L]} & \dfrac{\partial\tilde{N}[0]}{\partial\tilde{\varepsilon}[L]} \\ \dfrac{\partial\tilde{M}[L]}{\partial\tilde{\chi}[0]} & \dfrac{\partial\tilde{N}[0]}{\partial\tilde{\varepsilon}[0]} & \dfrac{\partial\tilde{N}[0]}{\partial\tilde{\chi}[L]} & \dfrac{\partial\tilde{N}[0]}{\partial\tilde{\varepsilon}[L]} \\ \dfrac{\partial\tilde{N}[L]}{\partial\tilde{\chi}[0]} & \dfrac{\partial\tilde{N}[L]}{\partial\tilde{\varepsilon}[0]} & \dfrac{\partial\tilde{N}[L]}{\partial\tilde{\chi}[L]} & \dfrac{\partial\tilde{N}[L]}{\partial\tilde{\varepsilon}[L]}\end{bmatrix}=\begin{bmatrix}\widetilde{EI}[0] & \widetilde{ES}[0] & 0 & 0 \\ \widetilde{ES}[0] & \widetilde{EA}[0] & 0 & 0 \\ 0 & 0 & \widetilde{EI}[L] & \widetilde{ES}[L] \\ 0 & 0 & \widetilde{ES}[L] & \widetilde{EA}[L]\end{bmatrix} \tag{5.251}$$

The block diagonal Jacobian matrix $\mathbf{J}_{\eta}^{\mathrm{II}}$ is given by

$$\mathbf{J}_{\eta}^{\mathrm{II}}\equiv\begin{bmatrix}\overline{\mathbf{J}}_{\eta,1}^{\mathrm{II}} & & & \\ & \overline{\mathbf{J}}_{\eta,2}^{\mathrm{II}} & & \\ & & \ddots & \\ & & & \overline{\mathbf{J}}_{\eta,m}^{\mathrm{II}}\end{bmatrix} \tag{5.252}$$

where the generic elemental matrix $\overline{\mathbf{J}}_{\eta}^{\mathrm{II}}$ is

$$\overline{\mathbf{J}}_{\eta}^{\mathrm{II}}=\begin{bmatrix}\beta_{\chi,1} & -\gamma_{\mathrm{EI},1} & 0 & 0 \\ -\gamma_{\mathrm{EA},1} & \beta_{\varepsilon,1} & 0 & 0 \\ 0 & 0 & \beta_{\chi,2} & -\gamma_{\mathrm{EI},2} \\ 0 & 0 & -\gamma_{\mathrm{EA},2} & \beta_{\varepsilon,2}\end{bmatrix} \tag{5.253}$$

with, see (5.67), (5.69), (5.58) and (5.59)

$$\beta_{\chi,1}=\frac{EI_{\mathrm{A}}-\widetilde{EI}[0]}{EI_{\mathrm{A}}}=1-\frac{\widetilde{EI}[0]}{E_{\mathrm{A}}I}=1-\frac{\tilde{E}_{\mathrm{EI}}[0]}{E_{\mathrm{A}}} \tag{5.254}$$

$$\beta_{\chi,2}=\frac{EI_{\mathrm{A}}-\widetilde{EI}[L]}{EI_{\mathrm{A}}}=1-\frac{\widetilde{EI}[L]}{E_{\mathrm{A}}I}=1-\frac{\tilde{E}_{\mathrm{EI}}[L]}{E_{\mathrm{A}}} \tag{5.255}$$

$$\beta_{\varepsilon,1}=\frac{EA_{\mathrm{A}}-\widetilde{EA}[0]}{EA_{\mathrm{A}}}=1-\frac{\widetilde{EA}[0]}{E_{\mathrm{A}}A}=1-\frac{\tilde{E}_{\mathrm{EA}}[0]}{E_{\mathrm{A}}} \tag{5.256}$$

$$\beta_{\varepsilon,2} = \frac{EA_{\mathrm{A}} - \widetilde{EA}[L]}{EA_{\mathrm{A}}} = 1 - \frac{\widetilde{EA}[L]}{E_{\mathrm{A}}\,A} = 1 - \frac{\tilde{E}_{\mathrm{EA}}[L]}{E_{\mathrm{A}}} \tag{5.257}$$

$$\gamma_{\mathrm{EI},1} = \frac{\widetilde{ES}[0]}{EI_{\mathrm{A}}} \quad ; \quad \gamma_{\mathrm{EI},2} = \frac{\widetilde{ES}[L]}{EI_{\mathrm{A}}} \quad ; \quad \gamma_{\mathrm{EA},1} = \frac{\widetilde{ES}[0]}{EA_{\mathrm{A}}} \quad ; \quad \gamma_{\mathrm{EA},2} = \frac{\widetilde{ES}[L]}{EA_{\mathrm{A}}} \tag{5.258}$$

or

$$\overline{\mathbf{J}}_{\eta}^{\mathrm{II}} = \begin{bmatrix} \mathbf{J}_{\eta,1}^{\mathrm{II}} & \mathbf{0}_2 \\ \mathbf{0}_2 & \mathbf{J}_{\eta,2}^{\mathrm{II}} \end{bmatrix} \tag{5.259}$$

with

$$\mathbf{J}_{\eta,i}^{\mathrm{II}} = \begin{bmatrix} \beta_{\chi,i} & -\gamma_{\mathrm{EI},i} \\ -\gamma_{\mathrm{EA},i} & \beta_{\varepsilon,i} \end{bmatrix} \tag{5.260}$$

Thence, the spectral radius of $\mathbf{J}_{\eta}^{\mathrm{II}}$ is equal to the greatest spectral radius of the cross-sectional matrices $\mathbf{J}_{\eta,1}^{\mathrm{II}}$ and $\mathbf{J}_{\eta,2}^{\mathrm{II}}$. On the other hand, it was shown in § 5.2.4 that $\left|\mathbf{J}_{\eta,1}^{\mathrm{II}}\right| < 1$ and $\left|\mathbf{J}_{\eta,2}^{\mathrm{II}}\right| < 1$ if the relation $E_{\mathrm{A}} > E_{\max}$ is satisfied at each fibre of every cross section. This proves, as desired, that the FFM(MN)$_{\mathrm{Def}}$ discrete description converges when the latter condition is satisfied.

Finally, note that in the case of the simplified uncoupled constitutive relation, $\widetilde{ES} = 0$, and thence the nonlinear stiffness matrix (5.251) gets reduced to

$$\overline{\mathbf{s}} = \begin{bmatrix} \widetilde{EI}[0] & 0 & 0 & 0 \\ 0 & \widetilde{EA}[0] & 0 & 0 \\ 0 & 0 & \widetilde{EI}[L] & 0 \\ 0 & 0 & 0 & \widetilde{EA}[L] \end{bmatrix} \tag{5.261}$$

Recall that, as mentioned in § 5.4.6.1, the auxiliary axial stiffness is $\widetilde{EA}_{\mathrm{A}} = EA = \mathrm{const}$. This way, the fictitious axial force is null and $\beta_{\varepsilon,1} = \beta_{\varepsilon,2} = 0$. In this case, the Jacobian matrix (5.253) gets reduced to

$$\overline{\mathbf{J}}_{\eta}^{\mathrm{II}} = \begin{bmatrix} \beta_{\chi,1} & 0 & 0 & 0 \\ 0 & 0 & 0 & 0 \\ 0 & 0 & \beta_{\chi,2} & 0 \\ 0 & 0 & 0 & 0 \end{bmatrix} \tag{5.262}$$

Thence, it is obvious that the sufficient convergence conditions for this case are those derived in chapters 3 for FFM (*M*).

5.6. Illustrative example

The application of FFM(MN)$_{\text{Def}}$ is now illustrated by means of the problem represented in Figure 5.11. The beam has length $L = 1$ and an idealized cross section formed by two single fibres kept at a distance $h = 0.2L$ one from the other, see Figure 5.11b. The area of each fibre is[14]

$$A_{\text{b}} = A_{\text{t}} = \frac{h^2}{2} \tag{5.263}$$

but it is supposed to be lumped at a point, so that each fibre is replaced by its axis.

The top fibre has a linear constitutive relation with stiffness $E_{\text{t}} = 1$,

$$\sigma_{\text{t}} = \widehat{\sigma}_{\text{t}}\left[e_{\text{t}}\right] = E_{\text{t}}\, e_{\text{t}} = e_{\text{t}} \quad \text{or} \quad e_{\text{t}} = \widehat{e}_{\text{t}}\left[\sigma\right] = \frac{1}{E_{\text{t}}}\sigma_{\text{t}} = \sigma_{\text{t}} \tag{5.264}$$

where e_{b} and e_{t} are the cross-sectional normal strains in the bottom and top fibres.

The bottom fibre follows the nonlinear constitutive relationship

$$\sigma_{\text{b}} = \widehat{\sigma}_{\text{b}}\left[e_{\text{b}}\right] = \frac{E_0\, e_{\text{b}}}{\sqrt{1+\left(\dfrac{E_0\, e_{\text{b}}}{\sigma_{\text{ref}}}\right)^2}} = \frac{e_{\text{b}}}{\sqrt{1+e_{\text{b}}^2}} \quad \text{or} \quad e_{\text{b}} = \widehat{e}_{\text{b}}\left[\sigma\right] = \frac{\sigma_{\text{b}}/E_0}{\sqrt{1-\left(\dfrac{\sigma_{\text{b}}}{\sigma_{\text{ref}}}\right)^2}} = \frac{\sigma_{\text{b}}}{\sqrt{1-\sigma_{\text{b}}^2}} \tag{5.265}$$

where $\sigma_{\text{ref}} = 1$ is a stress bounding value and $E_0 = 1$ is the initial stiffness. This constitutive relationship is similar to that of the examples presented in chapters 3 and 4.

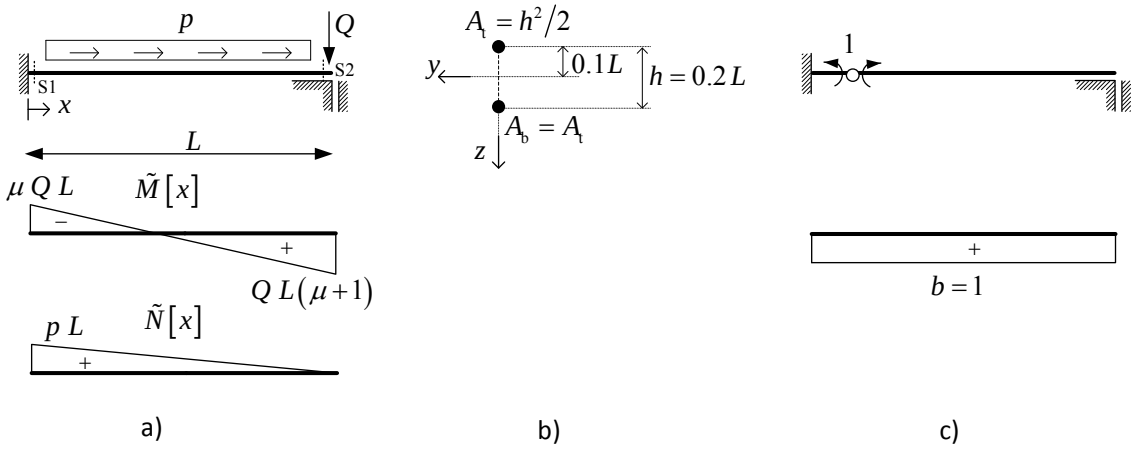

Figure 5.11. Example 5: a) Beam, boundary conditions and loading, b) idealized cross section and c) primary structure of the force method.

[14] The subscripts t and b denoting the top fibre and the bottom fibre, respectively.

The beam carries a uniformly distributed axial load $p = 0.08$ and a transverse point load $Q = 0.1$ at the right end section. Second-order effects are neglected.

In order to solve this problem, let us first define a system of coordinates whose longitudinal *x*-axis is at mid distance between the initial position of the two fibres and whose *z*-axis is vertical and points downwards, Figure 5.11b. The origin of the axes is contained in the beam left end section.

The cross-sectional compatibility relations are given by

$$\chi = \frac{e_{\mathrm{b}} - e_{\mathrm{t}}}{h} \tag{5.266}$$

$$\varepsilon = \frac{e_{\mathrm{b}} + e_{\mathrm{t}}}{2} \tag{5.267}$$

or, inverting the above relations,

$$e_{\mathrm{t}} = \varepsilon - \chi \frac{h}{2} \tag{5.268}$$

$$e_{\mathrm{b}} = \varepsilon + \chi \frac{h}{2} \tag{5.269}$$

The equilibrium cross-sectional relations are given by

$$M = \frac{h}{2}\left(\sigma_{\mathrm{b}} A_{\mathrm{b}} - \sigma_{\mathrm{t}} A_{\mathrm{t}}\right) \tag{5.270}$$

$$N = \sigma_{\mathrm{b}} A_{\mathrm{b}} + \sigma_{\mathrm{t}} A_{\mathrm{t}} \tag{5.271}$$

which can also be inverted,

$$\sigma_{\mathrm{t}} = \frac{1}{A_{\mathrm{t}}}\left(\frac{N}{2} - \frac{M}{h}\right) \tag{5.272}$$

$$\sigma_{\mathrm{b}} = \frac{1}{A_{\mathrm{b}}}\left(\frac{N}{2} + \frac{M}{h}\right) \tag{5.273}$$

The total cross-sectional area is $A = A_{\mathrm{b}} + A_{\mathrm{t}} = h^2$ and its second moment of area with respect to the *y*-axis is

$$I = \frac{h^2}{4}\left(A_{\mathrm{b}} + A_{\mathrm{t}}\right) = \frac{h^4}{4} \tag{5.274}$$

The stiffness of the bottom fibre is given by

$$E_{\mathrm{b}} = \widehat{E}_{\mathrm{b}}\left[e\right] \equiv \frac{d\widehat{\sigma}_{\mathrm{b}}\left[e_{\mathrm{b}}\right]}{de_{\mathrm{b}}} = E_0\left(1+\left(\frac{E_0\, e_{\mathrm{b}}}{\sigma_{\mathrm{ref}}}\right)^2\right)^{-3/2} = \frac{1}{\left(1+e_{\mathrm{b}}^2\right)^{3/2}} \tag{5.275}$$

with $\widehat{E}_{\mathrm{b}}\left[0\right] = E_0 = 1$. In order to determine the cross-sectional constitutive relations substitute successively (5.265.2), (5.264.2), (5.272) and (5.273) into (5.266) and (5.267), giving

$$\chi = \hat{\chi}\left[M, N\right] = \frac{1}{h}\left(\frac{\frac{1}{A_{\mathrm{b}}}\left(\frac{N}{2}+\frac{M}{h}\right)}{\sqrt{1-\left(\frac{1}{A_{\mathrm{b}}}\left(\frac{N}{2}+\frac{M}{h}\right)\right)^2}} - \frac{1}{A_{\mathrm{t}}}\left(\frac{N}{2}-\frac{M}{h}\right)\right) \tag{5.276}$$

$$\varepsilon = \hat{\varepsilon}\left[M, N\right] = \frac{1}{2}\left(\frac{\frac{1}{A_{\mathrm{b}}}\left(\frac{N}{2}+\frac{M}{h}\right)}{\sqrt{1-\left(\frac{1}{A_{\mathrm{b}}}\left(\frac{N}{2}+\frac{M}{h}\right)\right)^2}} + \frac{1}{A_{\mathrm{t}}}\left(\frac{N}{2}-\frac{M}{h}\right)\right) \tag{5.277}$$

Similarly, substituting successively (5.265.1), (5.264.1), (5.268) and (5.269) into (5.270) and (5.271), gives

$$M = \hat{M}\left[\chi, \varepsilon\right] = \frac{h}{2}\left(\frac{\varepsilon+\chi\frac{h}{2}}{\sqrt{1+\left(\varepsilon+\chi\frac{h}{2}\right)^2}}A_{\mathrm{b}} - \left(\varepsilon-\chi\frac{h}{2}\right)A_{\mathrm{t}}\right) \tag{5.278}$$

$$N = \hat{N}\left[\chi, \varepsilon\right] = \frac{\varepsilon+\chi\frac{h}{2}}{\sqrt{1+\left(\varepsilon+\chi\frac{h}{2}\right)^2}}A_{\mathrm{b}} + \left(\varepsilon-\chi\frac{h}{2}\right)A_{\mathrm{t}} \tag{5.279}$$

This structure has a single degree of static indeterminacy. The problem will be solved by the force method, considering the primary structure defined by releasing the bending moment at the left end section, *i.e.* the hyperstatic unknown is the bending moment at that section,

$$\tilde{M}\left[0\right] \equiv \mu Q L \tag{5.280}$$

Thence, static equilibrium gives the internal force fields

$$M = \tilde{M}\left[x\right] = QL\left(\mu+\frac{x}{L}\right) \tag{5.281}$$

$$N = \tilde{N}[x] = pL\left(1 - \frac{x}{L}\right) \tag{5.282}$$

Note that since the beam is axially isostatic the axial force field depends exclusively on the equilibrium conditions, *e.g.* $N_{S1} = \tilde{N}[0] = 0.08$. The compatibility condition corresponding to the hyperstatic unknown is given by

$$\int_0^L \tilde{b}_M \, \hat{\chi}\left[\tilde{M}[x], \tilde{N}[x]\right] dx = 0 \tag{5.283}$$

where $\tilde{b}_M = 1$ is the self-equilibrated bending moment distribution represented in Figure 5.11c. Thence,

$$\int_0^L \hat{\chi}\left[Q(\mu L + x), p(L - x)\right] dx = 0 \tag{5.284}$$

This equation is nonlinear in μ and its unique solution is $\mu = -0.612$, *i.e.* $M_{S1} = -0.0612$. To this value corresponds $M_{S2} = -0.0388$, $\chi_{S2} = 24.8$ and $\varepsilon_{S1} = 2.03$. The linear bending moment diagram is not symmetric w.r.t. the midspan section due to the axial-flexural coupling and the presence of the axial loading. Figure 5.12 presents the corresponding generalized strain fields and Figure 5.13 the normal strain at the top and bottom fibres. Note that, contrary to the axial force, the axial strain is not a monotonic (decreasing) function and that $\tilde{\varepsilon}[L] \neq 0$ even though $\tilde{N}[L] = 0$. Moreover, even though $|\tilde{M}[0]| > \tilde{M}[L]$, $|\tilde{\chi}[0]| < \tilde{\chi}[L]$. These results are justified by the interaction between flexural and axial behaviours.

Consider now the application of FFM(*MN*)$_{Def}$ to this problem. A constant auxiliary field E_A for both fibres along the beam was chosen. A first uniform mesh with two elements was consecutively refined by bisection, establishing a family of five uniform meshes with

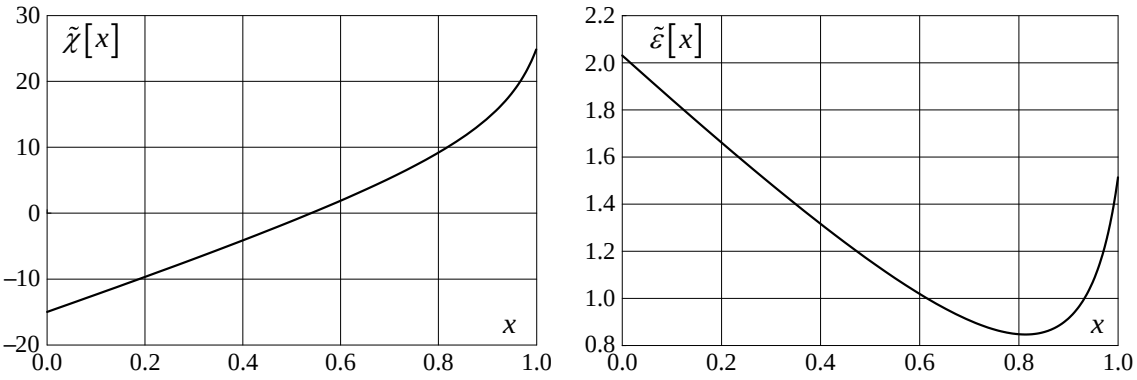

Figure 5.12. Example 5: Exact solution: curvature and axial strain fields.

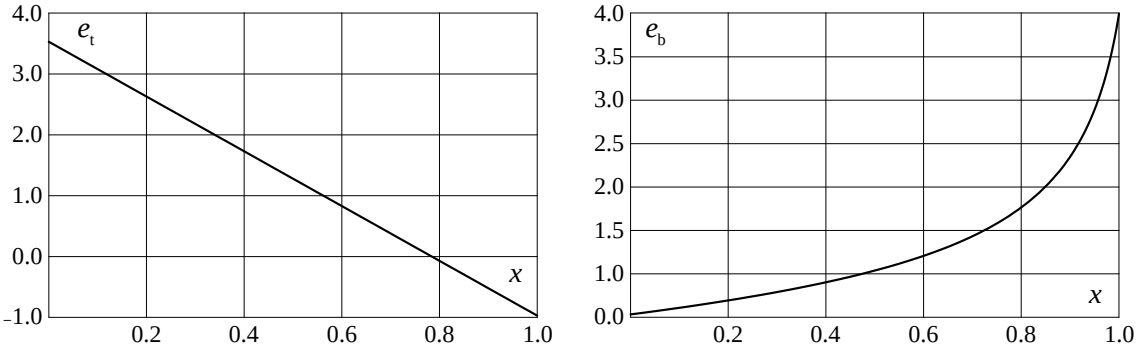

Figure 5.13. Example 5: Exact solution: normal stains at top fibre and bottom fibre.

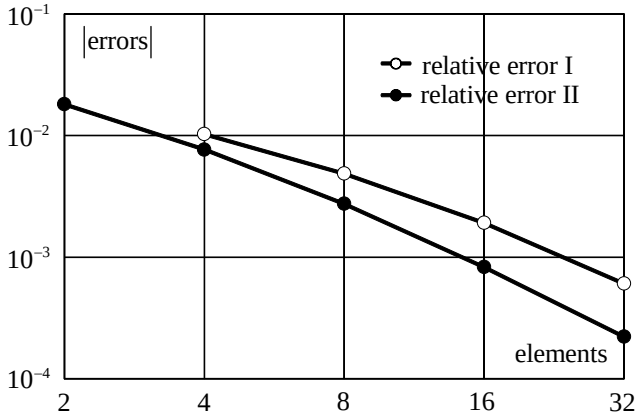

Figure 5.14. Example 5: Relative error I and relative error II for M_{S1} (logarithmic scale).

$2^i = 2,4,8,16$ and 32 elements. Similarly to the examples presented in § 3.7 and § 4.5, a convergence analysis was performed w.r.t. (i) the mesh refinement (*mesh*-convergence) and (ii) FFM iterative procedure itself (*FFM*-convergence). Both convergence analyses are based on relative error I (err_{I}) and relative error II (err_{II}) defined in § 3.7. Recall that, for a given mesh, the *i*th approximation of *x*, is *FFM*-convergent if $err_{\mathrm{I}}^{(i)} < tol_{\mathrm{FFM}}$ and that the *FFM*-convergent approximation of *x*, for the *j*th mesh, denoted x_j, is *mesh*-convergent if $\left\{err_{\mathrm{I},j}, err_{\mathrm{II},j}\right\} < tol_{\mathrm{mesh}}$, where the tolerance values $tol_{\mathrm{FFM}} = 0.001$ and $tol_{\mathrm{mesh}} = 0.01$ were chosen once again.

Figure 5.14 and Figure 5.15 summarise the mesh-convergence analysis results, each point representing an *FFM*-convergent solution. Table 5.1 presents the maximum generalised strains χ_{S2} and ε_{S1} and also the normalized bending moment μ of the *FFM*-convergent solutions of each mesh. The fifth mesh, with 32 elements, gives acceptable results, despite not being *mesh*-convergent in terms of χ_{S2}, see Figure 5.15.

For the fifth mesh, Figure 5.16 shows the number of iterations required by FFM(MN)$_{\mathrm{Def}}$ to converge for several values of E_{A} in the interval $]0.5, 2]$. FFM(MN)$_{\mathrm{Def}}$ did not converge

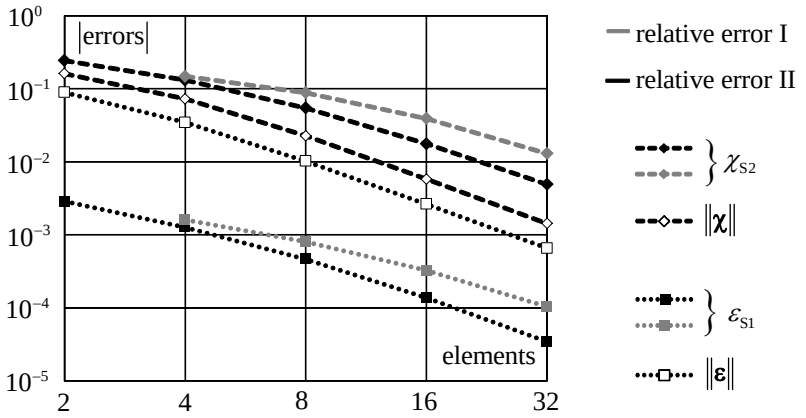

Figure 5.15. Example 5: Relative errors I and II for generalized strains (logarithmic scale).

Table 5.1 – Example 5: Exact and numerical solutions.

	number of elements (FFM)					exact solution
	2	4	8	16	32	
μ	-0.623	-0.617	-0.614	-0.612	-0.612	-0.612
χ_{S2}	18.801	21.579	23.484	24.402	24. 718	24.839
ε_{S1}	2.025	2.029	2.030	2.031	2.031	2.031

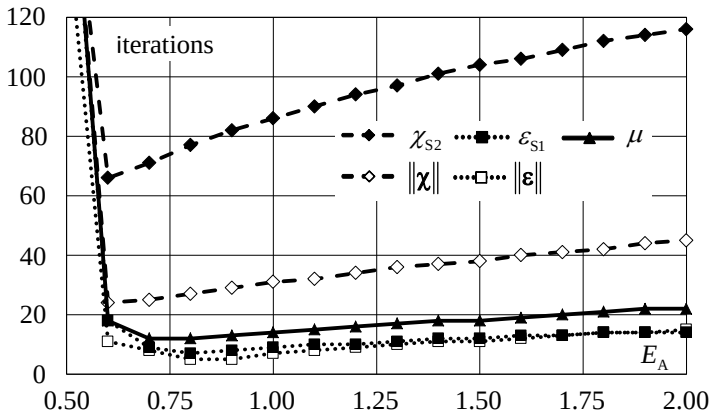

Figure 5.16. Example 5: Number of iterations required for convergence of FFM(*MN*)$_{Def}$.

numerically for $E_A \le 0.5$. Recall that $E_{max} = \max\{E_t, E_0\} = 1$. The results show that FFM(*MN*)$_{Def}$ sufficient convergence condition $E_A > E_{max}$ (5.82), is satisfied for this beam.

The parameter E_A is also seen to play an important role in terms of the convergence rate. Figure 5.16 shows that the number of iterations needed to achieve convergence in terms of χ_{S2} is much larger than with the remaining parameters.

Since no convergence conditions were derived for FFM_S, the corresponding iteration formulas were not used in this example.

5.7. Concluding remarks

In the context of *model MN*, FFM works with an auxiliary problem, where, differently from the effective coupled problem, bending and axial behaviours are uncoupled. As shown in § 5.2.2, the fictitious internal forces disguise the coupling of the effective problem and their incremental form can be related to the difference between the uncoupled auxiliary linear stiffness and the coupled effective nonlinear stiffness. This relationship is similar to the stiffness decomposition used in the Pseudo Force Method (Deng and Ghosn, 2001) to define the fictitious forces.

The general frameworks for the implementation of FFM(*M*) and FFM(*MN*) are similar, *i.e.* very similar operations are required in the implementation of these two models. Actually, the original idea of this particular implementation of FFM(*MN*), *i.e.* as a modification of FFM(*M*), is due to M. Ferreira, the author of *EvalS*.

Even though FFM(*M*) and FFM(*MN*) have a lot in common, the more accurate nature of the latter entails differences at the numerical level. This determines the difference in the convergence behaviour between the two models. The established sufficient convergence conditions for $FFM(MN)_{Def}$ are given by condition $E_A > E_{max}$, *i.e.* the auxiliary bending stiffness $EI_A = E_A I$ and axial stiffness $EI_A = E_A A$ are determined by E_A and the cross-sectional effective geometry.

Note that sufficient convergence conditions were derived for $FFM(MN)_{Def}$ only. The convergence of $FFM(MN)_S$ requires further investigation.

When applying FFM(*MN*) to the analysis of composite structural materials, like reinforced concrete, it may be possible to derive less restrictive sufficient convergence conditions. In fact, the developed sufficient convergence condition for $FFM(MN)_{Def}$, $E_A > E_{max}$, when applied to reinforced concrete structures, determines the use of an auxiliary stiffness E_A much larger that the initial Young's modulus of reinforced concrete E_c and this may lead to a high number of iterations. On the other hand, the use of smaller values for E_A does not necessarily cause the divergence of the iterative procedure. In fact, if the iterative procedure happens to converge

for a value of the auxiliary stiffness close to E_c, *i.e.* $E_A \approx E_c$, that solution might be numerically more efficient. Such a less demanding convergence condition could even be justified by a simple homogenisation of the cross section. This topic requires further investigation.

As already mentioned in chapter 3, a severe limitation of FFM, if one thinks of a method capable of generic nonlinear elastic analysis, is associated to constitutive relations which include horizontal or/and softening branches. Until now, it was not possible to derive any convergence condition for those types of behaviour. Even for such a common structural material like concrete, this type of behaviour must be considered, particularly, but not only, when the behaviour under service conditions of reinforced concrete structures is to be investigated. Another situation where the softening branch of a material may be reached is when the load-displacement curve approaches the vicinity of a limit point; in those cases, it is possible, and even likely for some materials, that the tangent stiffness at some points in the section is already negative (*i.e.* $E < 0$). It is worth noting that Costa (2013) has already applied FFM(*MN*) with success to RC problems where some points in the section do not present a positive stiffness.

A final comment must be made about the choice of the illustrative example presented in this chapter. Its simplicity offers an insight on the iterative procedure that other more complex examples would not provide. The main idea was to get rid of everything that might disturb the analysis. The example fulfils several objectives: (i) to illustrate the application of FFM(*MN*) in the simplest way possible; (ii) to study the *mesh*-convergence and (iii) to study the role played by the auxiliary stiffness in the efficiency of the iterative procedure. However, this example does not require from FFM(*MN*) as much as this method can give. As an example of more ambitious problems, Costa (2013) applied FFM(*MN*) to the quasi-static analysis of reinforced concrete frames with several floors and spans. Ferreira *et al.* (2011) offers another interesting application of FFM(*MN*) to the practical analysis of reinforced concrete skeletal structures.

Chapter 6
Application of FFM to reinforced concrete skeletal structures

6.1. Introduction

This chapter illustrates the application of FFM to the nonlinear elastic analysis of reinforced concrete skeletal structures. FFM was implemented in *EvalS* (Ferreira, 2011), a software for the analysis of plane skeletal structures which is briefly described in the next section. Subsequently, the analysis of two reinforced concrete structures is presented: a portal frame (Appleton, 1982) and a built-in beam (CEB, 1985, Favre *et al.*, 1989). These examples can also be found in (Gala *et al.,* 2010) and (Gala *et al.,* 2012), respectively.

The first example illustrates one of the most interesting features of FFM: a smeared approach is considered in this method to model the nonlinear deformations along the linear elements, instead of the lumped approach ("plastic hinges"). In the second example, the relevance of using a nonlinear elastic analysis to calculate deflections and crack width in a beam is investigated.

Reinforced concrete structures were chosen for these two illustrative examples, not because FFM is particularly adapted to this structural material, but because the nonlinear behaviour of reinforced concrete is as good as others to reveal the capabilities of this method.

6.2. Implementation of FFM in *EvalS*

EvalS is a software for the quasi-static analysis of plane skeletal structures, developed by Ferreira (2011). This program uses the Equivalent Force Method to model geometrically nonlinear behaviour and FFM_{Def} to perform nonlinear elastic analyses. From the user's viewpoint the latter analyses require the following steps:

(i) define the structural model:

   a. geometry;

   b. support conditions;

   c. constitutive relations;

   d. actions.

(ii) define the parameters required by a FFM analysis:

   a. finite elements mesh;

   b. constant auxiliary stiffnesses for each element;

   c. numerical tolerances and maximum number of iterations.

(iii) execute the "FFM analysis" option.

For this model and FFM parameters an iterative procedure is then internally performed, *i.e.* several iterations are made until *FFM*-convergence is achieved. In *EvalS*, the *FFM*-convergence is evaluated in terms of the relative error of the Euclidian norm of nodal displacements (excluding rotations),

$$err_{\mathrm{I},i}^{\mathbf{d}} = \left| \frac{\mathbf{d}^{(i)} - \mathbf{d}^{(i-1)}}{\mathbf{d}^{(i-1)}} \right| \tag{6.1}$$

Hence, the *i*th iteration of *EvalS* is FFM-convergent if

$$err_{\mathrm{I},i}^{\mathbf{d}} < tol_{\mathrm{FFM}} \tag{6.2}$$

where tol_{FFM} is a fixed tolerance. Each iteration consists in the following steps:

(i) compute the elemental fictitious internal forces at the interpolation sections;

(ii) compute the fictitious forces system;

(iii) solve the auxiliary problem;

(iv) compute relative errors;

(v) compare errors to tolerances.

Note that a *mesh*-convergence analysis should be performed by the user, *i.e.* the mesh should be refined, defining new meshes, until the difference between results for successive meshes becomes acceptable.

The three FFM models described in chapters 3 to 5 of this thesis have been implemented in *EvalS*, *e.g.*, the basic discrete description of FFM(*M*), the discrete description of FFM(*N*) and the discrete description of FFM(*MN*). The interpolation sections, *i.e.* the sections where the fictitious internal forces are determined, are the end sections of the linear elements.

With respect to FFM implementation of each model, the differences lie only in the format of the fictitious force system. In FFM(*MN*), the internal forces at the interpolation sections are determined by a discrete integration of the normal stress; each beam element is represented by a set of discrete fibers, which may have different nonlinear constitutive relations and which satisfy Euler-Bernoulli hypothesis at each cross section.

In the context of FFM implementation in *EvalS*, Ferreira extended FFM to point elements with nonlinear elastic constitutive relations. Based on these point elements, Costa (2013) developed a beam-column joint macro-element which he subsequently applied to the quasi-static analysis of reinforced concrete frames. The implementation in *EvalS* of the fibre-wise integration procedure and of FFM(*MN*) was made, tested and used by Costa (2013); see also Ferreira *et al.* (2011). Costa (2013) used FFM(*MN*) to determine the capacity curves required by push-over analyses and to study two specific aspects of the behaviour of reinforced concrete skeletal structures: beam growth and tension-stiffening. Other applications of FFM to reinforced concrete skeletal structures were presented by Gala *et al.* (2008) and Ferreira *et al.*(2011). Ferreira is presently expanding FFM(*N*) having in view the analysis based on adaptive stress fields, a generalization of strut and tie models.

6.3. First application example

In this section, FFM(*M*) is applied, via *EvalS*, to the nonlinear elastic analysis of the reinforced concrete portal frame represented in Figure 6.1 (Appleton, 1982). This frame is made up of

prismatic beams and columns, each of which is delimited by a pair of solid circles (critical sections) in Figure 6.1.

The effective load system is formed by the constant uniformly distributed load q and the incremental horizontal point forces F. The value of the latter suffers successive increments of $1\ \mathrm{kN}$ or, when approaching collapse, $0.01\ \mathrm{kN}$.

The main objective of this analysis is the determination of the capacity curve, *i.e.* the force-displacement (F-Δ) curve, required for a nonlinear static push-over analysis. The force-displacement curve is defined by the relation between the horizontal displacement of the frame upper beam Δ, *i.e.* its total drift, and the magnitude of the horizontal forces F. The structure collapses when the bending moment at section CS_{26} – located at the top of the right column – reaches the ultimate bending moment M_3, see Figure 6.1. This state is characterized by the ultimate displacement Δ_u and force F_u, and its numerical approximation depends on the nature, either smeared or lumped, of the nonlinear material formulation.

The nonlinear material behaviour was modelled in *EvalS* by elastic piecewise-linear bending moment-curvature relationships with five linear branches, as schematized in Figure 6.2. Table 6.1 gives the coordinates of the corner points of the constitutive relationship for each of

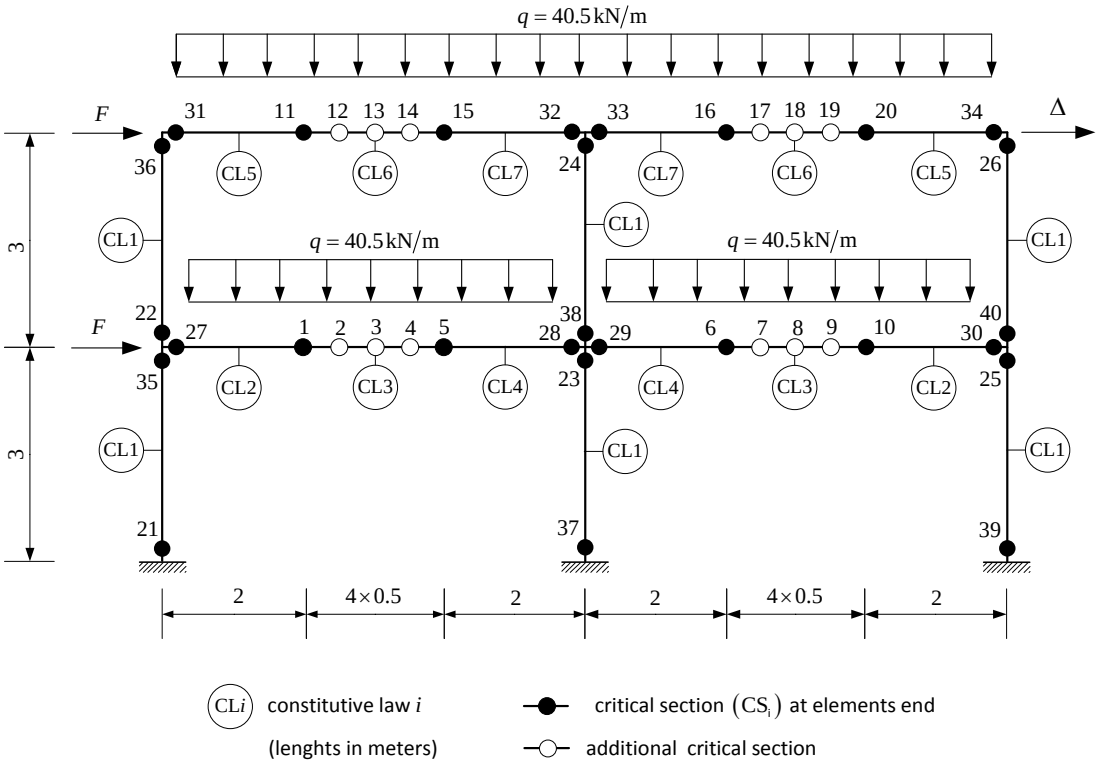

Figure 6.1. First application example: Frame, beam and column elements.

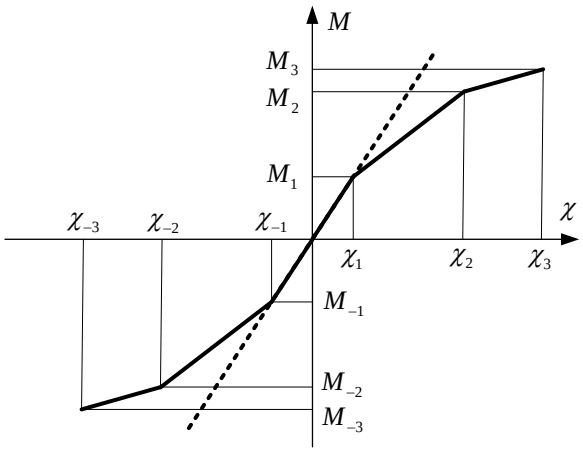

Figure 6.2. First application example: RC constitutive relationship.

Table 6.1 – First application example: corner points of the moment-curvature relationships.

	M [kNm]						χ [10^{-3}m^{-1}]					
	-3	-2	-1	1	2	3	-3	-2	-1	1	2	3
CL1	-72.3	-70.1	-20.7	20.7	70.1	72.3	-60.49	-4.31	-0.41	0.41	4.31	60.49
CL2	-156.0	-150.1	-45.0	44.2	115.2	118.5	-62.91	-2.77	-0.28	0.27	2.39	76.46
CL3	-118.5	-115.2	-44.2	45.0	150.1	156.0	-76.46	-2.39	-0.27	0.28	2.77	62.91
CL4	-234.1	-221.4	-47.5	44.2	115.2	118.5	-52.24	-3.23	-0.28	0.27	2.39	76.46
CL5	-76.2	-73.4	-42.0	42.0	73.4	76.2	-81.90	-1.68	-0.27	0.27	1.68	81.90
CL6	-76.2	-73.4	-42.0	43.0	109.7	113.5	-81.90	-1.68	-0.27	0.28	2.38	66.49
CL7	-191.3	-182.5	-45.5	42.0	73.4	76.2	-51.58	-3.47	-0.28	0.27	1.68	81.90

these beams and columns. These values are given in Appleton (1982), with the exception of the ultimate curvatures χ_3 and χ_{-3} which are not necessary for the analysis presented in that paper. The first corner point (M_1, χ_1) (resp. (M_{-1}, χ_{-1})) presented by Appleton, corresponds to the beginning of cracking in concrete. The second corner point (M_2, χ_2) (resp. (M_{-2}, χ_{-2})) presented by Appleton, corresponds to the beginning of yield of the steel reinforcement. Apparently, the axial forces are not considered in these constitutive relations. This explains the small slope of the last branch of the columns constitutive relation (CL1).

Appleton also determined a similar force-displacement curve admitting, however, that the nonlinear material deformations only can take place at plastic hinges located at specific fixed critical sections CS_i, identified in Figure 6.1 (i) by solid circles, those associated with beam-column joints and also to beam sections where the cross section of the longitudinal bars varies, and (ii) by hollow circles, those associated with sections where the bending moment

can have a (positive) maximum in the midspan region, due to the distributed load. The bending moment-rotation constitutive relation at those plastic hinges is based on the piecewise-linear bending moment-curvature relationships of Figure 6.2. and Table 6.1, admitting that the nominal length of the "plastic" hinge is $L_{\mathrm{P}} = 0.5\,\mathrm{m}$. The ultimate rotations ϕ_3 used by Appleton, corresponding to the neutral axis depth at the ultimate limit state, were estimated according to the experimental model proposed in CEB Model Code (1990). Hence, the following relation was adopted for the ultimate curvatures presented in Table 6.1 and used in *EvalS*/FFM analysis,

$$\chi_3 = \frac{\phi_3}{L_{\mathrm{P}}} \tag{6.3}$$

and, similarly, $\chi_{-3} = \phi_{-3} / L_{\mathrm{P}}$.

Appleton neglected second order effects and the first order axial deformation. The latter assumption was also used in the FFM analyses performed with *EvalS*, corresponding to the adoption of FFM(*M*). Actually, two analyses were performed with *EvalS*/FFM: in the first one, the geometrically nonlinear behaviour was considered using the Equivalent Forces Method; in the second one, this behaviour was ignored. The initial tangent stiffness of the nonlinear constitutive relations, characterized in Table 6.1, was chosen for the auxiliary bending stiffness distribution EI_{A}.

The nonlinear geometrical and material analysis performed with *EvalS*/FFM is now presented. Several meshes were considered, but only some of them were regular, with elements of equal length in the beams and elements of equal length in the columns. Regular mesh 1 has three elements in every beam and column. Regular mesh 2 results from the subdivision of each element of the previous mesh into three equal elements, as illustrated in Figure 6.3. The graphical output of *EvalS* in Figure 6.4 represents, for regular meshes 1 and 2, the distribution of the nonlinear component of curvature $\tilde{\chi}_{\mathrm{NL}}$ for the ultimate load F_{u}.

Figure 6.4 illustrates the localization process of the curvatures $\tilde{\chi}_{\mathrm{NL}}$ associated to mesh refinement, *i.e.*, to the progressive concentration of the higher strains as the mesh refinement increases. This result led to the definition of additional meshes, this time irregular meshes. Irregular mesh 1 results from subdividing into three elements the elements of regular mesh 2 where the absolute value of the curvature was maximum, see Figure 6.3. The following irregular meshes 2 and 3 result from subdividing into three elements the elements of the previous irregular mesh where the absolute value of the curvature was maximum: this

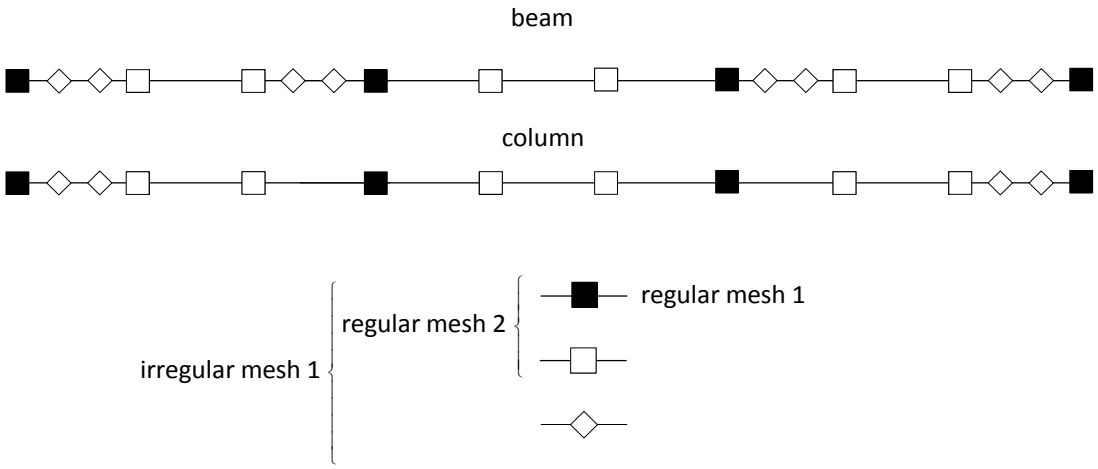

Figure 6.3. First application example: regular meshes 1 and 2 and irregular mesh 1.

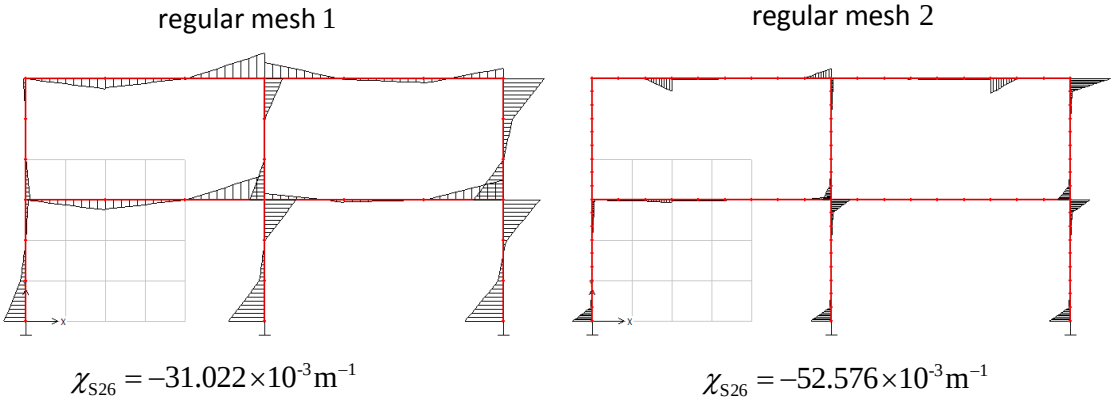

Figure 6.4. First application example: curvature fields $\tilde{\chi}_{\text{NL}}$ for ultimate load F_{u} for meshes 1 and 2 (note different curvature scales).

corresponds to a decrease of the finite elements dimension (partition norm) in the regions where the curvature is largest. It is easily observed that the solution for irregular mesh i is identical to the solution for regular mesh $i + 2$, which presents a larger number of elements. Figure 6.5 presents the force-displacement curves for the several meshes considered. Table 6.2 presents the value of relative error I for Δ (see § 3.7),

$$err_{\text{I},j}^{\Delta} = \left| \frac{\Delta_j - \Delta_{j-1}}{\Delta_{j-1}} \right| \tag{6.4}$$

for fixed values of the horizontal force F, where Δ_j is the value total drift for irregular mesh j ($err_{\text{I},1}^{\Delta}$ compares results for irregular mesh 1 and regular mesh 2). Table 6.3 presents the length L_{min} of the smallest element of each mesh, the values of F_{u}, Δ_{u} and their relative errors I,

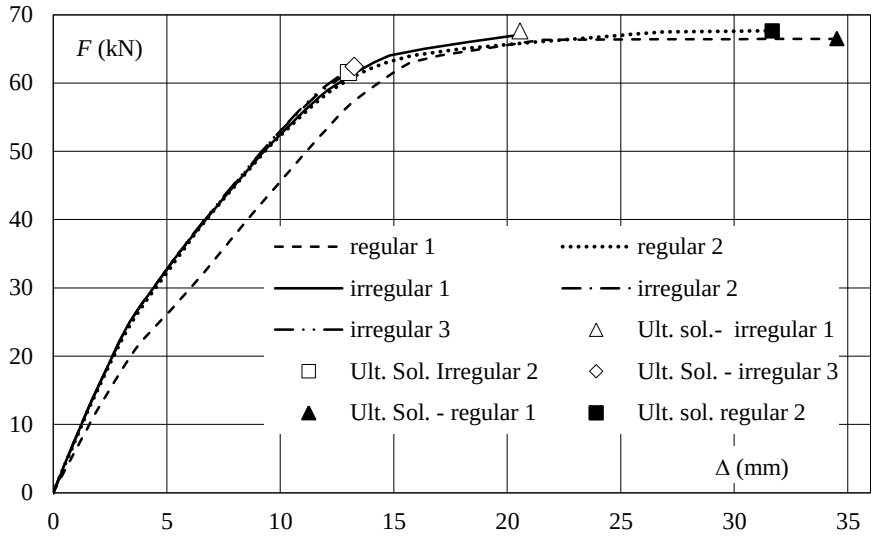

Figure 6.5. First application example: force-displacement curves computed with FFM in *EvalS*.

Table 6.2 – First application example: relative error I, $err_{\mathrm{I}}^{\Delta}[\%]$, for fixed values of force F.

mesh	$F\,[\mathrm{kN}]$					
	10	20	30	40	50	60
irregular 1	2.27	1.87	2.11	0.35	0.50	1.47
irregular 2	0.11	0.21	0.12	0.44	0.81	2.11
irregular 3	0.13	0.11	0.18	0.36	0.13	1.17

Table 6.3 – First application example: FFM solutions for several meshes.

mesh	$L_{\min}$ [cm]	F_{u} [kN]	Δ_{u} [mm]	$err_{\mathrm{I}}^{F_{\mathrm{u}}}$ [%]	$err_{\mathrm{I}}^{\Delta_{\mathrm{u}}}$ [%]
regular 1	100.00	66.47	34.51	–	–
regular 2	33.33	67.63	31.68	1.75	8.19
irregular 1	11.11	67.63	20.57	0.00	35.08
irregular 2	3.70	61.52	13.01	9.03	36.73
irregular 3	1.23	62.38	13.26	1.40	1.94

$$err_{\mathrm{I},j}^{F_{\mathrm{u}}} = \left| \frac{F_{\mathrm{u},j} - F_{\mathrm{u},j-1}}{F_{\mathrm{u},j-1}} \right| \tag{6.5}$$

$$err_{\mathrm{I},j}^{\Delta_{\mathrm{u}}} = \left| \frac{\Delta_{\mathrm{u},j} - \Delta_{\mathrm{u},j-1}}{\Delta_{\mathrm{u},j-1}} \right| \tag{6.6}$$

The results in Table 6.2 and Table 6.3 show that all relative errors err_{I}^{F}, $err_{\mathrm{I}}^{F_{\mathrm{u}}}$ and $err_{\mathrm{I}}^{\Delta_{\mathrm{u}}}$ for irregular mesh 3 have values less than 2%. Since this error is small, this solution is considered to be *mesh*-convergent.

Figure 6.6 presents the number of iterations needed to achieve *FFM*-convergence, considering geometrically nonlinear behaviour, with the irregular mesh 3 and $tol_{\text{FFM}} = 10^{-6}$. In a similar convergence analysis performed with *EvalS*/FFM, where the geometrically nonlinear behaviour was ignored, the solution for irregular mesh 3 proved again to be *mesh*-convergent.

The force-displacement curves calculated with *EvalS*/FFM will now be compared with those calculated by Appleton (1982), represented in Figure 6.7 by the solid circles. Because

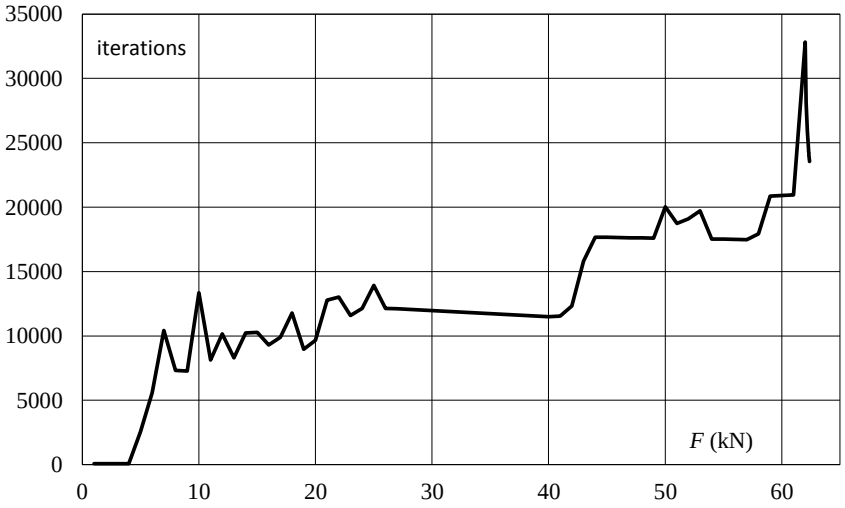

Figure 6.6. Number of iterations required to achieve *FFM*-convergence with $tol_{\text{FFM}} = 10^{-6}$ for irregular mesh 3, considering geometrically nonlinear behaviour.

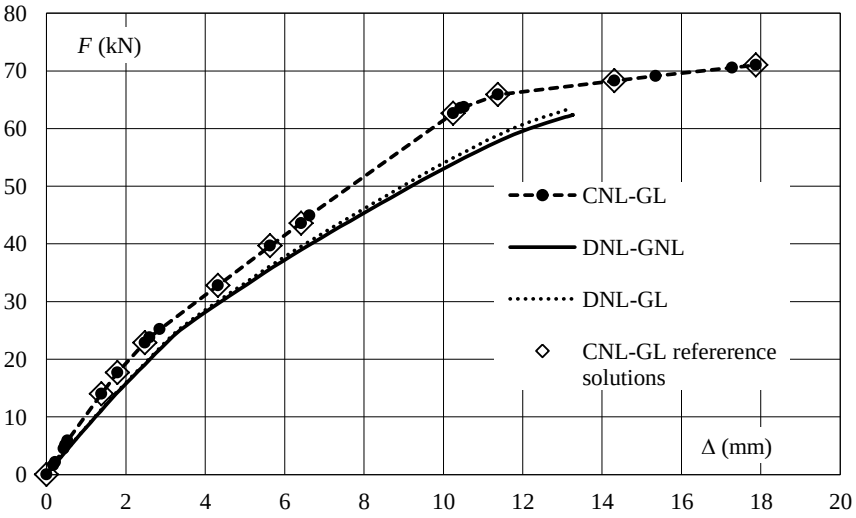

Figure 6.7. First application example: Force-displacement curves for concentrated (CNL) and distributed (DNL) material nonlinearity and for linear (GL) and nonlinear (GNL) geometrical analysis. The “reference solutions” are used in Table 6.4.

Table 6.4 – First application example: relative error of CNL and DNL-GL solutions.

Δ	[mm]	1.38	1.79	2.48	4.32	5.64	6.42	10.25	11.37	14.31	17.88
$F^{\mathrm{CNL,GL}}$	[kN]	13.98	17.66	22.88	32.81	39.67	43.59	62.64	65.89	68.27	71.00
$F^{\mathrm{DNL,GL}}$	[kN]	11.30	14.39	19.30	30.07	36.17	39.56	54.91	58.84	–	–
$F^{\mathrm{DNL,GNL}}$	[kN]	11.17	14.23	19.06	29.66	35.64	38.96	53.92	57.75	–	–
$err^{\mathrm{CNL,GL}}$	[%]	25.14	24.13	20.01	10.61	11.31	11.89	16.19	14.09	–	–
$err^{\mathrm{DNL,GL}}$	[%]	1.17	1.16	1.21	1.36	1.49	1.53	1.84	1.89	–	–

Table 6.5 – First application example: values of F_{u} and Δ_{u} for the three types of analysis.

model	F_{u} [kN]	Δ_{u} [mm]	$err^{F_{\mathrm{u}}}$ [%]	$err^{\Delta_{\mathrm{u}}}$ [%]
CNL-GL	71.00	17.88	13.82	34.79
DNL-GL	63.57	13.25	1.91	0.14
DNL-GNL	62.38	13.26	–	–

Appleton's model is based on lumped deformations at plastic hinges (CNL) in a geometrically linear (GL) analysis, the corresponding solution will be called the CNL-GL solution.

On the other hand, since *EvalS*/FFM is based on a *distributed* deformation model, its solution will be labelled DNL solution or, more precisely, DNL-GNL or DNL-GL solution, depending on the consideration, or not, of the geometrically nonlinear behaviour (using the Equivalent Forces Method).

Table 6.4 presents, for fixed values of Δ, corresponding to the CNL solutions which are labelled "reference solutions" in Figure 6.7, the relative error of the corresponding load F of the CNL and DNL-GL solutions when compared to the more accurate DNL-GNL solution,

$$err^{\mathrm{CNL,GL}} = \left| \frac{F^{\mathrm{CNL,GL}} - F^{\mathrm{DNL,GNL}}}{F^{\mathrm{DNL,GNL}}} \right| \tag{6.7}$$

$$err^{\mathrm{DNL,GL}} = \left| \frac{F^{\mathrm{DNL,GL}} - F^{\mathrm{DNL,GNL}}}{F^{\mathrm{DNL,GNL}}} \right| \tag{6.8}$$

Table 6.5 lists the values of the ultimate load F_{u} and displacement Δ_{u} calculated with the three types of analysis – CNL-GL, DNL-GL and DNL-GNL – and presents the relative error of the first two with respect, once again, to the third one,

$$err^{F_{\mathrm{u}}} = \left| \frac{F_{\mathrm{u}} - F^{\mathrm{DNL,GNL}}}{F^{\mathrm{DNL,GNL}}} \right| \tag{6.9}$$

$$err^{\Delta_u} = \left| \frac{\Delta_u - \Delta^{DNL,GNL}}{\Delta^{DNL,GNL}} \right| \tag{6.10}$$

These errors are not defined when the displacement reaches 14.31 mm, because the ultimate displacement of the DNL-GNL solution is less than this value.

The following conclusions can be extracted from the above results:

(i) The DNL-GNL solution is more flexible that the DNL-GL solution, although the difference between them is negligible – this means that geometrically nonlinear effects can be neglected in this problem, as initially admitted by Appleton (1982);

(ii) The CNL-GL model is always stiffer than the DNL-GL model, except in its last branch; actually, this last branch bestows a larger ductility to the CNL-GL model;

(iii) The ultimate displacement Δ_u is smaller for the DNL-GL model than for the CNL-GL model.

In brief, this example illustrates the importance of using spread models for nonlinear material behaviour instead of lumped models.

Finally, note that if the last branch of the constitutive relations of the columns was stiffer the difference between the CNL-GL and DNL-GL solutions would have been even greater, because in that case the nonlinear deformations would spread along the columns.

6.4. Second application example

In this second example, FFM(*M*) is applied to investigate the relevance of using a nonlinear material analysis to determine the deflections and crack width of the built-in $9\,\mathrm{m}$ long reinforced concrete beam represented in Figure 6.8. This problem was presented in the Manual on Cracking and Deformations of CEB (1985) and Favre *et al.* (1989) – note that Favre was the chairman of the task group that produced the former manual.

The concrete has the following properties: secant modulus of elasticity $E_{cm} = 30.5\,\mathrm{GPa}$, tensile strength $f_{ct} = 2.5\,\mathrm{MPa}$ and creep coefficient $\overline{\varphi} = \chi_\varphi\,\varphi = 0.8 \times 2.5$. The symmetrically disposed longitudinal reinforcement is schematically represented in Figure 6.8 (note that the concrete "cover" c is measured to center of the bars): four cases (**a** to **d**) are considered, corresponding to the reinforcement ratios given in Table 6.6. The sum of the reinforcement

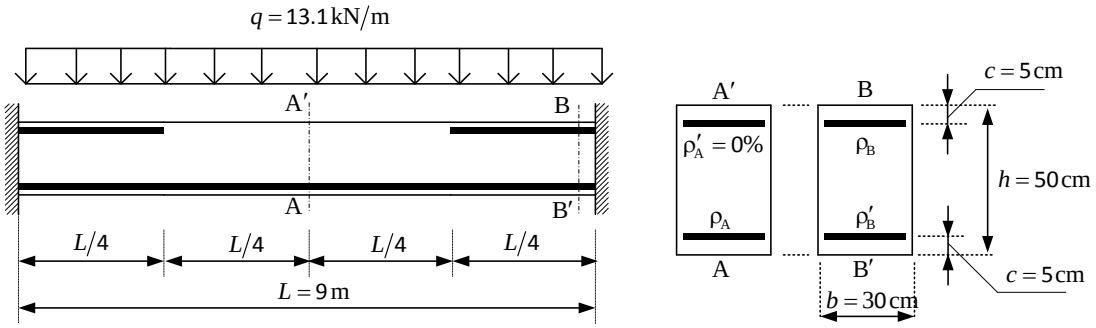

Figure 6.8. Second application example: reinforced concrete built-in beam and longitudinal reinforcement scheme.

Table 6.6 – Second application example: longitudinal reinforcement ratios.

reinforcement case	ρ_A [%]	ρ_B [%]	ρ'_B [%]	$\frac{\rho_B}{\rho_{B,E}}$	$\frac{\rho_B}{\rho_A}$	$A_{S,A}$ [cm²]	$A_{S,B}$ [cm²]	$A'_{S,B}$ [cm²]
a	0.20	0.80	0.20	1.20	4.00	2.70	10.80	2.70
b (elastic)	0.33	0.67	0.33	1.00	2.00	4.46	9.05	4.46
c (uniform)	0.50	0.50	0.33	0.75	1.00	6.75	6.75	4.46
d	0.67	0.33	0.50	0.50	0.50	9.05	4.46	6.75

ratios ($\rho_A = A_S / A_c$) at midspan, ρ_A, and at the built-in support, ρ_B, remains constant, $\rho_A + \rho_B = 1\%$. Thence, if the compression reinforcement at the supports is ignored, the ultimate plastic flexural load of the beam is the same for all cases. The distribution of steel in case **b** corresponds to a linear elastic bending moment distribution for constant cross sections ($\rho_{A,E} = \rho_{B,E} / 2 = 0.33\%$). In the fourth column of Table 6.6 the reinforcement ratio at the support is compared with this elastic value. This table shows also that, in the four cases **a** to **d**, the reinforcement is progressively transferred from the supports to midspan. This transfer is complemented with the increase of the compression reinforcement at the supports. In case **c** the tension reinforcement distribution is uniform.

The nonlinear moment-curvature relationships proposed by CEB (1985) and Eurocode 2 (CEN, 2004) were considered. Essentially, this model simulates flexure using an intermediate behaviour between the uncracked state I and the fully cracked state II.

Let us describe the methodology for computing this intermediate bending moment-curvature relationship. Consider the reinforced concrete linear element of length L with an axis of symmetry in the loading plane, top and bottom reinforcement as represented in Figure 6.9 and subjected to pure bending. The bending moment-curvature relationship of this element is

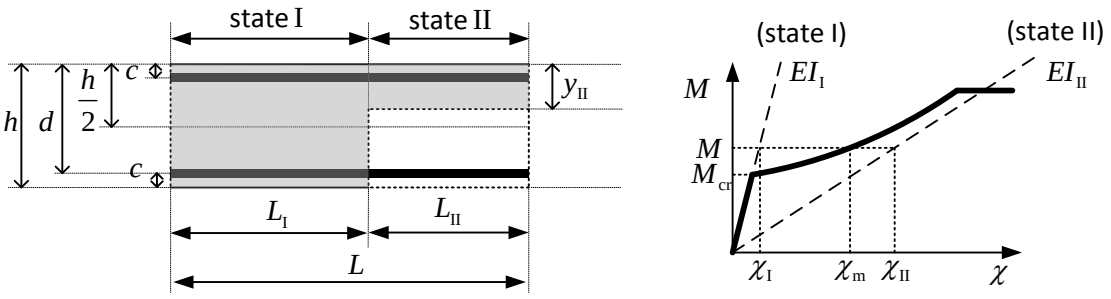

Figure 6.9. Second application example: reinforced concrete beam subjected to pure bending and bending moment-curvature relationship.

determined by an interpolation between the uncracked state I and the fully-cracked state II. Steel behaviour is admitted to be linear in both states I and II (service conditions). Concrete behaviour is admitted to be linear in state I. In state II, its tension stiffness is ignored (Ghali *et al.*, 2002) and its compressive behaviour is also admitted linear. The latter hypothesis is reasonable for the magnitude of the stresses in service conditions. Under these hypotheses, this beam can be modelled by a pair of beam segments with lengths L_1 and L_2 corresponding to sates I and II, see Figure 6.9, with an intermediate curvature given by,

$$\chi_{\mathrm{m}} = (1-\xi)\,\chi_{\mathrm{I}} + \xi\,\chi_{\mathrm{II}} \tag{6.11}$$

see right hand side of Figure 6.9. In this expression, χ_{I} and χ_{II} are the curvatures of the segments in state I and II and $\xi = L_{\mathrm{II}}/L$ is the fraction of the beam length in state II. This coefficient is given in § 7.4.3(3) of Eurocode 2 (CEN, 2004)

$$\xi = 1-\beta\left(\frac{M_{\mathrm{cr}}}{M}\right)^2 \tag{6.12}$$

where M_{cr} is the cracking bending moment and coefficient β represents the influence of loading duration or repetition: $\beta = 1.0$ for initial loading and $\beta = 0.5$ for loads applied in a sustained manner or for a large number of load cycles, see also Ghali *et al.* (2002).

This is all that is required for the calculation of the bending moment-curvature relationship, according to the following procedure (Ghali *et al.*, 2002):

(i) Determine the neutral axis positions in states I and II (both fixed, since the axial force is null);

(ii) Integrate over the cross section area the moment about those axes due to the normal stresses for a unit curvature, determining the bending stiffnesses EI_{I} and EI_{II}, which characterize the linear bending moment-curvature relations in states I and II;

(iii) Define a set of values of the bending moment;

(iv) For each of these bending moment values, determine the curvatures in states I and II,

$$\chi_{\mathrm{I}} = \frac{M}{EI_{\mathrm{I}}}, \qquad \chi_{\mathrm{II}} = \frac{M}{EI_{\mathrm{II}}} \tag{6.13}$$

(v) Calculate the coefficient ξ;

(vi) Determine the average curvatures with expression (6.11).

The influence of concrete creep is considered by modifying its modulus of elasticity, as suggested in §7.4.3(5) of Eurocode2 (CEN, 2004). The application of this procedure to the beam in analysis led to the bending moment-curvature diagrams represented in Figure 6.10.

The nonlinear material analysis performed with *EvalS*/FFM is now presented. Since a uniform mesh with less than four elements would not satisfactorily represent the longitudinal distribution of the reinforcement, three uniform meshes with 4, 8 and 16 elements were considered. The length of the elements of the third mesh is $1.125\ h$, where h is the cross section depth.

A constant auxiliary bending stiffness $EI_{\mathrm{A}} = E_{\mathrm{cm}}\, b h^3/12$, corresponding to the concrete gross cross section, was defined for all models. Table 6.7 present the number of iterations needed to achieve *FFM*-convergence with $tol_{\mathrm{FFM}} = 10^{-6}$.

Figure 6.11 represents the bending moment at the beam end sections and midspan, computed by *EvalS*/FFM and including creep, revealing the *mesh*-convergence of the solutions. For comparison purposes, this figure also shows the linear elastic solution for a beam with constant cross sections and the nonlinear solution determined in CEB (1985) using the above model (revealing that a rather coarse mesh was used in the latter case). In case **d** the (absolute value of the) bending moment decreases at the end sections B, because $\rho_{\mathrm{B}} < \rho_{\mathrm{B,E}}$, while in case **a** the bending moment decreases at midspan, because $\rho_{\mathrm{A}} < \rho_{\mathrm{A,E}}$.

Table 6.7 – Number of iterations required to achieve FFM-convergence with $tol_{\mathrm{FFM}} = 10^{-6}$.

reinforcement case	4 el	8 el	16 el
a	264	97	579
b	228	319	349
c	207	249	305
d	242	330	340

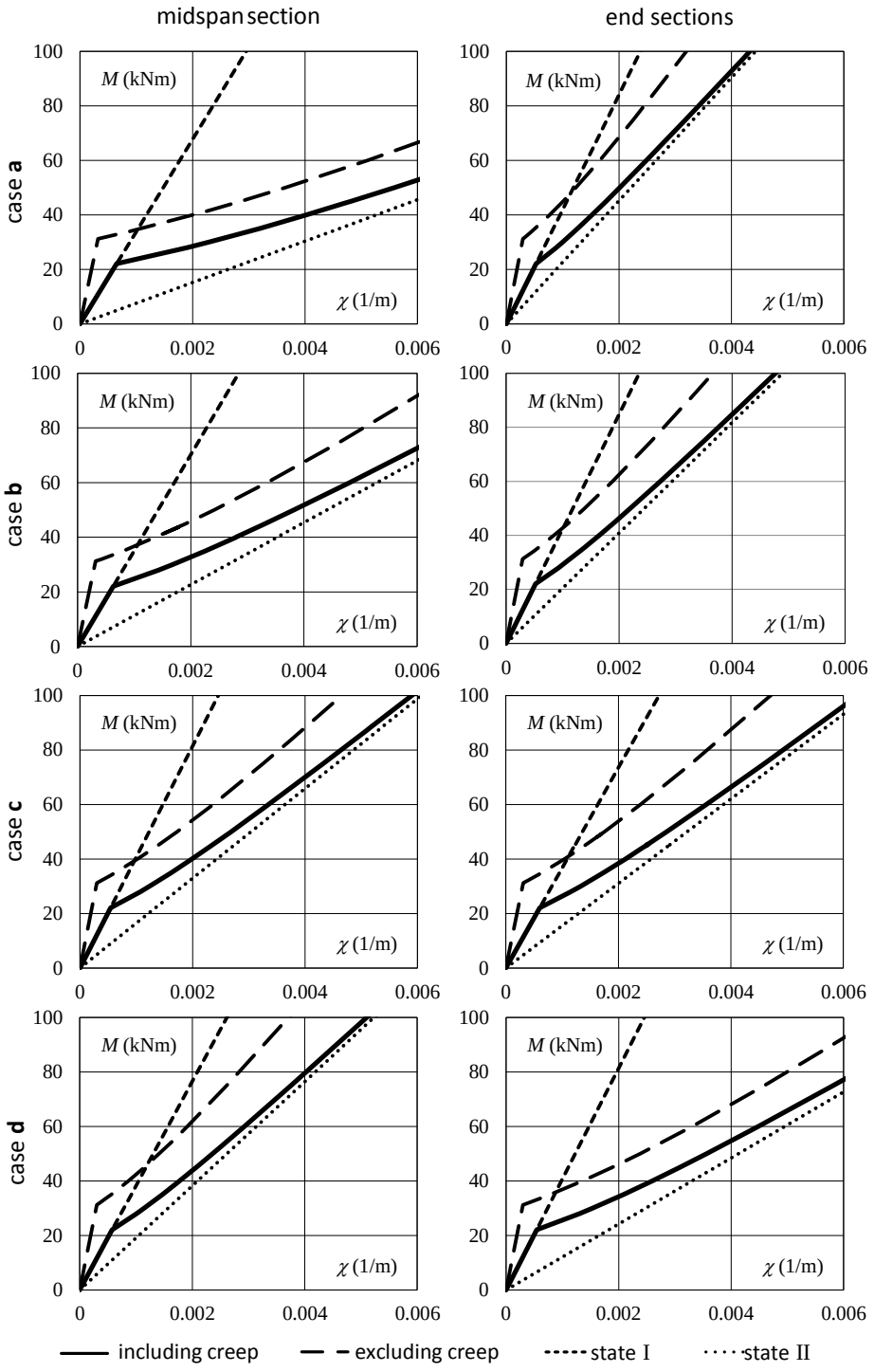

Figure 6.10. Second application example: computed RC moment-curvature relationships.

The values of the midspan deflection computed with *EvalS*/FFM are now compared to the values presented in CEB (1985) and Favre *et al.* (1989), designated CEB solutions. The latter solution is based on the constitutive model described above and the corresponding nonlinear bending moments represented in Figure 6.11. In CEB (1985) and Favre *et al.* (1989) the

deflection is also determined by the bilinear method, a simplified method based on the linear bending moments.

These results, presented in Figure 6.12 and in Table 6.8, show once more the *mesh*-convergence of the *EvalS*/FFM solutions. The difference between the results given by the nonlinear analyses and by the bilinear method show the relevance of the nonlinear material analysis. Actually, the redistribution of bending moments is not considered by the bilinear method because it is based on the linear elastic solution. This redistribution, patent in Figure 6.11, is coherent with the deflections presented in Figure 6.12.

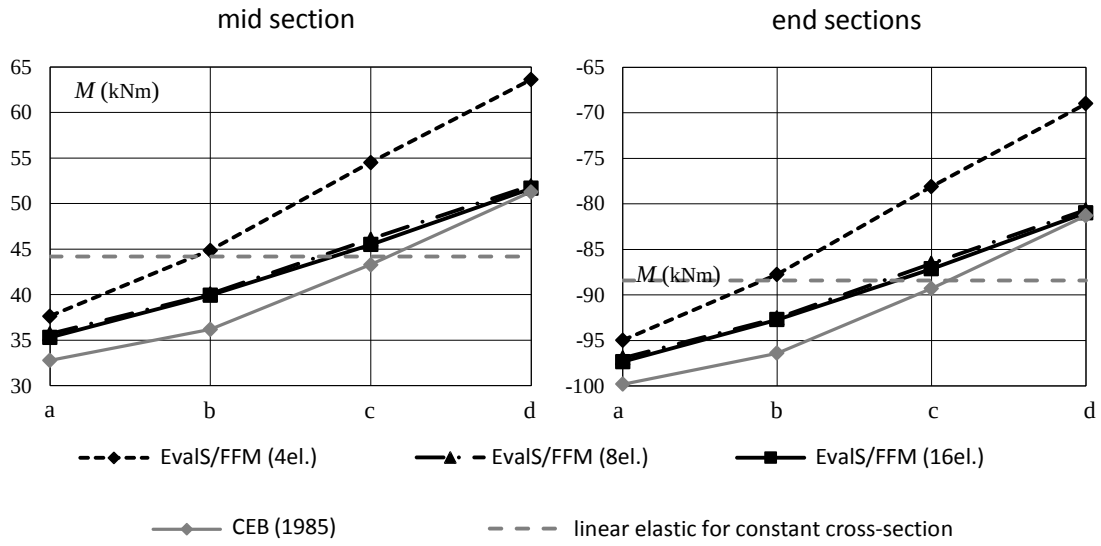

Figure 6.11. Second application example: bending moment at midspan and supports (including creep).

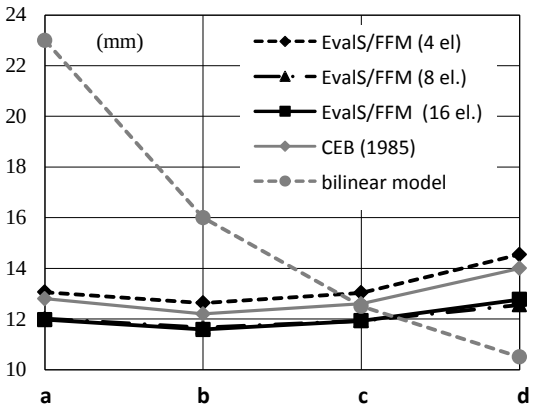

Figure 6.12. Second application example: midspan deflection (including creep).

Table 6.8 – Second application example: deflection and its relative errors w.r.t. the 16 elements *EvalS*/FFM solution (including creep).

reinforcement case	*EvalS*/FFM 4 elements		*EvalS*/FFM 8 elements		*EvalS*/FFM 16 elements		CEB (1985)		bilinear model	
	[mm]	[%]	[mm]	[%]	[mm]		[mm]	[%]	[mm]	[%]
a	13.06	9.08	12.01	0.32	11.97	–	12.80	6.91	23.00	92.10
b	12.63	9.05	11.67	0.71	11.58	–	12.20	5.32	16.00	38.12
c	13.03	9.23	11.93	-0.03	11.93	–	12.60	5.60	12.50	4.76
d	14.55	13.90	12.56	-1.68	12.77	–	14.00	9.62	10.50	-17.78

Determination of maximum crack width is considered next. According to Eurocode 2 (CEN, 2004), the crack width can be estimated by the expression

$$w_{\mathrm{k}} = s_{\mathrm{r,max}} \left(e_{\mathrm{sm}} - e_{\mathrm{cm}} \right) \tag{6.14}$$

where $s_{\mathrm{r,max}}$ is the maximum crack spacing, calculated according to the dispositions in Eurocode 2, and $e_{\mathrm{sm}} - e_{\mathrm{cm}}$ is the difference between the mean strains of reinforcement, e_{sm}, and of concrete between cracks, e_{cm}, which is determined by

$$e_{\mathrm{sm}} - e_{\mathrm{cm}} = \frac{\sigma_{\mathrm{s}} - \Delta\sigma}{E_{\mathrm{s}}} \geq 0.6 \frac{\sigma_{\mathrm{s}}}{E_{\mathrm{s}}} \tag{6.15}$$

where σ_{s} is the stress in the tension reinforcement assuming a cracked section, E_{S} is the modulus of elasticity of reinforcement and

$$\Delta\sigma = k_{\mathrm{t}} \frac{f_{\mathrm{ct,eff}}}{A_{\mathrm{s}} / A_{\mathrm{c,eff}}} \left(1 + \frac{E_{\mathrm{s}}}{E_{\mathrm{cm}}} \frac{A_{\mathrm{s}}}{A_{\mathrm{c,eff}}} \right) \tag{6.16}$$

where k_{t} is a load duration factor (0.6 for short term and 0.4 for long term loads), E_{cm} is the secant modulus of elasticity of concrete, $f_{\mathrm{ct,eff}}$ is the mean value of the tensile strength of the effective concrete at the time the first cracks are expected to occur, A_{S} is the total cross-sectional area of the longitudinal tensile reinforcement and $A_{\mathrm{c,eff}}$ is the effective area of concrete in tension surrounding the reinforcement, which is considered to be given by

$$A_{\mathrm{c,eff}} = b\, h_{\mathrm{eff}} \tag{6.17}$$

with

$$h_{\mathrm{eff}} = \min\left(2.5(h-d), \frac{h-x}{3}, \frac{h}{2} \right) \tag{6.18}$$

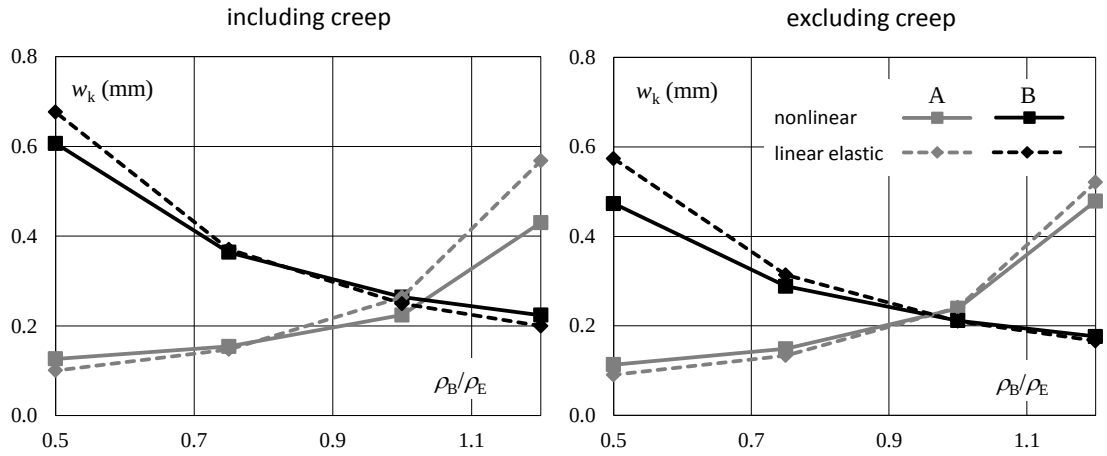

Figure 6.13. Second application example: crack width values.

Table 6.9 – Second application example: crack with and its relative errors w.r.t. the 16 elements *EvalS*/FFM solution (including creep).

reinforcement case	midspan			end sections		
	nonlinear [mm]	linear [mm]	error [%]	nonlinear [mm]	linear [mm]	error [%]
a	0.43	0.57	-24.24	0.22	0.20	12.19
b	0.22	0.26	-15.11	0.26	0.25	5.92
c	0.15	0.15	4.48	0.36	0.37	-1.74
d	0.13	0.10	25.40	0.61	0.68	-10.32

where x is the distance from the neutral axis to the top edge of the cross section, which is under compression. Using this model, the maximum crack width based on the nonlinear analysis performed with *EvalS*/FFM was determined. The normal stress σ_s in the reinforcement in state II, entering in (6.15), corresponds to the nonlinear bending moments computed for the mesh with 16 elements. Figure 6.13 and Table 6.9 present the crack width for this value of σ_s and also for the linear elastic bending moments, with and without the influence of creep. From these results, the following conclusions can be extracted:

(i) the crack width increases when the effect of creep is considered;

(ii) the relation between crack widths based on linear elastic bending moments and on a nonlinear analysis is not affected by creep;

(iii) the nonlinear analysis determines smaller crack widths than the linear analysis when $\rho \neq \rho_E$, see Table 6.9. This difference is greater when ρ is significantly different from ρ_E, which may be explained by the larger redistribution of bending moments for such cases.

In conclusion, these results show the relevance of performing a nonlinear material analysis when the crack width is required.

Chapter 7
Conclusions and further developments

7.1. Conclusions

The two central objectives of this thesis were the presentation and justification of the 1D Fictitious Force Method, in its several forms, and the clarification of the meaning of its iterative procedures from both physical and mathematical points of view. Both these objectives were fully accomplished: (i) FFM, a method for the quasi-static nonlinear elastic analysis of plane skeletal structures, was developed from a rigorous mechanical framework, (ii) a deep insight on its historical antecedents and basic fundaments was offered and (iii) the way the method operates was portrayed, *e.g.* including several flowcharts and schematic illustrations.

The main idea behind FFM, *i.e.* the solution of a problem with the help of a much simpler auxiliary problem, which must be solved iteratively, is shared by other methods of structural analysis. However, it appears that, for different reasons, the common points between these methods had never been illuminated before. Thence, our bibliographic review, instead of a more traditional approach, sought to reveal the common roots of several methods which, at first sight, could appear to be completely dissimilar. One important conclusion is that the systematisation of similar processes is possible and helpful, because it avoids the need to start everything from the very beginning.

Two distinct FFM approaches are possible, depending on the chosen control variable: either stresses or strains. The first is associated to FFM_S and the second to FFM_{Def}. Even though these two approaches are conceptually distinct and lead to different convergence conditions and different performances, most of the general procedure of FFM is common to both, as the shaded areas in the presented flowcharts reveal. In practical terms, this means that the analyst can chose the approach that suits him better. According to the presented analysis and comparison of results, FFM_{Def} seems to be more interesting for use in practise, since its convergence criterion is more easily satisfied.

When first established (Gala, 2007), FFM was anchored on the beam *model M*. Actually, a structural analysis method should be independent of specific application limitations. Moreover, as is well known (Blaauwendraad, 1972), the beam *model M*, which considers the constitutive relation at the cross-sectional level, is not always an acceptable model for the nonlinear material analysis of skeletal structures. The truss *model N* and beam column *model MN*, developed in chapters 4 and 5, demonstrate that the FFM idea is perfectly general. In particular, since in *model MN* the constitutive relation is considered at the fibre level, this model provides a much larger versatility than the most familiar beam *model M*. In the case of composite materials, such as reinforced concrete, the gains in terms of accuracy afforded by *model* MN are of course enormous.

Since FFM is an iterative method, its convergence conditions had to be established. Moreover, because the auxiliary stiffness field must be defined by the analyst and because this choice strongly affects the convergence conditions, the range of admissible values and the ideal values for this stiffness had to be determined. This was clearly achieved in the form of the proposed sufficient convergence conditions and associated commentaries.

FFM should be simple to apply, its implementation in linear analysis programs should be easy and, obviously, it should be capable of effectively tackling the quasi-static nonlinear elastic analysis of skeletal structures. Having this in mind, two types of application examples were presented in the thesis: while the first group of examples has a pedagogical objective, because of their simplicity, the second group reveals the potential of the method. Moreover, ever since the method was integrated in the structural analysis program *EvalS* it has also been employed by other authors in their studies.

The examples presented in chapters 3 to 5 are basic illustrations of the application of FFM. These examples served also to show the influence of the auxiliary stiffness in terms of the

numerical efficiency of the method. This parameter plays a relevant role: the examples confirm that its value can and must be chosen in a certain range and that the speed of convergence if affected by the analyst choice.

The development of a new method of structural analysis should not be concluded with the presentation of the corresponding governing equations. Even though structural systems are recurrently simple, more often than not they are large, which means that appropriate software is required for their analysis. The flowcharts included along the thesis have in mind the implementation of FFM in any program of linear structural analysis. Actually, these flowcharts were used to implement FFM in the program *EvalS* (2011) by Ferreira, its author, and Costa, who investigated the behaviour of beam-column joints in reinforced concrete frames (Costa, 2013). In fact, those flowcharts and other parts of the thesis also reflect the experience and many valuable suggestions by these two authors.

The practical application of FFM to the analysis of reinforced concrete skeletal structures was illustrated with two last examples. FFM or, more precisely, its implementation in *EvalS*, proved to be suitable to tackle these nonlinear problems. An interesting specificity is it capacity to consider the material nonlinearity distributed along the linear elements, in alternative to the lumped models provided by many structural analysis programs. Reinforce concrete was chosen for these examples not because of a special aptitude of FFM for this material but only to demonstrate its capabilities: they are better illustrated with the strong nonlinearities of reinforced concrete than with other more well-behaved structural materials.

As a final comment to these conclusions, it must be stressed that it is not consider that this line of investigation is ended. The next section presents suggestions of some topics that require more research.

7.2. Further developments

The origin of the suggestions for further developments of this work is threefold: (i) during the present investigation some new problems and questions appeared naturally, (ii) there are also some topics that, initially, were ment to be investigated, but which were left behind, and, finally, (iii) there is a group of issues whose investigation could not be concluded.

The numerical investigation of the role played by the auxiliary stiffness in the efficiency of the method should be pursued in order to establish more objective criteria, *i.e.* criteria which are less problem dependent, regarding the characteristics that the auxiliary stiffness field should have in order to lead to a small number of iterations for convergence.

The convergence of FFM(MN)$_S$ should be further investigated and convergence conditions established. In case the analytical approach reveals to be unfruitful, a numerical investigation of the convergence conditions, e.g. the determination of admissible values and also of optimal values of the auxiliary stiffness, should be carried out.

FFM must be extended to consider constitutive laws with softening branches. It is important to derived sufficient convergence conditions for such behaviour, for both FFM(*M*) and FFM(*MN*).

The convergence conditions of FFM(*MN*) should be improved for the particular case of composite structural materials, see the concluding remarks of chapter 5.

The use of higher order interpolation in the discrete descriptions of FFM, should also be developed and studied. Particularly, it should be evaluated if more complex systems of fictitious forces, with more elemental interpolation sections, is interesting from the numerical point of view, because fewer elements will be needed to achieve *mesh*-convergent solutions. This was illustrated with the second example in chapter 3, which compared the performance of FFM(M)$_2$ and FFM(M)$_3$, particularly with respect to the *mesh*-convergence. Ferreira (2013) is already investigating this matter, having in mind the application of FFM *model N* to the analysis of adaptative stress field models.

An important further development is the possibility of the combination of the Equivalent Force Method with FFM for the nonlinear material and geometrical analysis of skeletal structures. The convergence of the simultaneous application of these two methods should be studied. In particular, it should be investigated how the convergence criteria of these two methods change when they are combined.

FFM should be extended to non-holonomic elastic-plastic analysis, which requires the development of an incremental description of the method. Ferreira (2013) is also currently working on this topic having in view the analysis of adaptative stress field models.

As a last topic, a deeper investigation of the operators G^{I} which transform initial deformations (resp. initial stresses) into effective generalized deformations (resp. effective generalized stresses) can be a relevant development. Moreover, in the discrete case, the close

relation between matrices $\mathbf{T}$ and the similar matrices established by Fellipa *et al.* (1997, 2001) should be investigated.

References

Adams, P. F. (1974). *The Design of Steel Beam-Columns.* Canadian Steel Industries Construction Council, Wilowdale: 58.

Aguado, A., (1980). *Estudio del análisis no lineal de estructuras de hormigón mediante superposición de problemas lineales en deformaciones [Nonlinear Analysis of Reinforced Concrete Structures by Superimposing the Effect of Deformations].* Universidad Politécnica de Barcelona, Barcelona, PhD Thesis: 406.

Aguado, A., Murcia, J. and Mari, A. (1981). *Nonlinear Analysis of Concrete Structures by the Imposed Deformations Method. Comparison with Experimental Results*. IABSE Colloquium on Advanced Mechanics of Reinforced Concrete, Delft: 255-262.

Akgun, M. A. Garcelon, J. H. and Haftka R. T. (2001). *Fast Exact Linear and Non-linear Structural Reanalysis and the Sherman-Morrison-Woodbury Formulas.* International Journal for Numerical Methods in Engineering, 50(7): 1587-1606.

Appleton, J. (1982). *Análise Não-linear de Pórticos Planos de Betão Armado Sujeitos à Flexão [Nonlinear Analysis of Reinforced Concrete Portal Frames].* Laboratório Nacional de Engenharia Civil, Seminário 295, Lisboa: 130.

Arantes e Oliveira, E. R. (1975). *Foundations of the Mathematical Theory of Structures.* Springer-Verlag, Wien-New York: 223.

Arantes e Oliveira, E. R. (1999). *Elementos da Teoria da Elasticidade [Elements of the Theory of Elasticity*]. ISTPress, Lisboa: 176.

Argyris, J. H. and Kelsey, S. (1960). *Energy Theorems and Structural Analysis – A Generalised Discourse with Applications on Energy Principles of Structural Analysis Including the Effects of Temperature and Non-Linear Stress-Strain Relations*. London Butterworths, London: 60.

Argyris, J. H. and Kelsey, S. (1957). *The Matrix Force Method of Structural Analysis and Some New Applications.* Ministry of Supply, Aeronautical Research Council Reports and Memoranda, Reports and Memoranda nº 3034, London: 44.

Argyris, J. H. (1965). *Elasto-plastic Matrix Displacement Analysis of Three-Dimensional Continua.* Journal of Royal Aeronautic Society, 69: 633-636. *Cited by* Argyris, J. H. and Scharpf, D. W. (1972). *Methods of Elastoplastic Analysis.* Journal of Applied Mathematics and Physics (ZAMP), 23: 517-552.

Argyris, J. H. and Scharpf, D. W. (1972). *Methods of Elastoplastic Analysis.* Journal of Applied Mathematics and Physics (ZAMP), 23: 517-552.

Atkinson, K. and Han, W. (2001). *Theoretical Numerical Analysis: a Functional Analysis Framework.* Texts in Applied Mathematics, Springer-Verlag, New York: 450.

Bailey, P. B., Shampine L. F. and Waltman, P. E. (1968). *Nonlinear Two Point Boundary Value Problems*. Academic Press, New York: 171.

Becker, E. B., Carey, G. F. and Oden, J. T. (1981). *Finite Elements: an Introduction.* Prentice-Hall, Englewood Cliffs, 1: 258.

Beer, F. P., Johnston, E. R., Eisenberg, E. R., Staab, G. H. (2005). *Vector Mechanics for Engineers: Statics*. 7th ed., McGraw-Hill Higher Education: 648.

Blaauwendraad, I. J. (1972). *Realistic Analysis of Reinforced Concrete Framed Structures*. Heron, 18(4): 31.

Borkowski, A. (1988). *Analysis of Skeletal Structural Systems in the Elastic and Elastic-plastic Range.* Elsevier, New York: 223.

CEB (1974). *Bulletin d'Information nº 103: CEB – Buckling Manual.* Comité Euro-International du Béton, Paris: 234.

CEB (1985). CEB Design Manual on Cracking and Deformations. Comité Euro-International du Béton, Lausanne: 243.

CEN (2004). *EN 1992-1-1, Eurocode 2: Design of Concrete Structures – Part 1.1: General Rules and Rules for Buildings.* European Committee for Standardisation, Brussels: 225.

Chapra, S. C. and Canale, R. P. (2010). *Numerical Methods for Engineers.* 6th ed., McGraw-Hill Higher Education, New York: 960.

Chen, P. F. and Powell, G. H. (1982). *Generalized Plastic Hinge Concepts for 3D Beam-Column Elements.* University of California, Report UCB/EERC-82/20, Berkeley: 275.

Chen, W.F. and Lui, E. M. (1991). *Stability Design of Steel Frames.* CRC Press: 380.

Costa, R. (2013). *Modelação de ligações viga-pilar na análise de estruturas porticadas planas de betão armado [Beam-column joints modelling in framed reinforced concrete structures analysis].* Universidade de Coimbra, Coimbra, PhD Thesis: 491.

Cross, H. (1936). *Analysis of Flow in Networks of Conduits or Conductors.* University of Illinois, Engineering Experiment Station, Bulletin nº 286, Urbana: 29. *Cited by* Kolakowski, P., Wiklo, M. and Holnicki-Szulc, J. (2008). *Virtual Distortion Method – a Versatile Reanalysis Tool for Structures and Systems.* Review Article, Structural and Multidisciplinary Optimization, 36(3): 217-234.

Deng, L. and Ghosn, M. (2001). *Pseudoforce Method for Nonlinear Analysis and Reanalysis of Structural Systems.* Journal of Structural Engineering ASCE, 127(5): 570-578.

Dias da Silva, V. (2006). Mechanics and Strength of Materials, Springer, Berlin Heidelberg: 478.

Favre, R., Jaccoud, J. P., Koprna, M. and Radojicic, A. (1989). *Dimensionnement des Structures en Béton [Design of Concrete Structures].* Traité de la Génie Civil de l´École Polytechnique Fédérale de Lausanne, Presses Polytechniques et Universitaires Romandes, Lausanne, 8: 591.

Felippa, C. A. (2001). *A Historical Outline of Matrix Methods of Structural Analysis: a Play in Three Acts.* Computers and Structures, 79,14; 1313-1324.

Felippa, C. A. and Park, K. C. (2001). *The Construction of Free-Free Flexibility Matrices for Multilevel Structural Analysis.* University of Colorado, Centre for Aerospace Structures, Report CU-CAS-01-06, Boulder: 31.

Felippa, C. A. and Park, K. C. and Filho, M. R. J. (1997). *The Construction of Free-Free Flexibility Matrices as Generalized Stiffness Inverses.* University of Colorado, Centre for Aerospace Structures, Report CU-CAS-97-09, Boulder: 14.

Ferreira, M. (2011). *EvalS 2.2 – User's Manual*, Leiria.

Ferreira, M. (2013).*Estudo de Zonas de Descontinuidade com Modelos de Campos de Tensões Sujeitos a Acções Cíclicas [Analysis of Discontinuity Regions Under Ciclic Loads with Stress Field Models under].* Universidade de Lisboa, Instituto Superior Técnico, PhD Thesis (work in progress).

Ferreira. M., Costa, R., Gala, P. and Providência, P. (2011). *O Método das Forças Fictícias com Modelo de Fibras Aplicado à Análise de Estruturas de Betão Armado [The Fictitious Force Method with a Fibre Model Applied to the Analysis of Reinforced Concrete Structures].* Congresso de Métodos Numéricos em Engenharia 2011, Coimbra: 18.

Ferry Borges, J. and Arantes e Oliveira, E. R. (1964). *Non-Linear Analysis of Reinforced Concrete Structures.* Laboratório Nacional de Engenharia Civil, Technical Paper nº 223, Lisbon: 19.

Fertis, D. G. (2009). *Nonlinear Structural Engineering.* Springer, Berlin: 347.

Fertis, D. G. and Keene, M. E. (1990). *Elastic and Inelastic Analysis of Nonprismatic Members.* Journal of Structural Engineering ASCE, 116(2): 475-489.

Fertis, D. G. and Taneja, R. (1991). *Equivalent Systems for Inelastic Analysis of Prismatic and Nonprismatic Members.* Journal of Structural Engineering ASCE, 117(2): 473-488.

Gala, P., (2007). *O Método das Forças Fictícias na Modelação da Não Linearidade Material em Estruturas Reticuladas [The Fictitious Force Method in Modelling the Nonlinear Material Behaviour of Skeletal Structures]*. Universidade de Coimbra, Coimbra, MSc Thesis: 148.

Gala, P., Providência, P., Dias da Silva, V. and Ferreira, M., (2010). *O Método das Forças Fictícas na Modelação 1D da Não Linearidade Material em Estruturas Porticadas de Betão Armado – Aplicação à Análise Push-Over [The Fictitious Force Method in Modelling the Nonlinear Material Behaviour of Reinforced Concrete Skeletal Structures - an Application to the Determination of the Resistant Capacity Curve]*. Encontro Nacional de Betão Estrutural 2010, Lisboa: 10.

Gala, P., Ferreira, M., Providência, P. and Dias da Silva, V. (2012). *Avaliação da Fendilhação e Deformação em estruturas de Betão Armado com Análise Materialmente Não Linear [Assessing Cracking and Deformation in Reinforce Concrete Structures with Nonlinear Material Analysis]*. National Meeting of the Portuguese Association of Structural Concrete, Porto: 10.

Ghali, A., Favre, R. and Elbadry, M. (2002). *Concrete Structures - Stresses and Deformations.* 3rd ed., E&FN Spon, New York: 609.

Golub, G. H. and Van Loan, C. F. (1996). *Matrix Computation.* 3rd ed., John Hopkins University Press, Baltimore: 728. *Cited by* Deng, L. and Ghosn, M. (2001). *Pseudoforce Method for Nonlinear Analysis and Reanalysis of Structural Systems.* Journal of Structural Engineering ASCE, 127(5): 570-578.

Holnicki-Szulc, J. (1989). *Optimal Structural Remodelling – Simulation by Virtual Distortion.* Communications in Applyed Numerical Methods, 5: 289-298.

Holnicki-Szulc, J. (1991). *Virtual Distortion Method.* Springer-Verlag, Berlin: 176.

Jennings, A. and McKeown, J. J. (1992). *Matrix Computation.* 2nd ed., Wiley, Chichester: 427.

Kolakowski, P., Wiklo, M. and Holnicki-Szulc, J. (2008). *Virtual Distortion Method – a Versatile Reanalysis Tool for Structures and Systems.* Review Article, Structural and Multidisciplinary Optimization, 36(3): 217-234.

Lang, S. (2010). Undergraduate Analysis (Undergraduate Texts in Mathematics). 2nd ed., Springer, New Haven: 642.

Lin, T.H. (1968). *Theory of Inelastic Structures.* John Wiley & Sons, New York: 454.

Lui, E.M. (1988). *A Practical P-Delta Analysis Method for Type FR and PR Frames.* Engineering Journal AICS, 25(3): 85-98.

Lui, E. M. and Zhang, C. Y. (1990). *Nonlinear Frame Analysis by The Pseudo Load Method.* Computers and Structures, 37(5): 707-716.

Macchi, G. (1973). *Méthode des Rotations Imposés. Exposé de la Méthode et Example de Calcul [Method of Imposed Rotations. Explanation of the method and Aplication Example].* CEB International Course on Structural Concrete, Lisbon. *Cited by* Aguado, A., (1980). *Estudio del análisis no lineal de estructuras de hormigón mediante superposición de problemas lineales en deformaciones [Nonlinear Analysis of Reinforced Concrete Structures by Superimposing the Effect of Deformations].* Universidad Politécnica de Barcelona, Barcelona, PhD Thesis: 406.

Maier, G. (1970). *A Matrix Structural Theory of Piecewise-Linear Elastoplasticity With Interacting Yield Planes.* Meccanica 7: 51-66. *Cited by* Kolakowski, P., Wiklo, M. and Holnicki-Szulc, J. (2008). *Virtual Distortion Method – a Versatile Reanalysis Tool for Structures and Systems.* Review Article, Structural and Multidisciplinary Optimization, 36(3): 217-234.

Maier, G. (1972). *Mathematical Programming Methods in Structural Analysis.* International Conference on Variational Methods in Engineering., Southampton University Press. *Cited by* Teixeira de Freitas (1990). *Elastoplastic Analysis of Skeletal Structures.* in Mathematical Programming Methods in Structural Plasticity, CISM – International Centre for Mechanical Sciences, Courses and Lectures nº 299, Springer-Verlag, Udine: 153:169.

Makode, P. V., Ramirez, M. R. and Corotis, R. B. (1996). *Reanalysis of Rigid Frame Structures by the Virtual Distortion Method.* Structural Optimization 11: 71-79.

Makode, P. V., Corotis R. B. and Ramirez, M. R. (1999a). *Nonlinear Analysis of Frame Structures by Psuedo Distortions.* Journal of Structural Engineering ASCE, 125(11): 1309-1317.

Makode, P. V., Corotis R. B. and Ramirez, M. R. (1999b). *Geometric Nonlinear Analysis of Frame Structures by Pseudo Distortions.* Journal of Structural Engineering ASCE, 125(11): 1318-1327.

Mari, A., Murcia, J. and Aguado, A. (1982). *Second Order Analysis of Reinforced Concrete Frames.* In CEB Bulletin d'Information nº 153, Comité Euro-International du Béton, Paris: 183-197.

MC90 (1990). CEB-FIP Model Code 1990 - Design Code. Comite Euro-International du Beton – The International Federation for Structural Concrete. Thomas Telford Services Ltd, London: 437.

Morisset, A. (1976). *Stabilité des Piles et des Pylônes - Théories et Méthodes de Calcul.* Annales de L'Institut Technique du Bâtiment et des Travaux Publics nº 335.

Nowacki, W. (1970). *Teoria Sprężystości [Theory of Elasticity].* PWN, Warsaw: 769. *Cited by* Kolakowski, P., Wiklo, M. and Holnicki-Szulc, J. (2008). *Virtual Distortion Method – a Versatile Reanalysis Tool for Structures and Systems.* Review Article, Structural and Multidisciplinary Optimization, 36(3): 217-234.

Ortega, J. M. and Rheinboldt, W. C. (1970). *Iterative Solution of Nonlinear Equations in Several Variables.* SIAM, New York: 572.

Pina, H. (2010). *Métodos Numéricos [Numerical Methods].* Escolar Editora: 932.

Powell, G. H. and Chen, P. F. (1986). *3D Beam-Column Element with Generalized Plastic Hinges.* Journal of Engineering Mechanics ASCE, 112(7): 627-641.

Reddy, J. N. (1984). *An introduction to the Finite Element Method.* McGRaw-Hill International Editions, New York.

Reis, A. and Camotim, D. (2001). *Estabilidade Estrutural [Structural Stability].* McGraw-Hill Portugal, Alfragide: 470.

Richard, R. M. and Abbott, B. J. (1975). *Versatile Elastic-Plastic Stress-Strain Formula.* Journal of the Engineering Mechanics Division ASCE, 101(EM-4): 511-515.

Santana, A. P. and Queiró, J. F. (2010). *Introdução à Álgebra Linear [Introduction to Linear Algebra]*. Gradiva Publicações: 492.

Shampine, L. F. (1968). *Boundary Value Problems For Ordinary Differential Equations.* SIAM Journal of Numerical Analysis, 5(2): 219-242.

Sherman, J. and Morrison, W. J. (1949). *Adjustment of an Inverse Matrix Corresponding to Changes in the Elements of a Given Column or a Giving Row of the Original Matrix.* Annals of Mathematical Statistics, 20(4): 621. *Cited by* Akgun, M. A. Garcelon, J. H. and Haftka R. T. (2001). *Fast Exact Linear and Non-linear Structural Reanalysis and the Sherman-Morrison-Woodbury Formulas.* International Journal for Numerical Methods in Engineering, 50(7): 1587-1606. *and* Deng, L. and Ghosn, M. (2001). *Pseudoforce Method for Nonlinear Analysis and Reanalysis of Structural Systems.* Journal of Structural Engineering ASCE, 127(5): 570-578.

Simmons, F. G. (1991). *Differential Equations with Applications and Historical Notes.* 2nd ed., McGraw-Hill International Editions: 655.

Teixeira de Freitas (1990). *Elastoplastic Analysis of Skeletal Structures.* in Mathematical Programming Methods in Structural Plasticity, CISM – International Centre for Mechanical Sciences, Courses and Lectures nº 299, Springer-Verlag, Udine: 153:169.

Timoshenko, S. (1976). *Strength of Materials, Part II, Advanced Theory and Problems.* 3rd ed., Robert E. Krieger Publishing Co., New York: 588.

Veiskarami, M. and Pourzeynali, S. (2012). *Green's Function for the Deflection of Non-Prismatic Simply Supported Beams by an Analytical Approach.* Estonian Journal of Engineering, 18(4): 336-351.

Wolfram (2008). Wolfram Mathematica 6, v6.0.3

Woodbury, M. (1950). *Inverting Modified Matrices.* Princeton University, Statistical Research Group, Memorandum report 42, Princeton: 4. *Cited by* Akgun, M. A. Garcelon, J. H. and Haftka R. T. (2001). *Fast Exact Linear and Non-linear Structural Reanalysis and the Sherman-Morrison-Woodbury Formulas.* International Journal for Numerical Methods in Engineering, 50(7): 1587-1606.

Zienkiewicz O. C., Valliapan, S. and King, I. P. (1969). *Elasto-Plastic Solutions of Engineering Problems Initial Stress. Finite Element Approach.* International Journal for Numerical Methods in Engineering, 1(1): 75-100.